KU LEUVEN

ARENBERG DOCTORAL SCHOOL
Faculty of Science

Finding the ringdown of rotating black holes in higher-derivative gravity

Simon Maenaut

Supervisors:
Prof. dr. Thomas Hertog
Prof. dr. Tjonnie Li

Dissertation presented in partial fulfilment
of the requirements for the degree of
Doctor of Science (PhD): Physics

August 2025

FINDING THE RINGDOWN OF ROTATING BLACK HOLES IN HIGHER-DERIVATIVE GRAVITY

Simon MAENAUT

Supervisors:
Prof. dr. Thomas Hertog
Prof. dr. Tjonnie Li

Members of the
Examination Committee:
Prof. dr. Eva Laplace, chair
Prof. dr. Thomas Van Riet
Prof. dr. Hugues Sana
Dr. Henri Inchauspé
Prof. dr. Chris Van Den Broeck
(Utrecht University)

Dissertation presented in partial fulfilment
of the requirements for the degree of
Doctor of Science (PhD): Physics

August 2025

Statement on the use of Generative AI

The research and writing process of my thesis was completed without the use of generative AI assistance tools.

The text, code, and images in this thesis are my own (unless otherwise specified). Generative AI has only been used in accordance with the KU Leuven guidelines and appropriate references have been added. I have reviewed and edited the content as needed and I take full responsibility for the content of the thesis.

© 2025 Simon Maenaut
Uitgegeven in eigen beheer, Simon Maenaut, Celestijnenlaan 200D box 2415, B-3001 Leuven (Belgium)

Alle rechten voorbehouden. Niets uit deze uitgave mag worden vermenigvuldigd en/of openbaar gemaakt worden door middel van druk, fotokopie, microfilm, elektronisch of op welke andere wijze ook zonder voorafgaande schriftelijke toestemming van de uitgever.

All rights reserved. No part of the publication may be reproduced in any form by print, photoprint, microfilm, electronic or any other means without written permission from the publisher.

In memory of my grandfathers
Opa Piet and Opa Roger

Acknowledgements

Research is seldom carried out in isolation and it would not have been possible for me to complete this journey without the help and support of so many people. To each and every one of these individuals: Thank you!

To the reader, let me express my appreciation for your interest in my thesis.

The content of several publications is presented in this work. I would like to credit the funding and collaborations that supported me and my co-authors. Please refer to the original publications for a full acknowledgement thereof.

There are, at this point, several persons that I explicitly would like to thank. First and foremost, I would like to thank my supervisors Thomas Hertog and Tjonnie Li, who have guided me on my doctoral journey and without their continued advice, guidance and encouragement it would not have been possible. I am very grateful to have had two supervisors with such an extensive and profound set of – often complementary – knowledge, experience, and skills. Thank you, Thomas, for always sharing your scientific perspective and wisdom. Tjonnie, thank you for challenging me to always be more ambitious.

I would like to express my gratitude to Pablo Cano for always taking the time to explain concepts to me and to discuss different approaches to solving a problem. Thank you for guiding me as a student and for the wonderful collaborations on many of the research projects to study the fascinating nature of black holes. Let me thank Thomas Van Riet, who guided me when I started my journey into theoretical physics as a student. Together with Nikolay Bobev, you have taught me the most theoretical physics over the years and inspired me to do research.

Also, I want to thank Thomas Van Riet as well as Eva Laplace, Hugues Sana, Henri Inchauspé, and Chris Van Den Broeck for serving on my examination committee, taking the time to read my thesis, and providing valuable feedback.

It brought me great joy during my PhD to work with many wonderful people, and I would like to thank in particular those with whom I collaborated closely. Thank you Kwinten, Pablo, and Thomas for setting up a good start to my PhD, taking the time to involve me in the first projects and to teach me so much. Thank you Ania for your help with running the ringdown analysis and the enlightening conversations. Thank you Gregorio for all your invaluable advice, all the time debugging the analysis code and letting me discover Copenhagen. Thank you Vitor for all your words of wisdom. Thank you Nicola and Lodovico for insightful discussions on quasinormal modes. Even though this thesis does not include Euclidean wormholes, thank you Thomas (both), Bruno and Rob for bringing the saga on the stability of these strange objects to a proper conclusion. Thank you to all the students I had the honour of guiding throughout my PhD. In particular, I would like to thank Maxim, Alessia, Gorik, Karel, and Robrecht for being such fantastic and enthusiastic master students.

To all my colleagues: fellow PhDs, postdocs, professors from high-energy physics, gravitational waves, and beyond, I thank you for sharing your time with me. To everyone in the Leuven Gravity Institute, especially the managers, thank you. Annelien and Marina, thank you for putting up with me in your office and accepting the resulting increase in entropy, and for all the outreach activities. Thank you Caroline for your willingness to always listen and share advice.

There are many more people who contributed to my grasp of physics, throughout the Physics and Astronomy Department and especially from a special place up high called the Institute of Theoretical Physics. To all of you: Thank you! This includes Pierre, who visits the institute seasonally. Thank you for taking the time to also read my thesis and provide detailed feedback on my writing. Thank you Anneleen for all you have done and keeping the institute running all those years. Filip, thanks for the IT support and distractions when needed.

In my PhD I gained precious experience as a teaching assistant. Thank you Cassandra for helping out with the Quantum Mechanics course for engineers. Jozefien, thank you for working with me to support the phsyics master students.

To my friends from Leuven, Brussels, and abroad, thank you for your support and encouragements. A special thanks goes to Joris, Vincent and Soetkin for all the wonderful times throughout our studies, the games, and the vacations. I would also like to thank my housemates: Tom, Estelle, Nick, and Clannad, for living with me, sharing small moments of joy, and all your understanding.

To my family, thank you for your persistent motivation and confidence in me. Last but definitely not least, I want to thank my parents and my sister Emilia. For all your love, patience, and support, I am eternally grateful.

— Simon

Abstract

Black holes are among the most intriguing and fascinating objects in our universe. They are a key feature of general relativity, Einstein's theory of gravity, and their existence leads to many of the current questions in theoretical physics. Astronomical observations indicate the presence of black holes in a variety of astrophysical phenomena, including in star systems and at the centre of galaxies. Although inherently dark by nature, the presence of black holes could be inferred from the influence these massive compact objects have on their surroundings. The detection of gravitational waves provides a new lens to study black holes.

Gravitational waves are ripples in the fabric of spacetime, and are predicted by general relativity as a form of gravitational radiation. The gravitational waves we can measure come from astrophysical events with strong and dynamical gravitational fields, e.g. mergers of massive compact objects like black holes. The first detection of gravitational waves in 2015 was from the merger of two black holes. Since then about a hundred black hole mergers have been observed. The gravitational-wave signal from the merger of black holes can be described in three phases: the inspiral, when the two black holes orbit around each other, they gradually draw closer and spiral inward; the merger, when the event horizons of the two black holes start to overlap, and they coalesce together; and the ringdown, whereby the new black hole relaxes towards its stationary state and the surrounding spacetime rings with the black hole's quasinormal modes.

Each quasinormal mode has a specific complex frequency, which describes its oscillation frequency and damping time, intrinsic to the black-hole spacetime. The quasinormal mode spectrum of a Kerr black hole, which consists of these complex frequencies, is uniquely determined by the black hole's mass and spin. Quasinormal modes are solutions of the Teukolsky equation, which is derived from the perturbation of curvature scalars in the Newman-Penrose formalism. Black-hole spectroscopy aims to study the nature of black holes by analysing the gravitational-wave signal of the ringdown and to compare the observed spectrum of quasinormal mode frequencies with theoretical predictions.

With advances in the sensitivity of gravitational-wave detectors, it is pertinent to explore gravitational-wave signatures of corrections to general relativity. On a fundamental level, there are strong arguments to consider that general relativity is incomplete, at least at very high energies. Higher-derivative gravity is an extension of general relativity that follows the principles of effective field theory. Higher-curvature terms are added to the Einstein-Hilbert action, order by order in curvature dimension, with a length scale ℓ much smaller than the black hole. The leading effect from these terms then comes from the lowest-order terms that modify the black-hole solutions and the dynamics of general relativity.

We study the leading effect of higher-derivative corrections to general relativity on the quasinormal modes that describe perturbations of rotating black holes. Initially, we only consider static and slowly-rotating black holes and calculate the effect of higher-derivative corrections on their quasinormal mode spectrum. The isospectrality between modes of opposite parity is lifted by these corrections. Subsequently, to study any rotating black hole with higher-derivative corrections, we describe curvature perturbations in terms of a universal Teukolsky equation. This requires a Newman-Penrose description of the corrected background and a metric reconstruction of Kerr perturbations. We are able to reduce the equations to a decoupled set of radial equations that form modified Teukolsky equations.

Since higher-derivative corrections lead to deviations in the effective potential of the modified Teukolsky equation, we studied a general parametrisation of such deviations, any of which can be captured by a limited number of coefficients. Small deviations should cause small shifts in the quasinormal mode spectrum. We calculate the leading corrections to the quasinormal mode frequencies related to each coefficient with a generalisation of Leaver's continued-fraction method. This allows for the fast computation of corrections to the quasinormal modes of rotating black holes in any theory that yields a modified Teukolsky equation. We apply this method to calculate the shifts from higher-derivative corrections in the quasinormal mode spectrum of black holes with a wide range of spins.

We conduct an analysis of all gravitational-wave signals with a detectable ringdown, with a waveform template for the ringdown of rotating black holes that includes higher-derivative corrections and allows for isospectrality breaking. This model was implemented in pyRing to perform the first time-domain spectroscopic search for these corrections with quasinormal mode frequency shifts that are accurate for rapidly rotating black holes. We find no evidence of higher-derivative corrections, and we set an upper bound on the length scale of these corrections from a joint analysis of all the observed ringdown signals.

In this thesis, we strive to connect the theoretical study of gravity to the analysis of ringdown observations through the explicit calculation of the impact of higher-derivative corrections on the ringdown signal of rotating black holes.

Contents

Abstract **iv**

1 Introduction **1**
1.1 Motivation 5
1.2 Aim 7
1.3 Structure 8

2 Metric perturbations of Schwarzschild black holes **10**
2.1 Metric perturbations 14
2.2 Master equations 17
2.3 Isospectrality 20

3 Newman-Penrose formalism and Kerr black holes **22**
3.1 Tetrad formalism 23
3.2 Kerr black hole 30
3.3 Teukolsky equation 33

4 Corrections from Higher-derivative gravity **38**
4.1 The EFT of gravity and its black holes 40
4.2 Perturbations of slowly-rotating black holes 42
4.3 Slowly-rotating black holes quasinormal modes 48

5 Setting up a modified Teukolsky equation **54**
5.1 The universal Teukolsky equation 56
5.2 Newman-Penrose description of the background geometry . . . 63
5.3 Metric reconstruction of Kerr perturbations 66
5.4 Separation of Teukolsky equations 69
5.5 Radial master equations 73
5.6 Quasinormal modes in six-derivative gravity 75
5.7 Conclusions 84

6 Quasinormal-mode spectra of black holes beyond Kerr 86
6.1 Parametrised formalism . . . 87
6.2 Computation of the coefficients . . . 91
6.3 The modified Teukolsky equations . . . 97
6.4 Quasinormal modes in higher-derivative gravity . . . 105
6.5 Conclusions . . . 115

7 Observational constraints 118
7.1 Bayesian inference . . . 119
7.2 Time-domain likelihood . . . 122
7.3 Kerr ringdown model . . . 124
7.4 EFT Analysis . . . 126
7.5 Conclusions . . . 133

8 Conclusion 134

A Appendix to Chapter 2 136
A.1 Equations from General Relativity . . . 136
A.2 Vector and tensor spherical harmonics . . . 138

B Appendix to Chapter 3 139
B.1 (Newman/Geroch-Held)-Penrose . . . 139
B.2 Nollert's improvements of continued fraction . . . 142

C Appendix to Chapter 4 145
C.1 Slowly-rotating metric . . . 145
C.2 Numerical results . . . 146
C.3 Chandrasekhar transformation linear in spin . . . 149
C.4 QM-like perturbation theory . . . 150
C.5 Solving the coupled equations using uncoupled equations . . . 152

D Appendix to Chapter 5 154
D.1 Starobinsky-Teukolsky identities . . . 154

E Appendix to Chapter 6 157
E.1 Ambiguity of the potential modifications . . . 157
E.2 Derivation of the boundary conditions . . . 158
E.3 Splitting of the potential . . . 159
E.4 Diagonal quadratic coefficients . . . 161

F Appendix to Chapter 7 162
F.1 Excluded regions for quartic corrections . . . 162

Bibliography 164

Chapter 1

Introduction

Black holes are one of the most fascinating astrophysical objects in the universe. Intuitively, a black hole can be described as a massive compact object in space that is so dense that its gravity prevents anything, even light, from escaping. From a theoretical point of view, black holes are described by general relativity, Albert Einstein's theory of gravity. General relativity models gravity as resulting from the geometry of space and time, or more accurately, of a unified spacetime. In this theory, the presence of mass and energy curves the spacetime geometry, whilst curved spacetime affects the motion of matter and radiation as gravity. How the spacetime geometry behaves is encoded in the Einstein field equations. Discovering that general relativity generically predicts the existence of black holes and that they are uniquely described was a process of several decades.

Just a few months after Einstein had developed general relativity in 1915 [1], Karl Schwarzschild found a solution to the Einstein field equations that describes the gravitational field generated by a point mass and a spherical static mass [2]. Later, it was found that the solution becomes singular at a specific distance from the origin called the Schwarzschild radius related to the mass of the object. The implications of these singularities were not well understood at the time. These solutions were only considered physically valid for the spacetime region outside a massive object such as a star, and what happens near the centre of this vacuum spacetime solution was long considered a mathematical curiosity. Arthur Eddington showed in 1924 that the singularity could be removed by applying a coordinate transformation [3] and this implies, as was concluded in 1933 by Georges Lemaître, that the coordinate singularity was non-physical [4]. It was only in 1958 that David Finkelstein identified this as a surface across which travel is only allowed in one direction [5], therefore called a horizon.

Schwarzschild's solution to the field equations was quickly extended to describe the spacetime around a charged point mass with the Reissner-Nordström metric, which was found independently by several physicists in the subsequent years [6–9]. However, finding an exact solution for a generically rotating object proved to be significantly more difficult. It was nearly half a century later, only in 1963, that Roy Kerr found an exact solution for a rotating black-hole metric [10]. The solution for a black hole that is both rotating and electrically charged was found two years later by Ezra Newman [11] and provided a common solution when combining general relativity with Maxwell's theory of electromagnetism. Although black holes are regular at the horizon, all these black holes have a physical singularity at the centre, where the curvature diverges. This was first suspected to be an artefact from the symmetry conditions imposed when solving the field equations and it was assumed that a generic solution would avoid these. However, in 1965 Roger Penrose [12] proved that singularities appear generically whenever black holes form, due to the presence of a closed trapped surface. These singularities are not observable outside the black hole, as according to the *cosmic censorship conjecture* [13] these are hidden by an event horizon.

From a theoretical perspective, black holes are very special and elegant objects. What was conjectured and proven under various assumptions by Werner Israel [14], Brandon Carter [15], David Robinson [16] and others was that the intrinsic properties of an isolated, stationary black hole (at rest) are fully characterised by its mass, its angular momentum and any electromagnetic charge it carries. This is the *no-hair theorem* (i.e., a black hole retains no other information "hair" about how it has formed or what fell into it, except for these properties). Since astrophysical black holes are expected to possess negligible charge, we will primarily focus on a black hole's mass and its angular momentum (or spin). This implies that once these parameters are measured for a specified black hole, all other intrinsic properties of the black hole can be predicted with fixed values. As a consequence, precise observations of black-hole properties provide excellent opportunities to either validate, or search for the limits, of general relativity.

Black holes will by nature not emit any detectable electromagnetic radiation, hence the evidence for black holes has historically relied on indirect observations. The first evidence for stellar mass black holes came in 1971 from the spectroscopic observation of Cygnus X-1, a high-mass x-ray binary, where a blue supergiant has a companion so compact and massive that it is likely a black hole [17, 18], and careful observation of binary systems have since yielded more candidates. Supermassive black holes are expected to be present at the centre of all galaxies. This was first supported by a redshift measurement of a quasar in 1963 [19, 20] which implied quasars could be the accretion disks of supermassive black holes. Radio interferometry by the Event Horizon Telescope of the centre of M87 [21] and Sagittarius A* [22] confirmed the presence of supermassive black holes.

The dynamics of black holes can be observed by their gravitational radiation. Gravitational waves are ripples in the fabric of spacetime created by the presence of strong dynamical gravitational fields found in some astrophysical phenomena. The existence of gravitational waves was another prediction of general relativity. As massive objects move, the geometry of spacetime around them also changes. When these objects accelerate, it causes ripples in the fabric of spacetime called gravitational waves, which propagate outwards at the speed of light.

Henri Poincaré had, in 1905, proposed the concept of gravitational radiation, such that gravitational interactions would propagate at the speed of light [23]. After having published his theory of general relativity, Einstein speculated that if this radiation exists, it is so weak it would be impossible to detect [24]. At the time, there was some discussion as to whether this radiation was physical, since Eddington showed in 1922 that some forms of gravitational radiation were actually mathematical artefacts from the choice of coordinate system [25]. In 1936, Einstein and Nathan Rosen proved that gravitational waves exist in general relativity (although originally they were convinced of the opposite) [26]. The ambiguities regarding various possible coordinate choices were resolved by Felix Pirani in 1957, as he expressed gravitational waves in terms of an invariant of the curvature tensor, showing that gravitational waves exert tidal forces [27]. The first indirect evidence for gravitational waves came in 1974 through the observation of a pulsar in a binary system with another neutron star, where the orbital decay matched the prediction from general relativity [28, 29].

The first direct detection of gravitational waves occurred on 14 September 2015 by the LIGO and Virgo collaborations, when both LIGO observatories were able to detect gravitational radiation from the merger of two black holes [30]. The observed gravitational-wave signal [31] is consistent with the merger of two black holes of 30 and 35 solar masses at a distance of around 440 Mpc. The remnant black hole has a mass of 62 solar masses, meaning that the merger emitted the equivalent of 3 solar masses in energy through gravitational waves. The observed signal was still very faint, with a strain of the order of $\sim 10^{-21}$, which highlights the incredible sensitivity needed in gravitational-wave detectors.

We can describe the merger of two black holes in roughly three distinct phases. As the black holes circle around their common centre of mass they slowly lose orbital energy and spiral inwards due to the emission of gravitational radiation. This inspiral is gradual at first when the black holes are relatively far apart, but as they come closer, the orbital frequency increases and the orbit decays faster. The merger happens roughly when the event horizons of the two black holes start to overlap, and they coalesce together into one highly distorted black hole. Finally, the newly formed black hole relaxes into its stationary state during the so-called ringdown, as the perturbed spacetime around the black hole oscillates and perturbations either cross the horizon or propagate as gravitational waves.

A perturbation in the spacetime around a black hole causes damped oscillations due to the dissipative nature of the system. The energy of such an oscillation disappears as it is absorbed at the horizon and as it radiates away to infinity. Such a perturbation can be described by a superposition of quasinormal modes, and their dynamics will be represented by the linearised Einstein field equations. Each quasinormal mode has a specific complex frequency, which describes its oscillation frequency and damping time, intrinsic to the black-hole spacetime. Together these frequencies form the quasinormal mode spectrum of a black hole. Since in general relativity the spacetime solution for an astrophysical black hole is fully described by its mass and spin, as a consequence of the no-hair theorem, this will uniquely determine the quasinormal mode spectrum of the black hole. The idea of *black-hole spectroscopy* is to study the nature of black holes by analysing the ringdown signal from the merger of black holes and comparing the observed spectrum of quasinormal modes to the predictions of general relativity.

Initially, the interest to study the perturbations of scalar, electromagnetic and gravitational fields on a black-hole spacetime background was to figure out whether black holes were actually stable and therefore even physically possible. For a Schwarzschild black hole, Tullio Regge and John Wheeler found in 1957 that it was stable at linear order. They were able to express metric perturbations with one type of parity symmetry (axial) in terms of one master equation [32]. The master equation that describes metric perturbations with the other type of parity symmetry (polar) was discovered only later by Frank Zerelli in 1970 [33]. In the same year, it was shown by Vishveshwara that solutions to these master equations are given by damped oscillations with complex frequencies [34]. Subrahmanyan Chandrasekhar proved in 1974 the very remarkable property that the Regge-Wheeler and Zerilli equations for axial and polar metric perturbations have the same quasinormal mode spectrum; the equations are isospectral [35]. Finding a separable master equation to describe gravitational perturbations on the background of a Kerr black hole was a significant mathematical problem that Saul Teukolsky was able to resolve in 1972 by describing them not in terms of the metric perturbations, but as perturbations of curvature invariants [36].

In the subsequent decades, the focus has shifted towards applying black-hole perturbation theory specifically in the context of binary black-hole mergers. The modelling of the post-merger ringdown signal and the inverse problem of identifying quasinormal modes in a ringdown signal received much attention. Following the first numerical relativity simulation of a black-hole merger [37–39], it became possible to identify quasinormal modes in simulated signals [40, 41]. GW150914 was, aside from the first gravitational-wave detection and observation of a black-hole merger, also the first observed ringdown of a black hole [42]. This marked the dawn of observational black-hole spectroscopy [43].

1.1 Motivation

The direct observation of gravitational waves from the merger of black holes opened a window to probe the dynamics of strongly curved regions of spacetime. The signal that follows these mergers allows us to validate the *Kerr hypothesis*, which is the prediction from the no-hair theorem that the geometry of any rotating black hole is given by the Kerr metric. It could enable a distinction between black holes and potential black hole mimickers. In the light of these developments, it is of interest to study and identify what the possible signatures of corrections to general relativity could be within gravitational-wave signals.

There are good reasons to study the theoretical landscape of possible extensions, modifications or alternatives to general relativity as the theory of gravitation. The existence of black holes in general relativity leads to a number of puzzling theoretical questions closely associated with the fundamental nature of gravity. The diverging curvature at the centre of a black hole, and the loss of information once it crosses the horizon, hint that the classical description of these objects in general relativity is insufficient. On a fundamental level, there are strong arguments that general relativity is incomplete, at least at very high energies, since it is fully incompatible with our understanding of quantum mechanics. Although this point provides no specific predictions, and the implied deviations could be at scales far outside the reach of astrophysical observations, frameworks to reconcile these theories suggest possible methods to extend general relativity. As a theory described mathematically by a metric, general relativity satisfies Einstein's equivalence principle. However, it is by far not the only possible theory of gravity to preserve local Lorentz invariance and diffeomorphism invariance. Studying alternatives to see to which extent they are ruled out or constrained (if at all) by experiments can further our understanding of the nature of gravity. Furthermore, to gauge how well an observed gravitational-wave signal matches the signal waveform predicted by general relativity, or how strongly deviations (either agnostic or motivated by theory) can be constrained, it is very valuable to have waveform predictions from theories that extend general relativity.

To extend general relativity it should be possible to describe the modification following the principle of Effective Field Theory (EFT). When the curvature of spacetime is small, the theory should effectively yield general relativity, and to preserve its symmetries we consider corrections from higher-curvature terms as described by higher-derivative gravity [44]. To construct the EFT extension to general relativity we add to the Einstein-Hilbert action all the possible terms compatible with the symmetries of the theory and we group them following an increasing order of curvatures (in other words, an increasing energy dimension). The leading effect from these corrections should come from the lowest-order terms that modify the black-hole solutions and the dynamics of general relativity.

There is a abundant literature that explores black-hole solutions in alternative theories of gravity. We specifically consider four-dimensional solutions that modify in smooth and parametric manner the black holes of general relativity. The theories that contain such black-hole solutions have an action constructed from the Einstein-Hilbert action supplemented with higher-derivative terms, including possibly additional scalar fields that couple directly to these terms. This includes, as particular cases, Einstein-dilaton-Gauss-Bonnet (EdGB) and dynamical Chern-Simons (dCS) gravity, with an additional coupled scalar field and the general class of higher-derivative gravity, without any additional fields. The first step was to find a solution for a spherically-symmetric black hole in such a theory, which will be a modified version of the Schwarzschild metric. Rotating black-hole solutions are significantly more challenging to find and are usually in a small coupling or small spin approximation or expressed numerically. The general leading-order correction to the Kerr solution in the EFT extension of general relativity with higher-derivative terms, including possible non-minimally coupled scalars, has been computed as a series in the spin parameter [45].

For non-rotating black holes, which are spherically symmetric, it is possible to compute the quasinormal mode spectrum from the modified field equations. This was done in various theories, including EdGB gravity [46, 47], dCS gravity [48, 49] and theories with quartic [50, 51] and cubic [52] curvature terms, among other models [53–55], as well as in some theory-agnostic approaches [56, 57]. Calculating the quasinormal mode spectrum for rotating black holes is harder. This is due to the fact that the solution for rotating black holes is only known perturbatively or numerically, and that the modifications to general relativity break the special hidden symmetry of the Kerr black hole utilised by Teukolsky. The equations describing quasinormal modes are, therefore, no longer separable. The computation of quasinormal frequencies for a rapidly rotating black hole in modified theories of gravity remained until recently an open problem.

A complementary approach is to express possible deviations from the Kerr quasinormal mode spectrum in a parametric manner. This can be done at several different levels, depending on the theoretical assumptions that are made. The simplest is to allow arbitrary deviations in frequencies and damping times, with the Kerr quasinormal modes either predicted from the remnant mass and spin inferred from the pre-merger signal [58] or inferred from the ringdown [59]. If deviations to the Kerr quasinormal mode spectrum have a clear dependence on the remnant mass and spin, these can be expressed as deviation coefficients of an expansion of the frequency and damping time in the spin parameter [60]. Finally, when theoretical corrections appear in the master equation as small modifications to the effective potential, then the perturbative corrections to the quasinormal mode frequencies can be written in terms of these deviations [61].

1.2 Aim

This thesis aims to quantify the possible effect of extensions to general relativity, such as higher-derivative corrections, on the gravitational-wave signal emitted during the ringdown of astrophysical black holes, with the purpose to connect theoretical models to observational analysis. We aspire to demonstrate that black-hole spectroscopy provides a strong observational framework to study the nature of black holes, since the features that appear through these corrections are generally representative for a broad class of deviations from general relativity.

There are three objectives that guided the research into this topic:

1. Study the effect of higher-derivative corrections to general relativity on the quasinormal modes that describe perturbations of rotating black holes.

To begin, we discuss the case of non-rotating and slowly-rotating black holes, where we can leverage the advantage of a spherically-symmetric background to find the general features of such corrections on the quasinormal mode spectrum. Subsequently, we consider the general case of rotating black holes, where we study the perturbations with curvature invariants to find a separable equation. Having the slowly-rotating black hole case as a reference makes it possible to validate the results of the general case for rotating black holes by comparing the predicted corrections to the quasinormal mode frequencies in the static limit. This builds upon the known techniques of black-hole perturbation theory in general relativity, although the inclusion of higher-derivative gravity breaks the special symmetries of Kerr black holes, thereby requiring a careful approach to capture the deviations and reconstruct a master equation for the perturbations.

2. Calculate the leading corrections to the quasinormal mode spectrum of rotating black holes from parametric deviations in the Teukolsky equations.

We expect a small deviation in the effective potential of the Teukolsky equation that governs linear perturbations of Kerr black holes to induce a small correction in the spectrum of quasinormal modes and in the associated separation constants. We can take advantage of the inherent properties of the Teukolsky equation to significantly reduce the number of parameters required to model any deviation. The purpose of this framework is to allow the development of a theory-informed description of agnostic quasi-normal mode deviations for rotating black holes. We can validate the method with examples in the literature where the corrections to the quasinormal mode frequencies are known, and can apply it to compute shifts in the quasinormal mode spectrum from higher-derivative corrections.

3. Analyse current gravitational-wave observations of black-hole ringdown to constrain the scale of potential EFT corrections to general relativity.

The analysis of gravitational-wave signals from the ringdown of black holes is done with the signal expressed in the time domain in order to avoid spectral leakage and contamination from the preceding signal of the inspiral and merger. The results of the previous steps allow for the construction of a signal template with quasinormal mode frequencies that include higher-derivative corrections. This can be implemented into a ringdown analysis package called pyRing that the LIGO-Virgo-KAGRA collaboration uses in the analysis of ringdown signals. The analysis of gravitational-wave events with a detectable ringdown can be used to infer a constraint on the scale of EFT corrections to general relativity.

1.3 Structure

This thesis is structured to reflect the research process; some chapters were written to provide the reader with sufficient background knowledge to understand the research results, which are presented in subsequent chapters and appendices. Throughout this thesis, we work in geometric units, setting G and c to one, although occasionally these constants are reintroduced explicitly to add clarity. We provide a summary of the equations of general relativity in appendix A.1.

We start with the essentials of black-hole perturbation theory in general relativity, which was developed throughout the last century. We study metric perturbations of a Schwarzschild black hole in chapter 2 with tensorial spherical harmonics. The Regge Wheeler gauge makes it possible to separate metric perturbations by parity and to arrive at the master equations that govern these perturbations and we discuss how quasinormal modes are the physical solutions to these equations.

To study perturbations of the rotating Kerr black holes as covered in chapter 3, we introduce the tetrad framework and Newman-Penrose formalism to describe curvature invariants called Weyl scalars. Although heavy in notation, this leads to the derivation of the Teukolsky equation to describe curvature perturbations. We conclude with a method to calculate the quasinormal mode frequencies.

After the overview of the prerequisites, we consider the first research objective. In chapter 4, we introduce higher-derivative gravity and explain why it provides an EFT extension to general relativity. We review the general black-hole solution with higher-derivative corrections as derived from the modified field equations. The main result of this chapter is the study of gravitational perturbations of first static and then slowly-rotating black holes, extending the techniques developed for the Schwarzschild black hole and calculating its quasinormal mode spectrum.

The methods that were developed for the Kerr black hole to arrive at the Teukolsky equation had to be adapted to allow corrections to general relativity. Through a careful derivation, we arrive at the *universal Teukolsky equation*, which we discuss in chapter 5. The ingredients needed to solve this equation and arrive at a modified Teukolsky equation are a description of the corrected background geometry in the Newman-Penrose formalism and a reconstructed metric from the curvature perturbations that solves the Teukolsky equations. This method can be applied even to reasonably rapidly rotating black holes.

The second research objective comes into focus in chapter 6, as we calculate the corrections to the quasinormal modes from a modified Teukolsky equation. We start initially with an arbitrary deviation of the effective potential expressed as a series in the inverse radius and compute the effect of each term on the quasinormal mode frequency. Subsequently, we apply this parametrisation to the modified Teukolsky equation from higher-derivative gravity and calculate the shifts of quasinormal mode frequencies due to higher-derivative corrections.

For the final research objective we use these results within a ringdown analysis. We provide a brief overview of the principles behind the Bayesian analysis that can be considered foundational to the analysis of gravitational-wave observations. Thereafter, we discuss the reasons for analysing the ringdown in the time domain. We introduce a general waveform template for ringdown of a Kerr black hole and touch upon the main assumptions that enter into current ringdown analyses. This is then adapted to include the effect from higher-derivative corrections, and we analyse all available gravitational-wave events with a detectable ringdown to set a constraint on the scale of potential EFT corrections to general relativity.

Finally, we present briefly the general conclusions from this thesis in chapter 8, and discuss some insights that could provide opportunities for further research with current and future gravitational-wave observations of black holes.

Chapter 2

Metric perturbations of Schwarzschild black holes

Black holes formed through the coalescences of two black holes are highly perturbed after the merger, yet they quickly settle down to a stationary state. This rapid relaxation, known as the ringdown of a black hole, is characterised by a set of damped oscillations with specific frequencies and damping times. These oscillations, called quasinormal modes, describe the motion of linear perturbations in the spacetime around a black hole and define its spectrum. The simplest black hole to consider is one that is static and spherically-symmetric. In general relativity, there is a unique spherically symmetric vacuum solution given by the Schwarzschild metric. To start our exploration of the ringdown of black holes, we first study the spectrum of a Schwarzschild black hole.

In this chapter we introduce the methods to calculate the spectrum of metric perturbations for a static, spherically-symmetric black hole in general relativity. We start with a brief overview of the properties of a Schwarzschild black hole and the basics of scalar, vector and tensor spherical harmonics. Metric perturbations projected onto these spherical harmonics can be classified as perturbations with either even or odd parity, and a careful gauge choice makes it possible to reduce the field equations for each class of perturbations to a single master equation. After applying appropriate boundary conditions, the master equations can be solved to yield a spectrum of quasinormal modes, which we discuss in detail. This sets out the groundwork that will be used later to extend the method beyond general relativity for static and slowly-rotating black holes.

In spherical coordinates, the Schwarzschild metric [2] is given by

$$\mathrm{d}s^2 = -f(r)\,\mathrm{d}t^2 + (\,1/f(r)\,)\,\mathrm{d}r^2 + r^2\left(\mathrm{d}\theta^2 + \sin^2(\theta)\,\mathrm{d}\phi^2\right) \tag{2.1}$$

with $f(r) = 1 - 2M/r$, where M can represent the mass of the black hole.

Birkhoff's theorem [14] proves that this metric is the unique spherically symmetric solution of the vacuum field equations. The components of the metric in these coordinates are independent of time, implying that the spacetime is stationary. Since there are no time-space cross terms, it is possible to show that the spacetime is static. More formally, this occurs when a spacetime has a timelike Killing vector orthogonal to a family of spacelike hypersurfaces.

Notice that at $r = 0$ and $r = 2M$ components of the metric diverge, and whilst the origin ($r = 0$) is a physical singularity where the curvature becomes infinite, the divergence at Schwarzschild radius ($r = 2M$) is due to these coordinates and can be resolved with different coordinates.

We introduce the tortoise coordinate r_* defined as

$$\mathrm{d}r_* = \frac{\mathrm{d}r}{f(r)} \quad \text{such that} \quad \frac{\partial}{\partial r_*} = f(r)\frac{\partial}{\partial r}\,. \tag{2.2}$$

If we integrate this expression we can express r_* (up to constant) as

$$r_* = r + 2M\log\left(\frac{r}{2M} - 1\right)\,, \tag{2.3}$$

where $r_* \to -\infty$ at the horizon and $r_* \to +\infty$ towards spatial infinity.

Introduce coordinates that are constant for ingoing and outgoing null geodesics

$$u = t + r_* \quad \text{and} \quad v = t - r_*\,. \tag{2.4}$$

We can write the metric in terms of the Eddington-Finkelstein coordinates [12], so that the metric in terms of the ingoing coordinate becomes

$$\mathrm{d}s^2 = -f(r)\,\mathrm{d}v^2 + 2\,\mathrm{d}v\,\mathrm{d}r + r^2\left(\mathrm{d}\theta^2 + \sin^2(\theta)\,\mathrm{d}\phi^2\right)\,. \tag{2.5}$$

Although one metric component still vanishes at $r = 2M$, the metric remains regular and invertible at the Schwarzschild radius and is therefore non-singular.

Hence, from the perspective of a local observer there is no reason to suspect that this surface is special. However, if we consider the trajectory of lightlike or timelike particles moving radially, a remarkable condition is imposed.

The condition for radial null curves becomes

$$\text{For ingoing rays:} \qquad \frac{\mathrm{d}v}{\mathrm{d}r} = 0\,,$$

$$\text{For outgoing rays:} \qquad \frac{\mathrm{d}v}{\mathrm{d}r} = 2/f(r)\,. \tag{2.6}$$

The paths of null (or time-like particles) can travel past the Schwarzschild radius. However, for $r < 2M$ all paths will have a future-direction with decreasing r (since $f(r)$ will be negative). The surface at the Schwarzschild radius functions as a point of no return and past this point particles can never escape to infinity. This defines the event horizon for a Schwarzschild black hole.

A scalar field (on a spherically-symmetric spacetime) can be decomposed in terms of spherical harmonic, which we define as

$$Y^{lm}(\theta,\phi) = N_{lm} e^{im\phi} P_l^m(\cos\theta)\,, \tag{2.7}$$

where the labels set the degree l and order m of the Legendre polynomial P_l^m and N_{lm} is a suitably chosen normalisation factor (depending on convention).

We introduce Ω_{AB} to describe the metric on a unit sphere as

$$\mathrm{d}\Omega^2_{(2)} = \Omega_{AB}\,\mathrm{d}x^A\,\mathrm{d}x^B = \mathrm{d}\theta^2 + \sin^2\theta\,\mathrm{d}\phi^2 \tag{2.8}$$

and let D_A be the covariant derivative of this metric. We can then define the Laplacian operator on a sphere as

$$D^2 = \Omega^{AB} D_A D_B\,. \tag{2.9}$$

Spherical harmonics are eigenfunctions of this Laplacian operator and satisfy

$$D^2 Y^{lm} = -l(l+1) Y^{lm}\,. \tag{2.10}$$

To study vector and tensor fields (which come with indices) in a similar manner, we need to generalise the spherical harmonics to tensor objects with indices [62]. The idea is to find tensors that are eigenfunctions of the Laplacian and satisfy

$$D^2 Y_{A_1\ldots A_n} = \lambda\, Y_{A_1\ldots A_n}\,, \tag{2.11}$$

where λ will be the eigenvalue of this tensor related to the Laplacian.

Starting with vector spherical harmonics, which will have one index, we identify two types: a set with even parity written as Y_A^{lm} and a set with odd parity written as X_A^{lm}; where a parity transformation changes $\theta \to \pi - \theta$ and $\phi \to \phi + \pi$. We construct these with a covariant derivative of a scalar spherical harmonic as

$$Y_A^{lm} = D_A Y^{lm} \quad \text{and} \quad X_A^{lm} = -\epsilon_A{}^B D_B Y^{lm} \tag{2.12}$$

with ϵ_{AB} the Levi-Civita symbol of the sphere: $\epsilon_{\theta\phi} = \sin\theta$, and $\epsilon_A{}^B = \Omega^{BC}\epsilon_{AC}$.

These vector harmonics are eigenfunctions of the Laplacian

$$D^2 Y_A^{lm} = -(l^2+l-1)Y_A^{lm} \quad \text{and} \quad D^2 X_A^{lm} = -(l^2+l-1)X_A^{lm} \tag{2.13}$$

and they satisfy a number of orthogonality relations:

$$\int \bar{Y}^A_{lm} Y_A^{l'm'} \, \mathrm{d}\Omega = l(l+1)\,\delta_{ll'}\delta_{mm'}\,, \qquad \int \bar{Y}^A_{lm} X_A^{l'm'} \, \mathrm{d}\Omega = 0\,,$$

$$\int \bar{X}^A_{lm} X_A^{l'm'} \, \mathrm{d}\Omega = l(l+1)\,\delta_{ll'}\delta_{mm'}\,. \tag{2.14}$$

Two sets of tensor spherical harmonics have even parity, and one has odd parity. One even parity tensor harmonic set corresponds to $\Omega_{AB}Y^{lm}$, and the other is

$$Y^{lm}_{AB} = \left[D_A D_B + \frac{1}{2}l(l+1)\Omega_{AB}\right] Y^{lm}\,, \tag{2.15}$$

whilst the odd-parity tensor harmonic set can be constructed as

$$X^{lm}_{AB} = -\frac{1}{2}\big(\epsilon_A{}^C D_B + \epsilon_B{}^C D_A\big) D_C Y^{lm}\,. \tag{2.16}$$

These are eigenfunctions of the Laplacian on the sphere

$$D^2(\Omega_{AB}Y^{lm}) = \Omega_{AB}D^2 Y^{lm} = -l(l+1)\Omega_{AB}Y^{lm}\,,$$

$$D^2 Y^{lm}_{AB} = -(l^2+l-4)Y^{lm}_{AB}\,, \quad D^2 X^{lm}_{AB} = -(l^2+l-4)X^{lm}_{AB}\,, \tag{2.17}$$

and satisfy the following set of orthogonality relations

$$\int \bar{Y}^{AB}_{lm} Y^{l'm'}_{AB} \, \mathrm{d}\Omega = \frac{1}{2}(l-1)l(l+1)(l+2)\,\delta_{ll'}\delta_{mm'}\,,$$

$$\int \bar{X}^{AB}_{lm} X^{l'm'}_{AB} \, \mathrm{d}\Omega = \frac{1}{2}(l-1)l(l+1)(l+2)\,\delta_{ll'}\delta_{mm'}\,,$$

$$\int \bar{Y}^{AB}_{lm} X^{l'm'}_{AB} \, \mathrm{d}\Omega = 0 \quad \text{and} \quad \Omega^{AB} Y^{lm}_{AB} = \Omega^{AB} X^{lm}_{AB} = 0\,. \tag{2.18}$$

We list the components of these tensorial spherical harmonics in Appendix A.2.

2.1 Metric perturbations

The Einstein field equations (see Appendix A.1) in vacuum are given by:

$$G_{\mu\nu} = R_{\mu\nu} - \tfrac{1}{2}\, R\, g_{\mu\nu} = 0\,. \tag{2.19}$$

To study perturbations due to gravitational interactions, we apply a small metric perturbation $\epsilon\, h_{\mu\nu}$ to the background metric $g_{\mu\nu}$ as

$$g_{\mu\nu} \to g_{\mu\nu} + \epsilon\, h_{\mu\nu} \quad \text{for} \quad \epsilon \ll 1 \quad \text{and} \quad h_{\mu\nu} = \mathcal{O}(1)\,. \tag{2.20}$$

This should satisfy the field equations in vacuum up to linear order in ϵ so that

$$G^{(0)}_{\mu\nu} + \epsilon\, G^{(1)}_{\mu\nu} + \mathcal{O}\big(\epsilon^2\big) = 0\,. \tag{2.21}$$

Since the background metric satisfies the field equations at leading order ($G^{(0)}_{\mu\nu}$), the linearised Einstein tensor with the metric perturbation has to equal zero

$$G^{(1)}_{\mu\nu} = -\tfrac{1}{2}\nabla_\alpha\nabla^\alpha\hat{h}_{\mu\nu} - \tfrac{1}{2}g_{\mu\nu}\nabla^\alpha\nabla^\beta\hat{h}_{\alpha\beta} + \nabla^\alpha\nabla_{(\mu}\hat{h}_{\nu)\alpha} = 0\,, \tag{2.22}$$

where $g_{\mu\nu}$ is the background metric, ∇_μ its covariant derivative and we introduce the trace-reversed metric perturbation as $\hat{h}_{\mu\nu} = h_{\mu\nu} - \frac{1}{2}h_{\alpha\beta}\, g^{\alpha\beta}\, g_{\mu\nu}$.

To decompose $h_{\mu\nu}$ into spherical harmonics we split the metric into two parts

$$\mathrm{d}s^2 = g_{ab}\,\mathrm{d}x^a\,\mathrm{d}x^b + r^2\Omega_{AB}\,\mathrm{d}x^A\,\mathrm{d}x^B\ , \tag{2.23}$$

where we define the metric on each sub-manifold as

$$g_{ab}\,\mathrm{d}x^a\,\mathrm{d}x^b = -f(r)\,\mathrm{d}t^2 + \frac{\mathrm{d}r^2}{f(r)}\,, \quad \Omega_{AB}\,\mathrm{d}x^A\,\mathrm{d}x^B = \mathrm{d}\theta^2 + \sin^2(\theta)\,\mathrm{d}\phi^2\ . \tag{2.24}$$

The lower-case Latin indices $a, b, c, \ldots$ represent the time and radial coordinate whilst the upper-case Latin indices $A, B, C, ...$ represent the angular components. Any coordinates that separate the metric in this manner are a valid choice.

To decompose the metric perturbation we can use the vector and tensor spherical harmonics defined in the previous section and identify harmonics according to the lm labels and according to parity as

$$h_{\mu\nu} = \sum_{l,m} h^{lm}_{(+)\mu\nu} + \sum_{l,m} h^{lm}_{(-)\mu\nu} \tag{2.25}$$

where the even-parity $(+)$ and odd-parity $(-)$ components can be written as

$$\begin{aligned}
h^{lm}_{(+)ab} &= H^{lm}_{ab}Y^{lm}\,, & h^{lm}_{(-)ab} &= 0\,,\\
h^{lm}_{(+)aB} &= j^{lm}_a Y^{lm}_B\,, & h^{lm}_{(-)aB} &= h^{lm}_a X^{lm}_B\,,\\
h^{lm}_{(+)AB} &= r^2\left(K^{lm}\Omega_{AB}Y^{lm} + G^{lm}Y^{lm}_{AB}\right)\,, & h^{lm}_{(-)AB} &= h^{lm}_2 X^{lm}_{AB}\,,
\end{aligned} \tag{2.26}$$

and the functions $\{H_{ab}, j_a, K, G\}$ and $\{h_a, h_2\}$ only depend on t and r.

Since the physics of a system is independent of the choice of coordinates, expressions in general relativity are invariant under coordinate transformations. The perturbed field equations with the linearised Einstein tensor (2.22) are also invariant under the following gauge transformation for the metric perturbation

$$h'_{\mu\nu} = h_{\mu\nu} + \nabla_\mu k_\nu + \nabla_\nu k_\mu \,. \tag{2.27}$$

We can use this gauge freedom to reduce metric perturbation components.

To find the effect of such a gauge transformation on the metric (2.23) it suffices to write out the covariant derivative above in terms of a partial derivative and the Christoffel symbol (see Appendix A.1) and find all the non-zero components. A metric perturbation will transform as follows:

$$\begin{aligned} h'_{ab} &= h_{ab} - \hat{\nabla}_a k_b - \hat{\nabla}_b k_a \,, \\ h'_{aA} &= h_{aA} - \partial_A k_a - \partial_a k_A + \frac{2}{r}\,(\partial_a r) k_A \,, \\ h'_{AB} &= h_{AB} - D_A k_B - D_B k_A - \Omega_{AB}\, r\,(\partial_a r) k^a \,, \end{aligned} \tag{2.28}$$

where $\hat{\nabla}_a$ is the covariant derivative on the (t, r) sub-manifold with g_{ab} as metric, and as before D_A is the covariant derivative on the sphere with Ω_{AB} as metric. Similar to the decomposition of the metric perturbation, we can decompose the vector k_μ of the transformation into spherical harmonics of different parity,

$$k_\mu = \sum_{l,m} k^{lm}_{(+)\mu} + \sum_{l,m} k^{lm}_{(-)\mu} \,. \tag{2.29}$$

The odd-parity components of a gauge transformation are generated by a vector field $k_\alpha = (0, k_A)$ that is decomposed as

$$k^{lm}_{(-)A} = \xi^{lm} X^{lm}_A \,, \tag{2.30}$$

where ξ^{lm} is a function of only the (t, r) coordinates. The odd-parity metric perturbation $h_{(-)\mu\nu}$ (dropping the spherical-harmonic labels) is transformed as

$$\begin{aligned} h'_{ab} &= h_{ab} \,, \qquad h'_{aA} = h_{aA} - X_A\,(\partial_a \xi - (2/r)(\partial_a r)) \,, \\ h'_{AB} &= h_{AB} - \xi\,(D_A X_B + D_B X_A) \,, \end{aligned} \tag{2.31}$$

Since $D_A X_B + D_B X_A = 2 X_{AB}$, the transformed metric has the form of (2.26). and the transformation therefore changes h_a and h_2 according to

$$\begin{aligned} h_a \to h'_a &= h_a - \nabla_a \xi + (2/r)(\partial_a r)\xi \,, \\ h_2 \to h'_2 &= h_2 - 2\xi \,, \end{aligned} \tag{2.32}$$

We use these gauge transformations to simplify the form of the metric perturbations and set $h_2 = 0$ such that only h_a are non-vanishing components.

The even parity components of a gauge transformations are generated by a vector field $k_\alpha = (k_a, k_A)$ that is decomposed as

$$k^{lm}_{(+)a} = \xi^{lm}_a Y^{lm} \quad \text{and} \quad k^{lm}_{(+)A} = \xi^{lm} Y^{lm}_A \,, \tag{2.33}$$

where the fields ξ^{lm}_a and ξ^{lm} are again purely functions of the (t, r) coordinates. This transforms the even parity metric perturbation $h_{(+)\mu\nu}$ as

$$h_{ab} \to h'_{ab} = h_{ab} - \hat{\nabla}_a \xi_b - \hat{\nabla}_b \xi_a \,, \qquad j_a \to j'_a = j_a - \xi_a - \hat{\nabla}_a \xi + \frac{2}{r}(\partial_a r)\xi \,,$$

$$K \to K' = K + \frac{l(l+1)}{r^2}\xi - \frac{2}{r}(\partial^a r)\xi_a \,, \quad G \to G' = G - \frac{2}{r^2}\xi \,, \tag{2.34}$$

where once again we have dropped the spherical-harmonic labels for readability. We use these gauge transformations to simplify the metric perturbations and set $j_a = 0$ and $G = 0$ such that only h_{ab} and K are non-vanishing components. This choice for odd- and even-parity components is the Regge-Wheeler gauge.

Since each part of a decomposed metric perturbation with either even or odd parity for a specific spherical harmonic satisfies the field equations independently, metric perturbations of the following form can be studied separately:

$$h_{\mu\nu} = h^{lm}_{(\pm)\mu\nu} \,. \tag{2.35}$$

We choose the Regge-Wheeler gauge, setting some metric components to zero. With a stationary background spacetime and linear field equations, the time dependence can be expressed as a factor $e^{-i\omega t}$ with ω a complex frequency. As a result of spherical symmetry, the resulting field equations are actually independent of the choice of m and we therefore set $m = 0$ in these calculations.

A metric perturbation in the Regge-Wheeler gauge can explicitly be written as

$$h^{l0}_{(+)\mu\nu} = \begin{bmatrix} f(r)H_0(r) & H_1(r) & 0 & 0 \\ H_1(r) & H_2(r)/f(r) & 0 & 0 \\ 0 & 0 & r^2 K(r) & 0 \\ 0 & 0 & 0 & r^2 K(r)\sin^2(\theta) \end{bmatrix} e^{-i\omega t} Y_{l0}(\theta, \phi) \,,$$

$$h^{l0}_{(-)\mu\nu} = \begin{bmatrix} 0 & 0 & 0 & h_0(r) \\ 0 & 0 & 0 & h_1(r) \\ 0 & 0 & 0 & 0 \\ h_0(r) & h_1(r) & 0 & 0 \end{bmatrix} e^{-i\omega t} \left(\sin\theta \frac{\partial}{\partial\theta}\right) Y_{l0}(\theta, \phi) \,. \tag{2.36}$$

where odd-parity metric perturbations have radial functions $h_0(r)$ and $h_1(r)$, and even-parity metric perturbations have $H_0(r)$, $H_1(r)$, $H_2(r)$ and $K(r)$.

2.2 Master equations

To evaluate the field equations and find solutions, we calculate the linearised Einstein tensor for a metric perturbation of a specific parity and harmonic. Applying the properties of spherical harmonics allows us to reduce the equations to a set of coupled ordinary differential equations for the different functions. Surprisingly, for both even and odd perturbations the full solution can be written in terms of one master variable that satisfies a simple differential equation.

We start with the odd-parity perturbations, which leads to a simpler calculation, as was done by Regge and Wheeler in 1957 [32]. The linearised Einstein tensor (2.22) with the odd-parity metric perturbation in the Regge-Wheeler gauge (2.36) has only three independent non-zero components: $G^{(1)}_{t\phi}$, $G^{(1)}_{r\phi}$ and $G^{(1)}_{\theta\phi}$. Requiring that last two vanish, yields to two first-order differential equations

$$\omega h_0 - if\,\frac{\mathrm{d}}{\mathrm{d}r}(f\,h_1) = 0\,,$$

$$-ir^4\omega\frac{\mathrm{d}}{\mathrm{d}r}\left(\frac{h_0}{r^2}\right) + h_1\left(-f\left(-2rf' + l(l+1)\right) + 2f^2 + r^2\omega^2\right) = 0\,. \tag{2.37}$$

The first equation makes it possible to express h_0 in terms of h_1 as

$$h_0 = \frac{i}{\omega}f\,\frac{\mathrm{d}}{\mathrm{d}r}(f\,h_1)\,, \tag{2.38}$$

and the other equation becomes a second-order differential equation for h_1.

If we introduce the variable

$$\Psi^- = \frac{f\,h_1}{r}\,, \tag{2.39}$$

this equation can be written as

$$f\,\frac{\mathrm{d}}{\mathrm{d}r}\left(f\,\frac{\mathrm{d}\Psi^-}{\mathrm{d}r}\right) + \left(\omega^2 - V^-_{lm}\right)\Psi^- = 0\,, \tag{2.40}$$

$$\text{where}\quad V^- = f\left(\frac{l(l+1)}{r^2} - \frac{3f'}{r}\right)\,. \tag{2.41}$$

If we change to the tortoise coordinate r_* we can express this as

$$\frac{\mathrm{d}^2\Psi^-}{\mathrm{d}r_*^2} + \left(\omega^2 - V^-\right)\Psi^- = 0\,. \tag{2.42}$$

This is the master equation for odd-parity metric perturbations, known as the Regge-Wheeler equation. A solution for Ψ_- will define a specific odd-parity metric perturbation. There is no $l = 0$ odd-parity mode and the $l = 1$ mode is not radiative (since gravitational-waves are not emitted as dipolar radiation).

The even-parity perturbations are significantly more difficult to disentangle, and were first solved in terms of a master variable and equation by Zerelli 1970 [33]. The independent non-vanishing components of the linearised Einstein tensor are off-diagonal elements $G^{(1)}_{tr}$, $G^{(1)}_{t\theta}$, $G^{(1)}_{r\theta}$, and diagonal elements $G^{(1)}_{tt}$, $G^{(1)}_{rr}$, $G^{(1)}_{\theta\theta}$. Similar to the odd-parity perturbations gravitational emission occur when $l \geq 2$ as the angular components of the equation are then non-zero, which means that the radial factors in each term of every component has to vanish.

The $G^{(1)}_{\theta\theta}$ component has two terms with different angular dependence and requiring the $\partial^2 Y_{lm}/\partial\theta^2$ term to equal zero implies that H_0 and H_2 are equal. We therefore introduce $H = H_0 = H_2$ to refer to either of the two variables.

The aim is now to use these differential equations to express the first derivative of each of the remaining variables H, H_1 and K in terms of the other variables. From $\delta G^{(1)}_{tr} = 0$ we find an expressions for K' as

$$K' = \frac{1}{2r^2}\left(\frac{2r(r-3M)}{2M-r}K + 2rH + \frac{il(l+1)}{\omega}H_1\right), \tag{2.43}$$

and from $\delta G^{(1)}_{t\theta} = 0$ we find an expression for H_1' as

$$H_1' = \frac{1}{2Mr - r^2}\left(ir^2\omega K + ir^2\omega H + 2MH_1\right). \tag{2.44}$$

The equation for K' can be used with $G^{(1)}_{r\theta} = 0$ to find an expression for H' as

$$\begin{aligned} H' = \frac{1}{2r^2\omega(r-2M)^2}\big(&r\omega\left(2\left(l^2+l+2\right)Mr + r^2\left(-l^2-l+2r^2\omega^2\right) - 6M^2\right)K \\ &+ r\omega\left(4M^2 - 2\left(l^2+l+1\right)Mr + l(l+1)r^2\right)H \\ &+ i(2M-r)\left(l(l+1)(M-r) + 4r^3\omega^2\right)H_1\big). \end{aligned} \tag{2.45}$$

Substituting these equations into $G^{(1)}_{\theta\theta} = 0$ with $\lambda = \frac{1}{2}(l-1)(l+2)$ yields

$$\begin{aligned} &\left(2\lambda + \frac{6M}{r}\right)H + \left(2\lambda - \frac{2M}{r} - \frac{2r}{(2M-r)}\left(\frac{M^2}{r^2} + r^2\omega^2\right)\right)K \\ &\qquad + \left(2i\omega r - i\frac{l(l+1)M}{\omega r^2}\right)H_1 = 0, \end{aligned} \tag{2.46}$$

which can be used to express H fully in terms of H_1 and K.

We introduce a new variable $H_1 = \omega S$ and find two first-order differential equations dependent on K and S with the following structure

$$K' = (\alpha_0 + \alpha_2\,\omega^2)K + (\beta_0 + \beta_2\,\omega^2)S\,,$$
$$S' = (\gamma_0 + \gamma_2\,\omega^2)K + (\delta_0 + \delta_2\,\omega^2)S\,, \tag{2.47}$$

where α, β, γ and δ are functions of r, M and l, not of ω, given by

$$\alpha_0 = \frac{(\lambda-2)Mr + 6M^2}{r(r-2M)(\lambda r+3M)}\,, \qquad \alpha_2 = \frac{-r^3}{(r-2M)(\lambda r+3M)}\,, \tag{2.48}$$

$$\beta_0 = \frac{i(\lambda-1)(\lambda r+2M)}{r^2(\lambda r+3M)}\,, \qquad \beta_2 = \frac{ir}{(\lambda r+3M)}\,, \tag{2.49}$$

$$\gamma_0 = \frac{ir(4(\lambda-1)Mr - 2\lambda r^2 + 9M^2)}{(r-2M)^2(\lambda r+3M)}\,, \quad \gamma_2 = \frac{ir^5}{(r-2M)^2(\lambda r+3M)}\,, \tag{2.50}$$

$$\delta_0 = \frac{M(6M + r(3\lambda+1))}{(\lambda r+3M)(2Mr-r^2)}\,, \qquad \delta_2 = \frac{-r^3}{(\lambda r+3M)(2M-r)}\,, \tag{2.51}$$

where we introduce $\lambda = \frac{1}{2}(l-1)(l+2)$ to simplify the notation.

We define $\hat{K}(r_*)$ and $\hat{S}(r_*)$ as functions of the tortoise coordinate r_* with

$$K(r) = g(r)\hat{K}(r_*) + \hat{S}(r_*) \quad \text{and} \quad S(r) = h(r)\hat{K}(r_*) + k(r)\hat{S}(r_*)\,, \tag{2.52}$$

where $g(r)$, $h(r)$ and $k(r)$ are chosen so that $\hat{S}$ and $\hat{K}$ satisfy the system:

$$\frac{\mathrm{d}\hat{K}}{\mathrm{d}r_*} = \hat{S} \quad \text{and} \quad \frac{\mathrm{d}\hat{S}}{\mathrm{d}r_*} = (V^+(r) - \omega^2)\hat{K}\,. \tag{2.53}$$

We find that the solution is given by

$$g(r) = \frac{\lambda(\lambda+1)r^2 + 3\lambda Mr + 6M^2}{r^2(\lambda r+3M)}\,,$$
$$h(r) = i\frac{-\lambda r^2 + 3\lambda Mr + 3M^2}{(r-2M)(\lambda r+3M)}\,, \qquad \text{and} \quad k(r) = \frac{-ir^2}{r-2M}\,. \tag{2.54}$$

With this condition V^+ is given by

$$V^+ = \left(1 - \frac{2M}{r}\right)\frac{2\lambda^2(\lambda+1)r^3 + 6\lambda^2 Mr^2 + 18\lambda M^2 r + 18M^3}{r^3(\lambda r+3M)^2}\,. \tag{2.55}$$

We introduce $\Psi^+ = \hat{K}$ as the master variable and we find the master equation

$$\frac{\mathrm{d}^2\Psi^+}{\mathrm{d}{r_*}^2} + \left(\omega^2 - V^+\right)\Psi^+ = 0\,. \tag{2.56}$$

2.3 Isospectrality

We have found by analysing the field equations in vacuum at linear order that in general metric perturbations can be decomposed in terms of spherical harmonics labelled by the numbers l, m, and in parts with even $(+)$ and odd $(-)$ parity. For each of these modes the full metric perturbation can be expressed in terms of a simple master variable $\Psi^{\pm}_{lm}$ that satisfies a master equation of the form

$$\frac{\mathrm{d}^2\Psi^{\pm}_{lm}}{\mathrm{d}r_*^2} + \left(\omega^2 - V^{\pm}_{lm}\right)\Psi^{\pm}_{lm} = 0\,, \tag{2.57}$$

where we reintroduce the labels l, m into the notation.

The quasinormal modes a black hole correspond to the solutions of this simple differential equation, with the appropriate physical boundary conditions.

The potential V vanishes at the horizon as $r_* \to -\infty$ and therefore in this limit solutions to the master equation should behave as $\Psi \sim e^{-i\omega(t\pm r_*)}$ in general. As nothing should leave the black hole horizon, only incoming modes that correspond to a plus sign should be allowed, hence

$$\Psi \sim e^{-i\omega(t+r_*)} \quad \text{for} \quad r_* \to -\infty \qquad \text{(at the horizon)}. \tag{2.58}$$

This implies that outgoing modes are suppressed near the horizon.

In an asymptomatically flat spacetime the potential vanishes at spatial infinity. To avoid waves entering spacetime from infinity the boundary condition sets

$$\Psi \sim e^{-i\omega(t-r_*)} \quad \text{for} \quad r_* \to +\infty \qquad \text{(at infinity)} \tag{2.59}$$

and outgoing waves are allowed to leave the system and dissipate energy.

With these boundary conditions the master equation only has solutions for a discrete set of complex ω which are called the quasinormal mode frequencies. For each value of l and the polarisation $\pm$, we will have an infinite set of these frequencies $\omega^{\pm}_{l,n}$ labelled by the overtone index n in increasing order of the size of their imaginary component, starting with $n = 0$ for the fundamental mode. All these complex frequencies together form the quasinormal mode spectrum.

Notice that since we expect the absolute amplitude of a mode to decay over time, a quasinormal mode frequency should have a negative imaginary component. However, the amplitude towards infinity would then diverge as a consequence. Regular initial conditions on the background spacetime can therefore not be represented directly as a superposition of quasinormal modes. Rather, these modes represent quasistationary states that can not exist forever. These modes are excited at some precise time and then they decay exponentially. Quasinormal modes do not form a complete basis of wavefunctions [63].

A very important result for Schwarzschild black holes is that the spectra of odd and even perturbations are identical. This is due to the fact that a solution of the odd master equation with a specific quasinormal mode frequency can be transformed into a solution of the even master equation with the same frequency.

The effective potential for even and odd metric perturbations can be written as

$$V^{\pm} = W^2 \mp \frac{\mathrm{d}W}{\mathrm{d}r_*} - \beta^2 \tag{2.60}$$

where

$$W = \frac{3M(2M-r)}{r^2\,(3M+\lambda r)} - \beta \quad \text{and} \quad \beta = \frac{\lambda(\lambda+1)}{3M}\,. \tag{2.61}$$

A simple substitution with the following transformation changes a solution of the even master equation to a solution of the odd master equation and back

$$\Psi^{\pm} = -\frac{1}{\beta^2+\omega^2}\left(\mp W\,\Psi^{\mp} + \frac{\mathrm{d}\Psi^{\mp}}{\mathrm{d}r_*}\right) \tag{2.62}$$

which confirms that the even and odd perturbations are indeed isospectral [35].

Chapter 3

Newman-Penrose formalism and Kerr black holes

Astrophysical black holes, from stellar remnants to galactic centres, generally rotate as the spacetime curvature of these black holes carries angular momentum. The angular momentum from the formation of the black hole and any subsequent infalling matter is preserved and the spacetime surrounding the black hole is warped and dragged along in the direction of rotation. The assumption that the system is (nearly) spherically symmetric will not hold for rotating black holes and the method developed in the previous chapter is therefore not applicable. To find the gravitational quasinormal mode spectrum it is no longer possible to decompose metric perturbations and express them in terms of a master variable. Instead we will consider perturbations in terms of the curvature components of the Weyl tensor, with an adapted form of the Bianchi identity as main equation.

In this chapter we discuss the techniques needed to study rotating black holes and to calculate their quasinormal mode spectrum for gravitational perturbations. We start with an introduction of a tetrad frame to describe spacetime and discuss the Newman-Penrose (NP) formalism. This formalism chooses a special frame in terms of two real and two complex null (lightlike) vectors and describes the properties of a spacetime in terms of curvature components and spin coefficients. We explore the properties of rotating black holes in general relativity, which are described by the Kerr metric in terms of their mass and angular momentum. Finally we show how applying this formalism to a Kerr black hole can lead to the Teukolsky equations, whose solutions define its quasinormal mode spectrum. Later these methods will be extended to find the quasinormal modes of rotating black holes when considering small modifications to general relativity.

3.1 Tetrad formalism

When investigating a problem in general relativity, we often consider the field equations with a choice of local coordinates that is well-suited for the system. Instead of choosing specific coordinates, an alternative approach is to choose a frame of four linearly independent vector fields, called a tetrad frame, and to examine the equations satisfied by projecting tensors onto this tetrad frame. This is the core idea of the tetrad formalism and the choice of the tetrad frame should reflect the spacetime symmetries that are key to the problem at hand. We first present the formalism in general without choosing a specific frame and derive the relevant properties necessary for our application following [64].

At each point in spacetime we define a frame of four linearly independent vectors. We label a frame vector by a tetrad index, written as a Latin lower-case letter in bold upright characters to distinguish it from the tensor index of the vector written with a Greek lower-case letter (which is used to label its components). A frame vector is therefore written as

$$e_{\mathbf{a}}{}^{\mu} \tag{3.1}$$

with in this case $\mathbf{a}$ the frame index and μ the tensor index of the vector.

The tensor index can be lowered and raised with the metric $g_{\mu\nu}$ such that

$$e_{\mathbf{a}\,\mu} = g_{\mu\nu}\, e_{\mathbf{a}}{}^{\mu} \tag{3.2}$$

whilst we also define the inverse of a frame vector $e^{\mathbf{b}}{}_{\nu}$ to satisfy

$$e_{\mathbf{a}}{}^{\mu}\, e^{\mathbf{b}}{}_{\mu} = \delta^{\mathbf{b}}{}_{\mathbf{a}}\,, \qquad\qquad e_{\mathbf{a}}{}^{\mu}\, e^{\mathbf{a}}{}_{\nu} = \delta^{\mu}{}_{\nu}\,. \tag{3.3}$$

To raise and lower frame indices we introduce $\eta_{\mathbf{ab}}$ and its inverse $\eta^{\mathbf{ab}}$

$$\eta_{\mathbf{ab}} = e_{\mathbf{a}}{}^{\mu} e_{\mathbf{b}\,\mu}\,, \qquad\qquad \eta^{\mathbf{ab}}\,\eta_{\mathbf{bc}} = \delta^{\mathbf{a}}{}_{\mathbf{c}}\,. \tag{3.4}$$

where we assume that $\eta_{\mathbf{ab}}$ is a constant and symmetric.

With these definitions we can raise and lower frame indices

$$\eta_{\mathbf{ab}}\, e^{\mathbf{a}}{}_{\mu} = e_{\mathbf{b}\,\mu}\,, \qquad\qquad \eta^{\mathbf{ab}}\, e_{\mathbf{a}\,\mu} = e^{\mathbf{b}}{}_{\mu} \tag{3.5}$$

and confirm that

$$e_{\mathbf{a}\,\mu}\, e^{\mathbf{a}}{}_{\nu} = g_{\mu\nu}\,. \tag{3.6}$$

Any vector or tensor field can be projected onto the tetrad frame

$$A^{\mathbf{a}} = e^{\mathbf{a}}{}_{\mu}\, A^{\mu} = e^{\mathbf{a}\,\mu}\, A_{\mu}\,, \qquad\qquad A^{\mu} = e_{\mathbf{a}}{}^{\mu}\, A^{\mathbf{a}} = e^{\mathbf{a}\,\mu}\, A_{\mathbf{a}} \tag{3.7}$$

and more generally

$$T_{\mathbf{ab}} = e_{\mathbf{a}}{}^{\mu}\, e_{\mathbf{b}}{}^{\nu}\, T_{\mu\nu}\,, \qquad\qquad T_{\mu\nu} = e^{\mathbf{a}}{}_{\mu}\, e^{\mathbf{b}}{}_{\nu}\, T_{\mathbf{ab}}\,. \tag{3.8}$$

With the frame vectors $e_{\mathbf{a}}{}^{\mu}$ we can define directional derivatives

$$\partial_{\mathbf{a}} = e_{\mathbf{a}}{}^{\mu}\, \partial_{\mu} = e_{\mathbf{a}}{}^{\mu}\, \frac{\partial}{\partial x_{\mu}}\,, \tag{3.9}$$

which can be applied on a scalar, vector and tensor fields

$$\partial_{\mathbf{a}} \varphi = e_{\mathbf{a}}{}^{\mu}\, \partial_{\mu} \varphi = e_{\mathbf{a}}{}^{\mu}\, \nabla_{\mu} \varphi\,, \tag{3.10}$$

$$\begin{aligned} \partial_{\mathbf{c}} V_{\mathbf{b}} &= e_{\mathbf{c}}{}^{\nu}\, \partial_{\nu} \big(e_{\mathbf{b}}{}^{\mu}\, V_{\mu} \big) = e_{\mathbf{c}}{}^{\nu}\, \nabla_{\nu} \big(e_{\mathbf{b}}{}^{\mu}\, V_{\mu} \big) \\ &= e_{\mathbf{b}}{}^{\mu}\, e_{\mathbf{c}}{}^{\nu}\, \nabla_{\nu} V_{\mu} + V_{\mu}\; e_{\mathbf{c}}{}^{\nu}\, \nabla_{\nu}\, e_{\mathbf{b}}{}^{\mu} \\ &= e_{\mathbf{b}}{}^{\mu}\, e_{\mathbf{c}}{}^{\nu}\, \nabla_{\nu} V_{\mu} + V^{\mathbf{a}}\, e_{\mathbf{a}}{}^{\mu}\, e_{\mathbf{c}}{}^{\nu}\, \nabla_{\nu}\, e_{\mathbf{b}\,\mu}\,. \end{aligned} \tag{3.11}$$

We introduce the spin coefficients as

$$\gamma_{\mathbf{abc}} = e_{\mathbf{a}}{}^{\mu}\, e_{\mathbf{c}}{}^{\nu}\, \nabla_{\nu}\, e_{\mathbf{b}\,\mu} \tag{3.12}$$

in order to write

$$\partial_{\mathbf{c}} V_{\mathbf{b}} = e_{\mathbf{c}}{}^{\mu}\, e_{\mathbf{b}}{}^{\nu}\, \nabla_{\mu} V_{\nu} + V^{\mathbf{a}}\, \gamma_{\mathbf{abc}}\,. \tag{3.13}$$

We define the intrinsic derivative of a vector

$$\nabla_{\mathbf{c}} V_{\mathbf{b}} = e_{\mathbf{c}}{}^{\mu}\, e_{\mathbf{b}}{}^{\nu}\, \nabla_{\mu} V_{\nu} = \partial_{\mathbf{c}} V_{\mathbf{b}} - \eta^{\mathbf{ad}}\, \gamma_{\mathbf{abc}}\, V_{\mathbf{d}} \tag{3.14}$$

such that we can freely interchange covariant derivatives and intrinsic derivatives. The definition of intrinsic derivatives of tensor fields follows in a similar manner.

If we calculate

$$e_{\mathbf{b}}{}^{\mu}\,\nabla_{\nu}\,e_{\mathbf{a}\,\mu}+e_{\mathbf{a}}{}^{\mu}\,\nabla_{\nu}\,e_{\mathbf{b}\,\mu}=\nabla_{\nu}\big(e_{\mathbf{a}\,\mu}\,e_{\mathbf{b}}{}^{\mu}\big)=\nabla_{\nu}\eta_{\mathbf{ab}}=0\,, \tag{3.15}$$

we find that spin coefficients are antisymmetric in the first indices

$$\gamma_{\mathbf{abc}}=e_{\mathbf{a}}{}^{\mu}\,e_{\mathbf{c}}{}^{\nu}\,\nabla_{\nu}\,e_{\mathbf{b}\,\mu}=-e_{\mathbf{b}}{}^{\mu}\,e_{\mathbf{c}}{}^{\nu}\,\nabla_{\nu}\,e_{\mathbf{a}\,\nu}=-\gamma_{\mathbf{bac}}\,. \tag{3.16}$$

To find the Riemann tensor we start with the Ricci identity

$$\nabla_{\mu}\nabla_{\nu}\,e_{\mathbf{a}\,\sigma}-\nabla_{\nu}\nabla_{\mu}\,e_{\mathbf{a}\,\sigma}=R_{\rho\sigma\mu\nu}\,e_{\mathbf{a}}{}^{\rho}\,, \tag{3.17}$$

which we can project onto the tetrad frame

$$\begin{aligned}
R_{\mathbf{abcd}}&=R_{\rho\sigma\mu\nu}\,e_{\mathbf{a}}{}^{\rho}\,e_{\mathbf{b}}{}^{\sigma}\,e_{\mathbf{c}}{}^{\mu}\,e_{\mathbf{d}}{}^{\nu}\\
&=\big(\nabla_{\mu}\,\gamma_{\mathbf{afg}}\,e^{\mathbf{f}}{}_{\sigma}\,e^{\mathbf{g}}{}_{\nu}-\nabla_{\nu}\,\gamma_{\mathbf{afg}}\,e^{\mathbf{f}}{}_{\sigma}\,e^{\mathbf{g}}{}_{\mu}\big)\,e_{\mathbf{b}}{}^{\sigma}\,e_{\mathbf{c}}{}^{\mu}\,e_{\mathbf{d}}{}^{\nu}\\
&=\partial_{\mathbf{c}}\gamma_{\mathbf{abd}}-\partial_{\mathbf{d}}\gamma_{\mathbf{abc}}-\gamma_{\mathbf{abf}}\,\eta^{\mathbf{fe}}\big(\gamma_{\mathbf{ced}}-\gamma_{\mathbf{dec}}\big)\\
&+\gamma_{\mathbf{afc}}\,\eta^{\mathbf{fe}}\gamma_{\mathbf{ebd}}-\gamma_{\mathbf{afd}}\,\eta^{\mathbf{fe}}\gamma_{\mathbf{ebc}}\,,
\end{aligned} \tag{3.18}$$

where in the last step the brackets are expanded and covariant derivatives of the basis vectors are replaced with the respective spin coefficients.

The Bianchi identity (A.12) can also be written with frame indices:

$$\nabla_{[\mathbf{e}}R_{\mathbf{ab}]\mathbf{cd}}=0\,. \tag{3.19}$$

Changing the intrinsic derivative to a directional derivative, this becomes

$$\begin{aligned}
&\partial_{[\mathbf{e}}R_{\mathbf{ab}]\mathbf{cd}}+2\,\eta^{\mathbf{ij}}\gamma_{\mathbf{ai}[\mathbf{e}}R_{\mathbf{jb}]\mathbf{cd}}\\
&\qquad+2\,\eta^{\mathbf{ij}}\gamma_{\mathbf{ci}[\mathbf{e}}R_{\mathbf{ab}]\mathbf{jd}}=0\,,
\end{aligned} \tag{3.20}$$

where terms have been grouped together by careful use of symmetry properties.

The simplest example to consider is that in any (3+1) dimensional spacetime one can find a set of orthonormal vector fields where one is timelike $e_{\mathbf{0}}{}^{\mu}$ and three are spacelike $e_{\mathbf{i}}{}^{\mu}$ such that

$$e_{\mathbf{0}}{}^{\mu}e_{\mathbf{0}\,\mu}=-1\quad\text{and}\quad e_{\mathbf{i}}{}^{\mu}e_{\mathbf{j}\,\mu}=\delta_{\mathbf{ij}}\,. \tag{3.21}$$

The metric can then be projected on the tetrad frame

$$g_{\mu\nu}e_{\mathbf{a}}{}^{\mu}e_{\mathbf{b}}{}^{\nu}=\eta_{\mathbf{ab}}\,, \tag{3.22}$$

where $\eta_{\mathbf{ab}}$ is equivalent to the Minkowski metric in Cartesian coordinates which implies that $e_{\mathbf{a}}{}^{\mu}$ provides a local Lorentz frame at any spacetime point.

3.1.1 Newman-Penrose formalism

The Newman-Penrose formalism is an application of the tetrad formalism with a special choice of frame. First proposed by Newman and Penrose in 1962 [65], it chooses a frame with four null vectors of which two are real, l^μ and n^μ, whilst the other two, orthogonal to the first two, are complex conjugates m^μ and $\bar{m}^\mu$. This is different to the usual choice of orthonormal vectors for a frame, and was in part motivated with the aim to capture the light-cone structure of spacetime. For black-hole solutions in general relativity we will see that this formalism is indeed effective to capture the inherent symmetries in these spacetimes.

The four null-frame vectors are labelled

$$e_{\mathbf{1}}{}^\mu = l^\mu\,, \qquad e_{\mathbf{2}}{}^\mu = n^\mu\,, \qquad e_{\mathbf{3}}{}^\mu = m^\mu\,, \qquad e_{\mathbf{4}}{}^\mu = \bar{m}^\mu\,. \tag{3.23}$$

The first pair of (real) null vectors are chosen to satisfy

$$l^\mu l_\mu = n^\mu n_\mu = 0 \quad \text{and} \quad l^\mu n_\mu = -1 \tag{3.24}$$

and orthogonal spacelike directions are described by two complex null vectors

$$m^\mu m_\mu = \bar{m}^\mu \bar{m}_\mu = 0 \quad \text{and} \quad m^\mu \bar{m}_\mu = 1 \tag{3.25}$$

where m^μ and $\bar{m}^\mu$ have to be complex conjugates for the metric to be real. Subsequently we find that

$$\eta_{\mathbf{ab}} = \begin{bmatrix} 0 & -1 & 0 & 0 \\ -1 & 0 & 0 & 0 \\ 0 & 0 & 0 & +1 \\ 0 & 0 & +1 & 0 \end{bmatrix} \tag{3.26}$$

and the metric is constructed by writing

$$g_{\mu\nu} = -l_\mu n_\nu - n_\mu l_\nu + m_\mu \bar{m}_\nu + \bar{m}_\mu m_\nu\,. \tag{3.27}$$

A frame spanned by $e^\mu_{\mathbf{a}} = \{l^\mu, n^\mu, m^\mu, \bar{m}^\mu\}$ is a Newman-Penrose (NP) frame.

Raising the frame index provides the following relations:

$$\begin{aligned} e^{\mathbf{1}\,\mu} &= \eta^{\mathbf{12}} e_{\mathbf{2}}{}^\mu = -n^\mu\,, & e^{\mathbf{2}\,\mu} &= \eta^{\mathbf{21}} e_{\mathbf{1}}{}^\mu = -l^\mu\,, \\ e^{\mathbf{3}\,\mu} &= \eta^{\mathbf{34}} e_{\mathbf{4}}{}^\mu = \bar{m}^\mu\,, & e^{\mathbf{4}\,\mu} &= \eta^{\mathbf{43}} e_{\mathbf{3}}{}^\mu = m^\mu\,. \end{aligned} \tag{3.28}$$

We mostly follow the convention of [64] for spin coefficients as defined in (3.12):

$$\kappa = -m^\mu l^\nu \nabla_\nu l_\mu \,, \quad \sigma = -m^\mu m^\nu \nabla_\nu l_\mu \,, \quad \rho = -m^\mu \bar{m}^\nu \nabla_\nu l_\mu \,, \quad \tau = -m^\mu n^\nu \nabla_\nu l_\mu \,,$$

$$\kappa' = n^\mu n^\nu \nabla_\nu \bar{m}_\mu \,, \quad \sigma' = n^\mu \bar{m}^\nu \nabla_\nu \bar{m}_\mu \,, \quad \rho' = n^\mu m^\nu \nabla_\nu \bar{m}_\mu \,, \quad \tau' = n^\mu l^\nu \nabla_\nu \bar{m}_\mu \,,$$

$$\epsilon = -\tfrac{1}{2}(n^\mu l^\nu \nabla_\nu l_\mu + m^\mu l^\nu \nabla_\nu \bar{m}_\mu) \,, \quad \beta = -\tfrac{1}{2}(n^\mu m^\nu \nabla_\nu l_\mu + m^\mu m^\nu \nabla_\nu \bar{m}_\mu) \,,$$

$$\epsilon' = \tfrac{1}{2}(n^\mu n^\nu \nabla_\nu l_\mu + m^\mu n^\nu \nabla_\nu \bar{m}_\mu) \,, \quad \beta' = \tfrac{1}{2}(n^\mu \bar{m}^\nu \nabla_\nu l_\mu + m^\mu \bar{m}^\nu \nabla_\nu \bar{m}_\mu) \quad (3.29)$$

where a prime $'$ interchanges frame field vectors in the following way

$$l^\mu \leftrightarrow n^\mu \quad \text{and} \quad m^\mu \leftrightarrow \bar{m}^\mu \tag{3.30}$$

and we used the fact that spin coefficients are antisymmetric in the first indices (see (3.16)) to swap the vectors with tensor index μ in the primed definitions.

To describe spacetime curvature in the Newman-Penrose formalism we first start with the Weyl tensor, the traceless part of the Riemann tensor (see (A.8)). Projected onto the Newman-Penrose frame, the various tetrad components of the Weyl tensor are represented by five complex Weyl scalars:

$$\Psi_0 = C_{\alpha\beta\mu\nu} l^\alpha m^\beta l^\mu m^\nu \,, \quad \Psi_1 = C_{\alpha\beta\mu\nu} l^\alpha n^\beta l^\mu m^\nu \,, \quad \Psi_2 = C_{\alpha\beta\mu\nu} l^\alpha m^\beta \bar{m}^\mu n^\nu \,,$$

$$\Psi_3 = C_{\alpha\beta\mu\nu} l^\alpha n^\beta \bar{m}^\mu n^\nu \,, \quad \Psi_4 = C_{\alpha\beta\mu\nu} n^\alpha \bar{m}^\beta n^\mu \bar{m}^\nu \,. \tag{3.31}$$

The tetrad components of the Ricci tensor are typically represented in terms of three real scalars, three complex scalars and the Ricci scalar:

$$\phi_{00} = \tfrac{1}{2} R_{\mu\nu} l^\mu l^\nu \,, \quad \phi_{22} = \tfrac{1}{2} R_{\mu\nu} n^\mu n^\nu \,, \quad \phi_{11} = \tfrac{1}{4}(R_{\mu\nu} l^\mu n^\nu + R_{\mu\nu} m^\mu \bar{m}^\nu) \,,$$

$$\phi_{01} = \tfrac{1}{2} R_{\mu\nu} l^\mu m^\nu \,, \quad \phi_{12} = \tfrac{1}{2} R_{\mu\nu} n^\mu m^\nu \,, \quad \phi_{02} = \tfrac{1}{2} R_{\mu\nu} m^\mu m^\nu \,,$$

$$R = -2 R_{\mu\nu} l^\mu n^\nu + 2 R_{\mu\nu} m^\mu \bar{m}^\nu \,. \tag{3.32}$$

It is important to realise that although these scalars are by construction invariant under diffeomorphisms, they crucially depend on the choice of the tetrad frame. A local Lorentz transformation at each spacetime point can rotate the tetrad.

The advantage of these local Lorentz transformations is that for some special classes of metrics, it is possible to apply local Lorentz transformations to obtain a frame where one or several of the Weyl scalars vanish to simplify expressions. The classification of four-dimensional spacetime metrics, in terms what can be achieved with these local rotations, was first described by Petrov in 1954 [66].

In the NP formalism, these transformations are categorised in three classes:

Rotations of type I keep l^μ fixed ($a \in \mathbb{C}$):

$$l^\mu \mapsto l^\mu, \qquad n^\mu \mapsto n^\mu + a^* m^\mu + a\bar{m}^\mu + aa^* l^\mu,$$
$$m^\mu \mapsto m^\mu + a l^\mu, \qquad \bar{m}^\mu \mapsto \bar{m}^\mu + a^* l^\mu. \tag{3.33}$$

Rotations of type II keep n^μ fixed ($b \in \mathbb{C}$):

$$n^\mu \mapsto n^\mu, \qquad l^\mu \mapsto l^\mu + b^* m^\mu + b\bar{m}^\mu + bb^* n^\mu,$$
$$m^\mu \mapsto m^\mu + b n^\mu, \qquad \bar{m}^\mu \mapsto \bar{m}^\mu + b^* n^\mu. \tag{3.34}$$

Rotations of type III scale l^μ, n^μ and rotate m^μ in the complex plane ($A, \theta \in \mathbb{R}$):

$$l^\mu \mapsto A^{-1} l^\mu, \qquad n^\mu \mapsto A n^\mu, \qquad m^\mu \mapsto e^{i\theta} m^\mu, \qquad \bar{m}^\mu \mapsto e^{-i\theta} \bar{m}^\mu. \tag{3.35}$$

The transformation rules for the Weyl scalars under each rotation can be found by evaluating the projections of the Weyl tensor onto a transformed tetrad.

Type I:
$$\Psi_0 \mapsto \Psi_0,$$
$$\Psi_1 \mapsto \Psi_1 + a^* \Psi_0,$$
$$\Psi_2 \mapsto \Psi_2 + 2a^* \Psi_1 + (a^*)^2 \Psi_0$$
$$\Psi_3 \mapsto \Psi_3 + 3a^* \Psi_2 + 3(a^*)^2 \Psi_1 + (a^*)^3 \Psi_0,$$
$$\Psi_4 \mapsto \Psi_4 + 4a^* \Psi_3 + 6(a^*)^2 \Psi_2 + 4(a^*)^3 \Psi_1 + (a^*)^4 \Psi_0; \tag{3.36}$$

Type II:
$$\Psi_0 \mapsto \Psi_0 + 4b\Psi_1 + 6b^2 \Psi_2 + 4b^3 \Psi_3 + b^4 \Psi_4,$$
$$\Psi_1 \mapsto \Psi_1 + 3b\Psi_2 + 3b^2 \Psi_3 + b^3 \Psi_4,$$
$$\Psi_2 \mapsto \Psi_2 + 2b\Psi_3 + b^2 \Psi_4,$$
$$\Psi_3 \mapsto \Psi_3 + b\Psi_4,$$
$$\Psi_4 \mapsto \Psi_4; \tag{3.37}$$

Type III:
$$\Psi_0 \mapsto A^2 e^{-2i\theta} \Psi_0, \qquad \Psi_1 \mapsto A^{-1} e^{i\theta} \Psi_1, \qquad \Psi_2 \mapsto \Psi_2,$$
$$\Psi_3 \mapsto A e^{-i\theta} \Psi_3, \qquad \Psi_4 \mapsto A^2 e^{-2i\theta} \Psi_4. \tag{3.38}$$

3.1.2 Geroch-Held-Penrose formalism

After choosing a specific frame, there is some advantage to working covariantly with respect to the subset of local transformations that retain its key properties. This is the main principle of the Geroch-Held-Penrose (GHP) formalism, which adapts the NP formalism into a description covariant under type-III rotations. Every object X within the formalism has specific weights $\{p, q\}$ given by how it transforms under a type-III rotation (in terms of A and θ as in (3.35)) such that

$$X \mapsto A^{-(p+q)/2}\, e^{i\theta(p-q)/2} X\,, \tag{3.39}$$

The advantage is that only objects with the same weights can be added together. The product of objects has the weight of the sum of the weights of its factors.

The weights of the frame fields are

$$l^\mu : \{1,1\}\,, \qquad n^\mu : \{-1,-1\}\,, \qquad m^\mu : \{1,-1\}\,, \qquad \bar{m}^\mu : \{-1,1\}\,. \tag{3.40}$$

and we note that the weights of X' are $\{-p,-q\}$ and those of X^* are $\{q,p\}$.

The weights of the Weyl scalars come from the tetrad vectors in their definition,

$$\Psi_0 : \{4,0\}\,, \quad \Psi_1 : \{2,0\}\,, \quad \Psi_2 : \{0,0\}\,, \quad \Psi_3 : \{-2,0\}\,, \quad \Psi_4 : \{-4,0\}\,. \tag{3.41}$$

The spin coefficients with definite weight are

$$\kappa : \{3,1\}\,, \qquad \sigma : \{3,-1\}\,, \qquad \rho : \{1,1\}\,, \qquad \tau : \{1,-1\}\,, \tag{3.42}$$

whilst ϵ, ϵ', β, β' are used to construct GHP covariant derivatives

$$\text{Þ} = (l^\alpha \nabla_\alpha - p\epsilon - q\epsilon^*)\,, \qquad \text{Þ}' = (n^\alpha \nabla_\alpha + p\epsilon' + q\epsilon'^*)\,, \tag{3.43}$$

$$\eth = (m^\alpha \nabla_\alpha - p\beta + q\beta'^*)\,, \qquad \eth' = (\bar{m}^\alpha \nabla_\alpha + p\beta' - q\beta^*)\,, \tag{3.44}$$

acting on X with weights $\{p, q\}$. The weights of Þ are $\{1,1\}$ and of $\eth$ are $\{1,-1\}$.

A subset of the Bianchi identities in vacuum (see (3.20)) will be used:

$$\text{Þ}\Psi_1 - \eth'\Psi_0 = -\tau'\Psi_0 + 4\rho\Psi_1 - 3\kappa\Psi_2\,, \tag{3.45}$$

$$\text{Þ}\Psi_2 - \eth'\Psi_1 = \sigma'\Psi_0 - 2\tau'\Psi_1 + 3\rho\Psi_2 - 2\kappa\Psi_3\,, \tag{3.46}$$

$$\text{Þ}'\Psi_0 - \eth\Psi_1 = \rho'\Psi_0 - 4\tau\Psi_1 + 3\sigma\Psi_2\,, \tag{3.47}$$

$$\text{Þ}'\Psi_1 - \eth\Psi_2 = -\kappa'\Psi_0 + 2\rho'\Psi_1 - 3\tau\Psi_2 - 2\sigma\Psi_3\,, \tag{3.48}$$

whilst a complete set of equations can be found in Appendix B.1.

3.2 Kerr black hole

Finding the exact solution of the Einstein field equations in vacuum to describe the metric of a rotating black hole, is significantly more challenging than for a static black hole, such as the Schwarzschild black hole (see Chapter 2). Since crucially spherical symmetry is broken, the solution is only stationary and axisymmetric (symmetric around an axis of rotation). This means that the solution has an asymptotically timelike Killing vector and an axial Killing vector. In contrast to spherically symmetric spacetime solutions that were discovered soon after Einstein had formulated general relativity, the exact solution for a rotating black hole was found by Kerr in 1963 [10] (nearly half a century later). The Kerr black hole is the final state after the gravitational collapse of matter (assuming balanced charges). Astrophysical black holes are thus described by the Kerr metric, which makes it one of the most important metric solutions.

The Kerr metric in Boyer-Lindquist coordinates [67] is given by:

$$\begin{aligned} \mathrm{d}s^2 = &- \left(1 - \frac{2Mr}{\Sigma}\right) \mathrm{d}t^2 - \frac{4Mar\sin^2(\theta)}{\Sigma}\,\mathrm{d}t\,\mathrm{d}\phi + \Sigma\left(\frac{\mathrm{d}r^2}{\Delta} + \mathrm{d}\theta^2\right) \\ &+ \left(r^2 + a^2 + \frac{2Mra^2\sin^2(\theta)}{\Sigma}\right)\sin^2(\theta)\,\mathrm{d}\phi^2 \,, \end{aligned} \tag{3.49}$$

where

$$\Delta = r^2 - 2Mr + a^2 \quad \text{and} \quad \Sigma = r^2 + a^2\cos^2(\theta)\,, \tag{3.50}$$

and M represents the mass of the black hole and a represents the black hole's specific angular momentum, closesly related to its angular momentum $J = aM$. We also introduce $\chi = a/M$ as the dimensionless spin parameter. Note that the parameters M and a of the Kerr metric together uniquely identify a solution. We confirm that this metric has indeed two Killing vectors, given by ∂_t and ∂_ϕ, since all components of the metric above are independent of these coordinates.

Time reversal (changing t to $-t$) changes the direction of rotation of the black hole which reverses its angular momentum and modifies the cross-term $\mathrm{d}t\,\mathrm{d}\phi$ in the metric. Therefore although the Kerr solution is stationary it is not static, in contrast to the Schwarzschild solution. The cross-term can be interpreted as the black hole dragging the exterior spacetime along in the direction of rotation. This effect is called frame dragging and affects objects near a Kerr black hole.

There is a physical singularity in this metric at $\Sigma = 0$ since there are curvature invariants that diverge at those points. For non-zero values of a, this condition describes a ring of points and is called the ring singularity of a Kerr black hole.

In these coordinates, event horizons occur at the values of r where $\Delta = 0$ and the $\mathrm{d}r^2$ component of the metric diverges

$$\Delta = r^2 - 2Mr + a^2 = 0\,, \tag{3.51}$$

which occurs for

$$r_\pm = M \pm \sqrt{M^2 - a^2}\,, \tag{3.52}$$

where $r = r_-$ sets an inner horizon and $r = r_+$ the event horizon to the exterior. When $|a|$ exceeds M, the roots $r_\pm$ become complex and the singularity at $\Sigma = 0$ is not hidden by a horizon, violating Penrose's cosmic censorship principle [13].

Since the Kerr metric is not static and only stationary, the event horizons found at $r = r_\pm$ are not Killing horizons for the asymptotic timelike Killing vector. The norm of this vector ∂_t is given by the tt-component of the inverse metric

$$g^{tt} = -\frac{1}{\Sigma}(\Delta - a^2 \sin^2(\theta))\,, \tag{3.53}$$

which vanishes on the surface where

$$\Delta - a^2 \sin^2(\theta) = 0 \tag{3.54}$$

called the ergosphere. Inside of this surface the Killing vector becomes spacelike. The ergosphere is exterior to the event horizon found at $r = r_+$ where $\Delta = 0$, and coincides with it when $\theta = 0$ or π (precisely at the north and south pole). The region between these two surfaces is called the ergoregion. Inside of it everything has to move along the direction of the rotation of the black hole; there can be no stationary observer. However, the ergosphere is not an event horizon and it is possible for light and matter to cross the ergosphere in both directions. As viewed by an asymptotic observer, since the Killing vector becomes spacelike, energy acts more like a momentum component and can become locally negative while remaining globally positive. This makes it possible to extract energy from a Kerr black hole through, e.g., the Penrose process [68] or superradiance [69].

The Kerr metric has, maybe unexpectedly, some exceptional properties that we will touch upon in the following discussion. It is possible to find two orthogonal preferential null directions (l^μ and n^μ) to build the Newman-Penrose frame. These will be the degenerate principal null directions of the Weyl tensor and we can complete the frame form the Kinnersley tetrad [64]:

$$l^\mu = \frac{1}{\Delta}\left(r^2 + a^2, \Delta, 0, a\right), \qquad m^\mu = \frac{1}{\sqrt{2}\zeta^*}\left(ia\sin(\theta), 0, 1, \frac{i}{\sin(\theta)}\right),$$

$$n^\mu = \frac{1}{2\Sigma}\left(r^2 + a^2, -\Delta, 0, a\right), \quad \bar{m}^\mu = \frac{1}{\sqrt{2}\zeta}\left(-ia\sin(\theta), 0, 1, \frac{-i}{\sin(\theta)}\right), \quad (3.55)$$

where we introduce a scaling factor

$$\zeta = r - ia\cos(\theta)\,. \quad (3.56)$$

As a consequence of the tetrad choice and the nature of the Kerr spacetime, which we will discuss in more detail, the following spin coefficients vanish:

$$\kappa = \kappa' = \sigma = \sigma' = 0\,. \quad (3.57)$$

The other associated spin coefficients are given by:

$$\rho = -\frac{1}{\zeta}, \qquad \rho' = \frac{\Delta}{2\zeta^2\bar{\zeta}}, \qquad \beta = \frac{\cot\theta}{2\sqrt{2}\bar{\zeta}}, \quad \beta' = \frac{\cot\theta}{2\sqrt{2}\zeta} - \frac{ia\sin\theta}{\sqrt{2}\zeta^2},$$

$$\tau = -\frac{ia\sin\theta}{\sqrt{2}\zeta\bar{\zeta}}, \quad \tau' = -\frac{ia\sin\theta}{\sqrt{2}\zeta^2}, \quad \epsilon = 0, \qquad \epsilon' = \frac{\Delta}{2\zeta^2\bar{\zeta}} - \frac{r-M}{2\zeta\bar{\zeta}}. \quad (3.58)$$

Since spin coefficients $\kappa, \kappa', \sigma, \sigma'$ are zero, the Goldberg-Sachs theorem [70] allows us to conclude that the Kerr spacetime is classified as Petrov type D. This implies that in the chosen basis all except one of Weyl scalars vanish:

$$\Psi_0 = \Psi_1 = \Psi_3 = \Psi_4 = 0\,. \quad (3.59)$$

The only non-vanishing Weyl scalar is Ψ_2 which can be found by contracting the Riemann tensor with the tetrads according to its definition, which yields

$$\Psi_2 = -\frac{M}{\zeta^3}\,. \quad (3.60)$$

The null frame, spin coefficients and Weyl scalars provide a complete description in the NP formalism of the Kerr metric, which is of Petrov type D. Finding that all Weyl scalars except Ψ_2 vanish and that specific spin coefficients are equal to zero illustrates the special nature of this spacetime and makes the NP formalism very well-suited to describe the physics of Kerr black holes.

3.3 Teukolsky equation

The aim is now to analyse the linear perturbations of the Kerr black hole by applying the GHP formalism. This derivation can for example be found in [64]. The property that the Kerr metric is a Petrov type D spacetime and a frame aligned along the principal null directions of this spacetime ensures that all Weyl curvature components except for Ψ_2 vanish. Similarly, the spin coefficients $\kappa = \sigma = \kappa' = \sigma' = 0$ and, in vacuum, all ϕ_{ij} from the Ricci tensor vanish.

From the definition of the Riemann tensor in tetrad notation written in (3.18) (see Appendix B.1 for details) the non-vanishing equations are

$$\text{Þ}\rho = \rho^2\,, \qquad \eth\tau = \tau^2\,, \qquad \text{Þ}\tau = (\tau - \tau'^*)\rho\,, \qquad \eth\rho = (\rho - \rho^*)\tau\,,$$

$$\Psi_2 = -\text{Þ}'\rho + \eth'\tau + \rho\rho'^* - |\tau|^2\,, \tag{3.61}$$

The Bianchi identity reduces to

$$\text{Þ}\Psi_2 = 3\rho\Psi_2\,, \quad \eth\Psi_2 = 3\tau\Psi_2\,, \tag{3.62}$$

where this includes the primed and conjugate versions of these equations.

The final ingredient is the commutation relations of the GHP derivatives acting on an object with weights $\{p, q\}$ from Section 3.1.2 given by

$$\left[\text{Þ}, \text{Þ}'\right] = (\tau^* - \tau')\eth + (\tau - \tau'^*)\eth' - p(\Psi_2 - \tau\tau') - q(\Psi_2^* - \tau^*\tau'^*)\,, \tag{3.63}$$

$$[\text{Þ}, \eth] = \rho^*\eth - \tau'^*\text{Þ} + q\rho^*\tau'^*\,, \tag{3.64}$$

$$\left[\eth, \eth'\right] = (\rho'^* - \rho')\text{Þ} + (\rho - \rho^*)\text{Þ}' + p(\rho\rho' + \Psi_2) - q(\rho^*\rho'^* + \Psi_2^*)\,. \tag{3.65}$$

Consider perturbations of order ϵ around such a background[1] and let

$$\Psi_i = \bar{\Psi}_i + \epsilon\delta\Psi_i\,, \quad \gamma_{\mathbf{abc}} = \bar{\gamma}_{\mathbf{abc}} + \epsilon\delta\gamma_{\mathbf{abc}}\,. \tag{3.66}$$

On account of the vacuum Petrov type D assumption for the unperturbed case

$$\phi_{00} = \phi_{01} = \phi_{02} = \phi_{21} = \phi_{11} = \phi_{22} = R = 0\,, \tag{3.67}$$

$$\bar{\Psi}_0 = \bar{\Psi}_1 = \bar{\Psi}_3 = \bar{\Psi}_4 = 0 \quad \text{and} \quad \bar{\kappa} = \bar{\kappa}' = \bar{\sigma} = \bar{\sigma}' = 0 \tag{3.68}$$

We remark that the GHP derivatives will also be perturbed but only their leading order will play a role so we do not burden our notation even further by indicating this explicitly.

[1] This perturbation parameter ϵ should not be confused with the NP ϵ defined previously. Here, the latter will only appear implicitly in the GHP-derivatives.

Consider Þ acting on (3.47). The first contribution, at order ϵ, is given by

$$Þ Þ' \delta\Psi_0 - Þ ð \delta\Psi_1 = Þ\left(\bar{\rho}' \delta\Psi_0\right) - 4Þ\left(\bar{\tau} \delta\Psi_1\right) + 3Þ\left(\delta\sigma \bar{\Psi}_2\right) . \tag{3.69}$$

Similarly, acting with ð on (3.45) yields

$$ð Þ \delta\Psi_1 - ð ð' \delta\Psi_0 = -ð\left(\bar{\tau}' \delta\Psi_0\right) + 4ð\left(\bar{\rho} \delta\Psi_1\right) - 3ð\left(\delta\kappa \bar{\Psi}_2\right) . \tag{3.70}$$

Now commute Þ and ð in (3.69). To leading order with (3.63) we find

$$Þ Þ' \delta\Psi_0 - ð Þ \delta\Psi_1 - \left(\bar{\rho}^* ð - \bar{\tau}'^* Þ\right) \delta\Psi_1 = Þ\left(\bar{\rho}' \delta\Psi_0\right) - 4Þ\left(\bar{\tau} \delta\Psi_1\right) + 3Þ\left(\delta\sigma \bar{\Psi}_2\right) . \tag{3.71}$$

In (3.70) we can replace $ð\Psi_1$ by using (3.47). At the same time, within (3.71) we can replace $Þ\Psi_1$ by using (3.45) and also replace the additional $ð\Psi_1$ term from the commutation relation. We find respectively

$$\begin{aligned} ð Þ \delta\Psi_1 - ð ð' \delta\Psi_0 &= -ð\left(\bar{\tau}' \delta\Psi_0\right) + 4\delta\Psi_1 ð\bar{\rho} \\ &+ 4\bar{\rho}\left(Þ' \delta\Psi_0 - \bar{\rho}' \delta\Psi_0 + 4\bar{\tau}\delta\Psi_1 - 3\delta\sigma\Psi_2\right) - 3ð\left(\delta\kappa\bar{\Psi}_2\right) , \end{aligned} \tag{3.72}$$

$$\begin{aligned} Þ Þ' \delta\Psi_0 - ð Þ \delta\Psi_1 - \bar{\rho}^* \left(Þ' \delta\Psi_0 - \bar{\rho}' \delta\Psi_0 + 4\bar{\tau}\delta\Psi_1 - 3\delta\sigma\bar{\Psi}_2\right) &= Þ\left(\bar{\rho}' \delta\Psi_0\right) - 4\delta\Psi_1 Þ\bar{\tau} \\ - \left(4\bar{\tau} + \bar{\tau}'^*\right)\left(ð' \delta\Psi_0 - \bar{\tau}' \delta\Psi_0 + 4\bar{\rho}\delta\Psi_1 - 3\delta\kappa\bar{\Psi}_2\right) + 3Þ\left(\delta\sigma\bar{\Psi}_2\right) . \end{aligned} \tag{3.73}$$

To simplify this, we use (3.62) to replace $ð\bar{\Psi}_2$ with $3\bar{\tau}\bar{\Psi}_2$, and $Þ\bar{\Psi}_2$ with $3\bar{\rho}\bar{\Psi}_2$. We make use of (3.61) to replace $Þ\bar{\tau}$ with $(\bar{\tau} - \bar{\tau}'^*)\bar{\rho}$ and $ð\bar{\rho}$ with $(\bar{\rho} - \bar{\rho}^*)\bar{\tau}$. Then, with the following relation from the Riemann tensor (3.18) (see also B.1), we relate $ð\delta\kappa$ with $Þ\delta\sigma$ using $\delta\Psi_0$

$$ð\delta\kappa = -\delta\Psi_0 + Þ\delta\sigma - (\bar{\rho} + \bar{\rho}^*)\delta\sigma + (\bar{\tau} + \bar{\tau}'^*)\delta\kappa . \tag{3.74}$$

After some extra rewriting, the results are

$$\begin{aligned} \left(ð Þ + 4\bar{\rho}^*\bar{\tau} - 20\bar{\rho}\bar{\tau}\right)\delta\Psi_1 + 3\left(Þ - \bar{\rho}^* + 3\bar{\rho}\right)\bar{\Psi}_2\delta\sigma + 3(4\bar{\tau} + \bar{\tau}'^*)\bar{\Psi}_2\delta\kappa = \\ \left(ð ð' - ð\bar{\tau}' - \bar{\tau}' ð + 4\bar{\rho}\left(Þ' - \bar{\rho}'\right) + 3\bar{\Psi}_2\right)\delta\Psi_0 , \end{aligned} \tag{3.75}$$

$$\begin{aligned} \left(ð Þ + 4\bar{\rho}^*\bar{\tau} - 20\bar{\rho}\bar{\tau}\right)\delta\Psi_1 + 3\left(Þ - \bar{\rho}^* + 3\bar{\rho}\right)\bar{\Psi}_2\delta\sigma + 3\left(4\bar{\tau} + \bar{\tau}'^*\right)\bar{\Psi}_2\delta\kappa = \\ \left(Þ Þ' - \bar{\rho}^*\left(Þ' - \bar{\rho}'\right) - Þ\bar{\rho}' - \bar{\rho}' Þ + \left(4\bar{\tau} + \bar{\tau}'^*\right)\left(ð' - \bar{\tau}'\right)\right)\delta\Psi_0 . \end{aligned} \tag{3.76}$$

The difference between these equations has only $\delta\Psi_0$ as a perturbed quantity.

We have found the Teukolsky equation for $\delta\Psi_0$

$$-\left[\left(Þ - 4\bar{\rho} - \bar{\rho}^*\right)\left(Þ' - \bar{\rho}'\right) - \left(ð - 4\bar{\tau} - \bar{\tau}'^*\right)\left(ð' - \bar{\tau}'\right) - 3\bar{\Psi}_2\right]\delta\Psi_0 = 0 , \tag{3.77}$$

and the equation for Ψ_4 can be found by application of the prime transformation

$$-\left[\left(Þ' - 4\bar{\rho}' - \bar{\rho}'^*\right)\left(Þ - \bar{\rho}\right) - \left(ð' - 4\bar{\tau}' - \bar{\tau}^*\right)\left(ð - \bar{\tau}\right) - 3\bar{\Psi}_2\right]\delta\Psi_4 = 0 . \tag{3.78}$$

These equations (3.77) and (3.78) provide master equations that fully describe the first-order dynamics on the background of a Kerr black hole in terms of a single partial differential equation as first derived by Teukolsky in 1972 [36]. Linear perturbations are either gravitational waves encoded by $\delta\Psi_0$ and $\delta\Psi_4$, or changes to the mass and spin of the black hole, or coordinate transformations, which can be non-trivial due to the presence of the asymptotic symmetry group.

If we express these equations back in Boyer-Lindquist coordinates (t, r, θ, ϕ), the Teukolsky master equation is given by

$$\left[\frac{(r^2+a^2)^2}{\Delta} - a^2\sin^2\theta\right]\frac{\partial^2\psi}{\partial t^2} + \frac{4Mar}{\Delta}\frac{\partial^2\psi}{\partial t\partial\phi} + \left[\frac{a^2}{\Delta} - \frac{1}{\sin^2\theta}\right]\frac{\partial^2\psi}{\partial\phi^2}$$
$$- \Delta^{-s}\frac{\partial}{\partial r}\left(\Delta^{s+1}\frac{\partial\psi}{\partial r}\right) - \frac{1}{\sin\theta}\frac{\partial}{\partial\theta}\left(\sin\theta\frac{\partial\psi}{\partial\theta}\right) - 2s\left[\frac{a(r-M)}{\Delta} + \frac{i\cos\theta}{\sin^2\theta}\right]\frac{\partial\psi}{\partial\phi}$$
$$- 2s\left[\frac{M(r^2-a^2)}{\Delta} - r - ia\cos\theta\right]\frac{\partial\psi}{\partial t} + (s^2\cot^2\theta - s)\psi = 0\,, \tag{3.79}$$

where either $\psi = \delta\Psi_0$ when $s = 2$, or $\psi = \zeta^4\delta\Psi 4$ when $s = -2$.

The Teukolsky master equation is separable and a solution can be written as

$$\psi(t, r, \theta, \phi) = \frac{1}{2\pi}\int \mathrm{d}\omega \sum_{l,m} R^s_{lm\omega}(r)\, S^s_{lm\omega}(\cos\theta)\, e^{im\phi}\, e^{-i\omega t} \tag{3.80}$$

The spin-weighted spheroidal harmonics $S_{lm\omega}(\cos(\theta))$ satisfy

$$\frac{\mathrm{d}}{\mathrm{d}x}\left[(1-x^2)\frac{\mathrm{d}S_s}{\mathrm{d}x}\right] + \left[(a\omega)^2x^2 - 2sa\omega x + B_{lm} - \frac{(m+sx)^2}{1-x^2}\right]S_s = 0\,, \tag{3.81}$$

where $x = \cos(\theta)$ and B_{lm} is the angular separation constant.

The radial function $R_{lm\omega}(r)$ satisfies the radial Teukolsky equation:

$$\Delta^{-s}\frac{\mathrm{d}}{\mathrm{d}r}\left[\Delta^{s+1}\frac{\mathrm{d}R_s}{\mathrm{d}r}\right] + \left[\frac{K^2 - 2si(r-M)K}{\Delta} + 4si\omega r - \lambda\right]R_s = 0 \tag{3.82}$$

where the terms in the potential are

$$K = (r^2+a^2)\omega - am\,, \tag{3.83}$$

$$\lambda = B_{lm} + s + a^2\omega^2 - 2am\omega\,. \tag{3.84}$$

Together with the right boundary conditions these equations can be solved simultaneously to find the quasinormal mode spectrum of Kerr black holes.

3.3.1 Continued fractions for the Teukolsky equation

We present Leaver's method to compute the frequencies and the separation constant for a Kerr spacetime. The first step to find a continued fraction expansion is to assume an ansatz for the wavefunctions. Let us start from the radial equation, where we make the following ansatz [71]

$$R(r) = f^{-i\sigma-s}\,(r-r_-)^{p-1-2s}\,e^{qr}\sum_{n=0}^{N} R_n f^n\,, \tag{3.85}$$

where $r_\pm$ are the zeros of Δ,

$$f = \frac{r-r_+}{r-r_-}\,, \tag{3.86}$$

and we have defined $p = q = i\omega$ and

$$\sigma = \sigma_{\rm GR} \equiv \frac{r_+(\omega-\omega_c)}{r_+-r_-}\,, \qquad \omega_c = \frac{am}{r_+}\,, \tag{3.87}$$

$$r_\pm = \frac{1}{2}(1\pm\beta)\,, \qquad \beta = \sqrt{1-4a^2}\,. \tag{3.88}$$

With these definitions, the equation (3.82) takes the form

$$\sum_{n=0}^{N} R_n\left(\frac{\alpha^r_{n-1}}{f}+\beta^r_n+\gamma^r_{n+1}f\right)f^n = 0\,, \tag{3.89}$$

where the coefficients are

$$\alpha^r_n = (n+1)\,(n+1-s-2i\sigma)\,, \tag{3.90}$$

$$\begin{aligned}\beta^r_n =& 2n(2i\sigma+p+q\beta-1)-2n^2-1-s-B_{\ell m}\\ &+q\left(a^2q+\beta+s\right)-2i\sigma(p+\beta q+i\omega-1)\\ &-p(\beta q+q+s-1)\,,\end{aligned} \tag{3.91}$$

$$\gamma^r_n = (n-p-i\omega)\,(n+s-p-2i\sigma+i\omega)\,. \tag{3.92}$$

The equation is satisfied when each term proportional to a power of f vanishes

$$\beta^r_0 R_0 + \alpha^r_0 R_1 = 0\,, \tag{3.93}$$

$$\gamma^r_n R_{n-1} + \beta^r_n R_n + \alpha^r_n R_{n+1} = 0 \quad \text{for } n \geq 1\,. \tag{3.94}$$

The path for the angular equation is similar. We define an ansatz for $S(x)$ such that it is finite at the regular singular points $x = \pm 1$ [71]

$$S(x) = (1+x)^{k_1}\,(1-x)^{k_2}\,e^{a\omega x}\sum_{n=0}^{N} S_n (1+x)^n\,, \tag{3.95}$$

where $k_1 = |m-s|/2$ and $k_2 = |m+s|/2$. We can obtain a similar recurrence relation by inserting this ansatz into equation (3.81), which, with an analogous reshuffling, reads

$$\beta_0^\theta S_0 + \alpha_0^\theta S_1 = 0\,, \tag{3.96}$$

$$\gamma_n^\theta S_{n-1} + \beta_n^\theta S_n + \alpha_n^\theta S_{n+1} = 0 \quad \text{for } n \geq 1\,, \tag{3.97}$$

where the coefficients are

$$\alpha_n^\theta = -2(n+1)\,(n+1+2k_1)\,, \tag{3.98}$$

$$\begin{aligned}\beta_n^\theta =& \, n(n-1) + 2n(k_1+k_2+1-2a\omega) \\ & - 2a\omega(2k_1+s+1) + (k_1+k_2)(k_1+k_2+1) \\ & - a^2\omega^2 - s(s+1) - B_{\ell m}\,,\end{aligned} \tag{3.99}$$

$$\gamma_n^\theta = 2a\omega(n+k_1+k_2+s)\,. \tag{3.100}$$

To invert the relation we can define the ladder operators which have the following property $R_{n+1} = -\Lambda_n^r R_n$ and $S_{n+1} = -\Lambda_n^\theta S_n$ as (the superscripts r and θ are omitted for clarity)

$$\Lambda_n = \frac{\gamma_{n+1}}{\beta_{n+1} - \alpha_{n+1}\Lambda_{n+1}}\,. \tag{3.101}$$

By initializing Λ_N according to the Nollert expansion (explained in detail in Appendix B.2), the equations one needs to solve simultaneously to obtain the eigenfrequency ω and the separation constant $B_{\ell m}$ are

$$\mathcal{L}_r = \Lambda_1^r \alpha_0^r - \beta_0^r = 0\,, \tag{3.102}$$

$$\mathcal{L}_\theta = \Lambda_1^\theta \alpha_0^\theta - \beta_0^\theta = 0\,, \tag{3.103}$$

which are nothing but (3.93) and (3.96).

Chapter 4

Corrections from Higher-derivative gravity

Fundamental gravity theory and general effective-field-theory (EFT) arguments suggest that general relativity (GR) is modified by higher-derivative terms in the action. As it turns out, the Kerr geometry is typically not a solution of modified or 'corrected' gravity theories. This may give rise to deviations from GR predictions that might be observable. Since higher-derivative terms modify gravity at short distances, the most sensitive probes are those that involve physics in the near-horizon region of a black hole. In particular we study the ringdown signal, determined by the black hole's quasinormal modes (QNMs).

We consider a general effective-field-theory (EFT) extension of general relativity, without introducing extra degrees of freedom. The action we obtain represents the most general diffeomorphism-invariant purely metric deformation of GR and is thus of phenomenological interest. The aim of this chapter is to compute the QNM frequencies of slowly-rotating black holes in this class of theories.

In this chapter, which is based on [72][1], we start in Section 4.1 by reviewing the EFT under consideration and the slowly rotating black holes in this theory. We analyse gravitational perturbations of these slowly rotating black holes in Section 4.2, first describing our general approach and then applying this to derive master equations for respectively the parity-preserving corrections and the parity-violating corrections. We then proceed to use these master equations to compute quasinormal mode frequencies in 4.3 and end with conclusions.

[1] Written with P. A. Cano, K. Fransen and T. Hertog.

The corrections to the QNM frequencies of non-rotating black holes have been obtained in a number of theories, including dynamical Chern-Simons gravity [48, 49], Einstein-dilaton-Gauss-Bonnet gravity [46, 47], and theories with quartic [50, 51] and cubic [52] curvature terms, among other models [53–55, 73]. In addition, theory-independent approaches were studied in [51, 56, 57], whilst eikonal QNMs beyond GR were investigated in [74–76].

The calculation of QNMs of astrophysically more relevant, rotating black holes is much more involved. Only recently, some progress has been made. In the case of a test scalar field, ref. [77] gave a way of dealing with the non-separability of the wave equation, and obtained the QNMs for rotating black holes in a large class of higher-derivative theories were computed.[2] However, when it comes to gravitational perturbations the situation is more precarious, given the difficulty to perform fully-fledged perturbation theory for rotating black holes in modified gravity theories. Nevertheless, this problem can be alleviated by assuming that the spin is small [78, 79]. Working at linear order in the spin, the QNM frequencies of slowly-rotating black holes in Einstein-dilaton-Gauss-Bonnet gravity were recently obtained in [80], and an analogous analysis for dynamical Chern-Simons theory was done in [81, 82].

Taking an EFT viewpoint, we assume that the effect of the beyond-GR corrections is small and work perturbatively in the higher-order couplings. Still, given that a length scale $\ell \geq 1$ km is required for modifications of gravity to be detectable through gravitational waves generated in processes involving astrophysical black holes, one may wonder what are the experimental bounds on the couplings in the theory. In the weak-field limit, the leading correction to the Newtonian potential is $\sim \ell^4 M^3/r^7$. This means that the relative correction Δ compared to GR predictions is $\Delta \sim \ell^4 M^2/r^6$. If, say, $\ell \sim 10$ km, then $\Delta_\odot \sim 10^{-31}$ and $\Delta_\oplus \sim 10^{-30}$ at the surfaces of the sun and the earth, respectively. Hence the corrections we consider have a completely negligible effect on solar system physics. On the other hand, for a black hole of 10 solar masses $\Delta_{\rm BH} \sim 10^{-2} - 10^{-3}$, large enough to induce effects that are potentially observable through gravitational-wave observations.

[2] Another strategy consists in performing a general theory-independent parametrisation of the departure from the GR prediction, as in ref. [60], but this requires the introduction of a large number of parameters.

4.1 The EFT of gravity and its black holes

We consider a general EFT extension of GR, that includes only the metric and no extra fields. To eight derivatives one can expand the action as

$$S = \frac{1}{16\pi G}\int \mathrm{d}^4x\,\sqrt{|g|}\left(R + \ell^4\mathcal{L}_{(6)} + \ell^6\mathcal{L}_{(8)} + \ldots\right)\,, \tag{4.1}$$

where ℓ is a length scale and where $\mathcal{L}_{(n)}$ denotes a Lagrangian density with n derivatives of the metric. Note that the leading corrections appear at the six-derivative level, since all four-derivative theories have the same vacuum solutions as GR, and hence can be ignored from the EFT viewpoint we adopt. In order to derive the most general form of the Lagrangians $\mathcal{L}_{(6)}$ and $\mathcal{L}_{(8)}$, one has to take into account that terms with explicit Ricci curvature are either trivial - in the sense that they do not affect the vacuum solutions of GR - or that they can be removed via a redefinition of the metric, and hence neglected. Therefore, one is left with a set of pure Riemann invariants, where the number of independent operators can be further reduced using a diverse set of identities.[3] The resulting six-derivative Lagrangian contains two cubic invariants, one preserving and the other breaking parity,

$$\mathcal{L}_{(6)} = \lambda_{\rm ev} R_{\mu\nu}{}^{\rho\sigma} R_{\rho\sigma}{}^{\delta\gamma} R_{\delta\gamma}{}^{\mu\nu} + \lambda_{\rm odd} R_{\mu\nu}{}^{\rho\sigma} R_{\rho\sigma}{}^{\delta\gamma} \tilde{R}_{\delta\gamma}{}^{\mu\nu}\,, \tag{4.2}$$

where

$$\tilde{R}^{\mu\nu\rho\sigma} = \frac{1}{2}\epsilon^{\mu\nu\alpha\beta} R_{\alpha\beta}{}^{\rho\sigma}\,. \tag{4.3}$$

On the other hand, the eight-derivative Lagrangian can be expressed as the sum of three quartic Riemann operators,

$$\mathcal{L}_{(8)} = \epsilon_1 \mathcal{C}^2 + \epsilon_2 \tilde{\mathcal{C}}^2 + \epsilon_3 \mathcal{C}\tilde{\mathcal{C}}\,, \tag{4.4}$$

where

$$\mathcal{C} = R_{\mu\nu\rho\sigma} R^{\mu\nu\rho\sigma}\,, \quad \tilde{\mathcal{C}} = R_{\mu\nu\rho\sigma}\tilde{R}^{\mu\nu\rho\sigma}\,. \tag{4.5}$$

In this case, the ϵ_1 and ϵ_2 interactions preserve parity, whilst ϵ_3 violates parity. The ϵ_2 term vanishes for spherically symmetric configurations, as it is the square of an odd-parity term. The corrections to GR are controlled by only five dimensionless couplings ($\lambda_{\rm ev,odd}$ and $\epsilon_{1,2,3}$) and the overall length scale ℓ, which can be absorbed in these couplings making them dimensionful.

[3] See [45, 83] for a more complete discussion on the construction of this effective theory.

The Einstein field equations of the theory (4.1) are given by

$$\mathcal{E}_{\mu\nu} = G_{\mu\nu} + \ell^4 \mathcal{E}^{(6)}_{\mu\nu} + \ell^6 \mathcal{E}^{(8)}_{\mu\nu} = 0\,, \tag{4.6}$$

where

$$\mathcal{E}^{(n)}_{\mu\nu} = P^{(n)}_{(\mu\ \ \rho\sigma\gamma} R_{\nu)\rho\sigma\gamma} - \frac{1}{2} g_{\mu\nu} \mathcal{L}_{(n)} + 2\nabla^\sigma \nabla^\rho P^{(n)}_{(\mu|\sigma|\nu)\rho}\,, \tag{4.7}$$

and in each case the tensor $P^{(n)}_{\mu\nu\rho\sigma}$ is given by

$$\begin{aligned} P^{(6)}_{\mu\nu\rho\sigma} &= 3\lambda_{\rm ev} R_{\mu\rho}{}^{\alpha\beta} R_{\alpha\beta\rho\sigma} \\ &\quad + \frac{3\lambda_{\rm odd}}{2} \left(R_{\mu\rho}{}^{\alpha\beta} \tilde{R}_{\alpha\beta\rho\sigma} + R_{\mu\rho}{}^{\alpha\beta} \tilde{R}_{\rho\sigma\alpha\beta} \right)\,, \end{aligned} \tag{4.8}$$

$$\begin{aligned} P^{(8)}_{\mu\nu\rho\sigma} &= 4\epsilon_1 \mathcal{C} R_{\mu\nu\rho\sigma} + 2\epsilon_2 \tilde{\mathcal{C}} \left(\tilde{R}_{\mu\nu\rho\sigma} + \tilde{R}_{\rho\sigma\mu\nu} \right) \\ &\quad + \epsilon_3 \left[2\tilde{\mathcal{C}} R_{\mu\nu\rho\sigma} + \mathcal{C} \left(\tilde{R}_{\mu\nu\rho\sigma} + \tilde{R}_{\rho\sigma\mu\nu} \right) \right]\,. \end{aligned} \tag{4.9}$$

The (slowly-)rotating black-hole solutions of these theories have been studied in refs. [45, 50] at different orders in the spin expansion, but here we only work at first order in the spin, in which case the metric takes a relatively simple form

$$\mathrm{d}s^2 = -N^2 f\, \mathrm{d}t^2 + \frac{\mathrm{d}r^2}{f} - 2ah \sin^2\theta\, \mathrm{d}t\, \mathrm{d}\phi + r^2 (\mathrm{d}\theta^2 + \sin^2\theta\, \mathrm{d}\phi^2)\,. \tag{4.10}$$

Working perturbatively in the higher-order couplings and in the spin $a = M\chi$, we present here only a symbolic representation of the functions N, f and h, with the full expression provided Appendix C.1.

$$\begin{aligned} f &= 1 - \frac{2M}{r} + \lambda_{\rm ev} \ell^4 \delta f_{\rm ev} + \lambda_{\rm odd} \chi \ell^4 \delta f_{\rm odd} + \epsilon_1 \ell^6 \delta f_1 + \epsilon_3 \ell^6 \chi \delta f_3 + \mathcal{O}\left(\ell^8, \chi^2\right)\,, \\ N &= 1 + \lambda_{\rm ev} \ell^4 \delta N_{\rm ev} + \lambda_{\rm odd} \chi \ell^4 \delta N_{\rm odd} + \epsilon_1 \ell^6 \delta N_1 + \epsilon_3 \ell^6 \chi \delta N_3 + \mathcal{O}\left(\ell^8, \chi^2\right)\,, \\ h &= 1 + \lambda_{\rm ev} \ell^4 \delta h_{\rm ev} + \epsilon_1 \ell^6 \delta h_1 + \epsilon_2 \ell^6 \delta h_2 + \mathcal{O}\left(\ell^8, \chi^2\right)\,. \end{aligned} \tag{4.11}$$

Importantly, due to these corrections, the position of the horizon is modified. It corresponds to the largest root of f, which yields

$$r_+ = 2M - \frac{5\lambda_{\rm ev}\ell^4}{8M^3} - \frac{5\epsilon_1 \ell^6}{4M^5} + \mathcal{O}(\ell^8, \chi^2)\,. \tag{4.12}$$

Here M represents the mass, whilst the total angular momentum is $J = \chi M^2$. Other properties of these black-hole geometries were studied in Refs [45, 50].

4.2 Perturbations of slowly-rotating black holes

Let us now consider a perturbation $g_{\mu\nu} = g^{\rm BH}_{\mu\nu} + h_{\mu\nu}$ over the black-hole metric. The aim of this section is to simplify the corresponding linearised equations into a reduced set of equations for some master variables.

We have discussed in chapter 2 how to calculate metric perturbations on a spherically-symmetric background by changing to the Regge-Wheeler gauge, separating the axial and polar metric perturbations and reducing the equations to a master equation for each type of metric perturbation.

The higher-derivative corrections do not change this fact and we can always work in the Regge-Wheeler gauge. Evaluating the linearised equations of motion projected onto spherical harmonics yields a system of equations for the variables. These equations can be simplified to yield two equations for two master variables, which are coupled if there are parity-breaking corrections — see [50] for the case of the quartic theories and [52] for the parity-preserving cubic one.

In the presence of rotation, the tensor harmonics $h^{lm}_{(\pm)\mu\nu}$ are not eigenfunctions of the linearised Einstein equations anymore, but one can always expand the metric perturbation using these functions since they always form a full basis. We can therefore write

$$h_{\mu\nu} = \sum_{l,m} h^{lm}_{(+)\mu\nu} + \sum_{l,m} h^{lm}_{(-)\mu\nu}\,. \tag{4.13}$$

Now, in the case of a slowly-rotating black hole, at linear order in the spin, one can see that the quasinormal modes will necessarily have the following structure

$$h_{\mu\nu} = h^{lm}_{\mu\nu} + \chi h'_{\mu\nu} + \mathcal{O}(\chi^2)\,, \tag{4.14}$$

where $h'_{\mu\nu}$ contains the sum of modes with $l' \neq l$,

$$h'_{\mu\nu} = \sum_{l'\neq l} \left[h^{l'm}_{(+)\mu\nu} + h^{l'm}_{(-)\mu\nu} \right]\,. \tag{4.15}$$

In words, the perturbation is composed of a leading term corresponding to the result for the spherically-symmetric case, and the additional terms will be of order χ. At the same time, the linearised equations have the following structure,

$$\mathcal{E}_{\mu\nu} = \mathcal{E}^{(0)}_{\mu\nu} + \chi\, \mathcal{E}^{(1)}_{\mu\nu} + \mathcal{O}(\chi^2) = 0\,. \tag{4.16}$$

The tensor harmonics are eigenfunctions of $\mathcal{E}^{(0)}_{\mu\nu}$ but not of $\mathcal{E}^{(1)}_{\mu\nu}$. Each of these equations contains a contribution from Einstein's field equations as well as contributions from the higher-derivative terms.

When we evaluate the equations with the $h_{\mu\nu}$ defined in (4.14), we find

$$\mathcal{E}^{(0)}_{\mu\nu}(h^{lm}) + \chi\left[\mathcal{E}^{(1)}_{\mu\nu}(h^{lm}) + \mathcal{E}^{(0)}_{\mu\nu}(h')\right] + \mathcal{O}(\chi^2) = 0\,.$$

Then we can project this on the tensor harmonics with index l, and this projection deletes all the terms $\mathcal{E}^{(0)}_{\mu\nu}(h')$, since h' only contains modes with $l' \neq l$. Therefore, we obtain equations involving only h^{lm} and these can be written as

$$P_a = \int \mathrm{d}\Omega\, \bar{X}^{B,lm}\mathcal{E}_{aB}(h^{lm}) = 0\,, \tag{4.17}$$

$$P_2 = \int \mathrm{d}\Omega\, \bar{X}^{AB,lm}\mathcal{E}_{AB}(h^{lm}) = 0\,, \tag{4.18}$$

and

$$Q_{ab} = \int \mathrm{d}\Omega\, \bar{Y}^{lm}\mathcal{E}_{ab}(h^{lm}) = 0\,, \tag{4.19}$$

$$Q_a = \int \mathrm{d}\Omega\, \bar{Y}^{B,lm}\mathcal{E}_{aB}(h^{lm}) = 0\,, \tag{4.20}$$

$$Q_2 = \int \mathrm{d}\Omega\, \bar{Y}^{AB,lm}\mathcal{E}_{AB}(h^{lm}) = 0\,, \tag{4.21}$$

$$Q_3 = \int \mathrm{d}\Omega\, \bar{Y}^{lm}\Omega^{AB}\mathcal{E}_{AB}(h^{lm}) = 0\,. \tag{4.22}$$

This is the set of consistent equations from which we will find a master equations and subsequently the quasinormal mode frequencies.

In addition, we will make use of the Regge-Wheeler gauge, which can be applied to the slowly-rotating case as well. To show this, consider first a gauge transformation with parameter ξ_μ that would put the $h^{lm}_{\mu\nu}$ term in (4.14) in the Regge-Wheeler form had we set $\chi = 0$. However, in the presence of rotation, this transformation will fail to achieve the Regge-Wheeler gauge by $\mathcal{O}(\chi)$ terms:

$$h_{\mu\nu} + 2\nabla_{(\mu}\xi_{\nu)} = h^{lm,\mathrm{RW}}_{\mu\nu} + \chi h'_{\mu\nu} + \chi\delta h_{\mu\nu} + \mathcal{O}(\chi^2)\,. \tag{4.23}$$

However, $\delta h_{\mu\nu}$ can be decomposed into spherical harmonics, so that

$$h_{\mu\nu} + 2\nabla_{(\mu}\xi_{\nu)} = \left(h^{lm,\mathrm{RW}}_{\mu\nu} + \chi\delta h^{lm}_{\mu\nu}\right) + \chi\left(h'_{\mu\nu} + \delta h'_{\mu\nu}\right) + \mathcal{O}(\chi^2)\,. \tag{4.24}$$

Now, it is clear that a new gauge transformation of order χ can be made in order to put the term $\chi\delta h^{lm}_{\mu\nu}$ into the Regge-Wheeler gauge up to $\mathcal{O}(\chi^2)$ terms.

Likewise, $\mathcal{O}(\chi)$ transformations can be used to put all the terms in $h'_{\mu\nu}$ in the Regge-Wheeler form, although this will not be relevant for our calculations. Thus, we can reduce the number of variables by imposing this right away.

In order to make further progress, it is useful to make a distinction between the higher-derivative corrections that preserve parity and those that do not.

4.2.1 Parity-preserving corrections

For the parity-preserving corrections, the operator $\mathcal{E}^{(1)}_{\mu\nu}(h^{lm})$ does not mix between the perturbations $h^{lm}_{(+)}$ and $h^{lm}_{(-)}$, so we considered these separately.

Decoupled equations for odd perturbations

We start discussing the resolution of the odd-parity equations for parity-preserving corrections, which are simpler as they only involve two variables in the Regge-Wheeler gauge, h_0 and h_1. We have three equations[4] $P_t = P_r = P_2 = 0$, but there is a relation among them implied by the Bianchi identity of the gravitational tensor, and hence it is enough to keep only P_r and P_2, which are of first order in the case of Einstein gravity.

The aim is to solve these equations perturbatively in χ and in the higher-order couplings, that we denote collectively by λ, keeping all the terms of order $\lambda\chi$. To achieve this, we first solve the equations with $\lambda = 0$. This is easily done since in that case both equations are of first order and they give us h_0 as a function of h_1 and h'_1, as well as a second-order equation for h_1.

We then consider the equations with $\lambda \neq 0$, which contain higher derivatives of these variables. However, since we are only interested in the perturbative solution in λ, we can use the zeroth-order solution in all the terms proportional to λ, and this allows us to express those terms as functions of h_1 and h'_1 only. We can solve the equations $P_r = P_2 = 0$, to give a solution of the form

$$h_0 = a(r)h_1 + b(r)h'_1\,, \quad h''_1 + c(r)h_1 + d(r)h'_1 = 0\,, \tag{4.25}$$

for certain functions $a(r)$, $b(r)$, $c(r)$, $d(r)$. Finally, we can introduce a rescaled master variable

$$\Psi^- = \frac{A(r)r^2}{r - r_+}h_1\,, \tag{4.26}$$

where $A(r)$ is a factor that can be chosen so that Ψ^- satisfies a Schrödinger-type equation in terms of a preferred radial variable.

[4] The even-parity sector of the equations vanishes: $Q_{ab} = Q_a = Q_2 = Q_3 = 0$.

For instance, to facilitate numerical computations, we find it useful to write the master equation in terms of the "pseudo-tortoise coordinate" r_* defined as

$$r_* = r + 2M \log\left(\frac{r}{r_+} - 1\right) . \tag{4.27}$$

This has the property that $r_* \to -\infty$ at the event horizon. In the case of the Schwarzschild black hole, a Schrödinger-type equation for Ψ^- in terms of r_* is found for $A(r) = 1$. Thus, in order to take into account the effect of the spin and of the higher-derivative corrections, we must choose $A(r) = 1 + \delta A(r)$. With an appropriate choice of $\delta A(r)$, which is unique up to a constant term, we find the following equation for Ψ^-,

$$\frac{\mathrm{d}^2\Psi^-}{\mathrm{d}r_*^2} + \left(\omega^2 - V_{lm}^-\right)\Psi^- = 0 . \tag{4.28}$$

The potential V_{lm}^- has a GR part plus a specific contribution from each of the higher-derivative terms,

$$V_{lm}^- = V_{lm}^{-\mathrm{GR}} + \ell^4 \lambda_{\mathrm{ev}} V_{lm}^{-(\mathrm{ev})} + \ell^6 \left(\epsilon_1 V_{lm}^{-(1)} + \epsilon_2 V_{lm}^{-(2)}\right) , \tag{4.29}$$

At the same time, each of these contributions contains a term of zeroth order and another one of first order in the spin. For the GR part we have

$$\begin{aligned} V_{lm}^{-\mathrm{GR}} = &\left(1 - \frac{2M}{r}\right)\left(\frac{l(l+1)}{r^2} - \frac{6M}{r^3}\right) \\ &+ m\chi\left(\frac{4M^2\omega}{r^3} + \frac{24M^2(3r-7M)(r-2M)}{l(l+1)r^7\omega}\right) , \end{aligned} \tag{4.30}$$

which corresponds to the Regge-Wheeler potential [32] plus a spin correction. The expressions for the other potentials are shown in the appendix of [72].

Decoupled equations for even perturbations

The case of even perturbations is more intricate, as it involves four variables, H_0, H_1, H_2 and K, in the Regge-Wheeler gauge. The odd-parity sector of the equations is trivially satisfied, $P_a = P_2 = 0$. To solve the remaining equations we proceed iteratively, solving first the system with $\lambda = 0$, then substituting that result in the terms proportional to λ and solving the equations again.

When $\lambda = 0$, the equations $Q_2 = Q_{rr} = 0$ allow us to obtain H_1 and H_2 in terms of H_0, K and their derivatives. Then, working at first order in χ, the rest of the equations can be solved to obtain a relation of the form $H_0 = \tilde{a}(r)K + \tilde{b}(r)K'$, as well as a second-order differential equation for K. In this way, all the variables and their derivatives can be expressed as linear combinations of K and K'.

Now, coming back to $\lambda \neq 0$, since we are only interested in the linear corrections, we can substitute the zeroth-order solutions in the terms proportional to λ. By doing so, we rewrite all those terms as linear combinations of K and K'. Then we can solve the system of equations in an analogous way to the $\lambda = 0$ case. Thus, we get a master second-order equation for K and the rest of variables are linear combinations of K and K'. Finally, instead of working with K, it is customary to introduce the Zerilli function Ψ^+ as

$$\Psi^+ = \frac{2r\tilde{A}(r)}{l(l+1)}\left[K + \frac{2f}{\Lambda}\left(H_2 - rK'\right)\right], \tag{4.31}$$

where $\Lambda = (l-1)(l+2) + 6M/r$, and $\tilde{A}(r)$ is a normalisation factor. In the case of the Schwarzschild black hole in GR, this definition matches the original one by Zerilli when $\tilde{A}(r) = 1$. However, that factor has been introduced so that Ψ^+ satisfies a Schrödinger-type equation once rotation and higher-derivative corrections are taken into account, so that in general we will have $\tilde{A}(r) = 1 + \delta\tilde{A}(r)$. Again, by choosing $\delta\tilde{A}(r)$ suitably, where the choice is unique up to a constant term, we find that Ψ^+ satisfies the equation

$$\frac{\mathrm{d}^2\Psi^+}{\mathrm{d}r_*^2} + \left(\omega^2 - V_{lm}^+\right)\Psi^+ = 0\,, \tag{4.32}$$

where r_* is the pseudo-tortoise coordinate defined in (4.27) and V_{lm}^+ is the effective potential for even-parity perturbations. As before, the potential has contributions from the different terms in the gravitational action

$$V_{lm}^+ = V_{lm}^{+\mathrm{GR}} + \ell^4\lambda_{\mathrm{ev}}V_{lm}^{+(\mathrm{ev})} + \ell^6\left(\epsilon_1 V_{lm}^{+(1)} + \epsilon_2 V_{lm}^{+(2)}\right), \tag{4.33}$$

and for instance, the GR part reads

$$\begin{aligned} V_{lm}^{+\mathrm{GR}} = {} & \frac{1}{\Lambda^2}\left(1 - \frac{2M}{r}\right)\left[\mu^2\left(\frac{\mu+2}{r^2} + \frac{6M}{r^3}\right) + \frac{36M^2}{r^4}\left(\mu + \frac{2M}{r}\right)\right] \\ & + \frac{4mM^2\chi\omega}{(\mu+2)r^6\Lambda^3}\big(72(\mu+6)M^3 + 36\mu(\mu+8)M^2r \\ & + 6\mu^2(3\mu+16)Mr^2 + \mu^2\left(\mu^2+2\mu-12\right)r^3\big)\,, \end{aligned} \tag{4.34}$$

with $\mu = (l-1)(l+2)$. Note that for $\chi = 0$ this reduces to the well-known Zerilli potential for the Schwarzschild black hole [33, 84]. The expressions for the other contributions are given in the appendix of [72].

4.2.2 Parity-breaking corrections

The higher-derivative terms controlled by $\lambda_{\rm odd}$ and ϵ_3 violate parity, and hence their effect is somewhat different. Instead of modifying the equations of odd and even perturbations independently, there is a coupling between these modes. Proceeding along the same lines as in the previous subsection, we find the following coupled equations for the variables[5] $\Psi^{\pm}$:

$$\frac{\mathrm{d}^2\Psi^+}{\mathrm{d}r_*^2} + \left(\omega^2 - V_{lm}^{+\rm GR}\right)\Psi^+ = U_{lm}^+\Psi^- + W_{lm}^+\frac{\mathrm{d}\Psi^-}{\mathrm{d}r_*}\,, \tag{4.35}$$

$$\frac{\mathrm{d}\Psi^-}{\mathrm{d}r_*} + \left(\omega^2 - V_{lm}^{-\rm GR}\right)\Psi^- = U_{lm}^-\Psi^+ + W_{lm}^-\frac{\mathrm{d}\Psi^+}{\mathrm{d}r_*}\,. \tag{4.36}$$

Here $V_{lm}^{\pm\rm GR}$ are the GR potentials, whilst the coefficients $U_{lm}^{\pm}$ and $W_{lm}^{\pm}$ are controlled by the higher-derivative terms and hence they have two contributions,

$$U_{lm}^{\pm} = \lambda_{\rm odd}\ell^4 U_{lm}^{\pm(\rm odd)} + \epsilon_3\ell^6 U_{lm}^{\pm(3)}\,, \tag{4.37}$$

$$W_{lm}^{\pm} = \lambda_{\rm odd}\ell^4 W_{lm}^{\pm(\rm odd)} + \epsilon_3\ell^6 W_{lm}^{\pm(3)}\,. \tag{4.38}$$

Notice that, in the presence of parity-breaking corrections, the radius of the horizon is not modified at leading order, $r_+ = 2M$. Hence, r_* is the standard Schwarzschild tortoise coordinate, $r_* = r + 2M\log\left(\frac{r}{2M} - 1\right)$, so that

$$\frac{\mathrm{d}}{\mathrm{d}r*} = \left(1 - \frac{2M}{r}\right)\frac{\mathrm{d}}{\mathrm{d}r}\,. \tag{4.39}$$

We perform a Chandrasekhar transformation of one variable, say $\Psi^+ \to \tilde{\Psi}^+$, such that the zeroth-order equation $\frac{\mathrm{d}^2\Psi^+}{\mathrm{d}r_*^2} + \left(\omega^2 - V_{lm}^{+\rm GR}\right)\Psi^+$ is transformed into $\frac{\mathrm{d}^2\tilde{\Psi}^+}{\mathrm{d}r_*^2} + \left(\omega^2 - V_{lm}^{-\rm GR}\right)\tilde{\Psi}^+$. This is possible even at first order in the spin since $V_{lm}^{+\rm GR}$ and $V_{lm}^{-\rm GR}$ are isospectral at that order, and we show the explicit transformation in Appendix C.3. Of course, the functions $U_{lm}^{\pm}$, $W_{lm}^{\pm}$ are also affected by this change of variables, but expressed in this form we can devise a way to study the system of equations by solving only uncoupled equations. The idea is to decompose the corrections in contributions that are symmetric and antisymmetric under the exchange of $\Psi^{\pm}$, since for each of these contributions the equations can be decoupled. The effect of each correction can then be added up in an appropriate way to obtain, *e.g.*, the total shift in the QNM frequencies, that we study next. We explore this method in more detail in Appendix C.5.

[5] These are defined as in eqs. (4.26) and (4.31), but in the case of Ψ^+ we set $f = 1 - 2M/r$ in (4.31) instead of using the actual value of the metric function given in (4.11).

4.3 Slowly-rotating black holes quasinormal modes

Once we have set up the master equations that govern the perturbations of slowly-rotating black holes in our theory (4.1), our goal is to compute the corrections to the quasinormal modes of the Kerr black hole. Recall that these correspond to solutions in which the variables $\Psi^{\pm}$ behave as outgoing waves both at infinity and at the horizon and that this is only possible for a discrete set of complex frequencies. We are mostly interested in the shifts in the Kerr QNM frequencies induced by the higher-derivative corrections:

$$\omega = \omega^{\rm Kerr} + \delta\omega\,. \tag{4.40}$$

We recall that, in the case of Kerr, the spectrum of odd and even perturbations is identical. In order to show explicitly that for our GR potentials, to linear order in spin, this is still true, we present in Appendix C.3 an extension to the Chandrasekhar transformation which relates the Regge-Wheeler and Zerilli potentials. Now, for the higher-derivative corrections that preserve parity, the shifts in the QNM frequencies of odd and even modes are typically different, and hence one loses isospectrality. Thus, we have two families of frequencies.

$$\omega^{\pm} = \omega^{\rm Kerr} + \delta\omega^{\pm}\,. \tag{4.41}$$

If several parity-preserving interactions appear in the Lagrangian at the same time, one may obtain the total shifts $\delta\omega^{\pm}$ by simply adding up each of the individual contributions.

In the case of the corrections that violate parity, modes of even and odd parity couple and this actually produces a linear shift in the QNM frequencies [51].

The reason for this is that both GR potentials $V^{\pm{\rm GR}}$ are isospectral, and in that case, the problem (4.35)-(4.36) is analogous to performing quantum-mechanical perturbation theory with a degenerate Hamiltonian. In this situation, contrarily to the result with non-degenerate Hamiltonians, off-diagonal components in the Hamiltonian perturbation do introduce a linear correction into the energy states — the QNM frequencies in our case. In fact, one can see that, when there are only parity-breaking corrections, the shifts in the frequencies are opposite for the two families of modes

$$\omega^{\pm} = \omega^{\rm Kerr} \pm \delta\omega^{\rm break}\,, \tag{4.42}$$

for some $\delta\omega^{\rm break}$. Note that in this case the labels $\pm$ are unrelated to the parity of the perturbations. In addition to the frequency, since the QNMs in the presence of parity-violating interactions contain both the even- and odd-parity sectors, it is important to determine the relative normalisation of both modes.

Thus, we introduce the quantity,

$$\gamma = \lim_{r\to\infty} \frac{\Psi^+}{\Psi^-}\,, \tag{4.43}$$

which has to be determined as well (note that the two families of modes $\pm$ have relative normalisations $\pm\gamma$). [6]

Now, if there are several independent parity-violating operators in the action, the total value of $\delta\omega^{\rm break}$ cannot be easily obtained by adding up the contributions of each term. However, one can easily combine them if one knows separately the 'symmetric' ω_s and 'antisymmetric' ω_a contributions to the frequency with respect to interchange of Ψ^+ and Ψ^-. Roughly, by considering these contributions individually in equations (4.35)-(4.36), they can be decoupled, and for these decoupled equations the different contributions add linearly as usual. There are two caveats, though. The first is that one cannot actually use (4.35)-(4.36) as one should make a transformation to ensure the uncorrected (isospectral) potentials are identical, *i.e.* use the transformation given in Appendix C.3, as we mentioned earlier. Secondly, one must be able to recombine these 'symmetric' and 'antisymmetric' contributions. The procedure is analogous to what is used to combine the even-parity and odd-parity contributions discussed next, but for convenience it is made explicit in Appendix C.5. The final, full correction due to parity-breaking interactions can be written as $\delta\omega^{\rm break} = \sqrt{(\sum_i \omega_s^{(i)})^2 + (\sum_i \omega_a^{(i)})^2}$. Equivalently, in order not to work with these auxiliary frequencies, one can note that the ratio $\omega_a^{(i)}/\omega_s^{(i)}$ will characterise the mixing, so in principle one can combine the different odd-parity corrections if in addition to $\delta\omega^{(i)\rm break}$ one is given the mixing coefficients $\gamma^{(i)}$.

Once the contributions to the QNM frequencies from parity-preserving and parity-violating terms have been independently determined, we would like to obtain the total shift in these frequencies in the case in which all the higher-derivative operators appear simultaneously in the action. To obtain that result, one can note that the problem of obtaining the corrected QNMs is formally equivalent to the problem of obtaining the eigenvectors and eigenvalues of a perturbed Hamiltonian. Thus, the usual formulas from quantum-mechanical perturbation theory can be applied — see Appendix C.4 and references [51, 63, 85, 86]. Therefore, one can derive the total shift from the eigenvalue equation

$$\begin{vmatrix} \delta\omega^+ - \delta\omega & \delta\omega^{\rm break} \\ \delta\omega^{\rm break} & \delta\omega^- - \delta\omega \end{vmatrix} = 0\,, \tag{4.44}$$

coming from the perturbation of a degenerate 2×2 Hamiltonian.

[6] Let us remark that the variables $\Psi^\pm$ are defined according to (4.26) and (4.31), and that their normalisation factors satisfy $A = \tilde{A} = 1$ at $r\to\infty$.

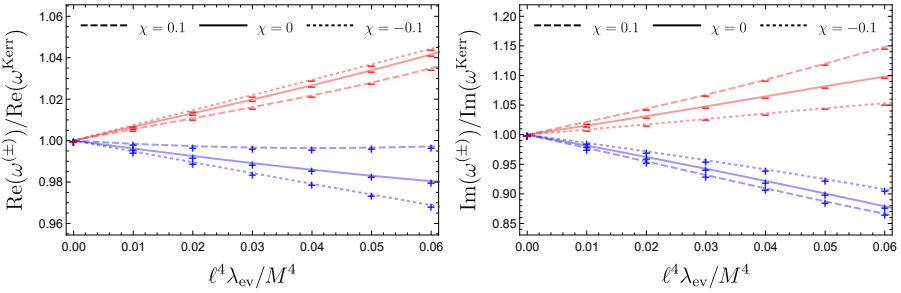


Figure 4.1: Fundamental QNM frequencies $l = m = 2$ relative to the Kerr values as we increase the cubic coupling λ_{ev}. Top: Ratio between the real parts of the corrected QNM frequency and of the Kerr one. Bottom: ratio of the imaginary parts. The lines represent a quadratic fit, whilst the points are numerical data. We observe that " + " and " − " modes are no longer isospectral and that the effect of the spin on the corrections is not negligible.

This yields the result

$$\delta\omega^{(\pm)}_{\mathrm{tot}} = \frac{1}{2}\left(\delta\omega^{+} + \delta\omega^{-}\right) \pm \sqrt{\frac{1}{4}\left(\delta\omega^{+} - \delta\omega^{-}\right)^2 + \left(\delta\omega^{\mathrm{break}}\right)^2}\,. \tag{4.45}$$

Note that we keep the ± labels, but one should bear in mind that these no longer represent defined-parity modes whenever $\delta\omega^{\mathrm{break}} \neq 0$. Finally, the relative normalisation between the even- and odd-parity master variables can be determined by applying again formulas from a 2×2 matrix eigenvalue problem.

$$\gamma^{\pm}_{\mathrm{total}} = \gamma^{\mathrm{break}}\left(\delta\omega^{\pm} - \delta\omega^{+}\right)/\delta\omega^{\mathrm{break}}\ . \tag{4.46}$$

We compute the coefficients $\delta\omega^{\pm,\mathrm{break}}$ and γ^{break} for each of the terms in (4.1).

4.3.1 Cubic corrections

In the cubic Lagrangian there is one parity-preserving correction and one parity-violating one. Thus, we have

$$\delta\omega^{\pm} = \lambda_{\mathrm{ev}}\frac{\ell^4}{M^5}\delta\omega^{\pm}_{\mathrm{ev}}\,, \tag{4.47}$$

$$\delta\omega^{\mathrm{break}} = \lambda_{\mathrm{odd}}\frac{\ell^4}{M^5}\delta\omega^{\mathrm{break}}_{\mathrm{odd}}\,, \tag{4.48}$$

where the factors of M have been introduced so that the coefficients $\delta\omega_i$ on the right-hand side are dimensionless.

In addition, at first order in the spin one can see that the dependence of these modes on the magnetic number m is always through the combination $m \cdot \chi$. Therefore, we can write

$$\delta\omega^{\pm}_{\rm ev} = \delta\omega^{\pm}_{\rm ev,0} + m\chi\,\delta\omega^{\pm}_{\rm ev,1} + \mathcal{O}(\chi^2)\,, \tag{4.49}$$

$$\delta\omega^{\rm break}_{\rm odd} = \delta\omega^{\rm break}_{\rm odd,0} + m\chi\,\delta\omega^{\rm break}_{\rm odd,1} + \mathcal{O}(\chi^2)\,, \tag{4.50}$$

and we only have to determine the $\delta\omega_{0,1}$ coefficients numerically for several values of l. As a check, we will also use our numeric results to obtain the Kerr QNM frequencies, that we express as

$$\omega^{\rm Kerr} = \omega_0 + m\chi\,\omega_1 + \mathcal{O}(\chi^2)\,. \tag{4.51}$$

On the other hand, the relative normalisation factor $\gamma_{\rm odd}$ for the parity-breaking corrections is mildly dependent on the value of $\lambda_{\rm odd}$. However, as a first approximation, we only need to consider its value in the limit $\lambda_{\rm odd} \to 0$, as the running of this parameter is sensitive to the presence of additional higher-derivative corrections. This value is a function of the spin and therefore we also expand it as

$$\gamma_{\rm odd} = \gamma_{\rm odd,0} + m\chi\,\gamma_{\rm odd,1} + \mathcal{O}(\chi^2)\,. \tag{4.52}$$

In order to compute all of these coefficients, we have performed a numerical integration of Eqs. (4.32), (4.28) and (4.35)-(4.36). This allows us to obtain the fundamental QNM frequencies for a range of values of χ and the corresponding coupling, $\lambda_{\rm ev}$ or $\lambda_{\rm odd}$. By fitting the resulting values to a quadratic polynomial in χ and $\lambda_{\rm ev,odd}$, we are able to extract the Schwarzschild value together with the linear shifts in the spin and in the coupling, as well as the coefficient of $\lambda_{\rm ev,odd}\cdot\chi$. In table C.1 (in Appendix C.2) we show the best-fit coefficients associated with the $\lambda_{\rm ev}$ correction, whilst in table C.2 we show the corresponding values for the $\lambda_{\rm odd}$ one, including in that case the value for $\gamma_{\rm odd}$. Also, in Fig. 4.1 we show the data points for the corrected QNM frequencies relative to the Kerr ones together with a quadratic fit in the case of $\lambda_{\rm ev}$ corrections, and in Fig. 4.2 we show an analogous plot for the parity-breaking corrections $\lambda_{\rm odd}$.

As a test of our results, we observe that the Kerr QNM frequencies obtained from these fits are in good agreement with the known values.[7] In addition, we have compared our results for non-rotating black holes with those in [52] for the $\lambda_{\rm ev}$ correction, and we have found that they agree within $\sim 1\% - 5\%$ accuracy.[8]

[7] There is only some discrepancy in the imaginary part of ω_1 as it is relatively small and therefore harder to capture.

[8] For the comparison we take into account that the $\lambda_{\rm ev}$ correction is related to the paramater d_9 in [52] according to $d_9 = \frac{M^2\lambda_{\rm ev}\ell^4}{16\pi G}$, where M is an energy scale used in that reference.

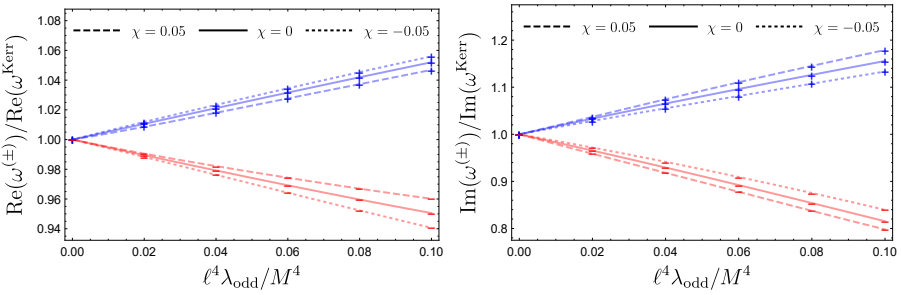


Figure 4.2: Fundamental QNM frequencies $l = m = 2$ relative to the Kerr values as we increase the cubic coupling λ_{odd}. Top: Ratio between the real parts of the corrected QNM frequency and of the Kerr one. Bottom: ratio of the imaginary parts. The lines represent a quadratic fit. We use " + " and " − " to label the different branches but these no longer represent defined-parity modes.

Finally, using the results in both tables together with (4.45) we can derive the total shift in the frequencies. For instance, for the $l = 2$ modes we get, explicitly,

$$\begin{aligned}\delta\omega^{\pm} = &\frac{\ell^4}{M^5}\Big[\lambda_{\mathrm{ev}}\left(0.0533 + 0.0255i + m\chi(0.0812 - 0.0489i)\right)\\ &\pm\Big(\left(0.0152 - 0.0556i - m\chi(0.155 + 0.0249i)\right)\lambda_{\mathrm{ev}}^2\\ &+\left(0.0139 - 0.0580i - m\chi(0.152 + 0.0086i)\right)\lambda_{\mathrm{odd}}^2\Big)^{1/2}\Big]\,. \end{aligned} \tag{4.53}$$

4.3.2 Quartic corrections

At quartic order, we have two parity-preserving terms and one parity-breaking one, and the shifts in the QNM frequencies accordingly take the form

$$\delta\omega^{\pm} = \frac{\ell^6}{M^7}\left(\epsilon_1\delta\omega_1^{\pm} + \epsilon_2\delta\omega_2^{\pm}\right)\,, \tag{4.54}$$

$$\delta\omega^{\mathrm{break}} = \epsilon_3\frac{\ell^6}{M^7}\delta\omega_3^{\mathrm{break}}\,, \tag{4.55}$$

where the coefficients $\delta\omega$ on the right-hand side are dimensionless.

Again, at linear order in the spin, these coefficients can be expanded as

$$\delta\omega_1^{\pm} = \delta\omega_{1,0}^{\pm} + m\chi\,\delta\omega_{1,1}^{\pm} + \mathcal{O}(\chi^2)\,, \tag{4.56}$$

$$\delta\omega_2^{\pm} = \delta\omega_{2,0}^{\pm} + m\chi\,\delta\omega_{2,1}^{\pm} + \mathcal{O}(\chi^2)\,, \tag{4.57}$$

$$\delta\omega_3^{\rm break} = \delta\omega_{3,0}^{\rm break} + m\chi\,\delta\omega_{3,1}^{\rm break} + \mathcal{O}(\chi^2)\,. \tag{4.58}$$

Similarly, we express the relative normalisation between the Ψ^+ and Ψ^- variables in the presence of ϵ_3 corrections as

$$\gamma_3 = \gamma_{3,0} + m\chi\,\gamma_{3,1} + \mathcal{O}(\chi^2)\,. \tag{4.59}$$

The values of these coefficients obtained by a quadratic fit of numerical data are shown in tables C.3, C.4 and C.5 (in Appendix C.2) for the ϵ_1, ϵ_2 and ϵ_3 corrections, respectively. As a first consistency check, we observe that we recover the Kerr QNM frequencies quite accurately from these fits. In addition, we have checked that our results for the corrections to the QNMs of non-rotating black holes are in good agreement with those in Refs [50] and [51] for the $\epsilon_{1,2}$ and ϵ_3 corrections, respectively — the discrepancies we get are of the order of $1\% - 6\%$ depending on the case.[9] Finally, a puzzling observation is that in the case of ϵ_3 corrections the value for the relative normalisation factor γ_3 is essentially coincident with the one for the cubic $\lambda_{\rm odd}$ corrections. Clearly, this cannot be a coincidence and indicates that there is more to be understood on the structure of QNMs with parity-breaking interactions. This will be explored elsewhere.

4.3.3 Concluding remarks

We have presented a complete calculation of the QNMs of black holes in a general effective theory extension of GR, taking into account the rotation at leading order. The next step is to predict the corrections to the QNM spectrum of fully rotating black holes, and to search for these deviations from GR.

Higher-derivative corrections to GR yield a rich phenomenology for the modified Kerr QNM spectrum. First, we observe that the isospectrality of the even- and odd-parity modes is broken. Furthermore, in the presence of parity-breaking corrections, even - and odd modes get coupled, so that QNMs are composed by a certain linear combination of both types of perturbations. Interestingly, the parity-breaking corrections also introduce a linear shift in the QNM frequencies due to the isospectrality of the Kerr QNMs.

[9] For the comparison, we have to take into account that the ϵ_i parameters of reference [50] compare to our own ϵ_i according to $(\epsilon_1, \epsilon_2, \epsilon_3)\big|_{\rm there} = -\ell^6/M^6(\epsilon_1, \epsilon_2/4, \epsilon_3/2)\big|_{\rm here}$

Chapter 5

Setting up a modified Teukolsky equation

We construct a set of universal Teukolsky equations, in the spirit of [87, 88]. That is, we formulate in full generality the specific combination of Bianchi identities that reduce to the usual Teukolsky equations when the background is a Ricci-flat Petrov type D spacetime. The universal Teukolsky equations apply to any background geometry and to any theory, since the theory-dependence only enters through the presence of an effective stress-energy tensor on the right-hand side of the Einstein equation. Next we describe in detail how to evaluate these equations for fluctuations around rotating black-hole solutions that deviate perturbatively from Kerr. Following the approach of [77], we show how to effectively separate these equations into a set of radial equations.

This chapter, which is based on [89][1], is structured as follows (see figure 5.1). In Section 5.1 we derive the universal Teukolsky equations and outline how to evaluate these perturbatively around a Kerr black hole, similarly to [87, 88]. In Sections 5.2 and 5.3 we provide the ingredients to evaluate these equations. In Section 5.4 we explain how the equations can effectively be separated, and in Section 5.5 how these equations can be reduced to a set of radial equations. In Section 5.6 we obtain these equations for the six-derivative EFT extension of general relativity, introduced in the previous chapter, to apply this technique. We solve these numerically in two different ways and obtain explicit results for the shifts in the QNM frequencies that pass several consistency tests.

[1] Written with P. A. Cano, K. Fransen and T. Hertog.

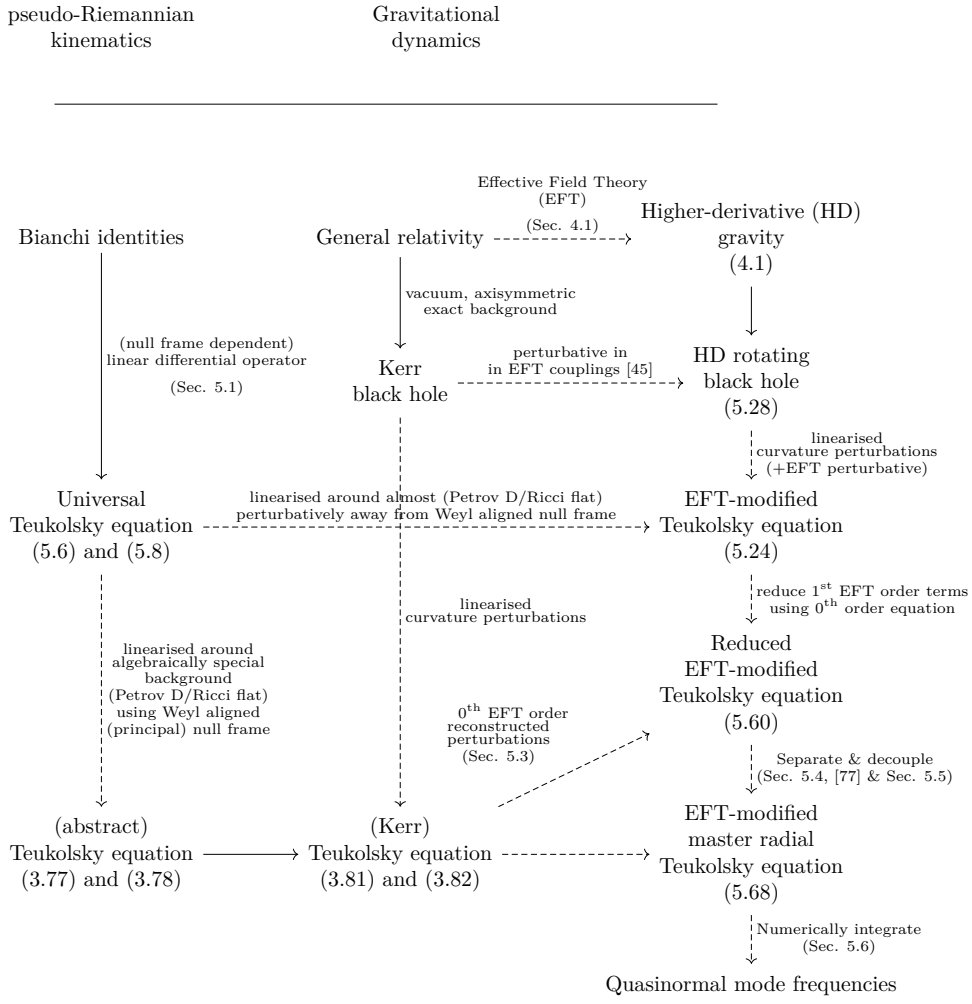


Figure 5.1: Schematic overview of the approach we develop in this chapter to compute the spectrum of quasinormal modes of black holes with significant spin beyond Kerr black holes in general relativity. Dashed lines indicate an approximate or perturbative relation.

5.1 The universal Teukolsky equation

In this section, we derive what we call the "universal Teukolsky equations". This should simply be taken to mean that we write down in full generality a particular combination of Bianchi identities that reduce to the Teukolsky equations for perturbations around a Petrov type D spacetime. This approach was used for higher-order perturbations of rotating black holes in general relativity [90].

5.1.1 Derivation

The schematic form of the Teukolsky equation is as follows

$$\hat{D}[e_{\mathbf{a}}{}^{\mu}, \gamma_{\mathbf{abc}}] \left(\nabla_{[\gamma} R_{\alpha\beta]\sigma\rho}\right) = 0\,, \tag{5.1}$$

with $\hat{D}[e_{\mathbf{a}}{}^{\mu}, \gamma_{\mathbf{abc}}]$ a linear, first-order differential operator depending on the choice of a null-frame tetrad $e_{\mathbf{a}}{}^{\mu}$ and the related spin connection $\gamma_{\mathbf{abc}}$.
We shall follow the Newman-Penrose (NP) and Geroch-Held-Penrose (GHP) approaches to (5.1), as seen in Section 3.3 but without making any assumptions on the spacetime or NP-frame along the way.

In this notation, the Bianchi identities that we will use are

$$\begin{aligned}
\text{Þ}'\Psi_0 - \eth\Psi_1 - \eth\phi_{01} + \text{Þ}\phi_{02} &= \rho'\Psi_0 - 4\tau\Psi_1 + 3\sigma\Psi_2 + \sigma'^*\phi_{00} \\
&\quad - 2\tau'^*\phi_{01} - 2\kappa\phi_{21}^* + 2\sigma\phi_{11} + \rho^*\phi_{02}\,, \qquad (5.2)\\
\text{Þ}\Psi_4 - \eth'\Psi_3 - \eth'\phi_{21} + \text{Þ}'{\phi_{02}}^* &= \rho\Psi_4 - 4\tau'\Psi_3 + 3\sigma'\Psi_2 + \sigma^*\phi_{22} \\
&\quad - 2\tau^*\phi_{21} - 2\kappa'\phi_{01}^* + 2\sigma'\phi_{11} + \rho'^*\phi_{02}^*\,, \qquad (5.3)\\
\text{Þ}'\Psi_3 - \eth\Psi_4 - \text{Þ}'\phi_{21} + \eth'\phi_{22} &= -\tau\Psi_4 + 4\rho'\Psi_3 - 3\kappa'\Psi_2 + \tau^*\phi_{22} \\
&\quad - 2\rho'^*\phi_{21} - 2\sigma'\phi_{21}^* + 2\kappa'\phi_{11} + \kappa'^*{\phi_{02}}^*\,, \qquad (5.4)\\
\text{Þ}\Psi_1 - \eth'\Psi_0 - \text{Þ}\phi_{01} + \eth\phi_{00} &= -\tau'\Psi_0 + 4\rho\Psi_1 - 3\kappa\Psi_2 + \tau'^*\phi_{00} \\
&\quad - 2\rho^*\phi_{01} - 2\sigma\phi_{01}^* + 2\kappa\phi_{11} + \kappa^*\phi_{02}\,. \qquad (5.5)
\end{aligned}$$

These expressions (and the additional identities) can be found, for instance, as (4.12.36)-(4.12.41) in [91]. We remark that this reference uses a "mostly minus" metric convention. In addition, the curvature tensor $R^{\mu}{}_{\nu\alpha\beta}$ is defined with opposite sign. Consequently, our definitions for the spin coefficients have the opposite signs compared to (4.5.22) of [91], as do the curvature scalars, compared to (4.11.10). On the other hand, (3.31) are the same as (4.11.9) of [91].

The result of these choices is that the Bianchi identities in our GHP notation agree with [91]. Nevertheless, as a check, we have independently derived them.

Now, applying Þ and ð the Bianchi equations (5.2) and (5.5), respectively, one finds, upon summing, the result

$$\mathcal{O}_2^{(0)}\left(\Psi_0\right)+\mathcal{O}_2^{(1)}\left(\Psi_1\right)+\mathcal{O}_2^{(2)}\left(\Psi_0\right)=8\pi\left(\mathcal{T}_2^{(0)}+\mathcal{T}_2^{(1)}+\mathcal{T}_2^{(2)}\right), \tag{5.6}$$

with

$$\mathcal{O}_2^{(0)}=2\left[(\text{Þ}-4\rho-\rho^*)(\text{Þ}'-\rho')-(\text{ð}-4\tau-\tau'^*)(\text{ð}'-\tau')-3\Psi_2\right], \tag{5.7a}$$

$$\mathcal{O}_2^{(1)}=4\left[2\kappa\left(\text{Þ}'-\rho'^*\right)-2\sigma\left(\text{ð}'-\tau^*\right)+2\left(\text{Þ}'\kappa\right)-2\left(\text{ð}'\sigma\right)+5\Psi_1\right], \tag{5.7b}$$

$$\mathcal{O}_2^{(2)}=6\left[\kappa\kappa'-\sigma\sigma'\right], \tag{5.7c}$$

$$\begin{aligned}\mathcal{T}_2^{(0)}&=(\text{ð}-\tau'^*-4\tau)[(\text{Þ}-2\rho^*)T_{lm}-(\text{ð}-\tau'^*)T_{ll}]\\&\quad+(\text{Þ}-4\rho-\rho^*)[(\eth-2\tau'^*)T_{lm}-(\text{Þ}-\rho^*)T_{mm}],\end{aligned} \tag{5.7d}$$

$$\begin{aligned}\mathcal{T}_2^{(1)}&=\frac{1}{2}\left[\sigma\text{Þ}-\kappa\text{ð}\right]T-\left[3\sigma\left(\text{Þ}'-\rho'^*\right)-\sigma'^*\left(\text{Þ}-4\rho-\rho^*\right)-\text{Þ}\left(\sigma'^*\right)\right]T_{ll}\\&\quad-2\left[\sigma\left(\text{ð}-\tau-\tau'^*\right)+\text{ð}\left(\sigma\right)\right]T_{l\bar{m}}+\left[3\sigma\left(\text{ð}'-2\tau^*\right)+3\kappa\left(\text{Þ}'-2\rho'^*\right)\right]T_{lm}\\&\quad-\left[3\kappa\left(\text{ð}'-\tau^*\right)-\kappa^*\left(\text{ð}-4\tau-\tau'^*\right)-\text{ð}\left(\kappa^*\right)\right]T_{mm}\\&\quad+\left[\kappa\text{ð}+\sigma\left(\text{Þ}-2\rho-2\rho^*\right)+2\text{Þ}\left(\sigma\right)-\Psi_0\right]\left(T_{ln}+T_{m\bar{m}}\right)\\&\quad-2\left[\kappa\left(\text{Þ}-\rho-\rho^*\right)+\text{Þ}\left(\kappa\right)\right]T_{nm},\end{aligned} \tag{5.7e}$$

$$\mathcal{T}_2^{(2)}=3\left[\kappa\kappa'^*T_{ll}+\sigma\sigma^*T_{mm}\right], \tag{5.7f}$$

and[2]

$$8\pi T_{ll}=2\phi_{00}\,,\quad 8\pi T_{lm}=2\phi_{01}\,,\quad 8\pi T_{mm}=2\phi_{02}\,,\quad 8\pi T_{n\bar{m}}=2\phi_{21}\,, \tag{5.7g}$$

$$8\pi T=-R\,,\quad 8\pi\left(T_{ln}+T_{m\bar{m}}\right)=4\phi_{11}\,. \tag{5.7h}$$

[2] Naturally, T_{ll}, T_{lm}, etc., are the components of the stress-energy tensor in the basis (3.23). This enters in the Einstein equations as $G_{\mu\nu}=8\pi T_{\mu\nu}$. In the case of the higher-derivative corrections we have the equations (4.6) and hence we must use $8\pi T_{\mu\nu}=\ell^4\mathcal{E}^{(6)}_{\mu\nu}$.

Here, (5.2) and (5.5) were additionally used to replace $\eth\Psi_2$ and $\text{Þ}\Psi_1$. Moreover, several other relations between the spin coefficients and curvature scalars were used along the way. Additional relevant identities and details can be found in Appendix B.1. Similarly, applying $\text{Þ}'$ and $\eth'$ to two of the the Bianchi equations, (5.3) and (5.4) respectively, one finds, upon summing, the result

$$\mathcal{O}^{(0)}_{-2}\left(\Psi_4\right)+\mathcal{O}^{(1)}_{-2}\left(\Psi_3\right)+\mathcal{O}^{(2)}_{-2}\left(\Psi_4\right)=8\pi\left(\mathcal{T}^{(0)}_{-2}+\mathcal{T}^{(1)}_{-2}+\mathcal{T}^{(2)}_{-2}\right), \tag{5.8}$$

with

$$\mathcal{O}^{(0)}_{-2}=2\left[(\text{Þ}'-4\rho'-\rho'^{*})(\text{Þ}-\rho)-(\eth'-4\tau'-\tau^{*})(\eth-\tau)-3\Psi_2\right], \tag{5.9a}$$

$$\mathcal{O}^{(1)}_{-2}=4\left[2\kappa'\left(\text{Þ}-\rho^{*}\right)-2\sigma'\left(\eth-\tau'^{*}\right)+2\left(\text{Þ}\kappa'\right)-2\left(\eth\sigma'\right)+5\Psi_3\right], \tag{5.9b}$$

$$\mathcal{O}^{(2)}_{-2}=6\left[\kappa\kappa'-\sigma\sigma'\right], \tag{5.9c}$$

$$\begin{aligned}\mathcal{T}^{(0)}_{-2}&=(\eth'-\tau^{*}-4\tau')[(\text{Þ}'-2\rho'^{*})T_{n\bar{m}}-(\eth'-\tau^{*})T_{nn}]\\&\quad+(\text{Þ}'-4\rho'-\rho'^{*})[(\bar{\eth}'-2\tau^{*})T_{n\bar{m}}-(\text{Þ}'-\rho'^{*})T_{\bar{m}\bar{m}}],\end{aligned} \tag{5.9d}$$

$$\begin{aligned}\mathcal{T}^{(1)}_{-2}&=\frac{1}{2}\left[\sigma'\text{Þ}'-\kappa'\eth'\right]T-\left[3\sigma'\left(\text{Þ}-\rho^{*}\right)-\sigma^{*}\left(\text{Þ}'-4\rho'-\rho'^{*}\right)-\text{Þ}'\left(\sigma^{*}\right)\right]T_{nn}\\&\quad-2\left[\sigma'\left(\eth'-\tau'-\tau^{*}\right)+\eth'\left(\sigma'\right)\right]T_{nm}+\left[3\sigma'\left(\eth-2\tau'^{*}\right)+3\kappa'\left(\text{Þ}-2\rho^{*}\right)\right]T_{n\bar{m}}\\&\quad-\left[3\kappa'\left(\eth-\tau'^{*}\right)-\kappa'^{*}\left(\eth'-4\tau'-\tau^{*}\right)-\eth'\left(\kappa'^{*}\right)\right]T_{\bar{m}\bar{m}}\\&\quad+\left[\kappa'\eth'+\sigma'\left(\text{Þ}'-2\rho'-2\rho'^{*}\right)+2\text{Þ}'\left(\sigma'\right)-\Psi_4\right]\left(T_{ln}+T_{m\bar{m}}\right)\\&\quad-2\left[\kappa'\left(\text{Þ}'-\rho'-\rho'^{*}\right)+\text{Þ}'\left(\kappa'\right)\right]T_{l\bar{m}},\end{aligned} \tag{5.9e}$$

$$\mathcal{T}^{(2)}_{-2}=3\left[\kappa'\kappa^{*}T_{nn}+\sigma'\sigma'^{*}T_{\bar{m}\bar{m}}\right], \tag{5.9f}$$

and

$$8\pi T_{nn}=2\phi_{22}\,,\quad 8\pi T_{lm}=2\phi_{01}\,,\quad 8\pi T_{\bar{m}\bar{m}}=2\phi^{*}_{02}\,,\quad 8\pi T_{n\bar{m}}=2\phi_{21}\,, \tag{5.10a}$$

$$8\pi T=-R\,,\quad 8\pi\left(T_{ln}+T_{m\bar{m}}\right)=4\phi_{11}\,. \tag{5.10b}$$

More details can be found in Appendix B.1. Aside from the key observations that were made long ago for the case of rotating black holes [36, 65, 92–95], the derivation of these expressions is an exercise in translation and algebra.

Yet it is important to emphasise that no assumptions are made on the spacetime or NP-frame to derive (5.6) and (5.8). Nevertheless, we have suggestively grouped together terms based on quantities that would vanish in a Petrov D spacetime in an aligned frame.

5.1.2 Linearisation

Contrary to the Teukolsky equations, the equations derived in the previous section apply for any four-dimensional spacetime and any choice of NP-frame. In contrast to the Teukolsky equations, they are in fact also totally impractical. Our goal is now to find a suitable regime, where we are close enough to the Teukolsky equations to use their nice properties whilst still being very general in terms of applicability. The key assumption going into this is the perturbative nature of the corrections. All observations so far indicate that this is likely a good assumption [96] but it should be stressed that non-perturbative corrections to the spectrum are also of interest [97–99]. These will not be captured here. Moreover, in light of the pseudospectral instability of these quasinormal modes such corrections could imply an entirely different spectrum of modes [100–102]. However, the time-domain response relevant for observations is more robust [103]. Therefore, we would still expect the perturbative corrections we compute to be relevant for the observed ringdown.

In general, although there are of course other relations between these variables, equations (5.6) and (5.8) involve the frame e_a, spin connection γ_{abc}, the (Ricci) curvatures[3] ϕ_{ab}, and Weyl scalars Ψ_i, so they take the form

$$\mathcal{E}_{\pm 2}(e_{\mathbf{a}}, \gamma_{\mathbf{abc}}, \phi_{ij}, \Psi_i) = \mathcal{E}_{\pm 2}(\Phi, \Psi_i) = 0\,, \tag{5.11}$$

where we will denote the variables excluding Ψ_i collectively as Φ. Consider a perturbation of a solution, so that we make $e_{\mathbf{a}} \to \bar{e}_{\mathbf{a}} + \delta e_{\mathbf{a}}$, $\gamma_{\mathbf{abc}} \to \bar{\gamma}_{\mathbf{abc}} + \delta\gamma_{\mathbf{abc}}$, $\phi_{ij} \to \bar{\phi}_{ij} + \delta\phi_{ij}$ (so in general $\Phi \to \bar{\Phi} + \delta\Phi$), and $\Psi_i \to \bar{\Psi}_i + \delta\Psi_i$, where the bar on top of a given quantity denotes that it is evaluated on the background. The equations above then yield two linear equations for the perturbations

$$\mathcal{E}_{\delta\Psi,\pm 2}\left(\delta\Psi_i\right) + \mathcal{E}_{\delta\Phi,\pm 2}\left(\delta\Phi\right) = 0\,, \tag{5.12}$$

where $\mathcal{E}_{\delta\Psi,\pm 2}\left(\cdot\right)$ and $\mathcal{E}_{\delta\Phi,\pm 2}\left(\cdot\right)$ are linear differential operators.

[3] Note however that the Ricci curvature will be replaced by the effective stress-energy tensor by imposing the Einstein equations. For higher-derivative theories, such as in (4.6), the effective stress-energy tensor is a function of the frame, spin connection and Weyl curvature, since at leading order in a perturbative expansion we only need to evaluate it on a solution of the vacuum Einstein equations (i.e. on a Ricci-flat spacetime).

In principle, these equations involve all perturbed variables. However, a simplification occurs if the background geometry corresponds to a corrected vacuum (Ricci flat) Petrov-D solution. By this we mean that the solution only departs perturbatively from the vacuum Petrov type D. In particular, this is the case for rotating black holes in the theory with higher-derivative corrections.

As a bookkeeping parameter, we introduce λ to keep track of the departure from vacuum Petrov type D (*e.g.*, in the case of higher-derivative corrections this could be ℓ^4 or ℓ^6 in (4.1)). We will work at linear order in λ, since we are only interested in the leading corrections. The background geometry will have

$$\bar{\Psi}_i = \bar{\Psi}_i^{(0)} + \lambda \bar{\Psi}_i^{(1)}\,, \quad \bar{\Phi}_i = \bar{\Phi}_i^{(0)} + \lambda \bar{\Phi}_i^{(1)}\,, \tag{5.13}$$

with, in particular

$$\bar{\Psi}_0^{(0)} = \bar{\Psi}_1^{(0)} = \bar{\Psi}_3^{(0)} = \bar{\Psi}_4^{(0)} = 0\,, \tag{5.14}$$

$$\bar{\phi}_{00}^{(0)} = \bar{\phi}_{01}^{(0)} = \bar{\phi}_{02}^{(0)} = \bar{\phi}_{21}^{(0)} = \bar{\phi}_{11}^{(0)} = \bar{\phi}_{22}^{(0)} = 0\,, \tag{5.15}$$

$$\bar{\kappa}^{(0)} = \bar{\kappa}'^{(0)} = \bar{\sigma}^{(0)} = \bar{\sigma}'^{(0)} = 0\,, \tag{5.16}$$

on the assumption that the uncorrected background is of Petrov type D and that the frame is chosen to be aligned to the principal null directions. The corrections to these quantities will nevertheless be non-vanishing in general.

When we evaluate the linearised equation (5.12) on this type of background, we can see that the operators $\mathcal{E}_{\delta\Phi,\pm 2}$ become of order λ, a fact which we denote by

$$\mathcal{E}_{\delta\Phi,\pm 2}\left(\delta\Phi\right) = \lambda \mathcal{E}^{(1)}_{\delta\Phi,\pm 2}\left(\delta\Phi\right)\,. \tag{5.17}$$

On the other hand,

$$\begin{aligned} \mathcal{E}_{\delta\Psi,+2}\left(\delta\Psi_i\right) &= \mathcal{D}^{(0)}_{2}\left(\delta\Psi_0\right) + \lambda \mathcal{E}^{(1)}_{\delta\Psi,+2}\left(\delta\Psi_i\right)\,, \\ \mathcal{E}_{\delta\Psi,-2}\left(\delta\Psi_i\right) &= \mathcal{D}^{(0)}_{-2}\left(\delta\Psi_4\right) + \lambda \mathcal{E}^{(1)}_{\delta\Psi,-2}\left(\delta\Psi_i\right)\,, \end{aligned} \tag{5.18}$$

where $\mathcal{D}^{(0)}_{\pm 2}$ are the Teukolsky operators for $\delta\Psi_{0,4}$ on the Kerr background:

$$\begin{aligned} \mathcal{D}^{(0)}_{+2} &= 2\left[(\text{Þ} - 4\rho - \rho^*)(\text{Þ}' - \rho') - (\eth - 4\tau - \tau'^*)(\eth' - \tau') - 3\Psi_2\right]\big|_{\text{Kerr}}\,, \\ \mathcal{D}^{(0)}_{-2} &= 2\left[(\text{Þ}' - 4\rho' - \rho'^*)(\text{Þ} - \rho) - (\eth' - 4\tau' - \tau^*)(\eth - \tau) - 3\Psi_2\right]\big|_{\text{Kerr}}\,. \end{aligned} \tag{5.19}$$

Then, to first order in λ, the equations become

$$\begin{aligned} \mathcal{D}^{(0)}_{+2}\left(\delta\Psi_0\right) + \lambda\left[\mathcal{E}^{(1)}_{\delta\Psi,+2}\left(\delta\Psi_i\right) + \mathcal{E}^{(1)}_{\delta\Phi,+2}\left(\delta\Phi\right)\right] &= 0\,, \\ \mathcal{D}^{(0)}_{-2}\left(\delta\Psi_4\right) + \lambda\left[\mathcal{E}^{(1)}_{\delta\Psi,-2}\left(\delta\Psi_i\right) + \mathcal{E}^{(1)}_{\delta\Phi,-2}\left(\delta\Phi\right)\right] &= 0\,. \end{aligned} \tag{5.20}$$

Now, the value of every perturbed quantity will be the one for the Kerr background plus a linear correction,

$$\delta\Phi = \delta\Phi^{(0)} + \lambda\delta\Phi^{(1)}\,. \tag{5.21}$$

Thus, at first order in λ, the previous equations are equivalent to

$$\begin{aligned}
&\mathcal{D}^{(0)}_{+2}\left(\delta\Psi_0\right) + \lambda\left[\mathcal{E}^{(1)}_{\delta\Psi,+2}\left(\delta\Psi_i^{(0)}\right) + \mathcal{E}^{(1)}_{\delta\Phi,+2}\left(\delta\Phi^{(0)}\right)\right] = 0\,,\\
&\mathcal{D}^{(0)}_{-2}\left(\delta\Psi_4\right) + \lambda\left[\mathcal{E}^{(1)}_{\delta\Psi,-2}\left(\delta\Psi_i^{(0)}\right) + \mathcal{E}^{(1)}_{\delta\Phi,-2}\left(\delta\Phi^{(0)}\right)\right] = 0\,.
\end{aligned} \tag{5.22}$$

Note that we intentionally do not split $\delta\Psi_{0,4} = \delta\Psi^{(0)}_{0,4} + \lambda\delta\Psi^{(1)}_{0,4}$, as we will write an equation for the complete variables $\delta\Psi_{0,4}$.

In fact, every zeroth-order perturbed quantity can be determined in terms of the Teukolsky variables $\delta\Psi^{(0)}_0$ and $\delta\Psi^{(0)}_4$:

$$\delta\Phi^{(0)} = \delta\Phi^{(0)}(\delta\Psi^{(0)}_0, \delta\Psi^{(0)}_4) = \delta\Phi^{(0)}(\delta\Psi_0, \delta\Psi_4) + \mathcal{O}(\lambda)\,. \tag{5.23}$$

Therefore, at the end of the day we should be able to write the equations explicitly as

$$\begin{aligned}
&\mathcal{D}^{(0)}_{+2}\left(\delta\Psi_0\right) + \lambda\left[\mathcal{E}^{(1)}_{\delta\Psi_0,+2}\left(\delta\Psi_0\right) + \mathcal{E}^{(1)}_{\delta\Psi_4,+2}\left(\delta\Psi_4\right)\right] = 0\,,\\
&\mathcal{D}^{(0)}_{-2}\left(\delta\Psi_4\right) + \lambda\left[\mathcal{E}^{(1)}_{\delta\Psi_0,-2}\left(\delta\Psi_0\right) + \mathcal{E}^{(1)}_{\delta\Psi_4,-2}\left(\delta\Psi_4\right)\right] = 0\,.
\end{aligned} \tag{5.24}$$

These are two coupled equations for the two variables $\delta\Psi_{0,4}$. In order to obtain these equations, we first need to obtain explicitly the relations (5.23). We will achieve this by finding the leading-order (general relativistic) metric perturbations associated to solutions to the Teukolsky equations in a procedure known as metric reconstruction.

5.1.3 Implementation

In practice, to obtain the equations (5.24) we proceed as follows. For every quantity $\Phi = \{\Psi_i, e_a, \gamma_{abc}\}$, we must find its explicit expression as

$$\Phi = \bar{\Phi} + \delta\Phi(\delta\Psi_0, \delta\Psi_4)\,, \tag{5.25}$$

where $\bar{\Phi}$ is the background value of the corresponding quantity, consisting of its Einstein-gravity value plus a correction,

$$\bar{\Phi} = \bar{\Phi}^{(0)} + \lambda\bar{\Phi}^{(1)}\,, \tag{5.26}$$

and $\delta\Phi(\delta\Psi_0, \delta\Psi_4)$ is the solution of the perturbed quantity in the Kerr background expressed in terms of $\delta\Psi_0$ and $\delta\Psi_4$. We remark that the term $\delta\Phi(\delta\Psi_0, \delta\Psi_4)$ involves no higher-derivative corrections; it is the perturbed quantity as obtained in Einstein gravity.

We then insert (5.25) into (5.6) and (5.8) keeping the terms linear in the fluctuations $\delta\Phi$ to first order in λ. In this process we can also reduce the number of derivatives in the terms proportional to λ by making use of the zeroth-order Teukolsky equations $\mathcal{D}^{(0)}_{\pm 2}(\delta\Psi_{0,4}) = 0$. The result is then the two equations (5.24). In order to carry out this computation we need two ingredients:

(1) the Newman-Penrose description of the background geometry (with the higher-derivative corrections),

(2) the solution for every perturbed quantity in the Einstein-gravity case (without corrections) expressed in terms of $\delta\Psi_0$ and $\delta\Psi_4$.

We address these points in the next section.

There is a last observation that must be made. In general, it will be convenient to work with complex metric perturbations. However, this comes at the price that complex conjugates in the NP formalism are not actual complex conjugates. Instead, these "conjugate" variables become independent and satisfy their own equations. We need to consider in particular the equations for $\delta\Psi_0^*$ and $\delta\Psi_4^*$. Thus, together with (5.6) and (5.8), we also need to consider their "conjugate" versions, which yield two equations for $\delta\Psi_0^*$ and $\delta\Psi_4^*$ analogous to (5.24). Therefore, at the end we will obtain altogether four coupled linear equations for $\delta\Psi_0$, $\delta\Psi_4$, $\delta\Psi_0^*$ and $\delta\Psi_4^*$.

5.2 Newman-Penrose description of the background geometry

The solutions of (4.1), perturbatively in the higher-derivative couplings, take the form

$$\bar{g}_{\mu\nu} = \bar{g}^{(0)}_{\mu\nu} + \lambda \bar{g}^{(1)}_{\mu\nu} \,, \tag{5.27}$$

where $\bar{g}^{(0)}_{\mu\nu}$ is a solution of the vacuum Einstein equations (*i.e.*, a Ricci flat metric) and $\bar{g}^{(1)}_{\mu\nu}$ is the correction at linear order in the higher-derivative couplings which, as in the previous section, we keep track of through the bookkeeping parameter λ. In the case of the rotating black-hole solutions, we use the following ansatz to capture the deviations with respect to Kerr [45],

$$\begin{aligned} \mathrm{d}\bar{s}^2 = &- \left(1 - \frac{2Mr}{\Sigma} - \lambda H_1\right) \mathrm{d}t^2 - (1 + \lambda H_2) \frac{4Mar(1-x^2)}{\Sigma} \,\mathrm{d}t\,\mathrm{d}\phi \\ &+ (1 + \lambda H_3)\, \Sigma \left(\frac{\mathrm{d}r^2}{\Delta} + \frac{\mathrm{d}x^2}{1-x^2}\right) \\ &+ (1 + \lambda H_4) \left(r^2 + a^2 + \frac{2Mra^2(1-x^2)}{\Sigma}\right) (1-x^2)\, \mathrm{d}\phi^2 \,, \end{aligned} \tag{5.28}$$

where

$$\Sigma = r^2 + a^2 x^2 \,, \quad \Delta = r^2 - 2Mr + a^2 \,, \tag{5.29}$$

and $x = \cos\theta$.[4] The metric $\bar{g}^{(0)}_{\mu\nu}$ is in this case the Kerr metric in Boyer-Lindquist coordinates, whilst $\bar{g}^{(1)}_{\mu\nu}$ is parametrised by the four functions $H_i(x, r)$,

$$\begin{aligned} \bar{g}^{(1)}_{\mu\nu}\, \mathrm{d}x^\mu\, \mathrm{d}x^\nu = &H_1\, \mathrm{d}t^2 - H_2 \frac{4Mar(1-x^2)}{\Sigma}\, \mathrm{d}t\, \mathrm{d}\phi + H_3 \Sigma \left(\frac{\mathrm{d}r^2}{\Delta} + \frac{\mathrm{d}x^2}{1-x^2}\right) \\ &+ H_4 \left(r^2 + a^2 + \frac{2Mra^2(1-x^2)}{\Sigma}\right) (1-x^2)\, \mathrm{d}\phi^2 \,. \end{aligned} \tag{5.30}$$

The solution depends on the two constants M and a, which represent the total mass and specific angular momentum as long as the H_i functions satisfy appropriate boundary conditions [45], which we assume. We also introduce the dimensionless spin parameter $\chi = a/M$. Here we consider solutions with $|\chi| < 1$, as the extremal limit $|\chi| \sim 1$ poses additional difficulties.

[4] We remark that it is computationally faster to use the algebraic x variable as opposed to the trigonometric θ variable.

For $|\chi| < 1$, the solutions for the H_i functions can be expressed as a convergent power series in χ, and they take the form[5]

$$H_i = \sum_{n=0}^{\infty} \chi^n \sum_{p=0}^{n} \sum_{q=0}^{q_{\max}(n,p)} H_i^{(n,p,q)} x^p r^{-q} \,, \tag{5.31}$$

for certain coefficients $H_i^{(n,p,q)}$ that one can compute. We have computed these solutions to order $\mathcal{O}(\chi^{30})$, which we believe would suffice for most purposes up to spins $\chi \sim 0.9$. For smaller spins, many fewer terms are required to obtain high accuracy. The availability of this high-order solution will not yet be fully exploited here, since we will only make use of a $\mathcal{O}(\chi^6)$ expansion in Section 5.6, but it is important for future applications. The solution could otherwise be obtained numerically by solving the system of linear partial differential equations satisfied by the H_i functions, but we find this less practical.

Let us also take note that the event horizon of the metric (5.28) is located at

$$r_+ = M + \sqrt{M^2 - a^2} \,, \tag{5.32}$$

and this is not modified by the higher-derivative corrections. This is because we are making a coordinate choice in (5.28) that guarantees that the horizon is always located at (5.32).

Let us now provide the Newman-Penrose description of this spacetime. We again consider a null tetrad $e_{\mathbf{a}}{}^{\mu}$ that we denote by

$$e_{\mathbf{1}}{}^{\mu} = l^{\mu} \,, \quad e_{\mathbf{2}}{}^{\mu} = n^{\mu} \,, \quad e_{\mathbf{3}}{}^{\mu} = m^{\mu} \,, \quad e_{4}{}^{\mu} = \bar{m}^{\mu} \,, \tag{5.33}$$

and that satisfies

$$\bar{g}_{\mu\nu} = -2 l_{(\mu} n_{\nu)} + 2 m_{(\mu} \bar{m}_{\nu)} \,. \tag{5.34}$$

Similar to the metric, the tetrad vectors equal their Kerr value plus a correction,

$$e_{\mathbf{a}}{}^{\mu} = e_{(0)\mathbf{a}}{}^{\mu} + \lambda e_{(1)\mathbf{a}}{}^{\mu} \,. \tag{5.35}$$

[5] In order to determine the convergence of the spin expansion one can perform standard convergence tests, like the root test, with a high-order expansion of the solution — in our case, we used the solution to order χ^{30}. These tests indicate that the power series is indeed convergent in the exterior of the black hole, with a radius of convergence $|\chi_{\max}| \sim 1$. Furthermore, in the case of certain observables the convergence of the spin expansion can be verified as the series can be summed up analytically [104, 105].

For the tetrad in the uncorrected Kerr geometry, we use the Kinnersley tetrad

$$\begin{aligned} l^{\mu}_{(0)} &= \left(\frac{r^2+a^2}{\Delta}\,, 1\,, 0\,, \frac{a}{\Delta} \right)\,, \\ n^{\mu}_{(0)} &= \left(r^2+a^2\,, -\Delta\,, 0\,, a \right) \frac{1}{\Sigma}\,, \\ m^{\mu}_{(0)} &= \left(ia\sqrt{1-x^2}\,, 0\,, -\sqrt{1-x^2}\,, \frac{i}{\sqrt{1-x^2}} \right) \frac{1}{\sqrt{2}\zeta^*}\,, \\ \bar{m}^{\mu}_{(0)} &= \left(-ia\sqrt{1-x^2}\,, 0\,, -\sqrt{1-x^2}\,, -\frac{i}{\sqrt{1-x^2}} \right) \frac{1}{\sqrt{2}\zeta}\,, \end{aligned} \tag{5.36}$$

where

$$\zeta = r - iax\,. \tag{5.37}$$

As is well-known, this frame has the property that it is aligned with the principal null directions of the Kerr metric. Therefore, in this frame, one in particular has (5.14) and (5.16)

$$\bar{\Psi}^{(0)}_0 = \bar{\Psi}^{(0)}_1 = \bar{\Psi}^{(0)}_3 = \bar{\Psi}^{(0)}_4 = 0\,, \tag{5.38}$$

$$\bar{\kappa}^{(0)} = \bar{\kappa}'^{(0)} = \bar{\sigma}^{(0)} = \bar{\sigma}'^{(0)} = 0\,, \tag{5.39}$$

as used in the previous section. The correction to the tetrad can then be found from the correction to the metric $\bar{g}^{(1)}_{\mu\nu}$ in (5.30) as

$$e_{(1)\mathbf{a}}{}^{\mu} = -\frac{1}{2}\,\bar{g}^{(1)}_{\alpha\beta}\,\bar{g}^{(0)\mu\alpha}\,e_{(0)\mathbf{a}}{}^{\beta}\,. \tag{5.40}$$

There is additional gauge freedom in the choice of $e_{(1)\mathbf{a}}{}^{\mu}$, corresponding to infinitesimal Lorentz transformations of the uncorrected frame. One may use this freedom to set to zero some of the components of the spin connection or some of the Weyl scalars (in particular, Ψ_1 and Ψ_3). However, this makes the form of the tetrad much more complicated, so in practice it seems more efficient to work with the simple choice given by (5.40). This will be the background tetrad we use throughout.

Once the tetrad is determined, obtaining the coefficients of the spin connection as well as the Weyl scalars, that we need for our computations,[6] is just a straightforward task that we carry out with the help of software.

[6] The Ricci curvature, although non-vanishing, is not needed.

5.3 Metric reconstruction of Kerr perturbations

In order to find the master equations (5.24) we also need to express every perturbed quantity on the Kerr background in terms of the Teukolsky variables. The most efficient way to accomplish this is by reconstructing the metric perturbation. From the metric perturbation, the remaining perturbed quantities can be straightforwardly computed.

Following [106], one can reconstruct the metric perturbation on the Kerr background as follows

$$M\partial_t h_{\mu\nu} = -\frac{1}{3}\nabla_\beta\left[\zeta^4\nabla_\alpha \mathcal{C}_{(\mu\ \ \nu)}^{\ \ \alpha\ \ \beta}\right] - \frac{1}{3}\nabla_\beta\left[(\zeta^*)^4\nabla_\alpha \bar{\mathcal{C}}_{(\mu\ \ \nu)}^{\ \ \alpha\ \ \beta}\right], \tag{5.41}$$

where

$$\mathcal{C}_{\mu\alpha\nu\beta} = 4\left(\psi_0 n_{[\mu}\bar{m}_{\alpha]}n_{[\nu}\bar{m}_{\beta]} + \psi_4 l_{[\mu}m_{\alpha]}l_{[\nu}m_{\beta]}\right), \tag{5.42}$$

$$\bar{\mathcal{C}}_{\mu\alpha\nu\beta} = 4\left(\psi_0^* n_{[\mu}m_{\alpha]}n_{[\nu}m_{\beta]} + \psi_4^* l_{[\mu}\bar{m}_{\alpha]}l_{[\nu}\bar{m}_{\beta]}\right). \tag{5.43}$$

The variables $\psi_{0,4}$ and $\psi^*_{0,4}$ satisfy the Teukolsky equations, but they are in general different from the Weyl scalars $\delta\Psi_{0,4}$, $\delta\Psi^*_{0,4}$. They are, however, proportional to them, as we show below. Let us also note that we will be working with a complex metric perturbation. This implies that conjugate quantities in the NP formalism are not complex conjugates anymore, but actually independent quantities. Therefore, $\psi_{0,4}$ and $\psi^*_{0,4}$ have to be treated as independent variables.

Since these variables satisfy Teukolsky equations, they can be separated as

$$\begin{aligned}
\psi_0 &= e^{-i\omega t+im\phi}R_2(r)S_2(x)\,,\\
\psi_0^* &= e^{-i\omega t+im\phi}R_2^*(r)S_{-2}(x)\,,\\
\psi_4 &= e^{-i\omega t+im\phi}\zeta^{-4}R_{-2}(r)S_{-2}(x)\,,\\
\psi_4^* &= e^{-i\omega t+im\phi}(\zeta^*)^{-4}R^*_{-2}(r)S_2(x)\,,
\end{aligned} \tag{5.44}$$

where $S_s(x)$, $R_s(r)$ and $R^*_s(r)$ satisfy the angular and radial Teukolsky equations

$$\frac{\mathrm{d}}{\mathrm{d}x}\left[(1-x^2)\frac{\mathrm{d}S_s}{\mathrm{d}x}\right] + \left[(a\omega)^2x^2 - 2sa\omega x + B_{lm} - \frac{(m+sx)^2}{1-x^2}\right]S_s = 0\,, \tag{5.45}$$

$$\mathfrak{D}_s^2 R_s = \Delta^{-s+1}\frac{\mathrm{d}}{\mathrm{d}r}\left[\Delta^{s+1}\frac{\mathrm{d}R_s}{\mathrm{d}r}\right] + VR_s = 0\,, \tag{5.46}$$

$$\mathfrak{D}_s^2 R^*_s = \Delta^{-s+1}\frac{\mathrm{d}}{\mathrm{d}r}\left[\Delta^{s+1}\frac{\mathrm{d}R^*_s}{\mathrm{d}r}\right] + VR^*_s = 0\,, \tag{5.47}$$

with

$$V = (am)^2 + \omega^2\left(a^2+r^2\right)^2 - 4amMr\omega + is\left(2am(r-M) - 2M\omega\left(r^2-a^2\right)\right) + \Delta\left(-a^2\omega^2 + s - B_{lm} + 2irs\omega\right), \tag{5.48}$$

and angular separation constants B_{lm}.[7] Note that the conjugate variables R_s^* satisfy the same equations as R_s. Now, since the time dependence is separated as $e^{-i\omega t}$, we can express the metric perturbation explicitly as

$$h_{\mu\nu} = -\frac{i}{3M\omega}\nabla_\beta\left[\zeta^4\nabla_\alpha\mathcal{C}_{(\mu\ \ \nu)}^{\ \ \alpha\ \ \beta}\right] - \frac{i}{3M\omega}\nabla_\beta\left[(\zeta^*)^4\nabla_\alpha\bar{\mathcal{C}}_{(\mu\ \ \nu)}^{\ \ \alpha\ \ \beta}\right], \tag{5.49}$$

We have checked by direct computation that this metric perturbation indeed satisfies the linearised Einstein equations $R_{\mu\nu} = 0$.

From $h_{\mu\nu}$ we can obtain the perturbation of the NP frame,

$$\delta e_{\mathbf{a}}{}^{\mu} = -\frac{1}{2}h_{\alpha\beta}\bar{g}^{(0)\mu\alpha}\bar{e}_{(0)a}{}^{\beta}, \tag{5.50}$$

where $g^{(0)}_{\mu\alpha}$ is the Kerr metric and $\bar{e}_{(0)a}{}^{\beta}$ is the frame (5.36). It is then straightforward (but computationally heavy) to obtain the perturbation of the spin connection $\delta\gamma_{abc}$ and of the Weyl scalars $\delta\Psi_i$, $\delta\Psi_i^*$ which are the quantities we need to evaluate the universal Teukolsky equations (5.6), (5.8) and their conjugates.

The missing crucial step is to establish the link between the metric variables ψ_i and the Teukolsky variables. To this end, it is important to observe the following relations between the four radial variables R_s and R_s^*. First of all, since R_s and the "conjugates" R_s^* satisfy the same equation (and, in the case of QNMs, the same boundary conditions), it follows that they must be proportional,

$$\begin{aligned} R^*_{+2}(r) &= q_{+2}R_{+2}(r), \\ R^*_{-2}(r) &= q_{-2}R_{-2}(r), \end{aligned} \tag{5.51}$$

for certain constants $q_{\pm2}$. We will refer to these constants as polarisation parameters, since they determine the polarisation of the perturbations. This will become clear in Section 5.6.

[7] These are related to the more conventional definition of angular separation constants in the literature, denoted ${}_sA_{lm}$, by $B_{lm} = {}_sA_{lm} + s$. However, the advantage of using B_{lm} is that they are the same for $s = +2$ and $s = -2$ and hence we do not need to distinguish between the two cases.

On the other hand, R_{+2} and R_{-2} can be related by means of Starobinsky-Teukolsky (ST) identities, which we review in the Appendix D.1. These read

$$\begin{aligned} R_{-2} &= C_{+2}\Delta^2 \left(\mathcal{D}_0\right)^4 \left(\Delta^2 R_{+2}\right) , \\ R_{+2} &= C_{-2} \left(\mathcal{D}_0^\dagger\right)^4 R_{-2} , \end{aligned} \tag{5.52}$$

where $\mathcal{D}_0$ and $\mathcal{D}_0^\dagger$ are the operators

$$\begin{aligned} \mathcal{D}_0 &= \partial_r + \frac{i\left(\omega(r^2+a^2) - ma\right)}{\Delta} , \\ \mathcal{D}_0^\dagger &= \partial_r - \frac{i\left(\omega(r^2+a^2) - ma\right)}{\Delta} . \end{aligned} \tag{5.53}$$

The two proportionality constants $C_{\pm 2}$ are not independent but related by

$$C_{+2}C_{-2} = \frac{1}{\mathcal{K}^2} , \tag{5.54}$$

where

$$\mathcal{K}^2 = D_2^2 + 144M^2\omega^2 , \tag{5.55}$$

and D_2 is the ST constant for the angular functions, given by (D.4). Thus, in sum, the relations (5.51) and (5.52) imply that the full metric perturbation is determined once we know one of the R_s or R_s^* and the constants q_s and C_s.

When we use all of these relations, together with the ST identities for the angular functions — see Appendix D.1 — we find that the Weyl scalars equal the metric variables up to proportionality constants,

$$\delta\Psi_{2-s} = P_s\psi_{2-s} , \quad \delta\Psi^*_{2-s} = P_s^*\psi^*_{2-s} , \quad s = \pm 2 . \tag{5.56}$$

The constants P_s, P_s^* depend on the polarisation parameters q_s and ST constants C_s and are given by

$$\begin{aligned} P_{+2} &= \frac{1}{2} + \frac{iD_2 q_{+2}}{24M\omega} - \frac{iC_{+2}q_{-2}\mathcal{K}^2}{6M\omega} , \\ P_{-2} &= \frac{1}{2} - \frac{iD_2 q_{-2}}{24M\omega} + \frac{iC_{-2}q_{+2}\mathcal{K}^2}{96M\omega} , \\ P^*_{+2} &= \frac{1}{2} + \frac{iD_2}{24M\omega q_{+2}} - \frac{iC_{+2}\mathcal{K}^2}{6M\omega q_{+2}} , \\ P^*_{-2} &= \frac{1}{2} - \frac{iD_2}{24M\omega q_{-2}} + \frac{iC_{-2}\mathcal{K}^2}{96M\omega q_{-2}} . \end{aligned} \tag{5.57}$$

Note that there are two choices for q_s and C_s for which $P_s = P_s^* = 1$, corresponding to $q_{+2} = q_{-2} = \pm 1$ with

$$C_{+2} = \frac{1}{4(D_2 - q_{+2}12iM\omega)}\,, \quad C_{-2} = \frac{4}{D_2 - q_{+2}12iM\omega}\,. \tag{5.58}$$

However, we will not restrict ourselves to this choice of constants. On the one hand, the choices $q_{+2} = q_{-2} = \pm 1$ correspond to modes of definite parity, and this is not suitable for theories that violate parity, in whose case modes of odd and even parity become mixed. On the other hand, by allowing the ST constants to be general we will be able to perform a strong consistency check on our results in Section 5.6.

5.4 Separation of Teukolsky equations

Let us assume that we are performing perturbation theory on the background of a rotating black hole in the theory (4.1) — although most of the discussion in this section can be applied in generality to any other theory. Our starting point is the two perturbed Weyl scalars $\delta\Psi_{0,4}$ and their conjugates $\delta\Psi^*_{0,4}$. We can always separate the dependence in the t and ϕ coordinates since these are isometric coordinates. Without loss of generality, we can additionally decompose the Weyl scalars in spin-weighted spheroidal harmonics, since these are a basis of functions, and write

$$\begin{aligned}
\delta\Psi_0 &= e^{-i\omega t + im\phi} \sum_l P_2^{lm} R_2^{lm}(r) S_2^{lm}(x)\,,\\
\delta\Psi_4 &= e^{-i\omega t + im\phi} \sum_l \zeta^{-4} P_{-2}^{lm} R_{-2}^{lm}(r) S_{-2}^{lm}(x)\,,\\
\delta\Psi_0^* &= e^{-i\omega t + im\phi} \sum_l P_2^{*lm} R_2^{*lm}(r) S_{-2}^{lm}(x)\,,\\
\delta\Psi_4^* &= e^{-i\omega t + im\phi} \sum_l (\zeta^*)^{-4} P_{-2}^{*lm} R_{-2}^{*lm}(r) S_{+2}^{lm}(x)\,.
\end{aligned} \tag{5.59}$$

This decomposition depends on the four sets of radial functions $R_s^{lm}(r)$, $R_s^{*lm}(r)$. Also, here we are including the constants P_s^{lm} and P_s^{*lm} that we found in (5.56). There is no loss of generality in doing this, as we can reabsorb these constants into the radial variables. However, the computation is clearer in this way.

Now, the logic to find the radial Teukolsky equations goes as follows. We start with a Weyl tensor that we have decomposed as (5.59). In order to obtain the equations (5.24) from (5.6) and (5.8) we need the metric that produced this Weyl tensor. Of course, we do not know the answer for higher-derivative gravities. However, we know the answer for Einstein gravity: every mode in (5.59) comes from a metric perturbation given by (5.49). Therefore, in the case of perturbative higher-derivative corrections, the metric perturbation associated to the Weyl tensor (5.59) will correspond to (5.49) plus $\mathcal{O}(\lambda)$ terms. But these are irrelevant in order to obtain (5.24), since all the terms coming from the metric reconstruction are already of order λ. Hence, we simply use (5.49).

Using the expansion (5.59), the metric reconstruction (5.49) and the background solution (5.28) in (5.6) and (5.8), and expanding to linear order in the fluctuations and in the higher-derivative corrections, yields equations

$$
\begin{aligned}
&\frac{\zeta^{s-2}}{\Delta\Sigma}\sum_l \Bigg[- S_s^{lm} P_s^{lm} \mathfrak{D}_s^2 R_s^{lm} \\
&+ \lambda\left(f^{lm}_{s,0,0} R_s^{lm} S_s^{lm} + f^{lm}_{s,1,0} \frac{\mathrm{d}R_s^{lm}}{\mathrm{d}r} S_s^{lm} + f^{lm}_{s,0,1} R_s^{lm} \frac{\mathrm{d}S_s^{lm}}{\mathrm{d}x} + f^{lm}_{s,1,1} \frac{\mathrm{d}R_s^{lm}}{\mathrm{d}r}\frac{\mathrm{d}S_s^{lm}}{\mathrm{d}x} \right) \\
&+ \lambda\left(h^{lm}_{s,0,0} R_s^{*lm} S_{-s}^{lm} + h^{lm}_{s,1,0} \frac{\mathrm{d}R_s^{*lm}}{\mathrm{d}r} S_{-s}^{lm} + h^{lm}_{s,0,1} R_s^{*lm} \frac{\mathrm{d}S_{-s}^{lm}}{\mathrm{d}x} + h^{lm}_{s,1,1} \frac{\mathrm{d}R_s^{*lm}}{\mathrm{d}r}\frac{\mathrm{d}S_{-s}^{lm}}{\mathrm{d}x} \right) \\
&+ \lambda\left(g^{lm}_{s,0,0} R_{-s}^{lm} S_{-s}^{lm} + g^{lm}_{s,1,0} \frac{\mathrm{d}R_{-s}^{lm}}{\mathrm{d}r} S_{-s}^{lm} + g^{lm}_{s,0,1} R_{-s}^{lm} \frac{\mathrm{d}S_{-s}^{lm}}{\mathrm{d}x} + g^{lm}_{s,1,1} \frac{\mathrm{d}R_{-s}^{lm}}{\mathrm{d}r}\frac{\mathrm{d}S_{-s}^{lm}}{\mathrm{d}x} \right) \\
&+ \lambda\left(j^{lm}_{s,0,0} R_{-s}^{*lm} S_s^{lm} + j^{lm}_{s,1,0} \frac{\mathrm{d}R_{-s}^{*lm}}{\mathrm{d}r} S_s^{lm} + j^{lm}_{s,0,1} R_{-s}^{*lm} \frac{\mathrm{d}S_s^{lm}}{\mathrm{d}x} + j^{lm}_{s,1,1} \frac{\mathrm{d}R_{-s}^{*lm}}{\mathrm{d}r}\frac{\mathrm{d}S_s^{lm}}{\mathrm{d}x} \right) \Bigg] = 0\,,
\end{aligned}
\tag{5.60}
$$

for $s = \pm 2$, plus another two conjugate equations. Here $\mathfrak{D}_s^2$ is the radial Teukolsky operator defined in (5.47) and $f^{lm}_{s,i,j}$, $h^{lm}_{s,i,j}$, $g^{lm}_{s,i,j}$ and $j^{lm}_{s,i,j}$ are functions of r and x as well as the black-hole spin a, the angular separation constants B_{lm} and the frequency ω. These functions additionally depend on the H_i functions of the corrected Kerr metric (5.28). They are given by very lengthy and uninformative expressions that we obtained explicitly for the six-derivative theories. Note that in the terms proportional to λ only first derivatives appear, as we have used the zeroth-order radial and angular Teukolsky equations to reduce the derivatives of higher order. For this reason, the functions $f^{lm}_{s,i,j}$, $h^{lm}_{s,i,j}$, $g^{lm}_{s,i,j}$ and $j^{lm}_{s,i,j}$ depend on the angular separation constants B_{lm}.

Let us now make the following two observations. First, the spin-weighted spheroidal harmonics satisfy the orthogonality relations[8]

$$2\pi \int_{-1}^{1} \mathrm{d}x\, S_s^{lm}(x;a\omega) S_s^{l'm}(x;a\omega) = \delta_{ll'}\,, \tag{5.61}$$

which hold even for complex ω. We can thus project the equations (5.60) into $S_s^{l'm}$ and obtain an infinite system of radial equations labelled by the number l',

$$-P_s^{l'm}\mathfrak{D}_s^2 R_s^{l'm} + \sum_l \lambda \left(f_{s,0}^{l'lm} R_s^{lm} + f_{s,1}^{l'lm} \frac{\mathrm{d}R_s^{lm}}{\mathrm{d}r} + h_{s,0}^{l'lm} R_s^{*lm} + h_{s,1}^{l'lm} \frac{\mathrm{d}R_s^{*lm}}{\mathrm{d}r} \right.$$
$$\left. + g_{s,0}^{l'lm} R_{-s}^{lm} + g_{s,1}^{l'lm} \frac{\mathrm{d}R_{-s}^{lm}}{\mathrm{d}r} + j_{s,0}^{l'lm} R_{-s}^{*lm} + j_{s,1}^{l'lm} \frac{\mathrm{d}R_{-s}^{*lm}}{\mathrm{d}r} \right) = 0\,, \tag{5.62}$$

where

$$\begin{aligned}
f_{s,i}^{l'lm} &= 2\pi \int_{-1}^{1} \mathrm{d}x\, S_s^{l'm} \left(f_{s,i,0}^{lm} S_s^{lm} + f_{s,i,1}^{lm} \frac{\mathrm{d}S_s^{lm}}{\mathrm{d}x} \right)\,, \\
h_{s,i}^{l'lm} &= 2\pi \int_{-1}^{1} \mathrm{d}x\, S_s^{l'm} \left(h_{s,i,0}^{lm} S_{-s}^{lm} + h_{s,i,1}^{lm} \frac{\mathrm{d}S_{-s}^{lm}}{\mathrm{d}x} \right)\,, \\
g_{s,i}^{l'lm} &= 2\pi \int_{-1}^{1} \mathrm{d}x\, S_s^{l'm} \left(g_{s,i,0}^{lm} S_{-s}^{lm} + g_{s,i,1}^{lm} \frac{\mathrm{d}S_{-s}^{lm}}{\mathrm{d}x} \right)\,, \\
j_{s,i}^{l'lm} &= 2\pi \int_{-1}^{1} \mathrm{d}x\, S_s^{l'm} \left(j_{s,i,0}^{lm} S_s^{lm} + j_{s,i,1}^{lm} \frac{\mathrm{d}S_s^{lm}}{\mathrm{d}x} \right)\,.
\end{aligned} \tag{5.63}$$

These are functions of r only.

Second, as the quasinormal modes of the Kerr black hole consist of a single term with a fixed l and m, in the corrected QNMs the sum in (5.59) will contain a leading term whilst the rest of the terms will be of order λ. That is, for the QNM that we would label with the numbers l_0 and m, we will have $R_s^{l_0 m} = \mathcal{O}(1)$ and $R_s^{lm} = \mathcal{O}(\lambda)$ for $l \neq l_0$.

[8] We remark that, addition to orthogonality, this relation defines our convention for their normalisation.

Therefore, at first order in λ, equation (5.62) becomes

$$-P_s^{l'm}\mathfrak{D}_s^2 R_s^{l'm} + \lambda\left(f_{s,0}^{l'l_0m}R_s^{l_0m} + f_{s,1}^{l'l_0m}\frac{\mathrm{d}R_s^{l_0m}}{\mathrm{d}r} + h_{s,0}^{l'l_0m}R_s^{*l_0m} + h_{s,1}^{l'l_0m}\frac{\mathrm{d}R_s^{*l_0m}}{\mathrm{d}r}\right.$$
$$\left. + g_{s,0}^{l'l_0m}R_{-s}^{l_0m} + g_{s,1}^{l'l_0m}\frac{\mathrm{d}R_{-s}^{l_0m}}{\mathrm{d}r} + j_{s,0}^{l'l_0m}R_{-s}^{*l_0m} + j_{s,1}^{l'l_0m}\frac{\mathrm{d}R_{-s}^{*l_0m}}{\mathrm{d}r}\right) = 0\,, \tag{5.64}$$

and similarly for the conjugate equations. For $l' = l_0$ these are in total four equations that only involve the variables $R_s^{l_0m}$, $R_s^{*l_0m}$. Dropping the labels for clarity, we find the master radial equations

$$-P_{+2}\mathfrak{D}_{+2}^2 R_{+2} + \lambda\left(f_{+2,0}R_{+2} + f_{+2,1}\frac{\mathrm{d}R_{+2}}{\mathrm{d}r} + h_{+2,0}R_{+2}^* + h_{+2,1}\frac{\mathrm{d}R_{+2}^*}{\mathrm{d}r}\right.$$
$$\left. + g_{+2,0}R_{-2} + g_{+2,1}\frac{\mathrm{d}R_{-2}}{\mathrm{d}r} + j_{+2,0}R_{-2}^* + j_{+2,1}\frac{\mathrm{d}R_{-2}^*}{\mathrm{d}r}\right) = 0\,,$$
$$-P_{-2}\mathfrak{D}_{-2}^2 R_{-2} + \lambda\left(f_{-2,0}R_{-2} + f_{-2,1}\frac{\mathrm{d}R_{-2}}{\mathrm{d}r} + h_{-2,0}R_{-2}^* + h_{-2,1}\frac{\mathrm{d}R_{-2}^*}{\mathrm{d}r}\right.$$
$$\left. + g_{-2,0}R_{+2} + g_{-2,1}\frac{\mathrm{d}R_{+2}}{\mathrm{d}r} + j_{-2,0}R_{+2}^* + j_{-2,1}\frac{\mathrm{d}R_{+2}^*}{\mathrm{d}r}\right) = 0\,, \tag{5.65}$$

together with their conjugate counterparts.

We still need to compute the integrals in (5.63) in order to determine the functions $f_{s,i}^{llm}$, $h_{s,i}^{llm}$, $g_{s,i}^{llm}$, and $j_{s,i}^{llm}$. This could be achieved numerically if a numerical solution for the corrected background is known. However, a possibility to obtain an analytic result consists in performing an expansion in the black-hole spin $\chi = a/M$. On the one hand, we know analytically the χ^n expansion of the functions H_i determining the background black-hole metric. On the other hand, the spin-weighted spheroidal harmonics $S_s^{lm}(x; a\omega)$ and the angular separation constants B_{lm} have analytic expansions for small $\gamma = a\omega$ [107].[9]

[9] Strictly speaking, one should perform a double series expansion both in χ and in γ, but for simplicity here we perform an overall expansion in χ using that $\gamma = M\omega\chi$. This could be problematic only if ω is large, so that $|\gamma| >> 1$, because in that case one may need to include more terms in the γ expansion. However, the result should converge anyways if enough terms are included in the overall χ expansion. Besides, for the most relevant QNMs, corresponding to the fundamental modes and a few overtones of the first few harmonics $l = 2, 3, ...$, we actually have $|\gamma| < \chi$.

When we expand the integrand of (5.63) in powers of χ, we find that every term can indeed be integrated analytically. Thus we are able to obtain explicit expressions for the functions

$$f^{llm}_{s,i}(r;a,\omega)\,, \quad h^{llm}_{s,i}(r;a,\omega)\,, \quad g^{llm}_{s,i}(r;a,\omega)\,, \quad j^{llm}_{s,i}(r;a,\omega) \tag{5.66}$$

as series expansions in a. By including enough terms in these expansions, one should be able to obtain an accurate result, even for moderate or large spins.

5.5 Radial master equations

So far we have been able to reduce the problem of studying black-hole perturbations to a system of four coupled radial equations (5.65) (and their conjugate versions) for the variables R_s and R^*_s. This problem can already be tackled with different methods in order to find the quasinormal modes [51], but it is still much more involved than the case of a decoupled equation. To decouple these equations, the idea is to use the Starobinsky-Teukolsky identities (5.52) as well as the relations with the conjugate variables (5.51). In fact, those relations are already implicitly assumed in (5.65) through the constants P_s.

We note that, upon using the zeroth-order Teukolsky equations, the ST relationships (5.52) can be expressed in the form of a first order operator,

$$\begin{aligned} R_{-2} &= C_{+2}\left(A_{+2}R_{+2} + B_{+2}\frac{\mathrm{d}R_{+2}}{\mathrm{d}r}\right)\,, \\ R_{+2} &= C_{-2}\left(A_{-2}R_{-2} + B_{-2}\frac{\mathrm{d}R_{-2}}{\mathrm{d}r}\right)\,, \end{aligned} \tag{5.67}$$

for given functions $A_{\pm 2}$, $B_{\pm 2}$. Taking a derivative in these expressions and using again the Teukolsky equations we obtain similar relations for the derivatives $dR_{\pm 2}/dr$. Combining these relations with (5.51), we can always express any of the R_s or R^*_s in terms of any of the other variables.

All of these relations hold at zeroth order in λ because the radial variables satisfy the zeroth-order Teukolsky equations. Therefore, we are allowed to assume those relations in the terms proportional to λ in (5.65). The result is four decoupled equations of the form (for $s = \pm 2$)

$$\begin{aligned} -P_s\mathfrak{D}_s^2 R_s + \lambda\left[f_{s,0}R_s + f_{s,1}\frac{\mathrm{d}R_s}{\mathrm{d}r}\right] &= 0\,, \\ -P^*_s\mathfrak{D}_s^2 R^*_s + \lambda\left[f^*_{s,0}R^*_s + f^*_{s,1}\frac{\mathrm{d}R^*_s}{\mathrm{d}r}\right] &= 0\,, \end{aligned} \tag{5.68}$$

The price to pay for the decoupling is that the functions $f_{s,i}$, $f^*_{s,i}$ now depend on the polarisation parameters q_s and the ST constants C_s. Let us take note that the dependence on these parameters is of the form

$$f_{s,i} = f_{s,i,1} + q_s f_{s,i,2} + C_s f_{s,i,3} + C_s q_{-s} f_{s,i,3}\,, \tag{5.69}$$

$$f^*_{s,i} = f^*_{s,i,1} + q_s^{-1} f^*_{s,i,2} + C_s q_s^{-1} f^*_{s,i,3} + C_s q_{-s} q_s^{-1} f^*_{s,i,3}\,, \tag{5.70}$$

where each of the $f_{s,i,j}$ and $f^*_{s,i,j}$ are functions or r. We recall that the coefficients P_s and P^*_s (5.57) also depend on these constants.

Now, besides the two polarisation parameters q_s and one of the C_s, there is a fourth undetermined constant in the problem: the frequency ω. In order to obtain the QNMs, we must proceed as follows. We can solve each equation in (5.68) independently to find the shift in Kerr's QNM frequency,

$$\omega_s = \omega_{\rm Kerr} + \lambda\delta\omega_s \quad \omega^*_s = \omega_{\rm Kerr} + \lambda\delta\omega^*_s\,, \tag{5.71}$$

where ω_s and ω^*_s denote the frequency obtained from the corresponding equation. The shifts $\delta\omega_s$ and $\delta\omega^*_s$ are functions of the various parameters and we can see that their dependence on them is of the form

$$\begin{aligned}
\delta\omega_s &= \frac{1}{P_s}\left[\delta\omega_{s,1} + q_s\delta\omega_{s,2} + C_s\delta\omega_{s,3} + C_s q_{-s}\delta\omega_{s,4}\right]\,,\\
\delta\omega^*_s &= \frac{1}{q_s P^*_s}\left[q_s\delta\omega^*_{s,1} + \delta\omega^*_{s,2} + C_s\delta\omega^*_{s,3} + C_s q_{-s}\delta\omega^*_{s,4}\right]\,,
\end{aligned} \tag{5.72}$$

where $\delta\omega_{s,i}$ and $\delta\omega^*_{s,i}$ are coefficients that we have to determine numerically. Now, for a QNM, the same frequency must be a solution of all the equations. Therefore, the following must hold in a QNM solution

$$\delta\omega_{+2}(q_s, C_s) = \delta\omega_{-2}(q_s, C_s) = \delta\omega^*_{+2}(q_s, C_s) = \delta\omega^*_{-2}(q_s, C_s)\,. \tag{5.73}$$

These equations fix the value of the polarisation parameters q_s, allowing us to obtain the QNM frequencies. On the other hand, as we show explicitly in the next section, the values of the ST constants C_s remain arbitrary because the frequencies are actually independent of these constants. This is a highly non-trivial fact that cannot be easily concluded from the form of the equations. Nevertheless, our numeric results confirm this, as will be discussed in the next section. This is a strong self-consistency test of our method: it tells us that the choice of ST constants represents a choice of gauge to reconstruct the metric perturbation from the Teukolsky variables. The same behaviour is found in general relativity, where one can reconstruct the metric perturbation in the ingoing or outgoing radiation gauges, or more generally, as a linear combination of both [64, 106].

5.6 Quasinormal modes in six-derivative gravity

As an application of our method, we compute the $(l, m) = (2, 2)$ and $(3, 3)$ fundamental QNM frequencies of the six-derivative theory to linear order in the higher-derivative couplings. By following the procedure outlined in the previous sections we have obtained the radial equations (5.68) for those modes at order a^6 and a^4, respectively. One last technical obstacle arises in the computation: we observe that the corrections to the Teukolsky equations in (5.68) have a singular character at the horizon because $f_{s,i}$ and $f^*_{s,i}$ behave as $f_{s,0} \sim (r - r_+)^{-1}$ and $f_{s,1} \sim (r - r_+)^0$. This behaviour, which arises due to the fact that we have reduced the order of the equations of motion by imposing the zeroth-order equations, is problematic for the following reason. Observe that we want our variables to behave as $R_s \sim (r - r_+)^\gamma$, near the horizon, for a certain γ. In that case we have $\mathfrak{D}_s^2 R_s \sim (r - r_+)^\gamma$, but due to the behaviour of the $f_{s,i}$ functions, the terms proportional to λ in (5.68) behave in turn as $(r - r_+)^{\gamma-1}$. This indicates that the variables R_s, R^*_s are not appropriate in the presence of corrections. In fact, we can redefine the variables as[10]

$$\begin{aligned} R_s &= \hat{R}_s + \lambda \left(\alpha_s \hat{R}_s + \beta_s \frac{\mathrm{d}\hat{R}_s}{\mathrm{d}r} \right) , \\ R^*_s &= \hat{R}^*_s + \lambda \left(\alpha^*_s \hat{R}^*_s + \beta^*_s \frac{\mathrm{d}\hat{R}^*_s}{\mathrm{d}r} \right) , \end{aligned} \tag{5.74}$$

for radial-dependent coefficients α_s, β_s, α^*_s, β^*_s. The equation for the new variables $\hat{R}_s$, $\hat{R}^*_s$ can again be rewritten — after making use of the zeroth-order Teukolsky equation in the terms proportional to λ — in the form of (5.68), with new functions $\hat{f}_{s,i}$, $\hat{f}^*_{s,i}$ that depend on the α_s, β_s, α^*_s, β^*_s functions. It suffices to choose these functions as

$$\alpha_s(r) = \frac{a_s}{r - r_+} , \quad \beta_s(r) = b_s , \tag{5.75}$$

for constants a_s, b_s, and analogously for α^*_s and β^*_s. By choosing the coefficients a_s, b_s appropriately, we can remove the divergences and obtain well-behaved equations for the variables $\hat{R}_s$, with the functions $\hat{f}_{s,i}$ satisfying $\hat{f}_{s,0} \sim (r - r_+)^0$, $\hat{f}_{s,1} \sim (r - r_+)$ for $r \to r_+$.

[10] We suspect the origin of these singularities lies in the choice of corrected NP frame (5.40), which is probably singular at the horizon. A redefinition of the radial variables is therefore equivalent to choosing a different NP frame.

In fact, with this choice we find that these functions take a polynomial form

$$\hat{f}_{s,0}(r) = M^2 \sum_{n=0}^{N} \left(\frac{r}{M}\right)^{4-n} \hat{f}_{s,0,n}\,, \quad \hat{f}_{s,1}(r) = M(r-r_+) \sum_{n=0}^{N} \left(\frac{r}{M}\right)^{3-n} \hat{f}_{s,1,n} \tag{5.76}$$

where $\hat{f}_{s,i,n}$ are coefficients and N increases with the order of the a-expansion. Thus, the resulting equations

$$\begin{aligned} -P_s \mathfrak{D}_s^2 \hat{R}_s + \lambda \left[\hat{f}_{s,0}\hat{R}_s + f_{s,1}\frac{\mathrm{d}\hat{R}_s}{\mathrm{d}r}\right] = 0\,, \\ -P_s^* \mathfrak{D}_s^2 \hat{R}_s^* + \lambda \left[\hat{f}_{s,0}^*\hat{R}_s^* + \hat{f}_{s,1}^*\frac{\mathrm{d}\hat{R}_s^*}{\mathrm{d}r}\right] = 0\,, \end{aligned} \tag{5.77}$$

now have the same behaviour as the zeroth-order Teukolsky equation for $r \to r_+$ and for $r \to \infty$, and we can impose the usual boundary conditions for QNMs. At $r = r_+$ the solution must behave as

$$R_s \sim \left(\frac{r}{r_+} - 1\right)^{\gamma_s}\,, \quad \gamma_s = -s - \frac{i}{r_+^2 - a^2}\left[2\omega M r_+ - ma\right] + \lambda\delta\gamma_s\,, \tag{5.78}$$

where the exponent corresponds to modes falling toward the black-hole horizon. The exponent takes the Kerr value plus a theory-dependent correction $\delta\gamma_s$. At infinity $r \to \infty$ we look for solutions corresponding to outgoing radiation, and hence R_s behaves as

$$R_s \sim r^{-1-2s} e^{-i\omega(1+\lambda\delta)r}\,, \tag{5.79}$$

where again δ is a theory-dependent coefficient.

In order to find the QNM frequencies we have applied two different numerical approaches. The first one consists in performing a direct numerical integration of (5.77) with the boundary conditions (5.78), (5.79), implementing a shooting-method strategy in order to find ω. The second one is based on the approach of [85, 86, 88], in the spirit of computing spectral shifts of a perturbed Hermitian operator. The results we report below were obtained from the first method, but we checked that the relative difference between the two methods for the shift in the QNM frequencies is smaller than 2% for $|\chi| \leq 0.12$ and remains this small on average for the complete range of values of the dimensionless spin we study. Let us discuss the cases of the even- and odd-parity theories independently.

5.6.1 Even-parity corrections

We consider Einstein gravity supplemented with the even-parity six-derivative operator. This will introduce corrections to the Kerr QNM frequencies that we can express as

$$\omega = \omega^{\rm Kerr} + \frac{\ell^4 \lambda_{\rm ev}}{M^5} \delta\omega \,, \tag{5.80}$$

so that $\delta\omega$ is a dimensionless coefficient that depends on the dimensionless spin χ. Our goal is to determine this coefficient.

In the case of parity-preserving corrections, perturbations can be naturally decoupled into modes of odd and even parity. For the background metric (5.28), a natural parity transformation corresponds to

$$(x, \phi) \to (-x, \phi + \pi) \,. \tag{5.81}$$

One can see that on the NP frame this has the effect $(m_\mu, \bar{m}_\mu) \to -(\bar{m}_\mu, m_\mu)$. In addition, the spheroidal harmonics verify $S_s(-x) = \pm S_{-s}(x)$. Therefore, up to a global sign, the parity transformation (5.81) is equivalent to $R_s \leftrightarrow R_s^*$ at the level of the metric perturbation (5.49). Hence, we conclude that the modes of definite parity are those with

$$R_s = \pm R_s^* \,, \tag{5.82}$$

or in other words, this fixes the polarisation parameters q_s to be $q_{+2} = q_{-2} = \pm 1$. The $+$ sign corresponds to polar perturbations whilst the $-$ sign to axial ones. When $q_s = \pm 1$, we check that, indeed, the conjugate equations in (5.77) are identical to the non-conjugate ones. Thus, we only need to consider the equations for $\hat{R}_{+2}$ and $\hat{R}_{-2}$, and only the ST constants C_s remain unspecified. By solving these equations and taking into account (5.72) and (5.57), we obtain that the shifts in the QNM frequencies for each polarisation $\pm$ take the form

$$\delta\omega_s^{\pm} = \sigma_s^{\pm} \frac{1 + \gamma_s^{\pm} C_s}{1 + \rho_s^{\pm} C_s} \,, \tag{5.83}$$

for coefficients $\sigma_s^{\pm}$, $\gamma_s^{\pm}$, $\rho_s^{\pm}$ that depend on the dimensionless spin χ and that we determine numerically. Then one may think that the ST constants are determined by the condition that the two shifts are the same (because all the equations should give the same QNM frequency), so that we would have the equation $\delta\omega_{+2} = \delta\omega_{-2}$ for the ST constants. However, the numerical results indicate strongly that

$$\gamma_s^{\pm} = \rho_s^{\pm} \,, \tag{5.84}$$

meaning that the QNM frequencies are, in fact, independent of these constants, which can be chosen arbitrarily. Furthermore, and even more importantly, the numerical results also indicate that $\delta\omega_{+2}^{\pm} = \delta\omega_{-2}^{\pm}$.

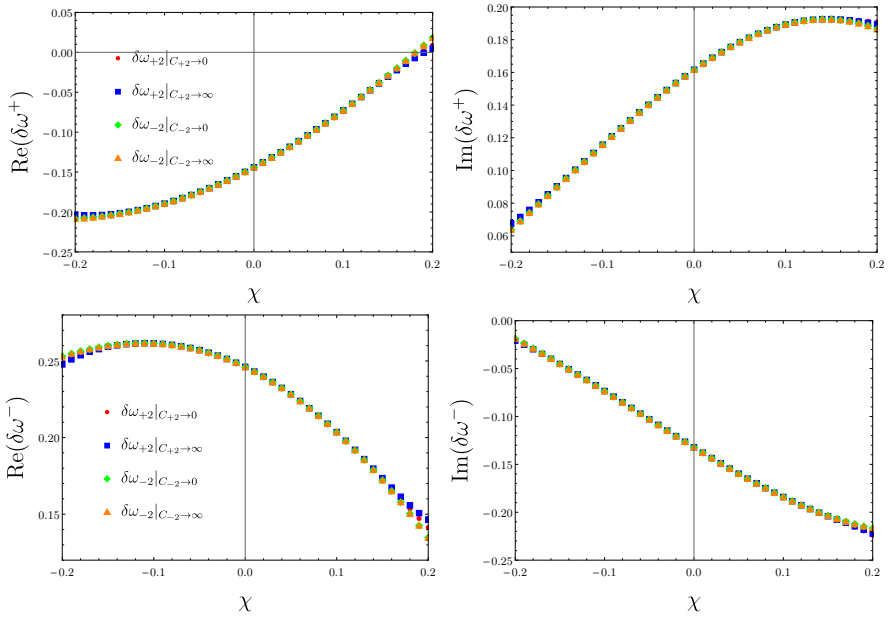


Figure 5.2: Shifts in the polar (top row) and axial (bottom row) QNMs frequencies with $(l, m) = (2, 2)$ due to the even-parity six-derivative correction.

To illustrate this, we compute the shifts $\delta\omega_s$ for $C_s = 0$ and $C_s \to \infty$. Let us first study the case of the $(l, m) = (2, 2)$ modes. In Fig. 5.2 we show the four different results,

$$\delta\omega_{+2}\big|_{C_{+2}=0}\,, \quad \delta\omega_{+2}\big|_{C_{+2}=\infty}\,, \quad \delta\omega_{-2}\big|_{C_{-2}=0}\,, \quad \delta\omega_{-2}\big|_{C_{-2}=\infty}\,, \tag{5.85}$$

for each polarisation obtained from a numerical integration of (5.77) expanded at order χ^6. We observe that all the frequencies are in fact almost identical for all the values of χ we are plotting. Especially, the two estimations for $\delta\omega_{-2}$ are indistinguishable in these plots, indicating that they are independent of C_{-2}. These two values remain very close to each other even for larger values of the spin, up to $|\chi| \sim 0.4$. On the other hand, we observe that the two estimations for $\delta\omega_{+2}$ differ slightly from each other and from $\delta\omega_{-2}$ already at $|\chi| \sim 0.2$. These small discrepancies can be explained by the truncation of the spin expansion and differences between the $s = +2$ and $s = -2$ equations.

In fact, we expect the equations to yield the same QNM frequencies only when the complete series in χ is included, but when the series in truncated at a given order we can only expect the results to agree for small enough χ.

In order to perform a quantitative comparison, we can fit the numerical results to a polynomial in χ. Performing a quadratic fit in the interval $-0.1 \leq \chi \leq 0.1$ we obtain the following result for the polar modes

$$\begin{aligned}
\delta\omega^{+}_{+2}\big|_{C_{+2}=0} &= (-0.144 + 0.162i) + (0.586 + 0.375i)\chi + (1.290 - 0.909i)\chi^2\,,\\
\delta\omega^{+}_{+2}\big|_{C_{+2}=\infty} &= (-0.144 + 0.162i) + (0.586 + 0.375i)\chi + (1.290 - 0.909i)\chi^2\,,\\
\delta\omega^{+}_{-2}\big|_{C_{-2}=0} &= (-0.144 + 0.162i) + (0.586 + 0.375i)\chi + (1.294 - 0.911i)\chi^2\,,\\
\delta\omega^{+}_{-2}\big|_{C_{-2}=\infty} &= (-0.144 + 0.162i) + (0.586 + 0.375i)\chi + (1.294 - 0.911i)\chi^2\,,
\end{aligned} \tag{5.86}$$

whilst for the axial ones we get

$$\begin{aligned}
\delta\omega^{-}_{+2}\big|_{C_{+2}=0} &= (0.246 - 0.132i) - (0.289 + 0.560i)\chi - (1.360 - 0.337i)\chi^2\,,\\
\delta\omega^{-}_{+2}\big|_{C_{+2}=\infty} &= (0.246 - 0.132i) - (0.289 + 0.560i)\chi - (1.360 - 0.337i)\chi^2\,,\\
\delta\omega^{-}_{-2}\big|_{C_{-2}=0} &= (0.246 - 0.132i) - (0.289 + 0.559i)\chi - (1.358 - 0.338i)\chi^2\,,\\
\delta\omega^{-}_{-2}\big|_{C_{-2}=\infty} &= (0.246 - 0.132i) - (0.289 + 0.559i)\chi - (1.359 - 0.338i)\chi^2\,.
\end{aligned} \tag{5.87}$$

These results pass several consistency tests. First, the agreement of the $\mathcal{O}(\chi^0)$ and $\mathcal{O}(\chi^1)$ coefficients is essentially perfect. In addition, those coefficients match with good accuracy the results obtained in Chapter 4 following a direct metric perturbation approach. In fact, in that case we got

$$\begin{aligned}
\delta\omega^{+} &= -0.137 + 0.161i + (0.612 + 0.376i)\chi + \mathcal{O}(\chi^2)\,,\\
\delta\omega^{-} &= 0.244 - 0.130i - (0.288 + 572i)\chi + \mathcal{O}(\chi^2)\,.
\end{aligned} \tag{5.88}$$

which coincide with the results above with an accuracy better than 5% for $\delta\omega^{+}$[11] and around 1% for $\delta\omega^{-}$.

Finally, the agreement among the $\mathcal{O}(\chi^2)$ coefficients is also excellent. The small discrepancies can be easily attributed to the numerical precision and to the different behaviour of the equations for a finite truncation of the spin series.

[11] We suspect that most of this error comes from the results in Chapter 4, since the result in (5.86), obtained in four different ways, seems to be very robust. Additionally, we can quote the results of [52] for static black holes, which in our conventions yield $\delta\omega^{+} \approx -0.144 + 0.163i$ and $\delta\omega^{-} \approx 0.246 - 0.133i$, matching our results here with an error less than 1%.

As a further test, we have also computed the $(l,m) = (3,3)$ modes. The convergence in the spin expansion seems to be faster than for $l = 2$ and in fact, we obtain a similar accuracy using an expansion of order χ^4 instead of χ^6. The four different estimations for the frequencies are shown in Fig. 5.3, where we again observe that all of them remain very close to each other.

Fitting these results to a quadratic polynomial in the range $-0.1 \leq \chi \leq 0.1$ yields

$$\begin{aligned}
\delta\omega^{+}_{+2}\big|_{C_{+2}=0} &= (-0.265 + 0.150i) + (0.575 + 0.418i)\chi + (1.405 - 0.473i)\chi^2\,, \\
\delta\omega^{+}_{+2}\big|_{C_{+2}=\infty} &= (-0.265 + 0.150i) + (0.576 + 0.418i)\chi + (1.411 - 0.473i)\chi^2\,, \\
\delta\omega^{+}_{-2}\big|_{C_{-2}=0} &= (-0.265 + 0.150i) + (0.573 + 0.418i)\chi + (1.398 - 0.463i)\chi^2\,, \\
\delta\omega^{+}_{-2}\big|_{C_{-2}=\infty} &= (-0.265 + 0.150i) + (0.573 + 0.418i)\chi + (1.401 - 0.463i)\chi^2\,,
\end{aligned} \tag{5.89}$$

and

$$\begin{aligned}
\delta\omega^{-}_{+2}\big|_{C_{+2}=0} &= (0.343 - 0.134i) - (0.373 + 0.444i)\chi - (1.295 - 0.319i)\chi^2\,, \\
\delta\omega^{-}_{+2}\big|_{C_{+2}=\infty} &= (0.343 - 0.134i) - (0.374 + 0.445i)\chi - (1.301 - 0.318i)\chi^2\,, \\
\delta\omega^{-}_{-2}\big|_{C_{-2}=0} &= (0.343 - 0.134i) - (0.372 + 0.445i)\chi - (1.291 - 0.316i)\chi^2\,, \\
\delta\omega^{-}_{-2}\big|_{C_{-2}=\infty} &= (0.343 - 0.134i) - (0.372 + 0.445i)\chi - (1.294 - 0.315i)\chi^2\,.
\end{aligned} \tag{5.90}$$

We observe excellent agreement among all the coefficients, including those of χ^2, and again the results to linear order reproduce the ones previously obtained in Chapter 4, which we rewrite here for convenience

$$\begin{aligned}
\delta\omega^{+} &= -0.258 + 0.151i + (0.597 + 0.426i)\chi + \mathcal{O}(\chi^2)\,, \\
\delta\omega^{-} &= 0.340 - 0.132i - (0.369 + 0.447i)\chi + \mathcal{O}(\chi^2)\,.
\end{aligned} \tag{5.91}$$

These results make us confident that the frequencies are indeed independent of the choice of ST constants and that both equations $s = 2$ and $s = -2$ yield the same frequencies. These highly non-trivial properties, together with the fact that we reproduce the results at linear order in the spin of Chapter 4, provide a strong test of the validity of our approach and computations.

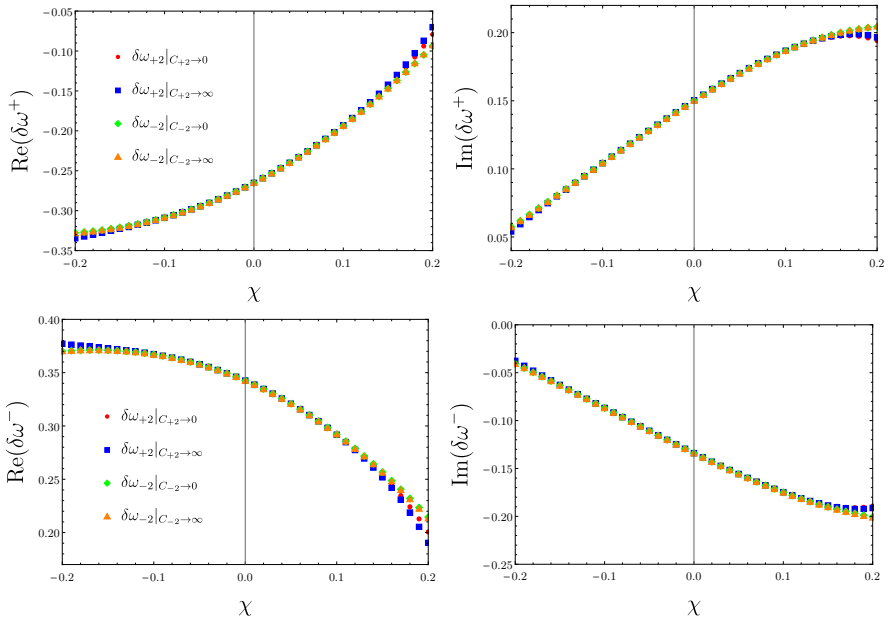


Figure 5.3: Shifts in the polar (top row) and axial (bottom row) QNMs frequencies with $(l, m) = (3, 3)$ due to the even-parity six-derivative correction.

5.6.2 Odd-parity corrections

Let us now consider the parity-breaking cubic interaction, and write the corresponding shift in the QNM frequencies as

$$\omega = \omega^{\text{Kerr}} + \frac{\ell^4 \lambda_{\text{odd}}}{M^5} \delta\omega \,. \tag{5.92}$$

Since this theory does not preserve parity, we can no longer decouple polar and axial modes, and these are unavoidably mixed. The polarisation parameters q_s have to be determined at the same time as the frequencies by solving (5.73). Now, based on our experience with the parity-preserving corrections, we expect the frequencies to be independent of the choice of ST constants, since these represent, essentially, a redundancy in our description of perturbations. To test this, we solve the equations (5.73) again in the limits $C_s \to 0$ and $C_s \to \infty$, in which case the $s = 2$ and $s = -2$ equations decouple. For instance, if we set $C_{+2} = 0$, then the condition $\delta\omega_{+2} = \delta\omega^*_{+2}$ gives us an equation for q_{+2} which has two solutions. Naturally these correspond to the two possible polarisations for QNMs, and in this case $q_{+2} \neq \pm 1$, indicating that these modes do not have a definite parity. If instead we set $C_{+2} \to \infty$ then the condition $\delta\omega_{+2} = \delta\omega^*_{+2}$ gives us an equation for q_{-2} which again has two solutions. A similar discussion applies for the case of $\delta\omega_{-2} = \delta\omega^*_{-2}$ for $C_{-2} = 0$ and $C_{-2} \to \infty$.

Proceeding in this way, we obtain four independent estimations for the shifts in the QNM frequencies. If everything is consistent, the four results should agree. As a first check, we observe that the two different polarisations $\delta\omega^{\pm}$ obtained in each case satisfy

$$\delta\omega^{+} = -\delta\omega^{-} \,. \tag{5.93}$$

This is expected for parity-breaking corrections since they couple odd- and even-parity modes [51, 72]. Thus, we show only the shifts with $\mathrm{Re}(\delta\omega) > 0$, as the other polarisation simply has a shift $-\delta\omega$. In Fig. 5.4 we show these shifts for the $(l,m) = (2,2)$ modes whilst in Fig. 5.5 we show the $(l,m) = (3,3)$ ones.

We observe that the four different estimations of the QNM frequencies match with very high accuracy.

Performing a quadratic fit in the interval $-0.1 < \chi < 0.1$ for the $(l,m) = (2,2)$ modes yields

$$\begin{aligned}
\delta\omega_{+2}\big|_{C_{+2}=0} &= (0.197\ -0.151i) - (0.447\ +0.506i)\chi - (1.371\ -0.291i)\chi^2 \,, \\
\delta\omega_{+2}\big|_{C_{+2}=\infty} &= (0.197\ -0.151i) - (0.447\ +0.506i)\chi - (1.373\ -0.289i)\chi^2 \,, \\
\delta\omega_{-2}\big|_{C_{-2}=0} &= (0.197\ -0.151i) - (0.445\ +0.506i)\chi - (1.356\ -0.293i)\chi^2 \,, \\
\delta\omega_{-2}\big|_{C_{-2}=\infty} &= (0.197\ -0.151i) - (0.445\ +0.505i)\chi - (1.354\ -0.296i)\chi^2 \,,
\end{aligned} \tag{5.94}$$

and in the case of the $(l,m) = (3,3)$ modes we obtain

$$\begin{aligned}
\delta\omega_{+2}\big|_{C_{+2}=0} &= (0.304\ -0.143i) - (0.475\ +0.432i)\chi - (1.354\ -0.396i)\chi^2 \,, \\
\delta\omega_{+2}\big|_{C_{+2}=\infty} &= (0.304\ -0.143i) - (0.475\ +0.433i)\chi - (1.359\ -0.395i)\chi^2 \,, \\
\delta\omega_{-2}\big|_{C_{-2}=0} &= (0.304\ -0.143i) - (0.473\ +0.433i)\chi - (1.348\ -0.389i)\chi^2 \,, \\
\delta\omega_{-2}\big|_{C_{-2}=\infty} &= (0.304\ -0.143i) - (0.473\ +0.433i)\chi - (1.347\ -0.388i)\chi^2 \,,
\end{aligned} \tag{5.95}$$

finding excellent agreement in all the coefficients. Finally, these results compare well with those in Chapter 4, which we reproduce here for convenience:[12]

$$\begin{aligned}
\delta\omega_{2,2} &= 0.192 - 0.151i - (0.466 + 0.414i)\chi + \mathcal{O}(\chi^2) \,, \\
\delta\omega_{3,3} &= 0.304 - 0.144i - (0.493 + 0.438i)\chi + \mathcal{O}(\chi^2) \,.
\end{aligned} \tag{5.96}$$

[12] As already observed in Footnote 11, we suspect that our results here are more accurate than those in Chapter 4 and hence the small discrepancies can likely be attributed to it.

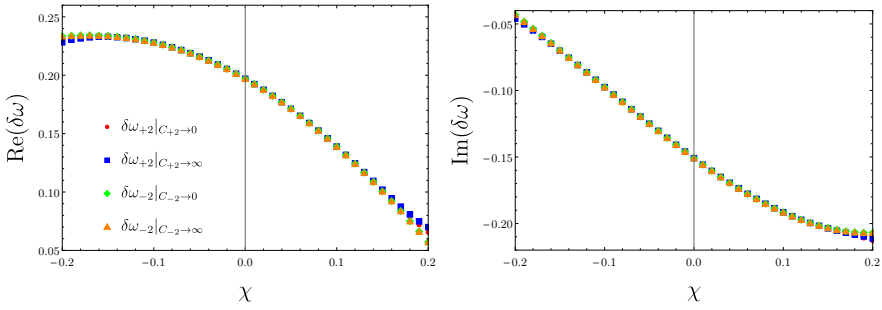


Figure 5.4: Shift in the $(l, m) = (2, 2)$ QNM frequency due to the odd-parity six-derivative correction.

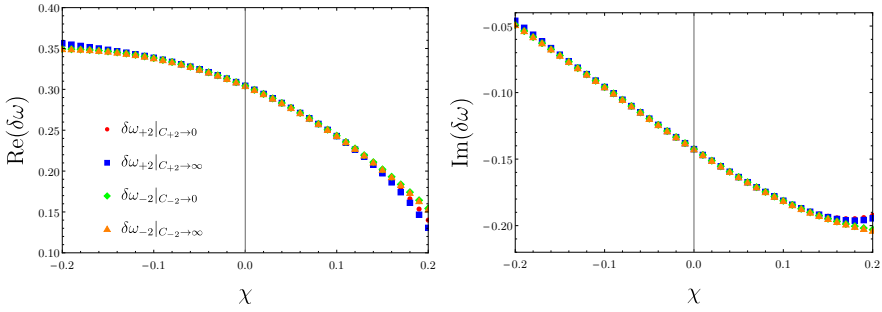


Figure 5.5: Shift in the $(l, m) = (3, 3)$ QNM frequency due to the odd-parity six-derivative correction.

5.7 Conclusions

We have put forward a general framework to analyse linearised excitations of rotating black holes that depart perturbatively from a Kerr spacetime. These rotating black holes arise, for instance, in theories of gravity beyond general relativity. Our approach, schematically summarised in Figure 5.1, has enabled us to reduce the study of such gravitational waves propagating on the background of these black holes to a system of four radial equations that stem from the effective separation of the universal Teukolsky equations.

The underlying perturbation theory philosophy, to exploit the vicinity of the algebraically special Kerr black hole, is in many ways evident and has been developed previously to various degrees of generality [77, 87, 88, 108]. Yet, to put this into practice has proven a technical challenge, which lay at the heart of this work. We have provided a detailed end-to-end strategy to implement the computation and we have presented the first results that emerge from this.

This entire computation is the synthesis of much previous work on the subject. On the one hand, the corrected Kerr background must be known, for which we used the results of [45] that expresses the corrections to the Kerr metric analytically as a series in the black-hole spin. On the other hand, it is necessary to reconstruct the metric perturbation (on the uncorrected Kerr background) from the Weyl scalars. By using the results of [106] we provided an explicit map between metric variables and the Teukolsky variables $\delta\Psi_s$ — see Section 5.3. Finally, we showed how one can effectively separate and decouple the Teukolsky equation by projecting it onto the spin-weighted spheroidal harmonics, as successfully applied by [77] for scalar perturbations. The series expansion in the black-hole spin is not strictly necessary, yet it turns out to be very important in practice. The reason is that, contrary to the Kerr metric in general relativity, rotating black-hole backgrounds are typically not known exactly. Nevertheless, a high-order expansion in spin allows us to obtain fully analytic radial equations, postponing the use of numerical methods until the very last step — the resolution of these equations.

We applied the approach just outlined explicitly to the case of the six-derivative EFT, in order to obtain the corrections to the QNMs. As we discussed, the QNMs are determined by the frequency ω, by the polarisation parameters $q_{\pm 2}$, and by the Starobinsky-Teukolsky (ST) constants $C_{\pm 2}$. In the case of even-parity higher-derivative corrections, one can decouple perturbations of odd and even parity, which fixes the polarisation parameters to be $q_{+2} = q_{-2} = \pm 1$. Given this choice, one should be able to obtain the QNM frequency by solving any of the radial Teukolsky equations. Therefore, in order for the result to be consistent, the two equations (for $s = \pm 2$) should yield the same frequencies.

On the other hand, parity-violating higher-derivative corrections mix modes of odd and even parity and one has to determine the QNM frequencies simultaneously with the polarisation parameters q_s by imposing that all radial equations for a given polarisation have the same frequencies. In both cases, the ST constants should be irrelevant. They represent a choice of gauge in which one reconstructs the metric perturbation. Thus, the QNM frequencies should actually be independent of the ST constants. This is highly non-trivial and provides a self-consistent check of our results.

The results in Section 5.6 pass three consistency checks with very high accuracy:

1. The $s = +2$ and $s = -2$ equations give the same QNM frequencies.
2. The shifts in the QNM frequencies are independent of the choice of Starobinsky-Teukolsky constants.
3. We reproduce the results of Chapter 4 for static and slowly-rotating black holes at linear order in the spin obtained from a metric perturbation approach.

Any one of these tests is, taken on its own, an impressive consistency check, when one considers the extensive calculations, expansions, transformations and the various numerical methods involved in obtaining the results. Given that they are all satisfied to a good approximation, we are confident that we have achieved a successful method to compute spectral shifts of QNMs of rotating black holes beyond general relativity.

We note that two of the above tests are based on redundancies in choices associated *e.g.* to gauge freedom. In addition to consistency checks, such redundancies allow some internal estimate of the precision we achieve. Moreover, the choices turn out to be not equally amenable to the combination of expansions and numerics that are used. For example, we observed that the $s = 2$ equation is quite sensitive to the order of the spin expansion, making it less precise. The $s = -2$ equation is much more stable. Indeed, the frequencies computed from the $s = -2$ equation pass the second test above with high precision even for high values of the black-hole spin.

It is rather straightforward to apply the computational strategy given here more generally in order to compute perturbative corrections to the QNM spectrum of Kerr black holes. Natural extensions include going further in the EFT of gravity, *e.g.*, by including eight-derivative terms in the effective action, as well as going to higher values of the black-hole spin. For the latter, one simply needs to include enough terms in the dimensionless spin expansion so as to get an accurate result [109], a process that is now entirely algorithmic.

Chapter 6

Quasinormal-mode spectra of black holes beyond Kerr

The necessity of having reliable quasinormal mode (QNM) frequencies at high spins and the fact that observations seem to narrow down the size of deviations from general relativity (GR), make the modified Teukolsky framework preferable for the study of QNMs beyond GR. We develop a general formalism for the quick computation of QNMs in theories which have a perturbative departure from GR. The advantage of this formalism is that it can be used also for the inverse problem, i.e. if a modification to GR is detected, one wants to be able to reconstruct the potential, the metric, or even the action from which the deviation originated [61, 110, 111]. In general, this framework opens the path to the development of a theory-informed description of QNM agnostic deviations.

This chapter, which is based on [112] and [113][1], starts with a comprehensive overview of the modified Teukolsky equation and the formalism in Section 6.1. We then show how to numerically compute the coefficients with a generalisation of the continued-fraction method and discuss its regime of validity in Section 6.2. This formalism is applied to higher-derivative corrections to GR in Section 6.3, and we compute corrections to the spectrum of quasinormal modes in Section 6.4. We give our conclusions on the formalism and the computation in Section 6.5. Throughout this chapter we scale the background metric such that the metric without corrections is a Kerr black hole with mass $M = 1/2$ and spin a, and due to this rescaling the spin parameter a ranges between 0 and $1/2$.

[1] Written with P. A. Cano, L. Capuano, N. Franchini and S. H. Völkel.

6.1 Parametrised formalism

6.1.1 The linear coefficients

Let us start from the radial Teukolsky equation for a spin s field as [94]

$$\frac{1}{\Delta^s R(r)}\frac{\mathrm{d}}{\mathrm{d}r}\left[\Delta^{s+1}R'(r)\right]+V(r)=0\,, \tag{6.1}$$

where the effective potential reads

$$V(r)=2is\frac{\mathrm{d}K}{\mathrm{d}r}-\lambda_{\ell m}+\frac{1}{\Delta}\left(K^2-isK\frac{\mathrm{d}\Delta}{\mathrm{d}r}\right)\,, \tag{6.2}$$

and we defined

$$\Delta=r^2-r+a^2\,,\qquad K=(r^2+a^2)\omega-am\,, \tag{6.3}$$

$$\lambda_{\ell m}=B_{\ell m}+a^2\omega^2-2am\omega\,. \tag{6.4}$$

It is worth mentioning that the zeros of the function Δ determine the location of the BH inner and outer horizons, given by

$$r_\pm=\frac{1\pm\sqrt{1-4a^2}}{2}\,. \tag{6.5}$$

On the other hand, the angular equation reads [94] (with $x=\cos\theta$)

$$\frac{1}{S(x)}\frac{\mathrm{d}}{\mathrm{d}x}\left[(1-x^2)S'(x)\right]+a^2\omega^2x^2-2sa\omega x+B_{\ell m}+s-\frac{(m+sx)^2}{1-x^2}=0\,. \tag{6.6}$$

We now assume that for a modified theory of gravity whose modifications are small with respect to GR the equation governing radial perturbations is the Teukolsky radial equation plus a correction to the potential linear in the coupling

$$\frac{1}{\Delta^s R(r)}\frac{\mathrm{d}}{\mathrm{d}r}\left[\Delta^{s+1}R'(r)\right]+V(r)+\delta V(r)=0\,, \tag{6.7}$$

and we assume that the modification is expanded in powers of r

$$\delta V(r)=\frac{1}{\Delta}\sum_{k=-K}^{4}\alpha^{(k)}\left(\frac{r}{r_+}\right)^k\,, \tag{6.8}$$

where K is the most negative coefficient of the power series and $\alpha^{(k)}$ are dimensionful coefficients we assume to be small.

This assumption is justified by the recent developments in obtaining modified Teukolsky equations by assuming small-coupling corrections to GR [87–89].

On the other hand, we can also assume that the angular equation remains unchanged. This is due to the fact that the spheroidal harmonics are a complete basis of the 2-sphere angular variables, and it can be shown that if one forces an angular expansion of the Weyl scalars in spin-weighted spheroidal harmonics, all the mixing terms would enter at second order in the coupling constants [89, 108]. Nevertheless, a modification on the QNM frequencies will induce a modification to the separation constant $B_{\ell m}$; hence, we also need to include equation (6.6) in our analysis.

If we assume the couplings to be small,[2] we are allowed to perform a Taylor expansion of QNMs and separation constants around their GR values [51, 57]. Hence, we can write

$$\begin{aligned} \omega_{n\ell m} &\simeq \omega^0_{n\ell m} + \sum_k d^{(k)}_{\omega,n\ell m}\alpha^{(k)}\,, \\ B_{\ell m}(a\omega) &\simeq B^0_{\ell m}(a\omega) + \sum_k d^{(k)}_{B,\ell m}\alpha^{(k)}\,. \end{aligned} \tag{6.9}$$

In the following steps, we omit the indices s, n, ℓ, m, a, ω for clarity. The linear coefficients d_ω and d_B can be identified as the derivatives of ω and B with respect to the single coupling α. To compute them, we perform the following steps. In the GR limit, one finds ω and $B_{\ell m}$ as simultaneous roots of two functions constructed from the radial and the angular equation

$$\mathcal{L}_r\left[\omega, B_{\ell m}\right] = 0\,, \qquad \mathcal{L}_\theta\left[\omega, B_{\ell m}\right] = 0\,. \tag{6.10}$$

The exact form of these functions depends on the chosen numerical method. For non-zero modifications, we can perform a Taylor expansion of the two functions around $\alpha = 0$

$$\mathcal{L}_j|_{\rm GR} + \alpha \left.\frac{\mathrm{d}\mathcal{L}_j}{\mathrm{d}\alpha}\right|_{\rm GR} + \mathcal{O}\big(\alpha^2\big) = 0\,, \tag{6.11}$$

where $j = [r, \theta]$ and we evaluate the derivative around their GR value $\omega = \omega^0$, $B = B^0$, $\alpha = 0$.

[2] We will provide a more quantitative comment about this assumption in Sec. 6.2.3. For now just consider these dimensionless parameters to be small enough to allow a linearisation of the eigenvalues $\omega_{n\ell m}$ and $B_{\ell m}$.

By requiring that equations (6.11) is satisfied at each order in α, and expanding the derivative by the chain rule, we obtain

$$\begin{aligned} \frac{\partial \mathcal{L}_r}{\partial \alpha} + \frac{\partial \mathcal{L}_r}{\partial \omega}\, d_\omega + \frac{\partial \mathcal{L}_r}{\partial B}\, d_B \bigg|_{\text{GR}} &= 0\,, \\ \frac{\partial \mathcal{L}_\theta}{\partial \omega}\, d_\omega + \frac{\partial \mathcal{L}_\theta}{\partial B}\, d_B \bigg|_{\text{GR}} &= 0\,, \end{aligned} \tag{6.12}$$

where we identified d_ω and d_B from their definition in equation (6.9). By solving the conditions above for d_ω and d_B, we get

$$\begin{aligned} d_\omega &= -\frac{\partial \mathcal{L}_r}{\partial \alpha}\frac{\partial \mathcal{L}_\theta}{\partial B}\left(\frac{\partial \mathcal{L}_r}{\partial \omega}\frac{\partial \mathcal{L}_\theta}{\partial B} - \frac{\partial \mathcal{L}_r}{\partial B}\frac{\partial \mathcal{L}_\theta}{\partial \omega}\right)^{-1}\bigg|_{\text{GR}}\,, \\ d_B &= \frac{\partial \mathcal{L}_r}{\partial \alpha}\frac{\partial \mathcal{L}_\theta}{\partial \omega}\left(\frac{\partial \mathcal{L}_r}{\partial \omega}\frac{\partial \mathcal{L}_\theta}{\partial B} - \frac{\partial \mathcal{L}_r}{\partial B}\frac{\partial \mathcal{L}_\theta}{\partial \omega}\right)^{-1}\bigg|_{\text{GR}}\,. \end{aligned} \tag{6.13}$$

In Section 6.2 we show how to numerically define the functions $\mathcal{L}_j$ with Leaver's continued fraction method.

6.1.2 Maximum number of independent coefficients

In reference [114], Kimura realised that in the case of spherically-symmetric perturbations, there is always an ambiguity in defining the modified potential, because the field can be freely reparametrised. The same reasoning can be applied to the Teukolsky equation as well. If we perform the following transformation in equation (6.7)

$$R(r) \to [1 + \varepsilon X(r)]\, R(r) + \varepsilon \Delta Y(r) R'(r)\,, \tag{6.14}$$

assuming that $\varepsilon \ll 1$, then the equation that $R(r)$ solves is

$$\frac{1}{\Delta^s R}\frac{\mathrm{d}}{\mathrm{d}r}\left[\Delta^{s+1} R'\right] + V + \delta V + \delta \overline{V} + \delta W \frac{R'}{R} = 0\,. \tag{6.15}$$

By imposing $\delta W = 0$ we uniquely obtain the free function $X(r)$ as

$$X(r) = c + \frac{s}{2}\Delta' Y - \frac{1}{2}\Delta Y'\,, \tag{6.16}$$

which yields the "ambiguous" potential in the form

$$\begin{aligned}\delta\overline{V} = \varepsilon\Delta\Bigg[Y'\left(\frac{\left(s^2-1\right)\left(\Delta'\right)^2}{2\Delta}+2s-2V-1\right)\\ +Y\left(\frac{s(s+1)\Delta'}{\Delta}-V'-\frac{V\Delta'}{\Delta}\right)\\ -\frac{1}{2}\Delta Y^{(3)}-\frac{3\Delta' Y''}{2}\Bigg].\end{aligned} \tag{6.17}$$

Now, after suitable choice of the function Y, we can express $\delta\overline{V}$ in the r basis. It turns out that the ansatz $Y = Y_j = y_j(r_+/r)^j$ yields

$$\delta\overline{V} = \frac{\varepsilon y_j}{\Delta}\sum_{k=-3}^{5} r_+^k \overline{A}_j^{(k)}\left(\frac{r}{r_+}\right)^{k-j}, \tag{6.18}$$

which implies that $j \geq 1$ since the maximum power of r in V is r^4, and the full expression of $\overline{A}_j^{(k)}$ can be found in Appendix E.1. In general, one can take a linear combination of the free functions Y_j and still get a potential that is equivalent to the starting one. Each term of this linear combination contains the free parameter y_j, which can be used to set to 0 one of the terms $\alpha^{(k)}$ in equation (6.8). This reasoning allows us to fix the negative limit in the power expansion to be $K = 3$.

It is possible that by choosing a different ansatz for Y one could further reduce the number of coefficients in the equation. In fact, for higher-derivative gravity, which we will study in 6.3, the number of independent coefficients reduces to four (being $k = [-2, 0, 1, 2]$) — see also [115]. Although we could not prove this is a general feature of arbitrary modifications of the Teukolsky equation, we suspect that it was possible in that case due to the expansion in the spin assumed for every coefficient. Indeed, we believe that the ansatz for Y that would reduce the potential to the lowest number of terms could be a rational function involving powers of a and r. To date, we could not find such reduction.

6.2 Computation of the coefficients

6.2.1 Continued fraction beyond Teukolsky

We turn our attention to the modified Teukolsky equation. It is always possible to bring equation (6.8) into the following form[3]

$$\begin{aligned}\delta V(r) = &\frac{A^{(0)}}{\Delta} + \frac{A^{(1)}}{r_+(r-r_-)} + \frac{1}{r_+^2}\sum_{k=0}^{2}\widetilde{\alpha}^{(k)}\left(\frac{r}{r_+}\right)^k \\ &+ \frac{1}{\Delta}\sum_{k=1}^{K}\alpha^{(-k)}\left(\frac{r_+}{r}\right)^k ,\end{aligned} \tag{6.19}$$

where $A^{(0)}$, $A^{(1)}$ and $\widetilde{\alpha}^{(k)}$ are constants that can be obtained from the constants $\alpha^{(k)}$ appearing in equation (6.8), as explained in Appendix E.3. First of all, we note that the terms multiplied by $1/\Delta$ modify the behaviour of the equation at the horizon. In order to take into account of these additional terms, we need to modify the definition of the exponent σ in the ansatz (3.85). To ensure that the solution is regular at the horizon, we must replace the value of σ by

$$\sigma = \frac{is}{2} + \sqrt{\left(\sigma_{\text{GR}} - \frac{is}{2}\right)^2 + \frac{1}{\beta^2}\sum_{k=-K}^{4}\alpha^{(k)}} , \tag{6.20}$$

where we took the positive sign of the square root in order to obtain the correct GR limit. On the other hand, the terms $\widetilde{\alpha}^{(1)}$ and $\widetilde{\alpha}^{(2)}$ modify the behaviour at infinity of the equation. This changes the values of p and q into

$$q = \pm\sqrt{-\frac{\widetilde{\alpha}^{(2)}}{r_+^4} - \omega^2} , \tag{6.21}$$

$$p = -\frac{r_+\widetilde{\alpha}^{(1)} + \widetilde{\alpha}^{(2)} - 2r_+^4\left(qs - is\omega - \omega^2\right)}{2qr_+^4} , \tag{6.22}$$

where the sign of q is chosen such that $\text{Re}(q) > 0$. See Appendix E.2 for the derivation of the appropriate boundary conditions for the beyond-Teukolsky case. This asymptotic behaviour is the reason why we truncate the series in equation (6.8) at $k = 4$.

[3] In Section 6.1.2 we showed that $K = 3$, but the following analysis works, in principle, for any value of K, hence we keep it unspecified.

By repeating the steps done for the GR case, we obtain a modified version of equation (3.89)

$$\sum_{n=0}^{N} R_n \left[\frac{\alpha^{\text{BG}}_{n-1}}{f} + \beta^{\text{BG}}_n + \gamma^{\text{BG}}_{n+1} f \right. \\ \left. + \frac{1}{\beta^2} \frac{(1-f)^2}{f} \sum_{k=1}^{K} \alpha^{(-k)} \left(\frac{1-f}{1-\eta f} \right)^k \right] f^n = 0 \,, \tag{6.23}$$

where $\eta = r_-/r_+$ and

$$\alpha^{\text{BG}}_n = \alpha^r_n - \frac{1}{\beta^2} \sum_{k=1}^{K} \alpha^{(-k)} \,, \tag{6.24}$$

$$\beta^{\text{BG}}_n = \beta^r_n - 2\left(\sigma_{\text{GR}} - \sigma\right)\left(\sigma_{\text{GR}} + \sigma - \omega\right) \,, \\ - 2\frac{A^{(0)}}{\beta^2} + \frac{A^{(1)}}{r_+ \beta} + \frac{\widetilde{\alpha}^{(0)}}{r_+^2} \tag{6.25}$$

$$\gamma^{\text{BG}}_n = \gamma^r_n + 2i\left(\sigma_{\text{GR}} - \sigma\right)\left(s + i\omega\right) \\ - \frac{1}{\beta^2} \sum_{k=1}^{K} \alpha^{(-k)} - \frac{A^{(1)}}{r_+ \beta} \,, \tag{6.26}$$

and we used the fact that

$$\Delta = \beta^2 \frac{f}{(1-f)^2} \,, \qquad r - r_- = \frac{\beta}{1-f} \,. \tag{6.27}$$

If we fix a single modification k, we can get rid of the rational behaviour in f by multiplying the equation by $(1-\eta f)^k$, obtaining the following expression

$$\sum_{n=0}^{N} R_n \left[\left(\frac{\alpha^{\text{BG}}_{n-1}}{f} + \beta^{\text{BG}}_n + \gamma^{\text{BG}}_{n+1} f \right) (1-\eta f)^k \right. \\ \left. + \frac{\alpha^{(-k)}}{\beta^2} \frac{(1-f)^{k+2}}{f} \right] f^n = 0 \,. \tag{6.28}$$

We can figure out the coefficient relation (equivalent to that of equation (3.94)), which at a given n takes the form

$$\sum_{j=-1}^{k+1} \left(\widetilde{\gamma}_{n,j-1} + \widetilde{\beta}_{n,j} + \widetilde{\alpha}_{n,j+1} \right) R_{n-j} = 0 \,. \tag{6.29}$$

The coefficients appearing in the relation are given by

$$\widetilde{\alpha}_{n,j} = (-\eta)^j \binom{k}{j} \alpha^{\text{BG}}_{n-j} + (-1)^j \binom{k+2}{j} \frac{\alpha^{(-k)}}{\beta^2}\,, \tag{6.30}$$

$$\widetilde{\beta}_{n,j} = (-\eta)^j \binom{k}{j} \beta^{\text{BG}}_{n-j}\,, \tag{6.31}$$

$$\widetilde{\gamma}_{n,j} = (-\eta)^j \binom{k}{j} \gamma^{\text{BG}}_{n-j}\,. \tag{6.32}$$

We notice that, from the definition of the binomial, $\widetilde{\alpha}_{n,j}$ is non-vanishing for $0 \leq j \leq k+2$, whilst $\widetilde{\beta}_{n,j}$ and $\widetilde{\gamma}_{n,j}$ are non-zero for $0 \leq j \leq k$. Now that we have a $(k+3)$-terms relation, we can perform a Gaussian elimination to reduce it to a three-terms relation (details can be found in the appendix of [61]). Once the three-terms relation is found, one can re-initialise the ladder operator Λ^r_n and obtain the modified frequency and separation constant from equations (3.102)–(3.103).

6.2.2 Numerical computation of the coefficients

In the previous two sections we explained how to obtain the functions $\mathcal{L}_r\,(\omega, B, \alpha)$ and $\mathcal{L}_\theta\,(\omega, B)$. To compute the coefficients d_ω and d_B as given in equation (6.13), we evaluate the derivatives numerically with a 4-point centred stencil. For each pair of coefficients, we initialise the ladder operators Λ_N to some arbitrary low integer N, and then increase it by one until the simultaneous relative change in d_ω and d_B is smaller than a given tolerance, which we chose to be 10^{-7} (the same accuracy has been required for the computation of the frequencies). We computed numerically all the coefficients for the following values $s = -2$, $n = [0, 2]$, $\ell = [2, 4]$, $m = [-\ell, \ell]$, $k = [-3, 4]$ in a uniform grid in $a = [0, 0.495]$ with spacing $\delta a = 0.005$. The full list of computed coefficients is available in a public git repository [116].

In figure 6.1 we show the results from this computation for the real and imaginary parts of the $d^{(k)}_\omega$ coefficients for $s = -2$, $n = 0$, $\ell = 2$, $m = [-2, 2]$. Specifically, we consider values of $k = [-3, 4]$ and of the spin a between 0 and 0.45, as well as the real and the imaginary part of $d^{(k)}_B$ for the same n, ℓ, m and $k = [-1, 2]$.

To directly apply our formalism to further studies, e.g., of ringdown analysis of non-linear computations or data analysis, we also provide some Python code and a Jupyter notebook with some examples [116]. It allows one to compute the QNMs and the separation constants as function of n, ℓ, m, a and $\alpha^{(k)}$ and can thus, in principle, be efficiently integrated in commonly used code infrastructure.

The code also allows one to access some of the earlier results for the parametrised QNM framework for modifications to the Regge-Wheeler and Zerilli potentials, for which coefficients beyond the fundamental mode have been computed in reference [61]. The GR values for the QNMs have been taken from reference [117, 118]. For more details about how the code is structured and how it can be used, we refer to the provided tutorial [116].

In principle, one should be able to compare the coefficients for $a = 0$ with those computed in [57, 61]. However, we stress that for $a = 0$, equation (6.7) reduces to the non-spinning limit of the Bardeen-Press equation [93], whereas the formalism of [57, 61] was developed for the Regge-Wheeler and the Zerilli equation. The transformation between the Bardeen-Press potential and the Regge-Wheeler/Zerilli potentials was obtained by Chandrasekhar [35], but generalizing this to the case of the modified potential with generic $\alpha^{(k)}$ couplings is non-trivial.

6.2.3 Linearised regime of validity

The framework we developed is motivated by the assumption that any modification of gravity produces only slight deviations from GR in astrophysical observables. In this section, we expand on the regime of validity of the formalism, by providing a quantitative assessment of the accuracy of this approach. It is worth noting that we can only assess the discrepancy from restricting to linear corrections to the frequencies, as defined in equation (6.9), and not taking into account higher-order corrections to the potential, which are beyond the scope of this chapter.

First of all, we give a heuristic motivation on the maximum size of the coefficients, by requesting that the perturbation equation is not strongly modified at the boundaries of our domain and that $\omega \simeq \mathcal{O}(1)$. At $r \to \infty$, we have seen from equations (6.21) and (6.22) that the only coefficients modifying the asymptotic structure of the potential are $\alpha^{(3)}$ and $\alpha^{(4)}$. From this we can infer that

$$\alpha^{(3)} \lesssim 1\,, \qquad \alpha^{(4)} \lesssim 1\,. \tag{6.33}$$

On the other hand, the modifications in the potential affect the near-horizon expansion as in equation (6.20). The condition is such that the sum of coefficients must behave as

$$\sum_k \alpha^{(k)} \lesssim \left| 2\beta^2 \sigma_{\rm GR} \left(\sigma_{\rm GR} - \frac{is}{2} \right) \right| . \tag{6.34}$$

It is worth noting that when the superradiant condition $\omega = \omega_c$ is activated, one has $\sigma_{\rm GR} = 0$, and we expect that the formalism is valid only if the sum of the $\alpha^{(k)}$ is approximately 0.

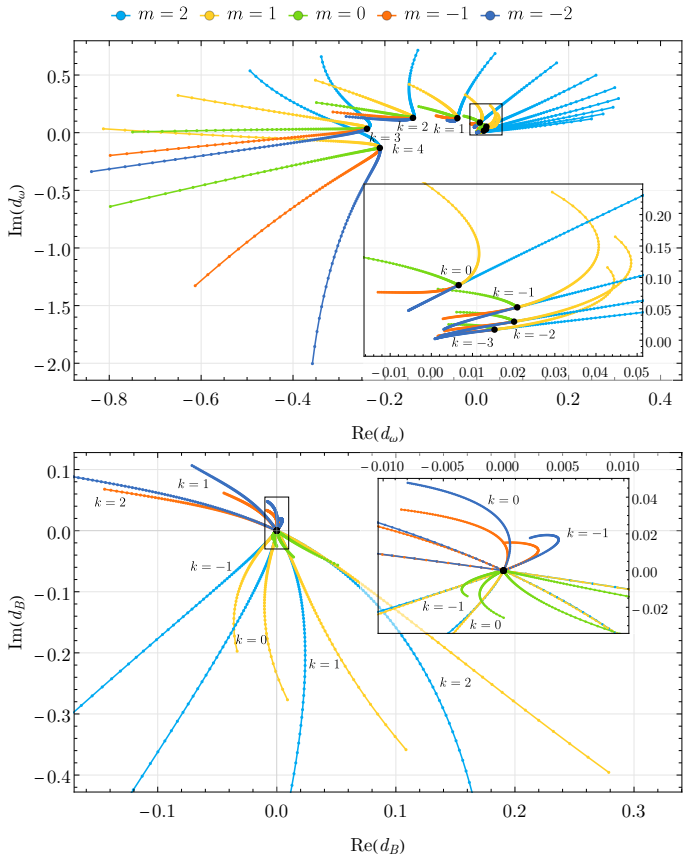


Figure 6.1: In the top panel we show the real and the imaginary part of d_ω for $n = 0$, $\ell = 2$, $m = [-2, 2]$, $k = [-3, 4]$ and values of the spin from $a = 0$ to $a = 0.45$, and each point is on a step of $\delta a = 0.005$. The inset focuses on the coefficients with $k = [-3, 0]$. In the bottom panel we show the real and the imaginary part of d_B for $n = 0$, $\ell = 2$, $m = [-2, 2]$, $k = [-1, 2]$ and same values of the spin. The inset focuses on the coefficients with $m \leq 0$ and $k = [-1, 0]$. In both plots the black dot indicates the coefficient value for $a = 0$.

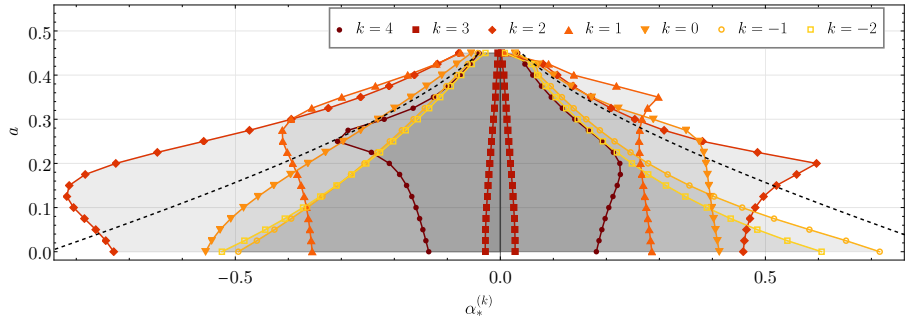


Figure 6.2: We plot the threshold values $\alpha_*^{(k)}$ against the spin for different values of k. With $\alpha_*^{(k)}$, we identify the limit value of a coupling at which a discrepancy of 1% between the linear and non-linear approximation is obtained. The plot uses as non-linear estimates the full continued fraction results. The discrepancy is evaluated for the $n = 0$, $\ell = m = 2$ mode and different values of k and of the spin a. The black dashed lines correspond to the estimate (6.34)

In general, however, each power of k affects the effective potential in a different way. In order to have a more quantitative estimate of the allowed regime of validity, we perform two separate analyses. First, we compare the QNM frequencies computed with the linear approximation against those obtained with a full continued-fraction method discussed above. We express the discrepancy between the frequencies as

$$\Delta_\omega \equiv \sqrt{\left(\frac{\Delta\omega_R}{\omega_R}\right)^2 + \left(\frac{\Delta\omega_I}{\omega_I}\right)^2}\,, \tag{6.35}$$

where $\omega_{R,I}$ are the real and imaginary parts of the QNM, respectively. We computed the discrepancy for several real positive and negative values of the couplings $\alpha^{(k)}$ and extracted the threshold values $\alpha_*^{(k)}$ at which Δ_ω reaches 1%. The results are represented in figure 6.2 for the mode $n = 0$, $\ell = m = 2$, for selected values of the spins between $a = 0$ and $a = 0.45$ and for $k = [-2, 4]$.

It can be seen in figure 6.2 that there is a complicated dependence of the thresholds on the type of modification we introduce in the potential. However, a main qualitative feature can be read off, i.e. that, for any modification, the threshold tends to get smaller for higher spins. The physical interpretation is that, for a given beyond-GR effect in the modified Teukolsky equation, rotation tends to exacerbate the deviation of the linear approximation with respect to the true values of the QNMs.

Since the computation of QNMs with the continued-fraction method is not immediate nor straightforward to implement, we want to provide a quick estimate for the uncertainty of the single-k contributions. In this respect, we compute the diagonal quadratic corrections, as explained in Appendix E.4. We checked the estimate $\alpha_*^{(k)}$ by computing Δ_ω, assuming that the non-linear frequencies are obtained including quadratic coefficients. By a qualitative comparison, the quadratic estimate works well to capture the uncertainty except for $k = 3$, and partially for $k = 4$. Even though it is not as precise as the full non-linear comparison, the quadratic coefficients can be used as a quick way to understand what threshold value to take for the couplings.

Lastly, we want to stress that the thresholds that we provided in this section are referred to the contribution of a single modification. Hence, it could be that, depending on the values of the coefficients, the combination of multiple k would need larger or smaller threshold values. This means that for a theory-specific case, the bounds on $\alpha^{(k)}$ might differ from what we inferred in this section, and need to be addressed case-by-case.

6.3 The modified Teukolsky equations

6.3.1 Radial Teukolsky equations

As a result of the computations in Chapter 5, Section 5.5, we get four equations for the radial variables (5.68). Removing the lm labels for clarity, they read:

$$\begin{aligned} \mathfrak{D}_s^2 R_s - \alpha \left[f_s R_s + g_s \Delta \frac{\mathrm{d}R_s}{\mathrm{d}r} \right] &= 0 \,, \\ \mathfrak{D}_s^2 R_s^* - \alpha \left[f_s^* R_s^* + g_s^* \Delta \frac{\mathrm{d}R_s^*}{\mathrm{d}r} \right] &= 0 \,, \end{aligned} \tag{6.36}$$

where $s = \pm 2$, and

$$\mathfrak{D}_s^2 = \Delta^{-s+1} \frac{\mathrm{d}}{\mathrm{d}r} \left[\Delta^{s+1} \frac{\mathrm{d}}{\mathrm{d}r} \right] + V_s \tag{6.37}$$

is the Teukolsky operator with a potential V_s given by

$$\begin{aligned} V_s = {} & (am)^2 + \omega^2 \left(a^2 + r^2\right)^2 - 4amMr\omega + is\left(2am(r-M) - 2M\omega\left(r^2 - a^2\right)\right) \\ & + \Delta\left(-a^2\omega^2 + s - B_{lm} + 2irs\omega\right) \,, \end{aligned} \tag{6.38}$$

and B_{lm} are the usual angular separation constants.

In addition, f_s and g_s are functions of r which, in the context of the spin expansion we are performing, take the form

$$\begin{aligned} f_s(r) &= r^4 \sum_{n=0}^{n_{\max}} \chi^n \sum_{k=0}^{k_{\max}(n)} \frac{f_{s,n,k}}{r^k}\,, \\ g_s(r) &= r^3 \sum_{n=0}^{n_{\max}} \chi^n \sum_{k=0}^{k_{\max}(n)} \frac{g_{s,n,k}}{r^k}\,, \end{aligned} \tag{6.39}$$

for certain coefficients $f_{s,n,k}$, $g_{s,n,k}$ that we determine analytically. Analogous expressions hold for f_s^*, g_s^*, and we remark that in general $f_s^* \neq f_s$, $g_s^* \neq g_s$ and that the star $*$ does not represent complex conjugation.

These coefficients depend on the frequency ω and on a number of parameters that relate the different radial functions when $\alpha = 0$ and that we use to fully decouple the corrected equations. In the Kerr case, the radial variables with $s = +2$ and $s = -2$ are related by the Starobinsky-Teukolsky (ST) identities [36, 119–121], that depend on two constants $C_{\pm 2}$ whose product is fixed — see Section 5.3. Thus, one of these constants is arbitrary, and it turns out to correspond to a gauge choice for the metric reconstruction. Physics should therefore be independent of this choice and we will come back to this later. This is a manifestation of the fact that the $s = +2$ and $s = -2$ variables contain the same information [122]. On the other hand, when $\alpha = 0$, the R_s variable and its NP conjugate R_s^* satisfy the same equation and boundary conditions, so that it follows that these variables must be proportional:

$$R_s^* = q_s R_s\,. \tag{6.40}$$

Contrary to the Starobinsky-Teukolsky constants, the q_s parameters are physical as they determine the polarisation of the perturbation. The reason why they do not show up in the study of Kerr perturbations has to do with isospectrality. But in theories beyond GR isospectrality is typically broken, and hence the corrections to the Teukolsky equations depend on the polarisation — see [123] for a study of isospectrality breaking in the Newman-Penrose formalism. We find that the correction to the Teukolsky equation, captured by the functions (6.39), depends explicitly on the ST constants C_s and the polarisation parameters q_s.

In order to simplify (6.36) we can perform a change of variables of the form

$$R_s \to R_s + \alpha \left(A_s R_s + B_s \Delta \frac{\mathrm{d}R_s}{\mathrm{d}r} \right)\,, \tag{6.41}$$

where the functions A_s and B_s are linear in the higher-derivative couplings.

At first order in α, this has the following effect on the corrected Teukolsky equation (6.36): $f_s \to \tilde{f}_s$, $g_s \to \tilde{g}_s$, where

$$\tilde{f}_s = f_s - \Delta\left(\Delta A_s'' + (s+1)A_s'\Delta' - 2V_sB_s' - B_sV_s'\right), \tag{6.42}$$

$$\tilde{g}_s = g_s - \Delta\left(2A_s' + \Delta B_s'' - (s-1)B_s'\Delta' - 2sB_s\right). \tag{6.43}$$

Then we can choose the functions A_s and B_s so that the corrected equation takes a simple form. In particular, we can fix $\tilde{g}_s = 0$, and determine A_s from this condition. With this choice, we rewrite equation (6.36) as

$$\Delta^{-s+1}\frac{\mathrm{d}}{\mathrm{d}r}\left[\Delta^{s+1}\frac{\mathrm{d}R_s}{\mathrm{d}r}\right] + \left(V_s + \alpha\delta V_s\right)R_s = 0, \tag{6.44}$$

where the correction to the potential, δV_s, reads

$$\begin{aligned}\delta V_s = &- f_s + \frac{1}{2}\Delta g_s' + sg_s\Delta' + B_s\Delta\left(-V_s' + s(1+s)\Delta'\right)\\ &+ \frac{1}{2}\Delta B_s'\left(-4V_s + 2(2s-1)\Delta + \left(s^2-1\right)\Delta'^2\right)\\ &- \frac{3}{2}\Delta^2\Delta'B_s'' - \frac{1}{2}\Delta^3B_s^{(3)}.\end{aligned} \tag{6.45}$$

We still have a functional freedom in the form of the potential δV_s, corresponding to the choice of $B_s(r)$. The quasinormal mode frequencies and other physical properties are nevertheless independent of this choice, as long as the function $B_s(r)$ is well behaved (*e.g.*, it must decay fast enough at infinity and be regular at the horizon). For convenience, let us from now on focus on the case of $s = -2$, although the discussion for the $s = 2$ is analogous.

In the context of the spin expansion and taking into account the expressions (6.39), it is also natural to assume a function B_{-2} of the form

$$B_{-2} = \sum_{n=0}^{n_{\max}}\sum_{k=-1}^{k_{\max}}\frac{\chi^n}{r^k}b_{n,k}. \tag{6.46}$$

Observe that we start the sum over k at $k = -1$, corresponding to a linear term in r. This is the highest power of r that preserves the asymptotic structure of the potential (which goes as r^4). Moreover, this function is clearly regular at the horizon. With this choice, the potential (6.45) also takes the form of a simultaneous expansion in χ and in $1/r$.

$$\delta V_{-2} = \sum_{n=0}^{n_{\max}}\sum_{k=-4}^{\tilde{k}_{\max}}\frac{\chi^n}{r^k}v_{n,k} \tag{6.47}$$

However, by tuning the coefficients $b_{n,k}$, we find that it is possible to remove almost all of the terms in this potential. All of the powers $1/r^k$ with $k > 2$ can be removed. That is, we can set $v_{n,k} = 0\ \forall k \geq 3, n \geq 0$. Interestingly, the term with $1/r^2$ cannot be removed. The remaining freedom in the $b_{n,k}$ coefficients can be used to impose additional constraints on the terms with $k = -1, 0, 1, 2, 3, 4$. We can for instance choose $v_{n,1} = 0$, so that there is no $1/r$ term, and we can also set $v_{n,-4} = 0$, so that the corrections to the potential are subleading at infinity. Interestingly, this choice also leads to $v_{n,-3} = 0$. Once we have set these conditions, we find that there is no additional freedom and the potential is uniquely reduced to the simple form

$$\delta V_{-2} = \frac{A_{-2}}{r^2} + A_0 + A_1 r + A_2 r^2 \,, \tag{6.48}$$

Thus, it is determined by the four coefficients A_k, which are expressed as a power expansion in the spin

$$A_k = \sum_{n=0}^{n_{\max}} \chi^n A_{k,n} \,. \tag{6.49}$$

We have checked that for all the theories considered and all the different l, m modes one can always write the potential as in (6.48). In addition, since the potential can always be brought to this form at any order in the spin expansion, we expect that (6.48) may be applicable even without expanding in the spin.

We have analytically computed the coefficients A_k at order $n_{\max} = 18$ for the $l = 2, 3$, $-l \leq m \leq l$ modes and at order $n_{\max} = 14$ for $l = 4$, $-l \leq m \leq l$, for all the theories in (4.1). These expressions are too lengthy to be displayed in the text, but we provide them in a public git repository [124].

6.3.2 Properties of the potentials

As we mentioned earlier, corrections to the Teukolsky equation depend on the Starobinsky-Teukolsky constants C_s, representing a gauge choice in the metric reconstruction, and on the polarisation parameters q_s. The dependence of the correction to the potential δV_s (and of the functions f_s , g_s we started with) on these parameters is of the form

$$\begin{aligned} \delta V_s &= \frac{1}{P_s}\left[\delta V_s^{(1)} + q_s \delta V_s^{(2)} + C_s \delta V_s^{(3)} + C_s q_{-s} \delta V_s^{(4)}\right] , \\ \delta V_s^* &= \frac{1}{q_s P_s^*}\left[\delta V_s^{*(1)} + q_s \delta V_s^{*(2)} + C_s \delta V_s^{*(3)} + q_{-s} C_s \delta V_s^{*(4)}\right] , \end{aligned} \tag{6.50}$$

where P_s and P_s^* are given by

$$\begin{aligned} P_s &= \frac{1}{2} + \frac{is}{48M\omega}\left(D_2 q_s - 2^s q_{-s} C_s \mathcal{K}^2\right) , \\ P_s^* &= \frac{1}{2} + \frac{is}{48 q_s M\omega}\left(D_2 - 2^s C_s \mathcal{K}^2\right) , \end{aligned} \tag{6.51}$$

D_2 is the Starobinsky-Teukolsky constant of the angular functions (D.4) and $\mathcal{K}^2 = D_2^2 + 144M^2\omega^2$. The origin of these P_s, P_s^* is explained in Section 5.3.

After removing the gauge freedom in the corrected Teukolsky equation by reducing the potential to its simplest form (6.48), this now manifestly exhibits certain important properties.

Parity-preserving corrections

First of all, the quasinormal mode frequencies should not depend on the ST constants, and at least in the case of parity-preserving corrections we can check this analytically. For those theories, the QNMs have definite parity and hence they are given by the polarisation $q_{+2} = q_{-2} = \pm 1$. When we use those values of $q_{\pm 2}$ in (6.48), with the coefficients A_k computed for each theory, we observe that the dependence on C_s drops off, leaving us with two different potentials $\delta V_{-2}^{\pm}$ — one for each polarisation — that only depend on M, a and ω. Thus, the result is manifestly independent of the gauge choice for the metric reconstruction. Furthermore, the conjugate potential becomes identical $\delta V_{-2}^{*\pm} = \delta V_{-2}^{\pm}$, so that the full equations for R_{-2} and R_{-2}^* are identical and have the same solutions. This ensures the consistency of the construction. On the other hand, the potentials for $s = +2$, that is, $\delta V_{+2}^{\pm}$, also become independent of C_s and they take a different form from $\delta V_{-2}^{\pm}$. However, they give rise to the same QNM frequencies, as checked in Chapter 5.

Parity-breaking corrections

In the case of parity-breaking corrections we also expect the result to be independent of the choice of the C_s constants, although in that case the equations have a more involved structure [115]. The key aspect about parity-breaking corrections is that one has to determine the polarisation $q_{\pm 2}$ by solving the different radial equations simultaneously. Since here we are only considering the $s = -2$ equations, we set $C_{-2} = 0$, which has the effect of decoupling these from the $s = +2$ ones.

Then we have to solve the $s = -2$ equation and its Newman-Penrose conjugate, which have different corrections to the potential, δV_{-2} and δV^*_{-2}. Remarkably, we find that these are given by[4]

$$\begin{aligned} \delta V_{-2} &= \frac{2}{1 - iq_{-2}K}\delta V_{\rm break}\,, \\ \delta V^*_{-2} &= -\frac{2}{1 - iK/q_{-2}}\delta V_{\rm break}\,, \end{aligned} \tag{6.52}$$

for the same $\delta V_{\rm break}$ that is independent of q_{-2}, and where

$$K = \frac{D_2}{12M\omega}\,. \tag{6.53}$$

Now, since we are interested in finding quasinormal mode solutions, the equations for R_{-2} and R^*_{-2} must be satisfied at the same time for the same QNM frequency. Clearly, this will only happen if

$$\frac{2}{1 - iq_{-2}K} = -\frac{2}{1 - iK/q_{-2}}\,, \tag{6.54}$$

so that the potentials become identical $\delta V_{-2} = \delta V^*_{-2}$. This leads to the following solution for the polarisation parameter

$$q^{\pm}_{-2} = \frac{iK}{1 \pm \sqrt{K^2 + 1}}\,, \tag{6.55}$$

which, remarkably, is independent of the specific theory. We also obtain the associated potentials for each of the polarisations

$$\delta V^{\pm}_{-2} = \delta V^{*\pm}_{-2} = \pm\frac{2}{\sqrt{1 + K^2}}\delta V_{\rm break}\,. \tag{6.56}$$

Thus, the polarisations + and − have opposite corrections to the QNM frequencies. This is a known property of parity-breaking higher-derivative corrections [51, 72, 115], and the fact that we can check it analytically provides a very strong test on the validity of our results.

[4] The denominators are (up to a factor) the P_{-2} and P^*_{-2} constants (6.51).

6.3.3 Convergence of the expansion

In order to determine the radius of convergence of the spin expansion of the A_k coefficients in (6.49) we must study how the coefficients $A_{k,n}$ behave for large n. Although we do not have a formula for $A_{k,n}$ for arbitrary n, our explicit results up to $n_{\max} = 18$ provide a good intuition. First, let us note that these coefficients depend on the frequency, so in order to obtain some numerical values we can set ω to be close to the frequency of the QNM in which we are interested. Our results show clearly that the coefficients $A_{k,n}$ grow exponentially with n, as

$$A_{k,n} \sim c_k \Lambda_1^n \,, \tag{6.57}$$

for some complex number Λ_1 which depends on the frequency. Generically, we find that $|\Lambda_1| > 1$, and hence the radius of convergence is $\chi^{\max} = |\Lambda_1|^{-1} < 1$. This, however, is just a problem of the series expansion, as we expect the full coefficients $A_k(\chi)$ to remain finite for every χ. Indeed, what (6.57) suggests is that the full expression of A_k can be written in the form

$$A_k(\chi) = \frac{\tilde{A}_k(\chi)}{1 - \Lambda_1 \chi} \,. \tag{6.58}$$

Here, the series expansion of the denominator precisely gives rise to the behaviour (6.57), but it does not introduce any divergence since Λ_1 is complex and χ is real. On the other hand, the series expansion of the numerator $\tilde{A}_k(\chi)$ should now have a much better convergence than the original $A_k(\chi)$, because we have absorbed in the denominator the terms that spoiled the convergence.

Now, the way to do this in practice is to transform our series expansion (6.49) into a Padé approximant with a denominator of order 1

$$A_k^{\text{Padé}(1)} = \frac{1}{1 - \tilde{\Lambda}_1 \chi} \sum_{n=0}^{n_{\max}-1} \chi^n \tilde{A}^{(1)}_{k,n} \,. \tag{6.59}$$

Remarkably, the value of $\tilde{\Lambda}_1$ obtained from the Padé approximant coincides very well with the value of Λ_1 estimated from the asymptotic behaviour of the coefficients. Thus, the Padé approximant is very powerful in identifying the complex pole in (6.58). The new series expansion in the numerator of (6.59) always has a better convergence than the original series (6.49), and there are two possibilities. If the coefficients $A^{(1)}_{k,n}$ remain bounded or grow slowly enough for $n \to \infty$, then the Padé approximant (6.59) has a radius of convergence of $\chi^{\max} = 1$, and therefore it is convergent for all subextremal values of the spin. Thus, taking $n_{\max}$ to be large enough, we should be able to consider arbitrarily high spins. The second possibility is that the new coefficients still grow exponentially, $A^{(1)}_{k,n} \sim \Lambda_2^n$, with $1 < |\Lambda_2| < |\Lambda_1|$.

In that case, the Padé approximant has a bigger radius of convergence than the original series, but it still diverges for high enough spin $\chi^{\max} = |\Lambda_2|^{-1}$. Thus, to improve the convergence, we proceed in the same way and apply a Padé approximant with order 1 denominator to the numerator of (6.59). Then we end up with an order-2 Padé approximant,

$$A_k^{\text{Padé}(2)} = \frac{1}{\left(1-\tilde{\Lambda}_1\chi\right)\left(1-\tilde{\Lambda}_2\chi\right)} \sum_{n=0}^{n_{\max}-2} \chi^n \tilde{A}^{(2)}_{k,n}\,, \tag{6.60}$$

where $\tilde{\Lambda}_2 \approx \Lambda_2$ is again complex and hence the full expression is finite. We can then analyse the convergence of the new series expansion with coefficients $\tilde{A}^{(2)}_{k,n}$ and proceed in the same way. If the new series converges for all values then we are done, otherwise we consider a Padé approximant of one more order.

In general, we get a Padé approximant with an order-N denominator

$$A_k^{\text{Padé}(N)} = \frac{\sum_{n=0}^{n_{\max}-N} \chi^n \tilde{A}^{(N)}_{k,n}}{\prod_{n=1}^{N}\left(1-\tilde{\Lambda}_n\chi\right)}\,, \tag{6.61}$$

and we consider the minimum value of N for which the numerator behaves as a convergent series $\forall|\chi| < 1$. The $\tilde{\Lambda}_n$ are always complex and hence this expression is regular for real values of χ. We note that increasing the value of N beyond the minimum value required to achieve convergence does not always result in a faster convergence, and it could in turn introduce spurious poles.

We have explored this strategy explicitly for the theories (4.1) using an expansion of order $n_{\max} = 18$ for the $l = 2, 3$ modes and of order $n_{\max} = 14$ and for the $l = 4$ ones. We have found that the order of the denominator of the Padé approximant that we should use typically increases with the magnitude of the angular numbers l and $|m|$. In practice, we used $N = 0$ for the $l = 2, 3$, $m = 0$ modes, $N = 1$ for $l = 2$, $m \neq 0$, and $N = 2$ for $l = 3$, $m \neq 0$ and all the $l = 4$ modes. Presumably, one needs to keep increasing the value of N as l and $|m|$ grow, but we do not have conclusive evidence of this. We illustrate the convergence of the Padé approximant in Fig. 6.3, where we show the coefficients $A_{-2,n}$ and $\tilde{A}^{(1)}_{-2,n}$ of the $l = m = 2$, $q_s = -1$ mode of the quartic theory $\mathcal{C}^2$. Although these results are only based on numerical evidence, they strongly indicate that the Padé approximant yields a convergent result. Therefore, this method allows us to study black holes of arbitrary spins as long as we include enough terms in the spin expansion.

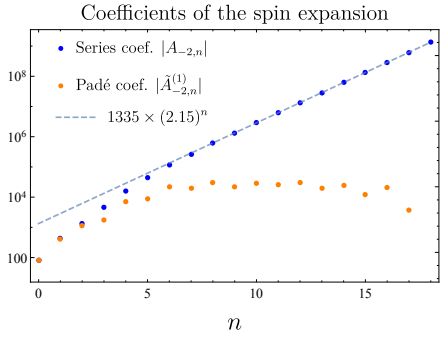


Figure 6.3: Absolute value of the coefficients $A_{-2,n}$ of the series expansion (6.49) and $\tilde{A}_{-2,n}$ of the Padé approximant (6.59) as a function of n. We show the values corresponding to the $l = m = 2$ mode with $q_s = -1$ of the quartic Lagrangian $\mathcal{C}^2$ and we set $M = 1$ and $\omega = 0.533 - 0.081$, corresponding to the $(2, 2, 0)$ QNM frequency of Kerr black holes with $\chi = 0.7$. A fit reveals that the coefficients of the series expansion grow exponentially as in (6.57) with $|\Lambda_1| \sim 2.1547$. Thus, the radius of convergence is $\chi^{\max} = |\Lambda_1|^{-1} \sim 0.46$. On the other hand, the coefficients of the Padé approximant are bounded, indicating that the series in (6.59) converges for all values of the spin $|\chi| < 1$. The numerator of the Padé approximant gives $\tilde{\Lambda}_1 = 0.2969 + 2.134i$, whose absolute agrees perfectly with $|\Lambda_1|$.

6.4 Quasinormal modes in higher-derivative gravity

Summarizing the results of the previous section, in order to study the quasinormal modes of the rotating black holes in the theory (4.1), it suffices to consider the equation (6.44) with either $s = +2$ or $s = -2$, since both are equivalent. We focus on the $s = -2$ case, so we have to solve the equation

$$\Delta^3 \frac{\mathrm{d}}{\mathrm{d}r}\left[\Delta^{-1}\frac{\mathrm{d}R_{-2}}{\mathrm{d}r}\right] + (V_{-2} + \alpha\,\delta V_{-2})\; R_{-2} = 0\,, \tag{6.62}$$

where δV_{-2} is given by the simple expression (6.48). This equation belongs to the class of parametrised modified Teukolsky equations analysed in the previous sections, which obtains the corrections to the QNM frequencies using a continued fraction method. Thus, the results of that work are directly applicable to study the QNMs of (6.62) and we refer back to Chapter 5 for the details.

In the previous section we considered potentials of the form (6.48) with free coefficients A_k (allowing for more values of k), but in our case these coefficients are not free but determined by the theory. Furthermore, they depend on

the frequency ω that one is trying to determine. However, at first order in the higher-derivative couplings, it suffices to evaluate those coefficients on the corresponding Kerr QNM frequency whose corrections we want to obtain. Thus, for each value of harmonic numbers (l, m), overtone index n, polarisation $\pm$ and angular momentum χ, each of the higher-derivative theories provides a numerical value for the coefficients A_k. Combining those values with the shift in the QNM frequencies associated to each individual A_k, computed previously, we obtain the full shift in the QNM frequencies due to higher-derivative corrections.

The magnitude of higher-curvature corrections depends on the curvature scale of the spacetime. In the case of a black hole, the curvature scale around the horizon is set by the black-hole mass M, and it is thus useful to introduce the dimensionless couplings

$$\alpha_{\rm ev} = \frac{\ell^4 \lambda_{\rm ev}}{M^4}\,, \quad \alpha_{\rm odd} = \frac{\ell^4 \lambda_{\rm odd}}{M^4}\,, \quad \alpha_i = \frac{\ell^6 \epsilon_i}{M^6}\,, \tag{6.63}$$

which characterise the magnitude of the relative corrections to GR. In order to be within the regime of validity of the EFT, we require that these couplings be small $|\alpha_{\rm q}| \ll 1$, where ${\rm q} \in \{{\rm ev}, {\rm odd}, 1, 2, 3\}$.

For each of the higher-derivative corrections, with couplings α_q defined in (6.63), we write

$$\omega^{\pm}_{lmn} = \omega^{\rm Kerr}_{lmn} + \frac{\alpha_{\rm q}}{M} \delta\omega^{{\rm q},\pm}_{lmn} + \mathcal{O}(\alpha^2_{\rm q})\,. \tag{6.64}$$

Thus, we define $\delta\omega^{\rm q}$ to be the coefficients of the linear-order corrections to the QNM frequencies. We note that these quantities are defined in a way such that they are dimensionless and they only depend on the dimensionless spin, $\delta\omega^{\rm q} = \delta\omega^{\rm q}(\chi)$. Our perturbative analysis of higher-derivative terms only allows us to compute these linear coefficients, but it is also interesting to look at the non-linear terms in (6.64) in order to determine the regime of validity of the linear corrections. We come back to this later.

We note that for these frequencies, similar to those of a Kerr black hole, considering negative values of χ is equivalent to the exchange $m \to -m$:

$$\delta\omega^{{\rm q},\pm}_{lmn}(-\chi) = \delta\omega^{{\rm q},\pm}_{l-mn}(\chi)\,. \tag{6.65}$$

By using the results of the previous sections, we have obtained $\delta\omega^{{\rm q},\pm}_{lmn}$ numerically for all the higher-derivative theories in (4.1), for $l = 2, 3, 4$, $m \in [-l, l]$, $n = 0, 1, 2$ and $0 \leq \chi \leq 0.95$ in the case of $l = 2, 3$ and $0 \leq \chi \leq 0.75$ for $l = 4$. We observe that the convergence of the spin expansions depends a great deal on the value of m. Typically, the $m = l$ modes have the slowest convergence, and we get reliable results up to $\chi \sim 0.7 - 0.8$. For smaller values of m, including negative values, the convergence is much faster, and for some modes we get an accurate result up to the maximum value of the spin that we computed, $\chi \sim 0.95$.

In Figure 6.4 we offer, as an example, a visualisation of the $\delta\omega^{\rm q}$ coefficients of the $(l,m,n)=(2,m,0)$ modes of the even-parity cubic theory.

As a test of our results, we have compared them with those of [115] for the $(l,m,n)=(2,2,0),(3,3,0)$ modes, which were obtained using an eigenvalue perturbation approach to solve the modified Teukolsky equation [85, 88]. We find that the two results agree quite well, with a relative difference in $\delta\omega^{\rm q}$ that increases approximately linearly with χ, and which is smaller than 9% for $\chi<0.7$. However, we found that the eigenvalue perturbation method that was employed in [115] was incomplete, as it did not take into account the variation in the angular separation constants B_{lm} due to the correction to the frequency. This explains the small difference between our results here and those in [115]. In fact, we have repeated the eigenvalue perturbation computation of $\delta\omega^{\rm q}$ including this effect, finding that the relative difference between that method and Leaver's method for $|\chi|\leq 0.4$ is $\lesssim 10^{-6}$ if $l=2$ and $\lesssim 10^{-5}$ if $l=3$. We have checked that this is the case as well for overtones, which were not computed in [115]. This impressive agreement serves as a consistency test of our methods and results.

6.4.1 Polynomial fits

Although we provided numerical results for the shifts in the QNM frequencies, it is most useful to express those results in terms of a fitting function that captures the dependence on the angular momentum. Here we follow a strategy similar to that of [115] and write our results in terms of polynomial functions using a weighted fit.

We consider the data set $\{(\chi_i,\delta\omega_i), i=1,\ldots,i_{\rm max}\}$, where $\delta\omega_i$ are the numerically computed values of $\delta\omega^{{\rm q},\pm}_{lmn}$ (we are dropping the labels for clarity) for $\chi=\chi_i$, and we include both positive and negative values of $\chi_i\in[-\chi_{\rm max},\chi_{\rm max}]$, with $\chi_{\rm max}=0.95$ for $l=2,3$, and $\chi_{\rm max}=0.75$ for $l=4$. We perform independent fitting procedures for the real and imaginary parts of the frequency, but in order to avoid introducing more notation let $\delta\omega_i$ denote either the real or the imaginary part of the frequency shift.

The data points $\delta\omega_i$ have two sources of uncertainty. On the one hand, there is a coming from the tolerance of the numerical method employed for the computation of QNM frequencies, which is around $\varepsilon_{\rm num}\sim 10^{-7}$. On the other hand, there is an uncertainty due to the convergence of the spin expansion, and we estimate it as the difference of the results using spin expansions of order $n_{\rm max}$ and of order $n_{\rm max}-1$, as we mentioned above. Let us denote this uncertainty by $\varepsilon_{{\rm spin},i}$, which indeed depends on the spin and is different for each data point.

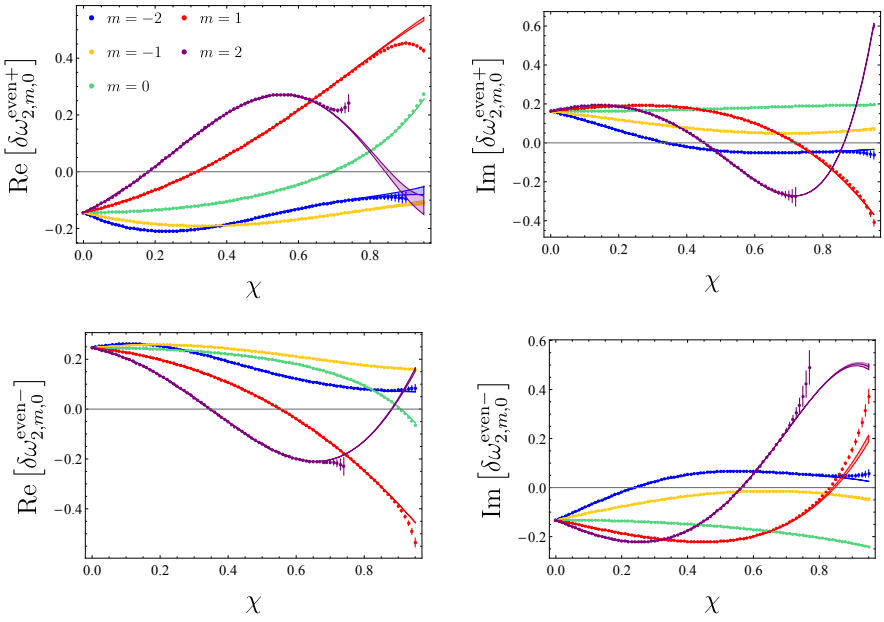


Figure 6.4: Shifts in the QNM frequencies of the $l = 2$ fundamental modes due to the even-parity cubic curvature corrections. The dots represent data points and the uncertainties are estimated from the convergence of the spin expansion (based on the difference with the frequency shift obtained with one less order). The lines and shaded regions correspond to the fitting polynomials of order $N_0 - 1$, N_0 and $N_0 + 1$, where N_0 is the optimum order.

We only include data points for which $\varepsilon_{\mathrm{spin},i}$ is less than 10% of the maximum value of $|\delta\omega_i|$ $\forall i$. Thus, the total uncertainty is

$$\varepsilon_{\mathrm{total},i} = \varepsilon_{\mathrm{num}} + \varepsilon_{\mathrm{spin},i}\,. \tag{6.66}$$

For small χ the spin expansion is very accurate and we have $\varepsilon_{\mathrm{spin},i} \ll \varepsilon_{\mathrm{num}}$, so the uncertainty from the numerical method dominates. For large spins, the uncertainty from the spin expansion dominates, with the transition happening at some critical value χ_c which grows as we increase the order of the expansion.

Then we wish to fit our data points to an Nth-degree polynomial

$$\delta\omega^N_{\mathrm{fit}}(\chi) = \sum_{j=0}^{N} c_j \chi^j\,. \tag{6.67}$$

In order to take the different accuracy of each data point into account, the fits are obtained by minimising the weighted sum of squared residuals

$$\Sigma_N = \sum_{i=1}^{i_{\max}} \frac{1}{\varepsilon^2_{\text{total},i}} \left|\delta\omega_i - \delta\omega^N_{\text{fit}}(\chi_i)\right|^2 , \tag{6.68}$$

where each weight is the inverse of the estimated variance of the data point.

In order to determine the optimum degree of the fitting polynomial, we compute the two-step ratios of the minimised squared residuals functions

$$d_N = \frac{\Sigma^{\min}_{N+1}}{\Sigma^{\min}_{N-1}} , \tag{6.69}$$

with $N = 1, 2, \ldots$. For the first few values of N, we typically have $d_N \ll 1$, indicating that increasing the degree of the polynomial results in a large increase of the goodness of the fit. For large enough N, we find that d_N saturates and approaches one, so increasing N does not significantly improve the fit. Thus, in order to avoid overfitting the data, we choose a value of N such that d_N is about to saturate. This is the maximum degree of the polynomial that guarantees that the fit is reliable and that we do not introduce spurious behaviour due to overfitting. For definiteness, we defined this optimum degree N_0 to be the lowest value of $N \geq 2$ for which $d_{N_0} > 0.2$.

We find that N_0 varies a lot: depending on the mode and the theory, we can have $6 \leq N_0 \leq 18$. The reason for this is not only the different accuracy of the results in each case, but it also has to do with the variability of $\delta\omega$ as a function of the spin. For some modes, $\delta\omega(\chi)$ has a mild dependence on χ and a low-order polynomial can fit it with very high accuracy. For others, it has a great variability (*e.g.*, it grows very fast, or shows several maxima and minima), so that a higher-degree polynomial is needed. We remark in particular that the order of the polynomial need not coincide with the order of the spin expansion, since the fitting polynomials are not the same as a Taylor expansion.

We expect that these fitting polynomials provide a reliable estimation for $\delta\omega$ even beyond the fitting range of χ. We show a test of this in Fig. 6.4. Along with the numerical data points, this figure shows the corresponding polynomial fits of degree N_0 and $N_0 \pm 1$. The shaded regions represent the area spanned by these three different polynomials, and they serve as a measure of the uncertainty in their prediction. We see that, even for the most problematic, $l = m = 2$ modes, the three fits agree very well, even beyond the fitting range. Thus, it is conceivable that the prediction from these fits is relatively accurate for spins as high as $\chi \sim 0.9$. For the other modes, where we have a better convergence of the spin expansion, the result is even more robust.

In the fitting region, all these polynomials are virtually indistinguishable from the data points, except when the uncertainties become large. In some cases, the fit departs from those data points, but this is the way in which the fit tells us that those points are not credible.

6.4.2 Overtones

Our results include, for the first time, the corrections to the overtones of rotating black holes. Thus, we take the opportunity to discuss some of the properties of these overtones.

As noticed long ago [100, 125], and recently revived by [102, 126], the spectrum of quasinormal modes of a black hole is unstable under small changes of the non-hermitian operator that defines the problem. The overtones are especially sensitive to this instability, and even a small deformation of the equations governing black-hole perturbations can lead to a total disruption of the spectrum of overtones. Thus, the corrections to the overtones are expected to be much larger than the corrections to the fundamental modes.[5] This effect has already been observed in some specific cases — see [61, 128–130].

In the case of higher-derivative corrections, there is yet another mechanism that will cause the corrections to the overtones to grow: the breakdown of the EFT at large frequencies. Indeed, for overtones of Schwarzschild and Kerr black holes, the nth-overtone frequency ω_n grows linearly with n in the imaginary direction [117]. Now, when $|\omega| \to \infty$, the potential V_s in the Teukolsky equation grows as $V_s \sim \omega^2$, but the correction to the potential δV_s can typically grow with a higher power of ω, hence producing larger corrections for higher overtones [130]. However, a direct comparison of δV_s with V_s is subtle (especially in the rotating case) since the powers of ω appear multiplying different powers of r. By exploring a few cases, we have found that the relative correction $|\delta V_s|/|V_s|$ indeed tends to grow for large enough n, although it does not necessarily show a monotonic behaviour for the first few values of n, since the growth of $|\omega_n|$ with n is relatively slow. We illustrate this in Fig. 6.5, where we see that for the first few values of n the correction to the potential actually decreases, although it eventually grows again. The growth appears to be faster in the quartic theory than in the cubic theory. On the other hand, the maximum of $|\delta V_s|/|V_s|$ tends to be closer to the horizon for higher overtones, although this behaviour does not seem to be universal.

[5] Here we are excluding "artificial" modifications of the perturbation equations, such as those involving adding an extra small bump to the potential at a large radius [127], which are known to disrupt the full spectrum of QNMs. The modifications due to higher-derivative corrections preserve the qualitative form of the potential and hence do not cause such a dramatic effect on the QNMs.

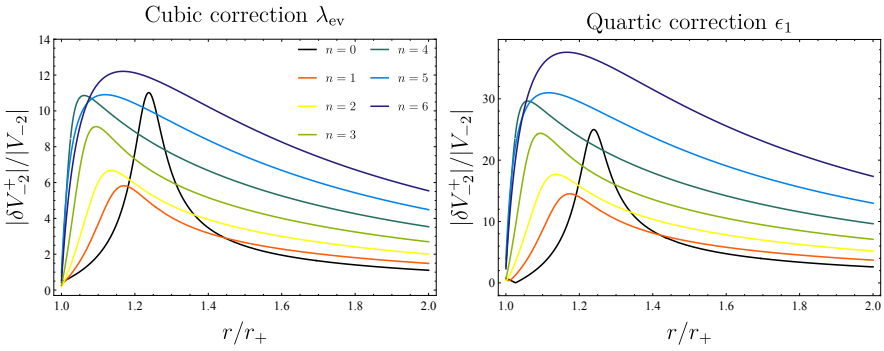


Figure 6.5: Relative correction to the potential for the first few overtones of modes with $l = m = 2$ and "+" polarisation for a black hole of spin $\chi = 0.3$. The left plot corresponds to the even-parity cubic theory, and the right plot to the quartic theory labelled by the parameter ϵ_1.

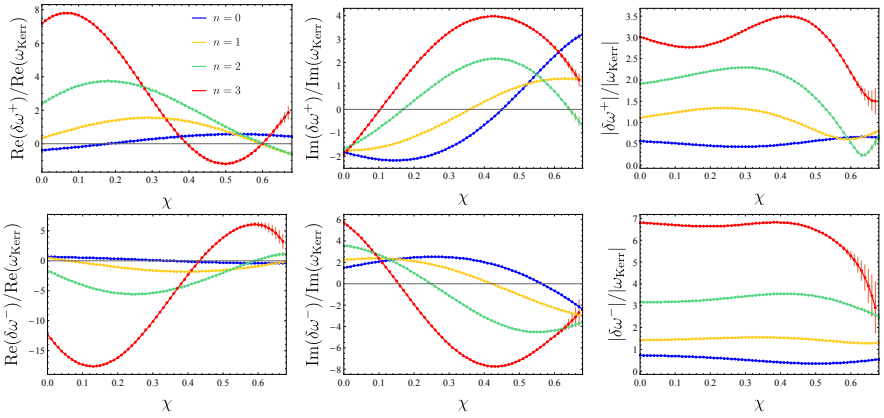


Figure 6.6: Corrections to the fundamental QNM frequency and to the first three overtones of $l = m = 2$ modes in the even-parity cubic curvature theory. The top and bottom row correspond to + and − polarisation, respectively. The first column shows the relative corrections to the real part of the frequency, the middle column the relative corrections to the imaginary part, and the last column, the absolute value of the relative correction.

Let us then show the corrections to the QNM frequencies. For definiteness we discuss the case of the even-parity cubic theory, but our full results are available in [113]. Fig. 6.6 shows the relative corrections to the QNM frequencies of the fundamental mode and three first overtones with $l = m = 2$ and for each of the two polarisations. The third column in that figure shows the relative correction

in absolute value, and it reveals that, quite consistently, higher overtones receive larger corrections. We recall from Fig. 6.5 that the corrections to the potential for these low overtones are not necessarily bigger than the correction to the potential of the fundamental mode. Thus, this growth is probably related to the unstable nature of the overtone spectrum. Although we have not computed higher overtones, we expect that these receive even larger corrections. The left and middle columns Fig. 6.6 also offer interesting information: the corrections to the real and imaginary parts of overtones vary a lot depending on the angular momentum of the black hole, with the curves becoming more nonlinear as we increase the overtone index. It would be interesting to understand how these overtones behave for angular momentum close to extremality, but a rigorous analysis of this limit is not possible with our current methods. In fact, we observe that the spin expansion converges more slowly as we increase the overtone index. The analysis of highly damped modes of rotating black holes thus requires a separate study. Our results with $n = 1, 2$ are nevertheless still accurate in the vicinity of $\chi \sim 0.7$ and beyond, depending on the case.

6.4.3 Regime of validity of the linear approximation

As we mentioned earlier, our analysis of the higher-derivative corrections is limited to first order in the coupling constants, which remains valid as long as these couplings are small enough. However, it is important to estimate exactly how small these couplings need to be. On the one hand, the modified Teukolsky equation receives corrections with higher powers of the $\alpha_{\rm q}$ couplings, but these are out of reach for now. On the other hand, even if we just consider the linearly modified Teukolsky equation, the QNM frequencies are in general non-linearly corrected. Here we explore these non-linear corrections to the QNM frequencies in order to estimate the regime of validity of the linear expansion, although we remark that this analysis is incomplete as we are missing the non-linear corrections to the Teukolsky equation.

In Section 6.2.3, we assessed the reliability of the linear approximation for single A_k modifications in the potential of the Teukolsky equation. Here we perform a similar analysis for the specific case of higher-derivative gravity, namely considering the potential modification of Eq. (6.48). We want to compare the prediction obtained with the linearised framework with the one from the full continued-fraction method. We define the measure of uncertainty as follows,

$$\Delta_{\delta\omega} \equiv \left| \frac{\omega_{\rm nl} - \omega_{\rm lin}}{\omega_{\rm lin} - \omega_{\rm Kerr}} \right| , \tag{6.70}$$

where $\omega_{\rm lin}$ is the frequency (6.64) truncated at first order in $\alpha_{\rm q}$ and $\omega_{\rm nl}$ represents the exact non-linear result obtained from the continued-fraction method.

This definition can be viewed as a relative uncertainty *on the correction* $\delta\omega$ to the GR quasinormal frequencies. We remark that this is different from the relative uncertainty on the full frequency, as $\delta\omega$ is itself small. Thus, the linear approximation remains valid as long as $\Delta_{\delta\omega} \ll 1$.

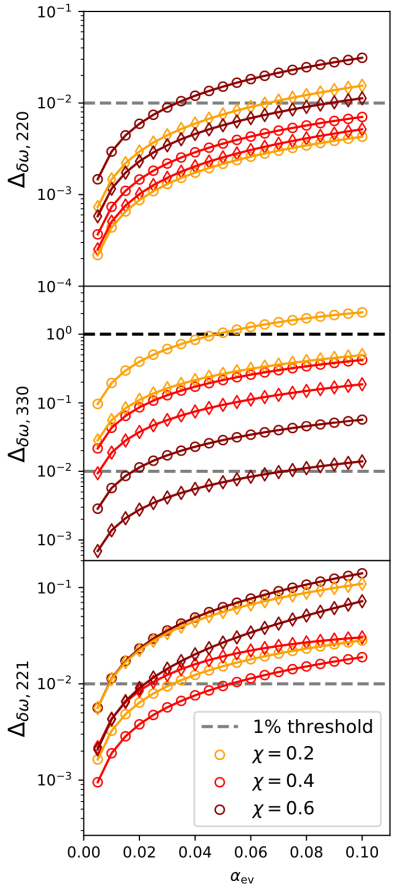


Figure 6.7: The relative uncertainty on the linear frequency correction versus dimensionless coupling in the cubic even theory for the 220 (upper panel), 330 (middle panel) and 221 (lower panel) modes at different spin parameters. The circles correspond to plus polarisation and the squares correspond to minus polarisation. The threshold at which the uncertainty reaches 1% and 100% values are indicated with dashed lines.

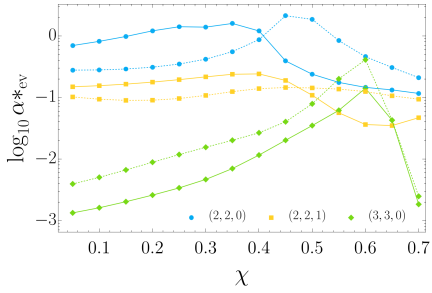


Figure 6.8: Threshold value of $\alpha^*_{\rm ev}$, for which the discrepancy between linear and non-linear approximations becomes larger than 5% in function of the spin. We report $\alpha^*_{\rm ev}$ for the $(2, 2, 0)$, $(2, 2, 1)$ and $(3, 3, 0)$ modes (respectively circle, square and diamonds) for the "+" (solid lines) and "−" (dashed lines) polarisations of the even-parity cubic curvature theory.

In Fig. 6.7 we show the results for the 220, 330 and 221 modes of the even-parity cubic theory at different values of the spin parameter for a range of dimensionless couplings $\alpha_{\rm ev} = \ell^4 \lambda_{\rm ev}/M^4$. As we naturally expect, these plots show that the uncertainty of the linear approximation grows as the value of coupling increases. In Fig. 6.8 we report the value of the coupling $\alpha^*_{\rm ev}$ for which $\Delta_{\delta\omega} = 5\%$ for a given mode at a given spin. We see that for 220 this happens for $\alpha_{\rm ev} \sim 0.1 - 1$, which are actually very large values of the coupling. For reference, at $\alpha_{\rm ev} \sim 0.1$ the Kerr QNM frequencies receive corrections of the order of 20%, and realistically we do not expect the EFT corrections to be valid beyond that. Thus, the linear approximation seems to perform better than expected. For the first overtone 221 the breakdown of the linear approximation occurs for somewhat smaller (but still fairly large) couplings, which is consistent with the fact that overtones receive larger corrections and with the observations of [130].

On the other hand, we observe that for the 330 modes, the linear approximation breaks down at much smaller couplings, especially for small spin. In this case we suspect that this is an artefact of the missing non-linear terms in the Teukolsky equation. Let us explain why. In the modified Teukolsky equation (6.62), the correction to the potential is only defined up to terms that do not modify the frequencies at linear order in the coupling. Let us denote such a term by $\delta V_{\rm trivial}$. Thus, if one makes $\delta V \to \delta V + C\delta V_{\rm trivial}$, where C is a constant, this has no effect at linear level in the coupling. However, $\delta V_{\rm trivial}$ will in general affect the frequencies non-linearly in the coupling, and this effect can be arbitrarily large if we take C to be large. This is what seems to be happening for the 330 modes.

We observe that for these modes the A_k coefficients in the Teukolsky equation are two orders of magnitude larger than for the 220 and 221 modes, but the linear correction to the frequency is of the same order of magnitude for all these cases. Thus, the potential for the 330 mode likely contains a large "trivial" piece $\delta V_{\rm trivial}$, which was probably introduced by all the manipulations we did to rewrite the potential in the form (6.48). This ambiguous term can only be fixed by computing the corrections to the Teukolsky equation at higher orders in the coupling. The conclusion is that our results should only be taken as an initial exploration, since the missing terms in the Teukolsky equation are crucial.

In any case, our results do confirm that a linear correction to the Teukolsky equation does imply a linear correction to the frequencies within a reasonable range of couplings. Another interesting observation that follows from Fig. 6.8 is that, contrary to what one could naively expect, increasing the rotation does not seem to imply an earlier breakdown of the linear regime.

6.5 Conclusions

In this chapter we have shown how to connect small deviations parametrised by powers of the radial coordinate r in the Teukolsky equation with small deviations in the eigenfrequencies and in the separation constants of modified Kerr BHs. We proved that for each value of n, ℓ, m there are up to nine independent coefficients in the radial parametrisation, but for specific cases they could be less. We presented a robust method to compute the coefficients that control the linear corrections to the QNM frequencies and separation constants through a generalisation of Leaver's continued fractions, and used it to compute them for $n = [0, 2]$, $\ell = [2, 4]$, $m = [-\ell, \ell]$ and $k = [-3, 4]$ for spins between 0 and 0.495.[6]

These coefficients will be particularly useful for the computation of QNMs of rotating BHs in alternative theories of gravity for which a modified Teukolsky equation is obtained, in the spirit of the method developed in [87–89]. So far, this method has been successfully applied to higher-derivative gravity, but theories like scalar-Gauss-Bonnet gravity and dynamical-Chern-Simons gravity (see [131]) are good candidates for this computation. The advantage of the parametrised method for the computation of QNMs of rotating BHs in alternative theories of gravity is that, in principle, one is not restricted to any mode, due to the flexibility of the continued-fraction method. We calculated the coefficients for a certain range of n, ℓ and m, but in principle one can compute them for each number and spin.

[6] We recall that in this chapter extremality corresponds to $a = 1/2$

The modified Teukolsky approach of [87–89] is currently limited by the fact that metric reconstruction is only available for GR, meaning that it is not yet possible to extend the method beyond first order in the coupling. For this reason, we did not explore further the quadratic coefficients as it was done in the non-rotating case [51, 61], and we limited the computation of the diagonal ones just to have a quick estimate of the uncertainty of the method itself.

The most intriguing open problem from our analysis is whether one can find a better way to exploit the potential ambiguity, as done in Section 6.1.2. We were able to reduce the number of independent coefficients $\alpha^{(k)}$ to 8. For the case of higher-derivative gravity we have been able to numerically reduce the number of free coefficients to just 4. One may wonder whether higher-derivative gravity has a special structure of the equations, or if there is a fundamental transformation of the potential that could diminish the number of free parameters. Such discussion is relevant especially if one wants to use this formalism in a theory-agnostic setup, *e.g.*, to perform ringdown tests of GR or the inverse problem. Since the coefficients $d^{(k)}$ have a spin dependence, it would be interesting to map them to ParSpec [60]. Another useful mapping would be with the WKB deviation coefficients, as done in [110].

We have provided the most complete calculation up to date of the corrections to the QNMs of Kerr black holes in a general EFT extension of GR. All our results can be found in the repository [124] that contains the analytically computed corrections to the potential (6.48), the numerical values of the shift in the QNM frequencies as defined in (6.64), and the coefficients of the polynomial fits (6.67). We computed these shifts for all the modes (l, m, n) with $l = 2, 3, 4$, $-l \leq m \leq l$, $n = 0, 1, 2$ of both polarisations $\pm$ for all the theories in (4.1) and for a large range of the black hole spin χ. The maximum spin that we can accurately capture depends on the mode, and it ranges between $\chi_{\rm max} \sim 0.7$ and $\chi_{\rm max} \sim 0.95$. We also performed a preliminary analysis of non-linear corrections to the QNM frequencies, finding that the first-order correction is accurate within a reasonable range of coupling constant values. Thus, these results should allow us to perform complete black-hole spectroscopy tests of higher-derivative gravity with ringdown observations.

Although our results capture the modes and black-hole solutions that are most relevant for astrophysical observations, there are still many unanswered questions about the QNM spectrum of rotating black holes beyond GR. For instance, our analysis does not yet include highly-damped modes or eikonal modes, since they require a separate treatment. Eikonal modes are especially interesting due to their connection with unstable null geodesics in GR [132, 133], which must have a generalisation for higher-derivative gravity [76, 134].

More importantly, the QNMs of highly rotating (*i.e.*, near-extremal) black holes cannot be accessed with our current methods based on a series expansion in the spin. The case of near-extremal black holes is particularly interesting since new phenomena appear close to extremality [135] and a possible amplification of higher-derivative effects could take place [136–138]. New methods will be required to study the QNM spectrum of these black holes. The analysis of perturbations in the near-horizon region recently reported by [139] may provide a promising starting point.

Chapter 7

Observational constraints

In the last decade we have been extremely fortunate to witness the direct detection of gravitational waves from compact binary mergers. The first observed gravitational-wave signal GW150914, already had a clear ringdown signature. In this and subsequent observed events, it was possible to clearly identify the fundamental mode of a quadrupole perturbation ($l = 2$, $m = 2$, $n = 0$). Ringdown measurements with the current generation of detectors, however, are limited as a black-hole ringdown is a relatively short signal dominated by noise. Although higher modes are still to be confidently detected, specific-data analysis techniques have been developed to start observational black-hole spectroscopy.

In this chapter, which is based on [140][1], we introduce the analysis, based on the principles of Bayesian inference, of current ringdown signal observations. We discuss some of the subtleties that are unique for this type of analysis compared the usual analysis of gravitational-wave signals from binary mergers. A consequence of the unique features of the ringdown signal is that the inference is preformed in the time domain (instead of the customary frequency domain). We discuss the general implementation of the Kerr ringdown model in pyRing, a specialised software package for ringdown analysis, and highlight some results. The higher-derivative corrections to the quasinormal-mode spectrum calculated previously were implemented in pyRing by adapting the Kerr ringdown model. We present and discuss the results of the analysis, which set an upper bound on the length scale of higher-derivative corrections to general relativity (GR).

[1] Written with G. Carullo, P. A. Cano, A. Liu, V. Cardoso, T. Hertog and T. G. F. Li.

The aim of a ringdown analysis is to fit a template based on a theoretical model from perturbation theory to the post-merger segment of a gravitational-wave signal from a binary black-hole coalescence. For a clean signal with little noise, as from a numerical relativity simulation, isolating the ringdown for a fit is done by discarding all data points before a specified starting time of the template. The ringdown analysis of actual detector measurements is more complicated as the template needs to be fitted to data with noise in a way that is independent of the preceding signal and takes into account the noise properties of the detector. Since the signal is buried deep in the detector noise, noise characterisation and signal modelling are required to apply Bayesian inference and find a probability distribution that quantifies the estimated signal parameters that fit the data. The noise in gravitational-wave detectors is frequency dependent (this is called coloured noise) and we assume that it is Gaussian and stationary within the observation window of an event (over longer time periods the noise slowly drifts). As a consequence, the noise is correlated in time and this makes it much harder to isolate a specific section of the signal in order to fit a ringdown model.

7.1 Bayesian inference

To describe an observed gravitational-wave signal with a specific signal model it is necessary to infer accurate estimates for the parameters within the model. This parameter estimation is done through the application of Bayesian inference. We start with some known information I (for example data treatment and detector noise properties) and signal model H dependent on parameters λ to provide a description for the observed data $\boldsymbol{d}$ (based on some signal template). The aim is to find the probability distribution of the parameters λ based on the available information: the observed data $\boldsymbol{d}$, the model H and information I. This probability is given by $p(\lambda \mid \boldsymbol{d}, H, I)$, which is the posterior distribution. Applying Bayes' theorem we find that

$$p(\lambda \mid \boldsymbol{d}, H, I) = \frac{p(\boldsymbol{d} \mid \lambda, H, I)\, p(\lambda \mid H, I)}{p(\boldsymbol{d} \mid H, I)}\,, \tag{7.1}$$

where we identify $p(\boldsymbol{d} \mid \lambda, H, I)$ as the likelihood, $p(\lambda \mid H, I)$ as the prior and $p(\boldsymbol{d} \mid H, I)$ as the model evidence, also known as the marginalised likelihood. The prior $p(\lambda \mid H, I)$ represents prior knowledge of the parameters λ before the data are analysed; for example a range of values expected for each parameter. The evidence $p(\boldsymbol{d} \mid H, I)$ does not depend on specific model parameters and is found by marginalising the likelihood over the parameters weighted by the prior

$$p(\boldsymbol{d} \mid H, I) = \int p(\boldsymbol{d} \mid \lambda, H, I)\, p(\lambda \mid H, I)\, \mathrm{d}\lambda\ . \tag{7.2}$$

Estimating parameters relies on selecting an appropriate model for the signal. If, however, the underlying model is not known, different models can be compared against each other. This is known as hypothesis testing or model comparison. Two models H_1 and H_2 can be compared by computing the odds ratio

$$O^{H_1}_{H_2} = \frac{p(H_1 \mid \boldsymbol{d}, I)}{p(H_2 \mid \boldsymbol{d}, I)} = \frac{p(\boldsymbol{d} \mid H_1, I)\, p(H_1 \mid I)}{p(\boldsymbol{d} \mid H_2, I)\, p(H_2 \mid I)}\,, \tag{7.3}$$

which is defined as the ratio between the posterior probabilities for the models. The first ratio $p(H_1 \mid I)/p(H_2 \mid I)$ forms the prior odds. This reflects any initial relative preference for a hypothesis and without prior preference is set to one. The other factor is the ratio of evidences, and better known as the Bayes factor

$$\mathcal{B}^{H_1}_{H_2} = \frac{p(\boldsymbol{d} \mid H_1, I)}{p(\boldsymbol{d} \mid H_2, I)}\,. \tag{7.4}$$

The evidence for a model is thus essential to compare models with each other.

In parameter estimation the data $\boldsymbol{d}$ only enter through the likelihood function $p(\boldsymbol{d}|\lambda, H, I)$, which depends on our understanding of the measurement process. We consider measurements made over a period T at intervals of Δt such that we have a uniform sampling time array $t_i = t_0 + i\Delta t$ with $N = T/\Delta t$ elements. A gravitational-wave signal $h(t)$ as a function of time can therefore be written as a time series $\boldsymbol{h} = (h_0, \ldots, h_{N-1})$ where $h_i = h(t_i)$. The detector noise present for each measurement can also be written as a time series $\boldsymbol{n} = (n_0, \ldots, n_{N-1})$. Assuming the noise is additive we write the detector output as

$$\boldsymbol{d} = \boldsymbol{n} + \boldsymbol{h}\,, \tag{7.5}$$

where in the time series $\boldsymbol{d}$ an element d_i represents the measurement at time t_i. For a signal template $\boldsymbol{h}(\lambda)$, the residual is therefore equal to $\boldsymbol{r}(\lambda) = \boldsymbol{d} - \boldsymbol{h}(\lambda)$. If the model is correct, the residuals for the true parameters (when $\boldsymbol{h} = \boldsymbol{h}(\lambda)$) should be drawn from the detector noise distribution. We therefore express the likelihood $p(\boldsymbol{d} \mid \lambda, H, I) = p(\boldsymbol{n} = \boldsymbol{r}(\lambda) \mid I)$ since the noise is model independent.

In the analysis of gravitational-wave observations we assume that, in the absence of a signal, the detector produces stochastic Gaussian noise that has zero mean. The probability-density function describing the noise samples $\boldsymbol{n}$ is therefore expressed as an N-dimensional multivariate normal distribution [141]:

$$p(\boldsymbol{n} \mid I) = \frac{1}{\det(2\pi\, \boldsymbol{C})^{1/2}} \exp\left[-\frac{1}{2}\, \boldsymbol{n}^{\intercal}\, \boldsymbol{C}^{-1}\, \boldsymbol{n}\right], \tag{7.6}$$

where $\boldsymbol{C} = \mathbb{E}\left[\boldsymbol{n}\boldsymbol{n}^{\intercal}\right]$ is the covariance matrix of the noise $\boldsymbol{n}$ from the detector. We assume $\boldsymbol{C}$ is known based on the instrument's properties such that I contains the values of $\boldsymbol{C}$ together with the assumption of Gaussian and additive noise.

Assuming the noise of the detector is wide-sense stationary, which is true for current detectors, the covariance matrix is only a function of time differences. We introduce the autocovariance function (ACF) $\boldsymbol{\rho}$ in terms of a time difference between sampling times so $\rho_k = \rho(k\Delta t)$. The covariance matrix then equals

$$C_{ij} = \rho_{|i-j|} \tag{7.7}$$

and is consequently a symmetric Toeplitz matrix, meaning $C_{ij} = C_{ji} = C_{i-1,j-1}$ for $i, j > 0$ and the matrix is therefore fully defined by its first column or row.

Imposing periodic boundary conditions where $\rho_k = \rho_{N-k}$, will make C circulant. Circulant matrices are diagonalised by applying a discrete Fourier transformation. The discrete Fourier transformation of the covariance matrix then yields

$$\tilde{C}_{ij} = \mathbb{E}[\tilde{n}_i^\intercal \tilde{n}_j^\intercal] = \frac{T}{2} S(|f_j|)\, \delta_{ij}\,, \tag{7.8}$$

where $S(|f_i|)$ is the one-sided power spectral density (PSD) and $f_j = j\Delta f = j/T$. The PSD is then related to the cyclic ACF through the transformation

$$S(|f_j|) = 2\Delta t \sum_{k=0}^{N-1} \rho_k\, e^{-2\pi i(jk/N)}\,, \tag{7.9}$$

conversely the ACF is related to the PSD with the inverse transformation

$$\rho_k = \frac{1}{2T} \sum_{j=0}^{N-1} S(|f_j|)\, e^{+2\pi i(jk/N)}\,, \tag{7.10}$$

which will be cyclic to satisfy the imposed periodic boundary conditions.

We can therefore write the likelihood in the frequency domain as

$$p(\boldsymbol{d} \mid \lambda, H, I) = \prod_{i=1}^{[\frac{N-1}{2}]} (\pi\, TS(f_i)/2)^{-1} \exp\left[-\frac{2}{T}\frac{\left|\tilde{d}_i - \tilde{h}_i(\lambda)\right|^2}{S(f_i)}\right], \tag{7.11}$$

where we would like to emphasise the fact that the residual in frequency domain will generally be complex. However, the time series $\boldsymbol{r}$ is real, so $\tilde{r}_k = \tilde{r}^*_{N-k}$ and $\tilde{r}_0$ and $\tilde{r}_{N/2}$ (for even N) are real. The residual has no zero-frequency component (any offset is removed) and the residual at the Nyquist frequency will be filtered. The bounds of the product can therefore be written from 1 to $[(N-1)/2]$ and we adjust the normalisation factor in front of the exponential accordingly [142].

It is more common to compute the log-likelihood, which is proportional to

$$\log(p(\boldsymbol{d} \mid \lambda, H, I)) \propto -\frac{2}{T} \sum_{i=1}^{[\frac{N-1}{2}]} \frac{\left|\tilde{d}_i - \tilde{h}_i(\lambda)\right|^2}{S(f_i)} \tag{7.12}$$

and represents a simple noise-weighted inner product in the frequency domain.

7.2 Time-domain likelihood

There were three assumptions regarding the noise properties that were required in order to arrive at (7.12) for signal analysis. The detector noise had to be Gaussian, wide-sense stationary and should satisfy periodic boundary conditions. In the analysis of the ringdown, where the aim is to isolate only the ringdown section of the signal, this last requirement is not enforceable whilst avoiding spectral leakage and not losing part of the signal.

In the regular analyses of gravitational-wave signals from compact binary coalescences, the time-series of detector data can selected to ensure that the signal is far enough from the segment edges, so that these can be tapered smoothly to prevent leakage when applying a Fourier transformation [141]. Although this removes information located close to the beginning or end of the observed data, this does not matter as long as there is no relevant signal content near the edges, or if the segment can be extended until this is satisfied.

Specifically, for the analysis of the ringdown this is not an option since most of the signal's power lies just at the start of the time series, right after the black holes have merged. Any smooth window function would therefore destroy a significant portion of the signal. Alternatively, keeping a short interval of data before the ringdown is also not valid, because the noise-weighted sum in the frequency domain couples points before and after the start of the ringdown, thereby modifying the actual frequency content of the observed ringdown signal. Finally, a simple Fourier transformation of the observed data beginning right at the start of the ringdown without a smooth window function will cause spectral leakage and inevitably correlate the beginning of the segment to its end.

These problems are avoided by analysing the signal fully in the time domain. We compute the likelihood directly based on the noise modelling of (7.6) as

$$p(\boldsymbol{d} \mid \lambda, H, I) = \frac{1}{\det(2\pi\,\boldsymbol{C})^{1/2}} \exp\left[-\frac{1}{2}\,(\boldsymbol{d}-\boldsymbol{h}(\lambda))^{\intercal}\,\boldsymbol{C}^{-1}\,(\boldsymbol{d}-\boldsymbol{h}(\lambda))\right] \tag{7.13}$$

and the log-likelihood to satisfy the following proportionality [143, 144]

$$\log(p(\boldsymbol{d} \mid \lambda, H, I)) \propto -\frac{1}{2}\,(\boldsymbol{d}-\boldsymbol{h}(\lambda))^{\intercal}\,\boldsymbol{C}^{-1}\,(\boldsymbol{d}-\boldsymbol{h}(\lambda))\,. \tag{7.14}$$

Given a specific analysis starting time, the only subtle points in the analysis are constructing the covariance matrix and any data conditioning that is applied. Typically for gravitational-wave observations the data conditioning includes downsampling, filtering and line-cleaning, all of which could impact the analysis. The duration of the data segment and its sampling rate are also crucial factors that can affect the results of a ringdown analysis (see [145] for a detailed study).

Assuming stationary noise, the matrix $\boldsymbol{C}$ only needs an estimate of the ACF. This can be obtained from noise-only observations by either computing the empirical autocorrelation of the noise or through (7.10) with an inverse Fourier transformation of an estimated PSD, for example from Welch's method. The ACF estimate has to be truncated to destroy the circularity that results from the Fourier transformation. The analysis segment for which the ACF is computed should be shorter than the segment length of noise-only data used in the empirical autocorrelation computation or the estimation of the PSD [143, 144].

The covariance matrix is by definition symmetric, real and positive semidefinite. It is therefore possible to apply a Cholesky decomposition on the matrix such that $\boldsymbol{C} = \boldsymbol{L}\boldsymbol{L}^\intercal$ where $\boldsymbol{L}$ is lower triangular. The inverse of $\mathbf{L}$ provides us with a way to define a whitened (or decorrelated) version of a time series array

$$\bar{\boldsymbol{x}} = \boldsymbol{L}^{-1}\boldsymbol{x}\,, \tag{7.15}$$

as each component of $\bar{\boldsymbol{n}}$ will independently be drawn from a normal distribution. If the parameters λ reflect the true parameters, the same should be true of $\bar{\boldsymbol{r}}(\lambda)$. This makes it possible to apply standard statistical tests to validate a model.

Looking back at equation (7.14), we can similarly use the covariance matrix to define a noise-weighted inner product in the time domain, where

$$\langle \boldsymbol{x}|\boldsymbol{y}\rangle = \boldsymbol{x}^\intercal \boldsymbol{C}^{-1}\boldsymbol{y} = \bar{\boldsymbol{x}}^\intercal \bar{\boldsymbol{y}}\,, \tag{7.16}$$

for any time-series arrays $\boldsymbol{x}$ and $\boldsymbol{y}$ of length N (equivalently, of duration T).

With this definition, we can introduce a notion of signal-to-noise ratio (SNR) for a limited time interval, as the normalised inner product over a time interval. We can write the matched-filter SNR at a given detector as

$$\mathrm{SNR}_{\mathrm{match}} = \frac{\langle \boldsymbol{d}|\boldsymbol{h}\rangle}{\sqrt{\langle \boldsymbol{h}|\boldsymbol{h}\rangle}}\,. \tag{7.17}$$

whilst the theoretical sensitivity of a detector for a signal can be estimated by

$$\mathrm{SNR}_{\mathrm{opt}} = \sqrt{\langle \boldsymbol{h}|\boldsymbol{h}\rangle}\,, \tag{7.18}$$

which is known as the optimal SNR (for a given PSD or ACF of the detector). This represents the expected value of the SNR (averaging over noise realisations) and is not per se the highest possible SNR, since any realisation of the noise could of course in practice have a higher or lower SNR value.

This time-domain definition of the SNR is better suited for ringdown analyses than usual definition in the frequency domain [144]. Although for a periodic ACF, $\boldsymbol{C}$ will be circulant and (7.16) becomes equivalent to the frequency-domain inner product used in (7.12) and the SNR definitions also become equivalent for an analysis segment that is extended to cover more than the full signal [144].

7.3 Kerr ringdown model

To analyse the ringdown we need to a construct waveform model that describes the gravitational-wave signal that is emitted after the merger of two black holes. As the newly formed remnant black hole gradually relaxes to its stationary state, the perturbed spacetime causes gravitational waves formed by a superposition of characteristic quasinormal modes (QNMs). For a Kerr black hole the frequency and damping time of QNMs solely depend on the black hole's mass and spin. Each mode that is excited (identified with labels l, m, n)[2] produces a signal

$$\mathcal{A}_{lmn}\, S^{\gamma}_{lm}(\iota, \varphi)\, e^{\,i\, t\, \omega_{lmn}}\,, \tag{7.19}$$

where $\mathcal{A}_{lmn}$ is the complex amplitude for the mode fitted freely to the data. $S^{\gamma}_{lm}(\iota, \varphi)$ is the spin-weighted spheroidal harmonic with oblateness $\gamma = a\omega_{lmn}$ with ι the inclination angle of the rotation axis with respect to the line of sight, and φ the azimuthal angle of the line of sight viewed in the black hole's frame. The complex QNM frequency ω_{lmn} can be interpreted as

$$\omega_{lmn} = \sigma_{lmn} + i/\tau_{lmn}\,, \tag{7.20}$$

where the imaginary part sets the inverse damping time of the mode $\tau_{lmn} > 0$ and the real part determines the oscillation frequency $\sigma_{lmn} = 2\pi f_{lmn}$.

An important point is that the QNM solutions for Kerr black holes come in pairs, since for a given (l, m, n) and value of a, the solutions $\omega_{lmn} = \pm\sigma_{lmn} + i/\tau_{lmn}$ are mirrored across the imaginary axis. For a correct template of the ringdown the two damped exponentials have to be present for each mode [118, 146].

We write the ringdown waveform starting at time t as the superposition

$$h_+ - ih_\times = \frac{M}{r} \sum_{lmn} \left[h^P_{lmn} + h^N_{lmn}\right] \theta(t - t_{\rm s})\,, \tag{7.21}$$

where we use P and N for the positive and negative frequency contributions

$$\begin{aligned} h^P_{lmn} &= \mathcal{A}^P_{lmn}\, S^{\gamma}_{lm}(\iota, \varphi)\, e^{+i\,(t-t_s)\,\omega_{lmn}}\,, \\ h^N_{lmn} &= \mathcal{A}^N_{lmn}\, S^{\bar\gamma}_{lm}(\iota, \varphi)\, e^{-i\,(t-t_s)\,\omega^*_{lmn}}\,, \end{aligned} \tag{7.22}$$

with $\bar\gamma = -\gamma^* = -a\omega^*$ and by symmetry $S^{\bar\gamma}_{lm}(\iota, \varphi) = (-1)^l S^{\gamma}_{l-m}(\pi - \iota, \varphi)^*$ [147]. Furthermore, if the progenitors' spins were aligned with the orbital rotation, reflection symmetry will relate the two amplitudes $\mathcal{A}^N_{lmn} = (-1)^l\, (\mathcal{A}^P_{lmn})^*$ [148]. We identify prograde modes for $m > 0$ that co-rotate with the black-hole spin and retrograde modes for $m < 0$ that counter-rotate.

[2] To follow convention we regretfully change from $e^{-i\omega t}$ in the previous chapter to $e^{+i\omega t}$.

In the literature there is an alternative mode identification, where modes are classified as prograde $\mathrm{sgn}(m) = \mathrm{sgn}(f_{lmn})$ and retrograde $\mathrm{sgn}(m) = -\mathrm{sgn}(f_{lmn})$. For $m \neq 0$ the complex frequencies are related by $\omega_{l-mn} = -\omega^*_{lmn}$ in a class. The reason for this choice is that retrograde modes are expected to be suppressed, and can thus be neglected in the analysis simplifying the expression to one sum. This is equivalent to requiring $m \geq 0$ in our classification of the modes.

The waveform written in (7.21) is expressed in the rest frame of the black hole. As a consequence of the expansion of the universe, all dimensionful quantities that are observed M, f_{lmn} and τ_{lmn} will be redshifted in the detector frame. Since the frequency and damping time scale with the black-hole mass, it suffices to replace the black-hole mass M with the observed mass $M_{\mathrm{obs}} = (1+z)M$ and the distance r with the luminosity distance D_{L} to account for the redshift [118].

The detector measures a signal projected by antenna patterns F_+ and $F_\times$

$$h = h_+ F_+(\theta, \phi, \psi) + h_\times F_\times(\theta, \phi, \psi)\,, \tag{7.23}$$

which depend on the polarisation of the gravitational wave ψ and the direction of the source relative to the orientation of the detector θ and ϕ, where

$$\begin{aligned} F_+(\theta, \phi, \psi) &= \tfrac{1}{2}(1 + \cos^2\theta)\cos 2\phi \cos 2\psi - \cos\theta \sin 2\phi \sin 2\psi\,, \\ F_\times(\theta, \phi, \psi) &= \tfrac{1}{2}(1 + \cos^2\theta)\cos 2\phi \sin 2\psi + \cos\theta \sin 2\phi \cos 2\psi\,, \end{aligned} \tag{7.24}$$

for a detector whose arms are at 90° from each other [141].

We briefly summarise how the Kerr model is implemented in pyRing [149] for the analysis of ringdown signals observed by the LVK collaborations [96, 150]. The $l = m = 2$ harmonic is the dominant mode in the ringdown [40, 151, 152], and only limited evidence exists for higher harmonics [153]. The first signal template we consider, called Kerr_{220}, consists of only the fundamental mode of this harmonic ($l = 2, m = 0, n = 0$) and models the signal once overtones, which have shorter damping times, become negligible (at roughly $10\,GM_{\mathrm{obs}}/c^3$ after merger) and the linearised ringdown description dominates the signal [59, 154]. The second signal template, called Kerr_{221}, consists of the same fundamental mode and its first overtone ($l = 2, m = 2, n = 1$). This allows us to start the ringdown analysis right at the estimated reference merger time [143, 155], disregarding higher overtones should not affect current observations [156, 157].

For the pyRing analysis the remnant mass and spin are assigned uniform priors, and the amplitude and phase are treated as free parameters with uniform priors. The reference time t_0 is computed from an estimate of the peak of the strain $(h_+^2 + h_\times^2)$ from the full IMR analyses (with approximant IMRPhenomXPHM). The sky location is fixed to coincide with the maximum likelihood value inferred from the full IMR analysis, whilst the polarisation receives a uniform prior.

7.4 EFT Analysis

A general EFT extension of GR constructed purely from Riemann tensor contractions that preserves parity to eight derivatives is given by the action

$$S = \int \mathrm{d}^4x \, \frac{\sqrt{|g|}}{16\pi} \left[R + \ell^4 \lambda_{\rm ev} \mathcal{R}^3 + \ell^6 \left(\lambda_1 \mathcal{C}^2 + \lambda_2 \tilde{\mathcal{C}}^2 \right) \right] . \tag{7.25}$$

This includes the higher-derivative curvature scalars $\mathcal{R}^3 = R_{\mu\nu}{}^{\rho\sigma} R_{\rho\sigma}{}^{\delta\gamma} R_{\delta\gamma}{}^{\mu\nu}$ with $\mathcal{C} = R_{\mu\nu\rho\sigma} R^{\mu\nu\rho\sigma}$ and $\tilde{\mathcal{C}} = R_{\mu\nu\rho\sigma} \tilde{R}^{\mu\nu\rho\sigma}$, where $\tilde{R}_{\mu\nu\rho\sigma} = \frac{1}{2} \epsilon_{\mu\nu\alpha\beta} R^{\alpha\beta}{}_{\rho\sigma}$ is the dual Riemann tensor. There is a new length scale ℓ related to the cut-off of the EFT, $\ell \sim 1/\Lambda_{\rm cutoff}$, whilst the coefficients $\lambda_{\rm ev,\,1,\,2}$ are dimensionless. With the physical scale of the system set by a black hole of mass M, we can introduce the dimensionless couplings:

$$\alpha_{\rm ev} = \frac{\ell^4 \lambda_{\rm ev}}{M^4} , \qquad \alpha_1 = \frac{\ell^6 \lambda_1}{M^6} , \qquad \alpha_2 = \frac{\ell^6 \lambda_2}{M^6} . \tag{7.26}$$

These characterise the size of the relative corrections to GR, which thus will become larger for smaller black holes. We assume $|\alpha_{\rm x}| \ll 1$ throughout the analysis, where $\mathrm{x} \in \{\mathrm{ev}, 1, 2\}$ so that we are well within the EFT regime and can apply an expansion in these couplings. We do not impose any further constraints in the present analysis.

The QNM frequencies with linear corrections to the Kerr values $\omega^{(0)}$ are

$$\omega^{\pm}_{\mathrm{x},lmn} = \omega^{(0)}_{lmn} + \alpha_{\rm x} \, \delta\omega^{\pm}_{\mathrm{x},lmn} , \tag{7.27}$$

where the label $\pm$ refers to the polarisation and isospectrality is generally broken.

We use a polynomial fit as a function of the dimensionless spin χ to model the corrections to the QNM frequencies for each polarisation and theory,

$$\delta\omega^{\pm}_{\mathrm{x},lmn} = \sum_{k=0}^{K} c^{(k)\pm}_{\mathrm{x},lmn} \, \chi^k , \tag{7.28}$$

where the coefficients for the dominant fundamental modes and their overtones were calculated in the previous chapter and we truncate the sum at $K = 12$.

To construct the waveform template used to analyse the data, we rely on the pyRing python package, which is tailored to model and analyse ringdown signals [149, 158]. Although a diverse set of GR and beyond-GR models are implemented in pyRing, we found it better to introduce a new parametrisation for the effect of the higher-derivative corrections on the ringdown waveform.

We start from the Kerr model and separate the metric polarisations as these are no longer isospectral

$$
\begin{aligned}
h_+ - i h_\times &= \frac{M_{\rm obs}}{D_{\rm L}} \sum_{lmn} \sum_{q=\pm} \left(h^{P,q}_{lmn} + h^{N,q}_{lmn} \right) , \\
h^{P,q}_{lmn} &= \mathcal{A}^{P,q}_{lmn}\, \mathcal{S}^{\gamma}_{lm}(\iota,\varphi)\, e^{+i\,(t-t_s)\,\omega^{q}_{lmn}}\, \theta(t-t_{\rm s}) \,, \\
h^{N,q}_{lmn} &= \mathcal{A}^{N,q}_{lmn}\, \mathcal{S}^{\bar{\gamma}}_{lm}(\iota,\varphi)\, e^{-i\,(t-t_s)\,\omega^{q*}_{lmn}}\, \theta(t-t_{\rm s}) \,,
\end{aligned}
\tag{7.29}
$$

where ω^{q}_{lmn} is the modified QNM frequency, expressed as a function of the redshifted mass of the remnant black hole as observed in the detector frame $M_{\rm obs}$, and its spin a. The angle ι denotes the inclination of the rotation axis of the final black hole relative to the observer's line of sight and φ the azimuthal angle of the line of sight in the black hole's frame. Here $\mathcal{S}_{lmn}$ are spin-weighted spheroidal harmonics, and $t_{\rm s} = t_0$ is the start time of the template.

Each QNM labelled by the indices lmn has two complex frequencies $\omega^{\pm}_{lmn}$ and a priori also two unknown complex amplitudes $\mathcal{A}^{P/N,\pm}_{lmn}$, where the contributions with a positive and negative real part of the frequency for each QNM are labelled with P and N respectively. Assuming the spins of the binary progenitors were aligned with the orbital angular momentum, reflection symmetry implies $\mathcal{A}^{N,\pm}_{lmn} = (-1)^l\, (\mathcal{A}^{P,\pm}_{lmn})^*$, which halves the number of free parameters per mode. For theories that preserve parity symmetry, as the ones considered in the analysis, this is a very good approximation for the current dataset for the purpose of searching for new physics. Here, $m < 0$ contributions represent counter-rotating modes [118, 146, 159], which are only significantly excited in systems with large progenitors spins anti-aligned with the orbital angular momentum, hence negligible for the current dataset.

To model the modified complex QNM frequency ω_{lmn} for a specific higher-derivative correction, we use (7.27) and (7.28). The theory-dependent coefficients $c^{(j)\pm}_{{\rm x},lmn}$ are made available within pyRing [158]. In what follows we remove the theory index x to ease the notation.

Assuming that we have a single correction in the action (7.25), we can reabsorb the corresponding coupling λ into the length scale of the EFT ℓ, so we can always set $\lambda = \pm 1$. From (7.26), we express α as

$$
\alpha = \lambda \left(\frac{\ell}{M} \right)^p = {\rm sign}(\ell) \left(\frac{|\ell| \cdot (1+z)}{M_{\rm obs}} \right)^p \,, \tag{7.30}
$$

where p is the power of the scaling of the coupling, equal to 4 for $\lambda = \lambda_{\rm ev}$ and 6 for $\lambda = \lambda_{1,2}$, and we allow ℓ to be negative to account for the sign of λ.

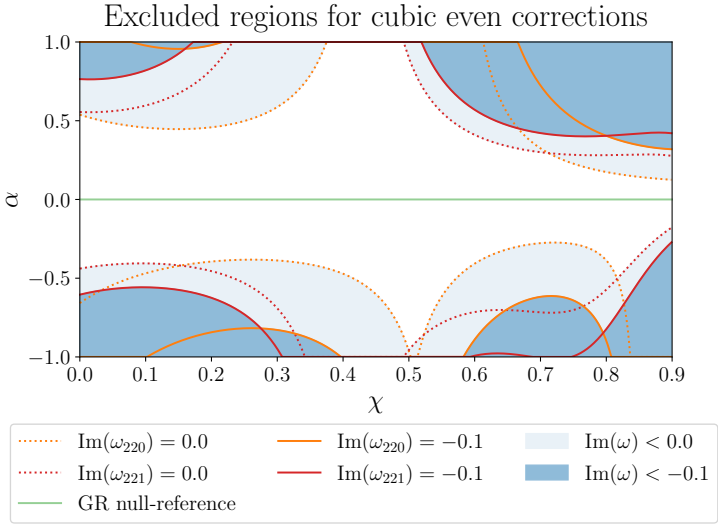


Figure 7.1: Parameter space of effective-field-theory corrections to the general relativistic quasinormal modes spectrum, as a function of coupling constant and black-hole rotational rate. Regions where the fundamental and first overtone $(l, m, n) = (2, 2, 0), (2, 2, 1)$ modes appear to grow exponentially ($\mathrm{Im}[\omega] < 0$) (dotted lines), or grow faster than $\mathrm{Im}[\omega] < -0.1$ (solid lines), are highlighted for cubic even corrections.

Since the length scale modifying the black-hole dynamics is related to the source dynamics, the mass scale of the black hole in the rest frame M needs to be scaled with the redshift factor compared to the mass observed in the detector $M_{\rm obs} = M\,(1 + z)$. This signals a breaking of GR scale invariance. If any EFT modification would be detected and consequently a specific value of ℓ inferred, it would then be possible to measure the source-frame mass M with subsequent observations. This would allow us to perform measurements of the redshift, hence the cosmological evolution, entirely using gravitational-wave signals from black-hole binaries.

A limitation of only knowing the QNM spectrum to linear order in the coupling is that it is still possible, even with $\alpha < 1$, to have exponentially growing modes for certain intervals of χ, depending on the polarisation and theory. These limitations, which are expected to be removed when including higher-order corrections, signal a breaking of the linear approximation. Hence, in our analysis, apart from limiting the correction factor to $|\alpha| < 1$, we also exclude regions of the parameter-space with modes that grow exponentially.

The reason to exclude these regions a priori, is that this behaviour also causes numerical issues when calculating the likelihood when modes grow quickly ($\mathrm{Im}[\omega] < -0.1$). Regions of the parameter space with exponentially growing modes would anyhow be excluded, given the damped morphology of the gravitational-wave signal. Fig. 7.1 illustrates the location of these effects, with the constraint on the parameter space added as a function of α and χ.

The spin of the final remnant black hole was limited to $\chi \leq 0.93$ in the analysis, since the uncertainty on the polynomial fit increases rapidly near extremal spin, whilst the magnitude of the linear corrections to most of the QNM frequencies seem to grow significantly. This limit does not affect the obtained constraints, since no near-extremal remnant spins have yet been observed.

Finally, in the analysis we searched for the dominant $lmn = 220$ fundamental mode and also its first overtone $lmn = 221$. Although adding overtones with constant amplitudes near the waveform peak [143, 155] does not correspond to physical black-hole vibrational spectra [160] (see also [161, 162] for wave packets scattering), their phenomenological usage significantly boosts the recovered signal-to-noise ratio, even beyond-GR [163]. We do not include other modes, since no higher angular mode has so far been confidently detected [96, 153, 164].

We now analyse the observed gravitational-wave events from the black-hole mergers contained in the GWTC-3 catalogue [165–167] that present detectable ringdown signatures. For this we make use of the ringdown analysis python code pyRing [149, 158], specifically written for the analysis of the post-merger phase signals with a time-domain likelihood formulation. Such a framework has been used within all ringdown-only spectroscopic analyses from the LVK collaboration in the GWTC-2 [168–170] and GWTC-3 [96] catalogues, and is thus extensively tested. We use the same event-selection criteria, and identical settings to the latter analyses also with regard to the data conditioning, the sampling and the likelihood parameters. We do not include in our dataset the event GW191109_010717 because of data-quality issues [96]. To increase slightly the amount of signal-to-noise ratio (SNR) captured [145, 171–173], at the expense of an increase in computational cost compared to the LVK analyses, we increase the analysis segment to 0.2 s. We isolate the gravitational-wave signal portion that follows the peak of the reconstructed $h_+^2 + h_\times^2$ and fix $t_{\rm start}$ to this peak. Following standard practice in spectroscopic analyses, we assume the maximum likelihood sky position extracted from a full signal template to propagate this estimate to multiple detectors [144, 166]. This is allowed since gravitational-wave propagation is not modified in our setup. We apply uniform priors on all the sampled parameters: the remnant black hole's observed mass $M_{\rm obs} \in [10, 500]\, M_\odot$, remnant spin $\chi \in [0.00, 0.93]$, the QNM amplitudes $A_{lmn} \in [0, 50]$, phases $\phi_{lmn} \in [0, 2\pi]$ and EFT scale $\ell \in [-740, +740]$ km (including $\mathrm{sign}(\lambda)$).

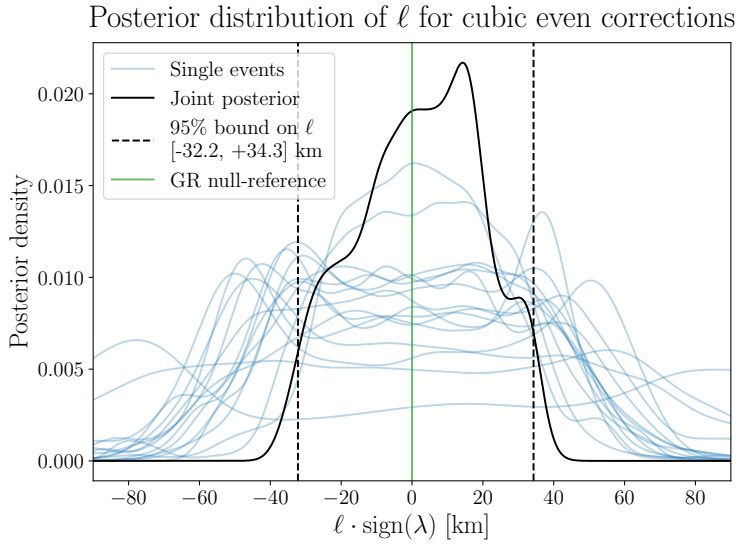


Figure 7.2: Posterior probability distributions of the length scale of new physics, ℓ, appearing in the effective-field-theory action (cubic even case). Constraints are derived from the time-domain spectroscopic analysis with pyRing of post-merger signals from binary black-hole coalescences, contained in the GWTC-3 catalogue from the LVK collaboration.

To avoid prior effects having a sizeable impact on the ℓ estimate, the luminosity distance is also sampled under a uniform prior, and constrained within the 95% bound obtained from GWTC-3 analyses. We repeat the analysis both when assuming QNM complex frequencies to be dictated by GR (in which case we fix $\ell = 0\,\mathrm{km}$), and by the EFT corrections under consideration, allowing us to construct an estimate of the Bayesian evidence for the presence of any deviations in the Einstein-Hilbert action. For all the events analysed, we verified that the range of ℓ (in km) supported by its marginalised posterior was at a clearly lower scale than the range of M supported by its marginalised posterior (converted from $M_\odot$ to km in geometric units and taking into account the redshift). A significant overlap between these posteriors would break the EFT assumption. There is one event, GW190708_232457, where the black-hole mass posterior is so broad that the ℓ range becomes comparable to the EFT cutoff, hence the results do not satisfy the EFT assumption (see e.g. Sec.IV.D of [174]). This event was therefore excluded from further analysis.

We report the marginalised posterior distributions of the ℓ parameter in Fig. 7.2, for the cubic even corrections and in Fig. 7.3 for the quartic corrections.

Posterior distributions for all events are centred around zero, with various degree of spread due to the difference in SNR among different events, together with a roughly corresponding degree of noisy features. Since ℓ is fixed by a universal fundamental constant that is common to all events, combining the single-event constraints into a unique posterior probability distribution can be achieved simply by first constructing a standard kernel-density estimation, and then multiplying the likelihood functions (under our assumption of a flat prior) [175]. The result of this is shown in Fig. 7.2 (solid black line). As expected, the combined result is less sensitive to noise-induced features of single events (light-blue lines). These constraints are robust even if individual events are removed, although the shape of the combined result is sensitive to changes.

Posterior distributions of remnant black-hole parameters and complex amplitudes are consistent between the GR and EFT analyses, with an expected broadening in the EFT case due to the increase in the number of parameters. We include in the supplemental material a comparison between the posterior distributions of the final observed mass and final spin for the ringdown analysis in GR and the analysis including EFT corrections for GW150914. The agreement of these two sets of posteriors, together with the large support for $\ell = 0$ shown in Fig. 7.2, indicates that no sign for violations of GR is present in the dataset. This result is made quantitative in Table 7.1, reporting the ratio of the global Bayesian evidences comparing the GR and EFT hypotheses, namely the Bayes Factors. We find no statistically significant evidence for a violation of GR.

We obtain these constraints with a method different from Ref. [174], which used a pSEOBNR waveform model that modified the ringdown to include corrections to the dominant QNM frequency and damping time linear in the spin. We do not use the pre-merger signal in our analysis and infer all parameters such as the final mass and spin, as well as the amplitudes and phases of each QNM from the ringdown. We also model isospectrality breaking and include the full non-linear dependence on spin of QNM corrections. As is evident from the previous chapters, the non-linear nature of these corrections is significant, implying their necessity for robust constraints on EFT corrections.

Theory	$\mathrm{sign}(\lambda) \cdot \ell$ in km	$\ln(\mathcal{B}_{\mathrm{EFT}}/\mathcal{B}_{\mathrm{GR}})$
Cubic even	$[-32.2, +34.3]$	$[-2.0, +1.0]$
Quartic 1	$[-24.9, +35.0]$	$[-2.1, +1.4]$
Quartic 2	$[-27.0, +38.7]$	$[-1.7, +0.9]$

Table 7.1: Summary of the constraints obtained at a 95 % level for each EFT correction, by combining posterior distributions of single events from GWTC-3, and the range of Bayes factors obtained from all events when comparing models.

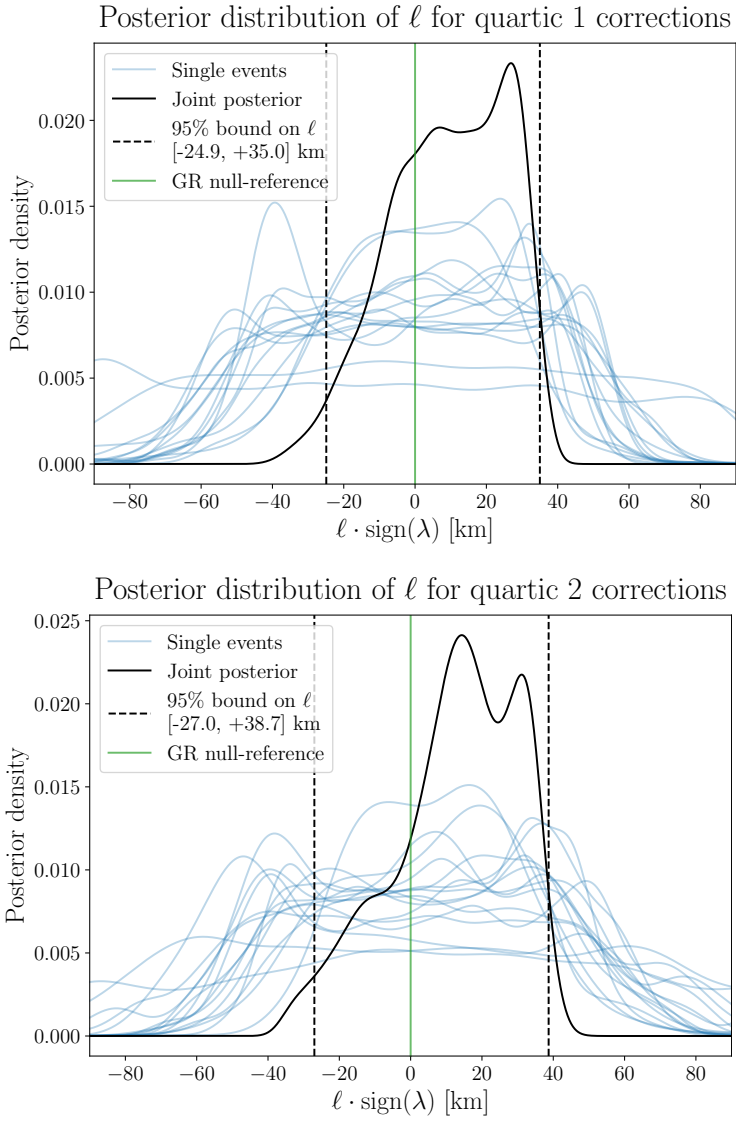


Figure 7.3: Posterior distributions of ℓ for quartic 1 and 2 corrections obtained from the analysis of the GWTC-3 catalogue.

7.5 Conclusions

We have presented the first time-domain spectroscopic search valid up to high black-hole rotation rates in a symmetry-preserving EFT extension of GR, constructed under minimal assumptions. Our study focused on the post-merger phase of binary black-hole mergers and relied crucially on the recent accurate predictions of the QNM frequency shifts in these theories. We find no evidence for new physics signatures in the quasinormal modes of the observed gravitational waves from the black-hole mergers in the GWTC-3 catalogue. The logarithm of the Bayes factor $[\ln(\mathcal{B}_{\rm EFT}/\mathcal{B}_{\rm GR})]$ of each EFT model with respect to GR was less than 1.5 for all events and negative for most events, compatible with statistical fluctuations [170]. Combining the information from all events we obtain a constraint on the length scale associated with each of the EFT corrections. These constraints are $\ell < 34.3\,\mathrm{km}$ for the cubic correction, $\ell < 35.0\,\mathrm{km}$ for quartic 1, and $\ell < 38.7\,\mathrm{km}$ for quartic 2.

Our analysis can readily be extended to EFTs with parity-violating terms. We leave such extension to future study, except to note that the assumption of symmetry that couples the amplitudes of modes would no longer be correct, implying a doubling of the number of free amplitude parameters and hence an increased computational cost. For other theory-specific corrections, including Einstein dilaton Gauss-Bonnet and dynamical Chern-Simons gravity, a similar analysis should be possible if leading corrections to the fundamental modes and the first overtones of QNM frequencies are known at higher spins (see [176]).

The next-generation ground-based gravitational-wave detectors such as the Einstein Telescope and Cosmic Explorer [177, 178] will enable the detection of black-hole mergers with much larger SNR. Moreover, given their improved sensitivity at higher frequencies, they will make it possible to observe the ringdown for smaller black holes. Since these have horizon regions with larger spacetime curvature, this will dramatically boost our capability to search for higher-derivative corrections to GR. The expected sensitivity of these detectors to theory-specific corrections to the ringdown signal was studied in Ref. [179], and it would be interesting to repeat a similar analysis in our setup. One way to improve the constraints might be by modelling the amplitudes of the QNMs for rotating black holes in these theories, either using numerical relativity simulations or from pre-merger predictions from parametrised-post-Newtonian or parametrised-post-Einsteinian frameworks. This method would allow one to extract significantly more information from the ringdown waveform, enabling even higher sensitivity. Overall, theory-specific predictions of QNM spectra for rotating black holes are essential to exploit the full potential of next-generation gravitational-wave detectors in searching for new physics in the high-curvature regime of gravity. Our results constitute a stepping-stone in this direction.

Chapter 8

Conclusion

Motivated by the idea that the direct measurement of gravitational waves from the merger of black holes could reveal the dynamics of gravity in spacetime regions with strong curvature, we studied the ringdown of black holes following such a merger that is characterised by a superposition of quasinormal modes. General relativity predicts that the frequencies and damping times of these modes are fully determined by the mass and spin of the remnant black hole. As we demonstrated, the spectrum of these quasinormal modes is sensitive to the black-hole geometry and the spacetime dynamics from the theory of gravity. The idea of black-hole spectroscopy is to use theoretical predictions to infer the properties of black holes from the gravitational waves emitted by the ringdown. We have strived in this thesis to connect the theoretical study of gravity to the analysis of ringdown observations through the explicit calculation of the impact of higher-derivative corrections on the ringdown signal of rotating black holes.

We have specifically studied the effect of higher-derivative corrections on the quasinormal modes spectrum of rotating black holes. The framework that was developed allows us to examine linear perturbations on a rotating black hole with small deviations from the Kerr geometry and the Einstein field equations. As this method allows an expansion in the spin parameter to very high orders, it is also applicable to rapidly rotating black holes. This is significant as astrophysical black holes can spin quite rapidly, and predictions from methods that do not fully capture the complex effects of rotation would be inaccurate. The isospectrality present in general relativity is broken by these corrections and some quasinormal mode shifts are significantly enhanced at higher spin. The validity of our implementation of the method was confirmed by matching the results in the slow-rotation limit and satisfying several consistency checks.

Since higher-derivative corrections lead to deviations in the effective potential of the modified Teukolsky equation, we studied a general parametrisation of such deviations, any of which can be captured by a limited number of coefficients. We calculated the linear corrections to the quasinormal mode frequencies related to each coefficient with a generalisation of Leaver's continued-fraction method. This allows for the fast computation of corrections to the quasinormal modes of rotating black holes in any theory that yields a modified Teukolsky equation. Another point of interest is the potential to connect a description for deviations in the quasinormal mode spectrum to modifications of the Teukolsky equation. We applied this method to calculate the corrections to the quasinormal modes from higher-derivative corrections for the modes of the most dominant harmonics, up to the second overtone and for nearly the full range of the black-hole spins. A preliminary analysis of non-linear corrections showed that the first-order correction seems accurate within a reasonable range of coupling-constant values. These results, therefore, are sufficiently robust to be used in a ringdown analysis.

We have provided an overview of the essentials for ringdown analysis, including a time-domain formulation of the likelihood and a waveform template, to describe the observed gravitational-wave signal from the ringdown of Kerr black holes. Together with the theoretical calculations of quasinormal mode frequencies with higher-derivative corrections, we constructed a template to model a ringdown waveform that included these corrections and allowed for isospectrality breaking. This waveform model was implemented in pyRing (a ringdown analysis package) to perform the first time-domain spectroscopic search for EFT corrections with accurate theoretical modelling of corrections for rapidly rotating black holes. We found no evidence for new physics signatures in the quasinormal modes of the observed black-hole mergers in the GWTC-3 catalogues and were able to set a constraint on the length scale associated with each type of EFT correction. We see these results as a first step in the development of theory-inspired searches for signs of deviations from general relativity with black-hole spectroscopy.

Gravitational-wave observations from the ringdown of black holes represent a unique opportunity to examine the fundamental nature of gravity in this regime. This requires that the full range of possible spins of astrophysical black holes be accounted for when modelling the ringdown, including during the calculation of their quasinormal mode frequencies. The framework and analysis we have developed should be applicable for other types of theoretical corrections to general relativity that have rotating black holes that deviate slightly from Kerr. With our research, we strive to contribute to further development of the field of black-hole spectroscopy in preparation for future gravitational-wave observations. We look forward to new discoveries in the study of the ringdown of black holes.

Appendix A

Appendix to Chapter 2

A.1 Equations from General Relativity

We provide a brief summary of some standard equations in general relativity. Numerous textbooks and notes (for example [180–182]) exist as references.

To denote the spacetime index of an object in the 4 dim. manifold of spacetime, we use lower-case Greek letters with value $0, 1, 2$ or 3. An event in spacetime is given by

$$x^\mu = (t, \mathbf{x}) \tag{A.1}$$

where t is the time coordinate and $\mathbf{x}$ is a 3 dim. vector with spatial coordinates. We use the mostly-plus signature convention $(-,+,+,+)$ for the metric and, as mentioned in the introduction, use geometric units $c = 1$ and $G = 1$.

The invariant line element can be written as

$$\mathrm{d}s^2 = g_{\mu\nu}(x)\,\mathrm{d}x^\mu\,\mathrm{d}x^\nu \tag{A.2}$$

where $g_{\mu\nu}$ is the metric tensor, a symmetric with ten independent components. Indices can be raised and lowered with the metric $g_{\mu\nu}$ and inverse metric $g^{\mu\nu}$.

In a flat Minkowski spacetime with (t, x, y, z) coordinates the metric equals

$$g^{\text{flat}}_{\mu\nu} = \eta_{\mu\nu} = \mathrm{diag}\,(-1, 1, 1, 1)\,. \tag{A.3}$$

where diag represents the diagonal components of the metric tensor.

We write partial derivatives and covariant derivatives as

$$\partial_\mu V^\nu = \frac{\partial V^\nu}{\partial x^\mu} \qquad \nabla_\mu V^\nu = \partial_\mu V^\nu + \Gamma^\nu_{\lambda\mu} V^\lambda \tag{A.4}$$

with the Christoffel symbol for a torsion-free and metric-compatible connection:

$$\Gamma^\sigma_{\mu\nu} = \frac{1}{2} g^{\sigma\lambda} \left(\partial_\mu g_{\nu\lambda} + \partial_\nu g_{\mu\lambda} - \partial_\lambda g_{\mu\nu} \right). \tag{A.5}$$

From the Christoffel symbols we can construct the Riemann tensor:

$$R^\mu{}_{\nu\sigma\tau} = \partial_\sigma \Gamma^\mu_{\nu\tau} - \partial_\tau \Gamma^\mu_{\nu\sigma} + \Gamma^\lambda_{\nu\tau} \Gamma^\mu_{\lambda\sigma} - \Gamma^\lambda_{\nu\sigma} \Gamma^\mu_{\lambda\tau}. \tag{A.6}$$

The Ricci tensor and the Ricci scalar are contractions of the Riemann tensor

$$R_{\mu\nu} = R^\lambda{}_{\mu\lambda\nu} \qquad \text{and} \qquad R = R^\lambda{}_\lambda \tag{A.7}$$

and the traceless part of the Riemann tensor is given by the Weyl tensor

$$C_{\mu\nu\rho\sigma} = R_{\mu\nu\rho\sigma} - g_{\mu[\rho} R_{\sigma]\nu} + g_{\nu[\rho} R_{\sigma]\mu} + \frac{1}{3} R\, g_{\mu[\rho} g_{\sigma]\nu}. \tag{A.8}$$

The action of general relativity in the presence of matter fields equals

$$S = \int \sqrt{|g|} \left(\frac{1}{16\pi} R + \mathcal{L}_\mathrm{m} \right) \tag{A.9}$$

where g is the determinant of the metric, R is the Ricci scalar, which represents the Einstein-Hilbert term of the action, and $\mathcal{L}_\mathrm{m}$ describes the matter fields.

The resulting energy momentum tensor is defined as

$$T_{\mu\nu} = -\frac{2}{\sqrt{|g|}} \frac{\delta S_\mathrm{m}}{\delta g^{\mu\nu}} = -2 \frac{\partial \mathcal{L}_\mathrm{m}}{\partial g^{\mu\nu}} + g_{\mu\nu} \mathcal{L}_\mathrm{m} \tag{A.10}$$

where S_m is the part of the action without the Einstein-Hilbert term. A variation of the action with respect to the inverse metric yields the Einstein field equations

$$G_{\mu\nu} = R_{\mu\nu} - \frac{1}{2} R\, g_{\mu\nu} = 8\pi T_{\mu\nu} \tag{A.11}$$

where $G_{\mu\nu}$ is the Einstein tensor defined in terms of the Ricci scalar and tensor. The Einstein field equations form a set of ten coupled differential equations.

The second Bianchi identity imposes that

$$\nabla_\lambda R_{\alpha\beta\mu\nu} + \nabla_\nu R_{\alpha\beta\lambda\mu} + \nabla_\mu R_{\alpha\beta\nu\lambda} = 0. \tag{A.12}$$

This implies that $\nabla_\mu G^{\mu\nu} = 0$ and as result of the Einstein equations above $\nabla_\mu T^{\mu\nu} = 0$, and energy and momentum are locally conserved quantities.

A.2 Vector and tensor spherical harmonics

We list the components of the vector and tensor spherical harmonics from [62]. For the vector spherical harmonics from (2.12) we find

$$Y^{lm}_{\theta} = \frac{\partial}{\partial\theta}Y^{lm}, \qquad X^{lm}_{\theta} = -\frac{1}{\sin\theta}\frac{\partial}{\partial\phi}Y^{lm}, \tag{A.13}$$

$$Y^{lm}_{\phi} = \frac{\partial}{\partial\phi}Y^{lm}. \qquad X^{lm}_{\phi} = \sin\theta\frac{\partial}{\partial\theta}Y^{lm}. \tag{A.14}$$

For the tensor spherical harmonics from (2.15) we find

$$\begin{aligned} Y^{lm}_{\theta\theta} &= \left[\frac{\partial^2}{\partial\theta^2} + \frac{1}{2}l(l+1)\right]Y^{lm}, \\ Y^{lm}_{\theta\phi} &= \left[\frac{\partial^2}{\partial\theta\partial\phi} - \frac{\cos\theta}{\sin\theta}\frac{\partial}{\partial\phi}\right]Y^{lm}, \\ Y^{lm}_{\phi\phi} &= \left[\frac{\partial^2}{\partial\phi^2} + \sin\theta\cos\theta\frac{\partial}{\partial\theta} + \frac{1}{2}l(l+1)\sin^2\theta\right]Y^{lm}. \end{aligned} \tag{A.15}$$

and from (2.16)

$$\begin{aligned} X^{lm}_{\theta\theta} &= -\frac{1}{\sin\theta}\left(\frac{\partial^2}{\partial\theta\partial\phi} - \frac{\cos\theta}{\sin\theta}\frac{\partial}{\partial\phi}\right)Y^{lm}, \\ X^{lm}_{\theta\phi} &= \frac{1}{2}\left(\sin\theta\frac{\partial^2}{\partial\theta^2} - \frac{1}{\sin\theta}\frac{\partial^2}{\partial\phi^2} - \cos\theta\frac{\partial}{\partial\theta}\right)Y^{lm}, \\ X^{lm}_{\phi\phi} &= \left(\sin\theta\frac{\partial^2}{\partial\theta\partial\phi} - \cos\theta\frac{\partial}{\partial\phi}\right)Y^{lm}. \end{aligned} \tag{A.16}$$

Appendix B

Appendix to Chapter 3

B.1 (Newman/Geroch-Held)-Penrose

Here we gather our conventions and useful identities of the Newman-Penrose (NP) and Geroch-Held-Penrose (GHP) formalism and is possible we follow [64].

The key starting point to derive the (universal) Teukolsky equations in Section 3.3 are the Bianchi identities. However, before presenting these, note the relations between spin coefficients and curvatures in GHP form

$$\phi_{00} = \text{Þ}\rho - \eth'\kappa - \rho^2 + \tau'\kappa + \tau\kappa^* - |\sigma|^2 \,, \tag{B.1a}$$

$$\Psi_0 = \text{Þ}\sigma - \eth\kappa - (\rho + \rho^*)\sigma + (\tau + \tau'^*)\kappa \,, \tag{B.1b}$$

$$\phi_{01} + \Psi_1 = -\text{Þ}'\kappa + \text{Þ}\tau - (\tau - \tau'^*)\rho - (\tau^* - \tau')\sigma \,, \tag{B.1c}$$

$$\phi_{01} - \Psi_1 = -\eth'\sigma + \eth\rho - (\rho - \rho^*)\tau + (\rho' - \rho'^*)\kappa \,, \tag{B.1d}$$

$$\phi_{02} = -\text{Þ}'\sigma + \eth\tau - \tau^2 - \kappa\kappa'^* + \rho'\sigma + \rho\sigma'^* \,, \tag{B.1e}$$

$$\Psi_2 + \frac{1}{12}R = -\text{Þ}'\rho + \eth'\tau + \rho\rho'^* + \sigma\sigma' - |\tau|^2 - \kappa\kappa' \,. \tag{B.1f}$$

These are simply a translation into the GHP language from (3.18)

$$\begin{aligned} R_{\mathbf{abcd}} = {} & \partial_{\mathbf{c}}\gamma_{\mathbf{abd}} - \partial_{\mathbf{d}}\gamma_{\mathbf{abc}} - \gamma_{\mathbf{abf}}\eta^{\mathbf{fe}}\big(\gamma_{\mathbf{ced}} - \gamma_{\mathbf{dec}}\big) \\ & + \gamma_{\mathbf{afc}}\eta^{\mathbf{fe}}\gamma_{\mathbf{ebd}} - \gamma_{\mathbf{afd}}\eta^{\mathbf{fe}}\gamma_{\mathbf{ebc}} \end{aligned} \tag{B.2}$$

Note that (B.1) is (Eq. 4.12.32) of [91] despite the different choices for the metric signature and Riemann curvature.[1] On the other hand it is (2.37) in [184] for a vacuum spacetime as well as (43) of [64] for a vacuum Petrov D spacetime (with an appropriately aligned tetrad). Similarly translating (3.20)

$$\partial_{[\mathbf{e}} R_{\mathbf{ab}]\mathbf{cd}} + 2\,\eta^{\mathbf{ij}}\gamma_{\mathbf{ai}[\mathbf{e}} R_{\mathbf{jb}]\mathbf{cd}} + 2\,\eta^{\mathbf{ij}}\gamma_{\mathbf{ci}[\mathbf{e}} R_{\mathbf{ab}]\mathbf{jd}} = 0 \tag{B.3}$$

one finds

$$\text{Þ}\Psi_1 - \eth'\Psi_0 - \text{Þ}\phi_{01} + \eth\phi_{00} = -\tau'\Psi_0 + 4\rho\Psi_1 - 3\kappa\Psi_2 + \tau'^*\phi_{00} - 2\rho^*\phi_{01} - 2\sigma\phi_{01}^* + 2\kappa\phi_{11} + \kappa^*\phi_{02}\,, \tag{B.4a}$$

$$\text{Þ}\Psi_2 - \eth'\Psi_1 - \eth'\phi_{01} + \text{Þ}'\phi_{00} + \frac{1}{12}\text{Þ}R = \sigma'\Psi_0 - 2\tau'\Psi_1 + 3\rho\Psi_2 - 2\kappa\Psi_3 + \rho'^*\phi_{00} - 2\tau^*\phi_{01} - 2\tau\phi_{01}^* + 2\rho\phi_{11} + \sigma^*\phi_{02}\,, \tag{B.4b}$$

$$\text{Þ}'\Psi_0 - \eth\Psi_1 - \eth\phi_{01} + \text{Þ}\phi_{02} = \rho'\Psi_0 - 4\tau\Psi_1 + 3\sigma\Psi_2 + \sigma'^*\phi_{00} - 2\tau'^*\phi_{01} - 2\kappa\phi_{21}^* + 2\sigma\phi_{11} + \rho^*\phi_{02}\,, \tag{B.4c}$$

$$\text{Þ}'\Psi_1 - \eth\Psi_2 - \text{Þ}'\phi_{01} + \eth'\phi_{02} - \frac{1}{12}\eth R = -\kappa'\Psi_0 + 2\rho'\Psi_1 - 3\tau\Psi_2 - 2\sigma\Psi_3 + \kappa'^*\phi_{00} - 2\rho'^*\phi_{01} - 2\rho\phi_{21}^* + 2\tau\phi_{11} + \tau^*\phi_{02}\,, \tag{B.4d}$$

$$\text{Þ}\phi_{11} + \text{Þ}'\phi_{00} - \eth\phi_{01}^* - \eth'\phi_{01} + \frac{1}{8}\text{Þ}R = (\rho' + \rho'^*)\phi_{00} + 2(\rho + \rho^*)\phi_{11} - (\tau' + 2\tau^*)\phi_{01} - (2\tau + \tau'^*)\phi_{01}^* - \kappa^*\phi_{21}^* - \kappa\phi_{21} + \sigma\phi_{02}^* + \sigma^*\phi_{02}\,, \tag{B.5a}$$

$$\text{Þ}\phi_{21}^* + \text{Þ}'\phi_{01} - \eth\phi_{11} - \eth'\phi_{02} + \frac{1}{8}\eth R = (\rho' + 2\rho'^*)\phi_{01} + (2\rho + \rho^*)\phi_{21}^* - (\tau' + \tau^*)\phi_{02} - 2(\tau + \tau'^*)\phi_{11} - \kappa'^*\phi_{00} - \kappa\phi_{22} + \sigma\phi_{21} + \sigma'^*\phi_{01}^*\,. \tag{B.5b}$$

Importantly, these include (2.2) and (2.3) in [94], but they were also presented in full as (4.12.36)-(4.12.41) of [91] as well as in special cases in (2.39) of [184], and (44) of [64]. They are, in short, well known in the literature but several

[1] It differs from [183] by oppositely defined spin coefficients. Their appendix also contains a useful discussion on sign conventions.

conventions are in circulation. The GHP formalism has a natural symmetry exchanging $l \leftrightarrow n$ and $m \leftrightarrow \bar{m}$. The associated equations are implicit in B.4 as what is known in this language as the "primed" versions of these equations. We will not present all of them explicitly but as a relevant example note that

$$\begin{aligned} \text{Þ}\Psi_1 - \eth'\Psi_0 - \text{Þ}\phi_{01} + \eth\phi_{00} = &- \tau'\Psi_0 + 4\rho\Psi_1 - 3\kappa\Psi_2 + \tau'^*\phi_{00} \\ &- 2\rho^*\phi_{01} - 2\sigma\phi_{01}^* + 2\kappa\phi_{11} + \kappa^*\phi_{02}\,, \end{aligned} \tag{B.6}$$

is related to

$$\begin{aligned} \text{Þ}'\Psi_3 - \eth\Psi_4 - \text{Þ}'\phi_{21} + \eth'\phi_{22} = &- \tau\Psi_4 + 4\rho'\Psi_3 - 3\kappa'\Psi_2 + \tau^*\phi_{22} \\ &- 2\rho'^*\phi_{21} - 2\sigma'\phi_{21}^* + 2\kappa'\phi_{11} + \kappa'^*\phi_{02}{}^*\,. \end{aligned} \tag{B.7}$$

A last GHP-ingredient that is useful for our derivations are the GHP-commutation relations is

$$\begin{aligned} \left[\text{Þ}, \text{Þ}'\right] &= (\tau^* - \tau')\eth + (\tau - \tau'^*)\eth' + (p+q)F_{B12} + (p-q)F_{\Omega 12}\,, \\ \left[\text{Þ}, \eth\right] &= \rho^*\eth + \sigma\eth' - \tau'^*\text{Þ} - \kappa\text{Þ}' + (p+q)F_{B13} + (p-q)F_{\Omega 13}\,, \\ \left[\eth, \eth'\right] &= (\rho'^* - \rho')\text{Þ} + (\rho - \rho^*)\text{Þ}' + (p+q)F_{B34} + (p-q)F_{\Omega 34}\,. \end{aligned} \tag{B.8}$$

when acting on an object of weight $\{p, q\}$. Here, we have used a notation associated to the more standard form of a covariant derivative

$$\text{Đ}_\mu = -n_\mu\text{Þ} - l_\mu\text{Þ}' + \bar{m}_\mu\eth + m_\mu\eth'\,, \tag{B.9}$$

written in terms of the connections B_μ and Ω_μ

$$\text{Đ}_\mu = \nabla_\mu + (p+q)B_\mu + (p-q)\Omega_\mu\,, \tag{B.10}$$

and defining the associated curvatures as

$$[\text{Đ}_\mu, \text{Đ}_\nu]V = \left((p+q)\,F_{B\mu\nu} + (p-q)\,F_{\Omega\mu\nu}\right)V\,, \tag{B.11}$$

where V has weight $\{p, q\}$. In terms of the gauge fields this becomes

$$F_{B\mu\nu} = \nabla_\mu B_\nu - \nabla_\nu B_\mu\,, \quad F_{\Omega\mu\nu} = \nabla_\mu\Omega_\nu - \nabla_\nu\Omega_\mu\,. \tag{B.12}$$

Spelled out explicitly, the commutation relations are

$$\begin{aligned}
\left[\text{Þ}, \text{Þ}'\right] &= (\tau^* - \tau')\eth + (\tau - \tau'^*)\eth' - p(\kappa\kappa' - \tau\tau' + \Psi_2 + \phi_{11} - \frac{1}{24}R) \\
&\quad - q(\kappa^*\kappa'^* - \tau^*\tau'^* + \Psi_2^* + \phi_{11} - \frac{1}{24}R)\,, \\
[\text{Þ}, \eth] &= \rho^*\eth + \sigma\eth' - \tau'^*\text{Þ} - \kappa\text{Þ}' - p(\rho'\kappa - \tau'\sigma + \Psi_1) \\
&\quad - q(\sigma'^*\kappa^* - \rho^*\tau'^* + \phi_{01})\,, \\
\left[\eth, \eth'\right] &= (\rho'^* - \rho')\text{Þ} + (\rho - \rho^*)\text{Þ}' + p(\rho\rho' - \sigma\sigma' + \Psi_2 - \phi_{11} - \frac{1}{24}R) \\
&\quad - q(\rho^*\rho'^* - \sigma^*\sigma'^* + \Psi_2^* - \phi_{11} - \frac{1}{24}R)\,,
\end{aligned} \tag{B.13}$$

as can again be compared against (4.12.33)-(4.12.35) in [91].

B.2 Nollert's improvements of continued fraction

The procedure to numerically solve Teukolsky equation through Leaver's method requires in practice an initialisation for the radial ladder operator Λ_n^r. Such quantity can be expanded for large initialisation number N as

$$\Lambda_N^r = \sum_{j=0}^{J} C_j N^{-j/2} + \mathcal{O}\left(N\right)^{-(J+1)/2}\,. \tag{B.14}$$

One can initialise the ladder operator just retaining the first term $C_0 = -1$. However, this approximation requires in general a very high initial value for N (which means long computational time) and appears to be insufficient for frequencies with large imaginary part (namely higher overtones). In [185], it was shown that adding further corrections to the initial Λ_N^r improves the accuracy of the method, also allowing to capture higher overtones. The $(k+3)$-terms recurrence relation of equation (3.89) for $n = N$ can be expressed as

$$\sum_{j=-1}^{k+1} M_{N,j}\, R_{N-j} = 0\,, \tag{B.15}$$

where we defined

$$M_{N,j} \equiv \widetilde{\gamma}_{N,j-1} + \widetilde{\beta}_{N,j} + \widetilde{\alpha}_{N,j+1}\,. \tag{B.16}$$

Dividing it by R_{N-k-1} and making use of the definition of ladder operator $\Lambda_N^r = -a_{N+1}/a_N$ one obtains the equation

$$\sum_{j=-1}^{k+1} (-1)^j \, M_{N,j} \prod_{i=j+1}^{k+2} \Lambda_{N-i}^r = 0 \,. \tag{B.17}$$

Plugging the definition (B.14) into the above formula, one can solve for the coefficients order by order. By the definition of $\widetilde{\gamma}_{N,j}$, $\widetilde{\beta}_{N,j}$ and $\widetilde{\alpha}_{N,j}$, they scale with N as

$$\widetilde{\alpha}_{N,j} = N^2 + \widetilde{\alpha}_1 N + \widetilde{\alpha}_0 \tag{B.18}$$

$$\widetilde{\beta}_{N,j} = -2N^2 + \widetilde{\beta}_1 N + \widetilde{\beta}_0 \tag{B.19}$$

$$\widetilde{\gamma}_{N,j} = N^2 + \widetilde{\gamma}_1 N + \widetilde{\gamma}_0 \tag{B.20}$$

If we fix $C_0 = -1$, then the other coefficients up to $J = 5$ can be written as

$$C_1 = \pm \sqrt{-\widetilde{\alpha}_1 - \widetilde{\beta}_1 - \widetilde{\gamma}_1} \,, \tag{B.21}$$

$$C_2 = \widetilde{\alpha}_1 + \frac{\widetilde{\beta}_1}{2} - \frac{1}{4} \,, \tag{B.22}$$

$$C_3 = \frac{C_2^2}{2C_1} - \frac{C_2}{4C_1} - \frac{\widetilde{\alpha}_0 + \widetilde{\beta}_0 + \widetilde{\gamma}_0}{2C_1} - \frac{1 + 2\widetilde{\alpha}_1}{4} C_1 \,, \tag{B.23}$$

$$C_4 = \widetilde{\alpha}_0 - \frac{4\widetilde{\alpha}_1 - 8\widetilde{\beta}_0 + 1}{16} - \frac{1 + 4\widetilde{\alpha}_1}{4} C_2 - \frac{C_3}{2C_1} \,, \tag{B.24}$$

$$\begin{aligned} C_5 = {} & \frac{2\widetilde{\alpha}_1 + 3}{4C_1} C_2^2 - \frac{8\widetilde{\alpha}_0 + 4\widetilde{\alpha}_1 + 3}{16} C_1 - \frac{C_3^2}{2C_1} \\ & - \frac{4\widetilde{\alpha}_1 + 3}{16C_1} C_2 + C_3 \left(\frac{C_2}{2C_1^2} - \widetilde{\alpha}_1 - 1 \right) \\ & + \left(\frac{C_2}{C_1} - \frac{3}{4C_1} \right) C_4 \,, \end{aligned} \tag{B.25}$$

and the sign of C_1 is chosen such that $\mathrm{Re}\,(C_1) > 0$.

We can do the same expansion for the angular part, by expanding

$$\Lambda_N^\theta = \sum_{j=0}^{J} D_j N^{-j/2} + \mathcal{O}\left(N\right)^{-(J+1)/2} \,. \tag{B.26}$$

From equations (3.98)–(3.100) we can schematically say that

$$\alpha_N^\theta = -2N^2 + \alpha_1 N + \alpha_0 \tag{B.27}$$

$$\beta_N^\theta = N^2 + \beta_1 N + \beta_0 \tag{B.28}$$

$$\gamma_N^\theta = \gamma_1 N + \gamma_0 \tag{B.29}$$

By solving perturbatively in $1/N$ the relation (3.101), we obtain the following expression for the coefficients D_j up to $J = 4$

$$D_0 = 0 \tag{B.30}$$

$$D_1 = \gamma_1 \tag{B.31}$$

$$D_2 = \gamma_0 - \gamma_1 \left(1 + \beta_1 + 2\gamma_1\right) \tag{B.32}$$

$$\begin{aligned} D_3 =& \gamma_1^2(\alpha_1 - 2) - \gamma_1(1 + \beta_0 + \beta_1) \\ & - D_2(\beta_1 + 4\gamma_1 + 2) \end{aligned} \tag{B.33}$$

$$\begin{aligned} D_4 =& \alpha_0\gamma_1^2 + \frac{2D_2^2\left(\beta_1 + 3\gamma_1 + 2\right)}{\gamma_1} \\ & + D_2\left(\beta_0 + \beta_1 + 2\gamma_1 + 1\right) \\ & + D_3\left(\frac{2D_2}{\gamma_1} - \beta_1 - 4\gamma_1 - 2\right) \end{aligned} \tag{B.34}$$

Appendix C

Appendix to Chapter 4

C.1 Slowly-rotating metric

$$
\begin{aligned}
f = 1 &- \frac{2M}{r} + 24\lambda_{\rm ev}\ell^4 M^2\left(\frac{9}{r^6} - \frac{49M}{3r^7}\right) + 1152\epsilon_1\ell^6 M^3\left(\frac{4}{r^9} - \frac{67M}{9r^{10}}\right) \\
&- \lambda_{\rm odd}\ell^4\chi\cos\theta\frac{27(2M-r)}{14M^2r^8}\left(704M^5 - 80M^4r - 32M^3r^2 - 12M^2r^3 - 4Mr^4 - r^5\right) \\
&- \epsilon_3\ell^6\chi\cos\theta\frac{3(2M-r)}{20M^4r^{11}}\left(139008M^8 - 13312M^7r - 5824M^6r^2 - 2496M^5r^3\right. \\
&\left. - 1040M^4r^4 - 416M^3r^5 - 156M^2r^6 - 52Mr^7 - 13r^8\right) + \mathcal{O}\left(\ell^8, \chi^2\right) \ . \quad \text{(C.1)} \\
N = 1 &- \frac{108\lambda_{\rm ev}\ell^4M^2}{r^6} - 1792\epsilon_1\ell^6\frac{M^3}{r^9} \\
&+ \lambda_{\rm odd}\ell^4\chi\frac{9\cos\theta}{14M^2r^7}\left(-1152M^5 + 80M^4r + 32M^3r^2 + 12M^2r^3 + 4Mr^4 + r^5\right) \\
&+ \epsilon_3\ell^6\chi\frac{\cos\theta}{20M^4r^{10}}\left(-177408M^8 + 13312M^7r + 5824M^6r^2 + 2496M^5r^3\right. \\
&\left. + 1040M^4r^4 + 416M^3r^5 + 156M^2r^6 + 52Mr^7 + 13r^8\right) + \mathcal{O}\left(\ell^8, \chi^2\right) \ , \quad \text{(C.2)} \\
h = &\frac{M}{r} - 20\frac{\lambda_{\rm ev}\ell^4M^3}{r^7} - \frac{64\epsilon_1\ell^6M^3}{11r^{10}}(108r - 121M) - 6912\epsilon_2\ell^6\frac{M^3}{11r^9} + \mathcal{O}\left(\ell^8, \chi\right) \ . \\
&\quad \text{(C.3)}
\end{aligned}
$$

C.2 Numerical results

In the tables below we show the Kerr QNM frequencies as well as the shifts associated to each type of higher-derivative correction obtained from fits to numerical data. By applying different numerical approaches, we estimate that the error in the shifts is of the order of $1\% - 5\%$ depending on the case, which is also in line with the comparison of these numbers with those in refs. [50–52] for non-rotating black holes. Thus, one should probably keep only the first two significant digits for the $\delta\omega_i^{\pm\text{break}}$ coefficients.

l	2	3	4	5
ω_0^+	$0.37367 - 0.08896i$	$0.59943 - 0.09270i$	$0.80917 - 0.09417i$	$1.01228 - 0.09487i$
ω_1^+	$0.0635 + 0.0012i$	$0.0678 + 0.00089i$	$0.0701 + 0.00054i$	$0.0715 + 0.00036i$
$\delta\omega_{\text{ev},0}^+$	$-0.137 + 0.161i$	$-0.258 + 0.151i$	$-0.357 + 0.149i$	$-0.452 + 0.148i$
$\delta\omega_{\text{ev},1}^+$	$0.306 + 0.188i$	$0.199 + 0.142i$	$0.178 + 0.103i$	$0.172 + 0.080i$
ω_0^-	$0.37367 - 0.08896i$	$0.59944 - 0.09270i$	$0.80917 - 0.09416i$	$1.01229 - 0.09487i$
ω_1^-	$0.0630 + 0.0011i$	$0.0677 + 0.00078i$	$0.0702 + 0.00048i$	$0.0715 + 0.00033i$
$\delta\omega_{\text{ev},0}^-$	$0.244 - 0.130i$	$0.340 - 0.132i$	$0.440 - 0.132i$	$0.540 - 0.133i$
$\delta\omega_{\text{ev},1}^-$	$-0.144 - 0.286i$	$-0.123 - 0.149i$	$-0.123 - 0.0992i$	$-0.125 - 0.0746i$

Table C.1: Best-fit coefficients for the fundamental quasinormal frequencies with λ_{ev} corrections. In the upper half of the table we show the results for the Kerr QNM frequencies and for the corresponding shifts in the case of even-parity perturbations, and in the lower half we show the results for odd-parity ones.

l	2	3
ω_0^+	$0.37366 - 0.08893i$	$0.59944 - 0.09270i$
ω_1^+	$0.0631 + 0.0011i$	$0.0673 + 0.00067i$
$\delta\omega_{\text{odd},0}^{\text{break}}$	$0.192 - 0.151i$	$0.304 - 0.144i$
$\delta\omega_{\text{odd},1}^{\text{break}}$	$-0.233 - 0.207i$	$-0.164 - 0.146i$
$\gamma_{\text{odd},0}$	$2.21 - 4.97i$	$0.705 - 3.253i$
$\gamma_{\text{odd},1}$	$-0.15 + 0.77i$	$-0.075 + 0.345i$

Table C.2: Best-fit coefficients for the fundamental quasinormal frequencies as well as for the relative normalisation factor γ with λ_{odd} corrections.

l	2	3	4	5
ω_0^+	$0.37367 - 0.08896i$	$0.59944 - 0.09270i$	$0.80918 - 0.09416i$	$1.01229 - 0.09487i$
ω_1^+	$0.0632 + 0.0012i$	$0.0677 + 0.00074i$	$0.0702 + 0.00039i$	$0.0716 + 0.00022i$
$\delta\omega_{1,0}^+$	$-0.172 - 0.245i$	$-0.653 - 0.594i$	$-1.45 - 1.07i$	$-2.71 - 1.65i$
$\delta\omega_{1,1}^+$	$-0.358 - 0.205i$	$-0.608 - 0.205i$	$-0.947 - 0.268i$	$-1.35 - 0.332i$
ω_0^-	$0.37367 - 0.08896i$	$0.59944 - 0.09270i$	$0.80917 - 0.09417i$	$1.01229 - 0.09487i$
ω_1^-	$0.0630 + 0.0013i$	$0.0676 + 0.00078i$	$0.0701 + 0.00043i$	$0.0715 + 0.00026i$
$\delta\omega_{1,0}^-$	$-0.079 - 0.054i$	$0.0059 - 0.038i$	$0.040 - 0.017i$	$0.057 - 0.0018i$
$\delta\omega_{1,1}^-$	$-0.096 + 0.171i$	$-0.041 + 0.048i$	$-0.0082 + 0.020i$	$0.0077 + 0.013i$

Table C.3: Best-fit coefficients for the fundamental quasinormal frequencies with ϵ_1 corrections. In the upper half of the table we show the results for the Kerr QNM frequencies and for the corresponding shifts in the case of even-parity perturbations, and in the lower half we show the results for odd-parity ones.

l	2	3	4	5
ω_0^+	$0.37367 - 0.08896i$	$0.59944 - 0.09270i$	$0.80918 - 0.09416i$	$1.01229 - 0.09487i$
ω_1^+	$0.0629 + 0.0010i$	$0.0674 + 0.00065i$	$0.0698 + 0.00033i$	$0.0712 + 0.00019i$
$\delta\omega_{2,0}^+$	0	0	0	0
$\delta\omega_{2,1}^+$	$-0.040 + 0.205i$	$-0.079 + 0.059i$	$-0.057 + 0.018i$	$-0.041 + 0.0047i$
ω_0^-	$0.37367 - 0.08896i$	$0.59944 - 0.09270i$	$0.80917 - 0.09416i$	$1.01229 - 0.09486i$
ω_1^-	$0.0630 + 0.0012i$	$0.0677 + 0.00074i$	$0.0702 + 0.00039i$	$0.0717 + 0.00021i$
$\delta\omega_{2,0}^-$	$-0.207 - 0.354i$	$-0.648 - 0.707i$	$-1.45 - 1.16i$	$-2.72 - 1.73i$
$\delta\omega_{2,1}^-$	$-0.273 - 0.416i$	$-0.586 - 0.313i$	$-0.943 - 0.332i$	$-1.37 - 0.368i$

Table C.4: Best-fit coefficients for the fundamental quasinormal frequencies with ϵ_2 corrections. In the upper half of the table we show the results for the Kerr QNM frequencies and for the corresponding shifts in the case of even-parity perturbations, and in the lower half we show the results for odd-parity ones.

l	2	3
ω_0^+	$0.37368 - 0.08896i$	$0.59945 - 0.09269i$
ω_1^+	$0.0630 + 0.0010i$	$0.0676 + 0.00071i$
$\delta\omega_{3,0}^{\rm break}$	$0.0755 + 0.132i$	$0.332 - 0.304i$
$\delta\omega_{3,1}^{\rm break}$	$0.117 + 0.235i$	$0.255 + 0.130i$
$\gamma_{3,0}$	$2.21 - 4.97i$	$0.705 - 3.25i$
$\gamma_{3,1}$	$-0.15 + 0.76i$	$-0.035 + 0.336i$

Table C.5: Best-fit coefficients for the fundamental quasinormal frequencies as well as for the relative normalisation factor γ with ϵ_3 corrections.

C.3 Chandrasekhar transformation linear in spin

The Regge-Wheeler and Zerilli equations are isospectral and this can be made explicit by performing a Darboux transformation, known in this context as the Chandrasekhar transformation, that relates them [186]. We extend this transformation here to linear order in spin in order to connect $V_{lm}^{-\mathrm{GR}}$ and $V_{lm}^{+\mathrm{GR}}$ in (4.30) and (4.34), respectively. Explicitly, we wish to transform

$$\frac{\mathrm{d}^2\tilde{\Psi}^+}{\mathrm{d}x^2} - V_{lm}^{+\mathrm{GR}}\tilde{\Psi}^+ = 0\,, \tag{C.4}$$

into

$$\frac{\mathrm{d}^2\Psi^+}{\mathrm{d}x^2} - V_{lm}^{-\mathrm{GR}}\Psi^+ = 0\,. \tag{C.5}$$

For a static black hole this can be done in a canonical way by

$$\Psi^+ = \frac{\mathrm{d}\tilde{\Psi}^+}{\mathrm{d}x} - f_*\tilde{\Psi}^+\,, \tag{C.6}$$

with

$$f_* = i\omega_* + \frac{3M(r-2M)}{r^2(\mu r/2+3M)}\,, \quad \omega_* = -i\frac{\mu(\mu/2+1)}{6M}\,. \tag{C.7}$$

In order to invert this transformation, note that

$$V^{-\mathrm{GR}} + \frac{\mathrm{d}f_*}{\mathrm{d}x} - f_*^2 = (-\omega^2+\omega_*^2)\,, \tag{C.8}$$

so

$$\tilde{\Psi}^+ = \frac{1}{(-\omega^2+\omega_*^2)}\Big(\frac{\mathrm{d}\Psi^+}{\mathrm{d}x} + f_*\Psi^+\Big)\,. \tag{C.9}$$

To include spin, a slightly more general type of transformation is needed making the procedure more arbitrary [186]. Nevertheless, an example that works to linear order in spin is given by

$$\Psi^+ = (1+m\chi\beta)\frac{\mathrm{d}\tilde{\Psi}^+}{\mathrm{d}x} - (f_* + m\chi f_*^{(1)})\tilde{\Psi}^+\,, \tag{C.10}$$

with

$$\beta = M\frac{24M^2+6(l+2)(l-1)Mr+l(-2-l+2l^2+l^3)r^2}{l(l+1)r^3(6M+(l+2)(l-1)r)\omega}\,, \tag{C.11}$$

$$\begin{aligned} f_*^{(1)} = -\big(&-864M^5 - 216(-4+l+l^2)rM^4 - l(1+l)(l+2)^3(l-1)^3r^7\omega^2 \\ &+ 36(l+2)(l-1)M^3r^2(-3+2r^2\omega^2)(l+1)(l+2)^2(l-1)^2Mr^4(1+4r^2\omega^2) \\ &- 6(l+2)(l-1)M^2r^3(2l^3+l^4+6r^2\omega^2-2l(1+3r^2\omega^2)-l^2(1+6r^2\omega^2))\big) \\ &/\left(3l(1+l)r^5(6+(l+2)(l-1)r)^2\omega\right)\,. \end{aligned} \tag{C.12}$$

C.4 QM-like perturbation theory

We will define a symmetric bilinear form with respect to which the zeroth order wave equations are self-adjoint in the following sense

$$\langle g|H_0 f\rangle = \langle H_0 g|f\rangle \ . \tag{C.13}$$

Up to boundary terms, this would hold for

$$\langle g|\psi\rangle = \int_C \mathrm{d}r_*\, g(r)\psi(r) = \int_C \mathrm{d}r\,(1+\frac{2M}{r-r_+})g(r)\psi(r)\,. \tag{C.14}$$

This needs to be made well-defined on functions satisfying the QNM boundary conditions $\sim e^{-i\omega r_*}$ as $r\to r_H$ and $\sim e^{i\omega r_*}$ as $r\to\infty$. In particular, given that the imaginary part of ω is negative, this means they diverge for both $r_*\to\pm\infty$ which prohibits the otherwise natural choice $r\in]r_+,\infty[$. Instead, one can take the contour C from $r\to r_+ +\epsilon+i\infty$ down around the branchcut at r_h and back up along $r\to r_+-\epsilon+i\infty$ [63, 86]. Given two coupled equations, we can instead choose

$$\begin{aligned}\langle g|\psi\rangle &= \int_C \mathrm{d}r\,(1+\frac{2M}{r-r_+})\begin{pmatrix}g^+(r) & g^-(r)\end{pmatrix}\begin{pmatrix}\psi^+(r)\\ \psi^-(r)\end{pmatrix}\\ &= \int_C \mathrm{d}r\,(1+\frac{2M}{r-r_+})(g^+(r)\psi^+(r)+g^-(r)\psi^-(r))\,,\end{aligned} \tag{C.15}$$

with respect to which the zeroth order uncoupled H_0 clearly satisfies (C.13). Now consider

$$\begin{aligned}&\begin{pmatrix}\frac{\mathrm{d}^2}{\mathrm{d}r_*^2}-(\omega^2-V^{+\mathrm{GR}}-\delta V^+) & \delta U^+ +\delta W^+\frac{\mathrm{d}}{\mathrm{d}r_*}\\ \delta U^- +\delta W^-\frac{\mathrm{d}}{\mathrm{d}r_*} & \frac{\mathrm{d}^2}{\mathrm{d}r_*^2}-(\omega^2-V^{-\mathrm{GR}}-\delta V^-)\end{pmatrix}\begin{pmatrix}\Psi^+(r)\\ \Psi^-(r)\end{pmatrix}\\ &\equiv (H_0+\delta H_+ +\delta H_- +\delta H_{\mathrm{break}})\,|\psi\rangle = 0\,.\end{aligned} \tag{C.16}$$

Expand both $|\psi\rangle = \left|\psi^{(0)}\right\rangle + \left|\psi^{(1)}\right\rangle$ and $\omega=\omega^{(0)}+\omega^{(1)}$as a zeroth order piece and a small correction

$$H_0\left|\psi^{(0)}\right\rangle = 0\,,\quad \left|\psi^{(0)}\right\rangle = c_+\,|+\rangle + c_-\,|-\rangle\ , \tag{C.17}$$

with

$$|+\rangle = \begin{pmatrix}\Psi^{+\mathrm{GR}}(r)\\ 0\end{pmatrix}\ ,\quad |-\rangle = \begin{pmatrix}0\\ \Psi^{-\mathrm{GR}}(r)\end{pmatrix}\ . \tag{C.18}$$

The first order equation is given by

$$H_0\left|\psi^{(1)}\right\rangle - 2\omega^{(0)}\omega^{(1)}\left|\psi^{(0)}\right\rangle + (\delta H_+ +\delta H_- +\delta H_{\mathrm{break}})\left|\psi^{(0)}\right\rangle = 0\,, \tag{C.19}$$

which, when acted on by respectively $\langle +|$, $\langle -|$ implies

$$-2\omega^{(0)}\omega^{(1)}c_+ \langle +|+\rangle + c_+ \langle +|\delta H_+ +\rangle + c_- \langle +|\delta H_{\rm break} -\rangle = 0\,,$$
$$-2\omega^{(0)}\omega^{(1)}c_- \langle -|-\rangle + c_- \langle -|\delta H_- -\rangle + c_+ \langle -|\delta H_{\rm break} +\rangle = 0\,. \qquad \text{(C.20)}$$

In order for this system to have a nontrivial solution, the following must hold

$$\begin{vmatrix} \frac{\langle +|\delta H_+ +\rangle}{2\omega^{(0)}\langle +|+\rangle} - \omega^{(1)} & \frac{\langle +|\delta H_{\rm break} -\rangle}{2\omega^{(0)}\langle +|+\rangle} \\ \frac{\langle -|\delta H_{\rm break} +\rangle}{2\omega^{(0)}\langle -|-\rangle} & \frac{\langle -|\delta H_- -\rangle}{2\omega^{(0)}\langle -|-\rangle} - \omega^{(1)} \end{vmatrix} = 0\,. \qquad \text{(C.21)}$$

From the individual corrections we identify

$$\delta\omega^+ = \frac{\langle +|\delta H_+ +\rangle}{2\omega^{(0)}\,\langle +|+\rangle}\,, \quad \delta\omega^- = \frac{\langle -|\delta H_- -\rangle}{2\omega^{(0)}\,\langle -|-\rangle}\,, \qquad \text{(C.22)}$$

$$(\delta\omega^{\rm break})^2 = \frac{\langle -|\delta H_{\rm break} +\rangle}{2\omega^{(0)}\,\langle -|-\rangle}\frac{\langle +|\delta H_{\rm break} -\rangle}{2\omega^{(0)}\,\langle +|+\rangle}\,. \qquad \text{(C.23)}$$

To conclude, we find (4.44)

$$(\delta\omega^+ - \omega^{(1)})(\delta\omega^- - \omega^{(1)}) - (\delta\omega^{\rm break})^2 = 0\,. \qquad \text{(C.24)}$$

In deriving this results, we have assumed the frequency dependence in H_0 comes only from ω^2. This is incorrect when including spin to linear order. However, this is easily corrected by simply replacing $2\omega^{(0)}$ by $(\frac{\partial(\omega^2 - V^{\pm{\rm GR}})}{\partial\omega})_{\omega=\omega^{(0)}}$ in the normalisations of (C.23). The associated eigenvectors can similarly be determined and, using

$$(\gamma^{\rm break})^2 = \frac{\langle -|\delta H_{\rm break} +\rangle}{\langle +|\delta H_{\rm break} -\rangle} \qquad \text{(C.25)}$$

they are found to lead to (4.46)

$$\gamma^\pm_{\rm total} = \gamma^{\rm break}\frac{\delta\omega^\pm - \delta\omega^+}{\delta\omega^{\rm break}}\,. \qquad \text{(C.26)}$$

when we write the eigenstate as

$$c_+ |+\rangle + c_- |-\rangle \propto \gamma^\pm_{\rm total}|+\rangle + |-\rangle\,, \qquad \text{(C.27)}$$

which corresponds to the definition if asymptotically $\Psi^{(+){\rm GR}} \sim \Psi^{(-){\rm GR}}$.

C.5 Solving the coupled equations using uncoupled equations

Consider the following set of coupled differential equations

$$\frac{\mathrm{d}^2\Psi^-}{\mathrm{d}x^2} - V^-\Psi^- + \lambda(C_{-+}\Psi^+ + D_{-+}\frac{\mathrm{d}\Psi^+}{\mathrm{d}x}) = 0\,, \tag{C.28}$$

$$\frac{\mathrm{d}^2\Psi^+}{\mathrm{d}x^2} - V^-\Psi^+ + \lambda(C_{+-}\Psi^- + D_{+-}\frac{\mathrm{d}\Psi^-}{\mathrm{d}x}) = 0\,, \tag{C.29}$$

with λ a small parameter. Note the appearance of V^- in the second equation: we can be bring the equations (4.35)-(4.36) into this form using the transformation described in Appendix C.3 (we are including the term ω^2 in V^- to shorten the formulas). Suppose we can independently consider the symmetric and antisymmetric parts of the perturbation, this is

$$\frac{\mathrm{d}^2\Psi^-}{\mathrm{d}x^2} - V^-\Psi^- + \lambda_s(\bar{C}\Psi^+ + \bar{D}\frac{\mathrm{d}\Psi^+}{\mathrm{d}x}) + \lambda_a(\delta C\Psi^+ + \delta D\frac{\mathrm{d}\Psi^+}{\mathrm{d}x}) = 0\,, \tag{C.30}$$

$$\frac{\mathrm{d}^2\Psi^+}{\mathrm{d}x^2} - V^-\Psi^+ + \lambda_s(\bar{C}\Psi^- + \bar{D}\frac{\mathrm{d}\Psi^-}{\mathrm{d}x}) - \lambda_a(\delta C\Psi^- + \delta D\frac{\mathrm{d}\Psi^-}{\mathrm{d}x}) = 0\,, \tag{C.31}$$

where for any quantity X we are defining

$$\bar{X} = \frac{1}{2}(X_{-+} + X_{+-})\,, \quad \delta X = \frac{1}{2}(X_{-+} - X_{+-})\,. \tag{C.32}$$

Here λ_s and λ_a are bookkeeping parameters, and we will eventually set them to 1, hence recovering the original equation. Now we can study the effect of each term in these equations. The λ_s coupled equations can be separated by $\Psi^s = \Psi^- \pm \Psi^+$ into an equation of the type

$$\frac{\mathrm{d}^2\Psi^s}{\mathrm{d}x^2} - V^-\Psi^s \pm \lambda_s(\bar{C}\Psi^s + \bar{D}\frac{\mathrm{d}\Psi^s}{\mathrm{d}x}) = 0\,. \tag{C.33}$$

On the other hand, the antisymmetric part can be separated by $\Psi^a = \Psi^- \pm i\Psi^+$ into an equation of the type

$$\frac{\mathrm{d}^2\Psi^a}{\mathrm{d}x^2} - V^-\Psi^a \mp i\lambda_a(\delta C\Psi^a + \delta D\frac{\mathrm{d}\Psi^a}{\mathrm{d}x})\,. \tag{C.34}$$

Keeping both, one can observe that diagonalizing either the symmetric or the antisymmetric part always makes the other completely off-diagonal and it is

therefore generically not possible to diagnolise both at the same time. One possible resolution to nevertheless consider both together, as is the original problem, is to define projections onto the leading radial wavefunctions and to use standard perturbation theory from quantum mechanics [51]. However, this is somewhat subtle as the QNMs are not square integrable [86] – see Appendix C.4. We will not take this approach but simply use it to argue for the form of the final equation in terms of solutions to (C.33) and (C.34). In particular, we can write (C.30) and (C.31) suggestively as

$$(H_0 + \lambda H') \equiv (H_0 + \lambda H_s + \lambda H_a) \left|\Psi\right\rangle \,. \tag{C.35}$$

We know from degenerate perturbation theory, as a special case of (4.44), that the correction due to an off-diagonal H' is given by

$$\omega_1 = \pm\sqrt{\left\langle\Psi^-\right| H' \left|\Psi^+\right\rangle \left\langle\Psi^+\right| H' \left|\Psi^-\right\rangle} = \pm\sqrt{\omega_s^2 + \omega_a^2}\,, \tag{C.36}$$

where in the second equality we wrote it in terms of the results from H_s and H_a separately. The value of ω_s can now be determined by the first order correction in (C.33), $\omega \approx \omega_0 + \lambda_s \omega_s$, whilst ω_a is similarly found from (C.34) and $\omega \approx \omega_0 + \lambda_a \omega_a$. The cross-terms had to cancel due to the symmetry under exchange $\Psi^+ \leftrightarrow \Psi^-$.

To find the normalisation coefficient, we can similarly use an analysis analogous to the one leading up to (4.46) to conclude that

$$(\gamma^{\text{break}})^2 = \frac{\left\langle\Psi^-\right| H' \left|\Psi^+\right\rangle}{\left\langle\Psi^+\right| H' \left|\Psi^-\right\rangle} = \frac{1 + (\frac{\omega_a}{\omega_s})^2}{(1 - i\frac{\omega_a}{\omega_s})^2}\,. \tag{C.37}$$

This again assumes asymptotically $\Psi^{(+)\text{GR}} \sim \Psi^{(-)\text{GR}}$. However, to compare with the results from the main text we actually need to translate to the original master variables $\tilde{\Psi}^{(+)\text{GR}}$, $\tilde{\Psi}^{(-)\text{GR}}$. Asymptotically, we can read of from the transformation (C.10)

$$\frac{\tilde{\Psi}^{(+)\text{GR}}}{\tilde{\Psi}^{(-)\text{GR}}} = \frac{1}{i(\omega^{\text{GR}} - \omega_*)} \frac{\Psi^{(+)\text{GR}}}{\Psi^{(-)\text{GR}}}\,, \tag{C.38}$$

so finally, for the original master variables

$$(\gamma^{\text{break}}) = \pm \frac{1}{i(\omega^{\text{GR}} - \omega_*)} \sqrt{\frac{1 + (\frac{\omega_a}{\omega_s})^2}{(1 - i\frac{\omega_a}{\omega_s})^2}}\,. \tag{C.39}$$

Appendix D

Appendix to Chapter 5

D.1 Starobinsky-Teukolsky identities

The Starobinsky-Teukolsky (ST) identities provide a relation between the Teukolsky equations of spins $\pm s$ [36, 119, 120] — see also [121] for a modern view on these identities.

Let us start by reviewing the ST identities for the angular functions[1] $S_s(x)$. Given two spin-weighted harmonic functions S_{+2} and S_{-2} that satisfy the equation (5.45) and that are normalised according to

$$2\pi \int_{-1}^{1} \mathrm{d}x\, S_s(x)^2 = 1\,, \tag{D.1}$$

these are related by

$$\begin{aligned} S_{-2} &= \frac{1}{D_2} L_{-1} L_0 L_1 L_2 S_{+2}\,, \\ S_{+2} &= \frac{1}{D_2} L^\dagger_{-1} L^\dagger_0 L^\dagger_1 L^\dagger_2 S_{-2}\,, \end{aligned} \tag{D.2}$$

where L_n and $L^\dagger_n$ are the operators

$$\begin{aligned} L_n &= \frac{m+nx}{\sqrt{1-x^2}} - a\omega\sqrt{1-x^2} - \sqrt{1-x^2}\frac{\partial}{\partial x}\,, \\ L^\dagger_n &= \frac{-m+nx}{\sqrt{1-x^2}} + a\omega\sqrt{1-x^2} - \sqrt{1-x^2}\frac{\partial}{\partial x}\,. \end{aligned} \tag{D.3}$$

[1] In this section we omit the lm labels for the sake of clarity.

The constant D_2 is in fact the same in the two identities on account of the normalisation of the functions, and it is given by

$$\begin{aligned} D_2 = \Big[& \left(8+6B_{lm}+B_{lm}^2\right)^2 - 8\left(-8+B_{lm}^2(4+B_{lm})\right)m\gamma + 4\left(8-2B_{lm}-B_{lm}^2+B_{lm}^3\right. \\ & \left.+2(-2+B_{lm})(4+3B_{lm})m^2\right)\gamma^2 - 8m\left(8-12B_{lm}+3B_{lm}^2+4(-2+B_{lm})m^2\right)\gamma^3 \\ & + 2\left(42-22B_{lm}+3B_{lm}^2+8(-11+3B_{lm})m^2+8m^4\right)\gamma^4 \\ & - 8m\left(3B_{lm}+4\left(-4+m^2\right)\right)\gamma^5 + 4\left(-7+B_{lm}+6m^2\right)\gamma^6 - 8m\gamma^7+\gamma^8\Big]^{1/2}, \end{aligned} \tag{D.4}$$

where $\gamma = a\omega$.

Consider now the radial ST identities. Suppose that we have two variables $R_{\pm 2}$ satisfying the corresponding radial Teukolsky equations (without corrections)

$$\mathfrak{D}^2_{+2}R_{+2} = 0\,, \quad \mathfrak{D}^2_{-2}R_{-2} = 0\,. \tag{D.5}$$

Then, let us define two auxiliary variables as follows

$$\begin{aligned} \tilde{R}_{-2} &= \Delta^2\left(\mathcal{D}_0\right)^4\left(\Delta^2 R_{+2}\right)\,, \\ \tilde{R}_{+2} &= \left(\mathcal{D}_0^\dagger\right)^4 R_{-2}\,, \end{aligned} \tag{D.6}$$

where $\mathcal{D}_0$ and $\mathcal{D}_0^\dagger$ are the operators

$$\begin{aligned} \mathcal{D}_0 &= \partial_r + \frac{i\left(\omega(r^2+a^2)-ma\right)}{\Delta}\,, \\ \mathcal{D}_0^\dagger &= \partial_r - \frac{i\left(\omega(r^2+a^2)-ma\right)}{\Delta}\,. \end{aligned} \tag{D.7}$$

Then, it follows by direct computation that the variables $\tilde{R}_{\pm 2}$ also satisfy the corresponding Teukolsky equation $\mathfrak{D}^2_{\pm 2}\tilde{R}_{\pm 2} = 0$. Furthermore, when studying black-hole perturbations, we are interested in solutions that satisfy outgoing boundary conditions at infinity and at the black-hole horizon. The map (D.6) preserves these conditions, meaning that if the original variables $R_{\pm 2}$ satisfy them, so do the transformed variables $\tilde{R}_{\pm 2}$. Due to the unicity of solutions of a second order ODE with fixed boundary conditions, it follows that, in fact, the transformed variables must be proportional to the original ones, $\tilde{R}_{\pm 2} \propto R_{\pm 2}$.

Therefore, there must exist two constants $C_{\pm 2}$ such that

$$\begin{aligned} R_{-2} &= C_{+2}\Delta^2 \left(\mathcal{D}_0\right)^4 \left(\Delta^2 R_{+2}\right) , \\ R_{+2} &= C_{-2} \left(\mathcal{D}_0^\dagger\right)^4 R_{-2} , \end{aligned} \tag{D.8}$$

The two constants are not independent due to the identity obtained by applying the map twice,

$$R_{-2} = C_{+2}C_{-2}\Delta^2 \left(\mathcal{D}_0\right)^4 \left(\Delta^2 \left(\mathcal{D}_0^\dagger\right)^4 R_{-2}\right) . \tag{D.9}$$

This allows one to conclude that

$$C_{+2}C_{-2} = \frac{1}{\mathcal{K}^2} , \tag{D.10}$$

where the constant $\mathcal{K}^2$ reads

$$\mathcal{K}^2 = D_2^2 + 144M^2\omega^2 . \tag{D.11}$$

Appendix E

Appendix to Chapter 6

E.1 Ambiguity of the potential modifications

Here we list the explicit form of the coefficients of equation (6.18) when one transforms the radial Teukolsky function as (6.14). These values hold for $s = -2$:

$$\overline{A}_j^{(-3)} = \frac{a^6}{2} j(j+1)(j+2)\,, \qquad \overline{A}_j^{(-2)} = -\frac{3a^4}{2} j(j+1)^2\,, \tag{E.1}$$

$$\overline{A}_j^{(-1)} = \frac{a^4}{2} j\left[3j(j+1) - 4B + 4m^2 - 8i\omega + 10\right] + 4ia^3 jm + \frac{3}{2}a^2 j\left(j^2 + j - 1\right)\,, \tag{E.2}$$

$$\begin{aligned}\overline{A}_j^{(0)} =& a^3(2j-1)\left[a\omega(\omega - 4i) - 2m(\omega + 2i)\right] - 4iajm - \frac{1}{2} j\left(j^2 - 4\right) \\ & - a^2\left[3j^3 - j\left(4B - 2m^2 + 4i\omega - 1\right) + B + 2\right]\,,\end{aligned} \tag{E.3}$$

$$\begin{aligned}\overline{A}_j^{(1)} =& 2a^4(j-1)\omega^2 + \frac{1}{2}a^2\Big[3j^2(j-1) + 4B + 2\omega(\omega - 16i) + 8 \\ & + j\left(-8B + 4m^2 - 4\omega(\omega - 8i) + 2\right)\Big] + 2am\left[2j(\omega + 3i) - \omega - 2i\right] \\ & + \frac{1}{2} j\left[3(j-1)j - 4B - 11\right] + B + 2\,,\end{aligned} \tag{E.4}$$

$$\overline{A}_j^{(2)} = a^2\omega\left[\omega - 16i(j-1)\right] - 2a(2j-1)m(\omega+2i) + \frac{1}{2}j(-3(j-2)j + 8B - 24i\omega + 13) - 3(B - 4i\omega + 2)\,, \tag{E.5}$$

$$\overline{A}_j^{(3)} = 2a^2(2j-3)\omega^2 + \frac{1}{2}(j-1)\left[(j-2)j - 4(B+2)\right] + 4i(5j-6)\omega\,, \tag{E.6}$$

$$\overline{A}_j^{(4)} = 2\omega\left[2(\omega+3i) - j(\omega+4i)\right]\,, \qquad \overline{A}_j^{(5)} = 2(j-2)\omega^2\,. \tag{E.7}$$

E.2 Derivation of the boundary conditions

The correct implementation of the continued fraction method requires that the ansatz that one assumes properly encodes the behavior of the solution close to the singular points of the equation. We will now show how such ansätze are properly derived in the beyond-Teukolsky case.

Following the discussion in [94], it is convenient to introduce the new master field

$$Y(r) = \Delta^{\frac{s}{2}}\left(r^2+a^2\right)^{\frac{1}{2}} R(r)\,, \tag{E.8}$$

and the tortoise coordinate r_* defined by

$$\frac{\mathrm{d}r_*}{\mathrm{d}r} = \frac{r^2+a^2}{\Delta}\,, \tag{E.9}$$

Note that this tortoise coordinate has the asymptotic behavior

$$\begin{aligned} r_* &\xrightarrow{r\to\infty} r\,, \\ r_* &\xrightarrow{r\to r_+} \frac{r_+}{\beta}\ln(r-r_+)\,. \end{aligned} \tag{E.10}$$

This choice allows to rewrite the modified Teukolsky equation in a form in which the first derivative of the master variable does not appear. For $r\to\infty$ it reads

$$\frac{\mathrm{d}^2}{\mathrm{d}r_*^2}Y + \left[\left(\omega^2 + \frac{\tilde{\alpha}^{(2)}}{r_+^4}\right) + \left(2is\omega + \frac{\tilde{\alpha}^{(1)}}{r_+^3} - \frac{\tilde{\alpha}^{(2)}}{r_+^4}\right)r^{-1}\right]Y = 0\,. \tag{E.11}$$

According with the boundary conditions for quasi-normal modes, we choose the solution that is purely outgoing, which reads $Y \sim r^{p-s}e^{qr_*}$, where the parameter p and q are the ones introduced in Eq. (6.21) and (6.22).

On the other hand, as $r \to r_+$, the modified Teukolsky equation reads

$$\frac{\mathrm{d}^2}{\mathrm{d}r_*^2}Y + r_+^{-2}\left[\left(K_+ - is\frac{\beta}{2}\right)^2 + \sum_{k=-K}^{4}\alpha^{(k)}\right]Y = 0\,, \tag{E.12}$$

where $K_+ = r_+\omega - am = \beta\sigma_{\mathrm{GR}}$. In this case, we want the solution to be purely ingoing, so we have

$$\begin{aligned} Y &\sim \exp\left\{\left(-\frac{ir_*}{r_+}\sqrt{\left(K_+ - is\frac{\beta}{2}\right)^2 + \sum_{k=-K}^{4}\alpha^{(k)}}\right)\right\} \\ &\sim (r-r_+)^{-i\sigma-\frac{s}{2}}\,, \end{aligned} \tag{E.13}$$

where σ is defined in Eq. (6.20). Considering the factor relating the master fields Y and R, we obtain

$$\begin{aligned} R &\xrightarrow{r\to\infty} e^{iqr}r^{p-2s-1}\,, \\ R &\xrightarrow{r\to r_+} (r-r_+)^{-i\sigma-s}\,. \end{aligned} \tag{E.14}$$

One can then easily verify that the ansatz of Eq. (3.85), with the generalised definitions of σ, p and q, correctly encodes the behavior of the solution $R(r)$ at the boundaries.

E.3 Splitting of the potential

In this section of the appendix we show how to transform the potential (6.8) into the potential (6.19). We start by splitting equation (6.8) into

$$\begin{aligned} \delta V(r) &= \frac{1}{\Delta}\sum_{k=-K}^{4}\alpha^{(k)}\left(\frac{r}{r_+}\right)^k \\ &= \frac{1}{\Delta}\sum_{k=0}^{4}\alpha^{(k)}\left(\frac{r}{r_+}\right)^k + \frac{1}{\Delta}\sum_{k=1}^{K}\alpha^{(-k)}\left(\frac{r_+}{r}\right)^k \end{aligned} \tag{E.15}$$

For $k \geq 1$, the first generic term in k of the sum can be rewritten as

$$\begin{aligned} \frac{\alpha^{(k)}}{\Delta}\left(\frac{r}{r_+}\right)^k &= \frac{\alpha^{(k)}}{\Delta}\left(\frac{r^k - r_+^k}{r_+^k} + 1\right) \\ &= \alpha^{(k)}\left[\frac{1}{\Delta} + \frac{1}{r_+(r-r_-)}\sum_{j=0}^{k-1}\left(\frac{r}{r_+}\right)^j\right] \end{aligned} \tag{E.16}$$

For $k \geq 2$ we can further simplify this term as

$$\begin{aligned}
\frac{\alpha^{(k)}}{\Delta}\left(\frac{r}{r_+}\right)^k &= \alpha^{(k)}\left[\frac{1}{\Delta} + \frac{1}{r_+(r-r_-)}\sum_{j=0}^{k-1}\frac{r^j - r_-^j + r_-^j}{r_+^j}\right] \\
&= \alpha^{(k)}\left[\frac{1}{\Delta} + \frac{1}{r_+(r-r_-)}\sum_{j=0}^{k-1}\left(\frac{r_-}{r_+}\right)^j + \frac{1}{r_-r_+}\sum_{j=1}^{k-1}\left(\frac{r_-}{r_+}\right)^j\sum_{n=0}^{j-1}\left(\frac{r}{r_-}\right)^n\right] \\
&= \alpha^{(k)}\left[\frac{1}{\Delta} + \frac{1}{r_+(r-r_-)}\sum_{j=0}^{k-1}\left(\frac{r_-}{r_+}\right)^j + \frac{1}{r_+^2}\sum_{j=0}^{k-2}\left(\frac{r}{r_-}\right)^j\sum_{n=j}^{k-2}\left(\frac{r_-}{r_+}\right)^n\right]
\end{aligned} \tag{E.17}$$

where we obtained the last line by expanding the series and collecting the terms in r to the same power. Summing over all the non-negative values of k yields

$$\begin{aligned}
\frac{1}{\delta}\sum_{k=0}^{4}\alpha^{(k)}\left(\frac{r}{r_+}\right)^k = \frac{1}{\delta}\sum_{k=0}^{4}\alpha^{(k)} + \frac{1}{r_+(r-r_-)}\sum_{k=1}^{4}\alpha^{(k)}\sum_{j=0}^{k-1}\left(\frac{r_-}{r_+}\right)^j \\
+\frac{1}{r_+^2}\sum_{k=0}^{2}\left(\frac{r}{r_+}\right)^k\sum_{j=k}^{2}\alpha^{(j+2)}\sum_{n=0}^{j}\left(\frac{r_-}{r_+}\right)^n
\end{aligned} \tag{E.18}$$

Now, we can perform a mapping between the coefficients $\alpha^{(k)}$ of equation (6.8) and the coefficients $A^{(0)}$, $A^{(1)}$ and $\widetilde{\alpha}^{(k)}$ introduced in equations (6.19). From a direct comparison we have

$$A^{(0)} = \sum_{k=0}^{4}\alpha^{(k)} \tag{E.19}$$

$$A^{(1)} = \sum_{k=1}^{4}\alpha^{(k)}\sum_{j=0}^{k-1}\left(\frac{r_-}{r_+}\right)^j \tag{E.20}$$

$$\widetilde{\alpha}^{(k)} = \sum_{j=k}^{2}\alpha^{(j+2)}\sum_{n=0}^{j}\left(\frac{r_-}{r_+}\right)^n \tag{E.21}$$

E.4 Diagonal quadratic coefficients

We show here how to compute the quadratic diagonal coefficients, defined from the next-to-leading-order expansion

$$\begin{aligned}\omega &\simeq \omega^0 + \sum_k d_\omega^{(k)} \alpha^{(k)} + \frac{1}{2} e_\omega^{(k)} {\alpha^{(k)}}^2 \,, \\ B &\simeq B^0 + \sum_k d_B^{(k)} \alpha^{(k)} + \frac{1}{2} e_B^{(k)} {\alpha^{(k)}}^2 \,.\end{aligned} \tag{E.22}$$

By extending the Taylor expansion (6.11) to the second order in α, we obtain

$$\mathcal{L}_j|_{\text{GR}} + \alpha \left.\frac{\mathrm{d}\mathcal{L}_j}{\mathrm{d}\alpha}\right|_{\text{GR}} + \frac{\alpha^2}{2} \left.\frac{\mathrm{d}^2\mathcal{L}_j}{\mathrm{d}\alpha^2}\right|_{\text{GR}} + \mathcal{O}\big(\alpha^3\big) = 0 \,. \tag{E.23}$$

By expanding with the chain rule the total derivative $\mathrm{d}^2\mathcal{L}_j/\mathrm{d}\alpha^2|_{\text{GR}}$, one can read off the quadratic coefficients as

$$\begin{aligned}
e_\omega = &\left(\frac{\partial\mathcal{L}_r}{\partial B}\frac{\partial\mathcal{L}_\theta}{\partial\omega} - \frac{\partial\mathcal{L}_r}{\partial\omega}\frac{\partial\mathcal{L}_\theta}{\partial B}\right)^{-1} \left[\frac{\partial^2\mathcal{L}_r}{\partial\alpha^2}\frac{\partial\mathcal{L}_\theta}{\partial B} + 2d_\omega \frac{\partial^2\mathcal{L}_r}{\partial\alpha\partial\omega}\frac{\partial\mathcal{L}_\theta}{\partial B} + 2d_B \frac{\partial^2\mathcal{L}_r}{\partial\alpha\partial B}\frac{\partial\mathcal{L}_\theta}{\partial B}\right. \\
&- d_\omega^2 \left(\frac{\partial^2\mathcal{L}_\theta}{\partial\omega^2}\frac{\partial\mathcal{L}_r}{\partial B} - \frac{\partial^2\mathcal{L}_r}{\partial\omega^2}\frac{\partial\mathcal{L}_\theta}{\partial B}\right) - d_B^2 \left(\frac{\partial^2\mathcal{L}_\theta}{\partial B^2}\frac{\partial\mathcal{L}_r}{\partial B} - \frac{\partial^2\mathcal{L}_r}{\partial B^2}\frac{\partial\mathcal{L}_\theta}{\partial B}\right) \\
&\left. + 2d_\omega\, d_B \left(\frac{\partial^2\mathcal{L}_r}{\partial\omega\partial B}\frac{\partial\mathcal{L}_\theta}{\partial B} - \frac{\partial^2\mathcal{L}_\theta}{\partial\omega\partial B}\frac{\partial\mathcal{L}_r}{\partial B}\right)\right] , \\
e_B = &-\left(\frac{\partial\mathcal{L}_r}{\partial B}\frac{\partial\mathcal{L}_\theta}{\partial\omega} - \frac{\partial\mathcal{L}_r}{\partial\omega}\frac{\partial\mathcal{L}_\theta}{\partial B}\right)^{-1} \left[\frac{\partial^2\mathcal{L}_r}{\partial\alpha^2}\frac{\partial\mathcal{L}_\theta}{\partial\omega} + 2d_\omega \frac{\partial^2\mathcal{L}_r}{\partial\alpha\partial\omega}\frac{\partial\mathcal{L}_\theta}{\partial\omega} + 2d_B \frac{\partial^2\mathcal{L}_r}{\partial\alpha\partial B}\frac{\partial\mathcal{L}_\theta}{\partial\omega}\right. \\
&- d_\omega^2 \left(\frac{\partial^2\mathcal{L}_r}{\partial\omega^2}\frac{\partial\mathcal{L}_\theta}{\partial\omega} - \frac{\partial^2\mathcal{L}_\theta}{\partial\omega^2}\frac{\partial\mathcal{L}_r}{\partial\omega}\right) - d_B^2 \left(\frac{\partial^2\mathcal{L}_r}{\partial B^2}\frac{\partial\mathcal{L}_\theta}{\partial\omega} - \frac{\partial^2\mathcal{L}_\theta}{\partial B^2}\frac{\partial\mathcal{L}_r}{\partial\omega}\right) \\
&\left. + 2d_\omega\, d_B \left(\frac{\partial^2\mathcal{L}_r}{\partial\omega\partial B}\frac{\partial\mathcal{L}_\theta}{\partial\omega} - \frac{\partial^2\mathcal{L}_\theta}{\partial\omega\partial B}\frac{\partial\mathcal{L}_r}{\partial\omega}\right)\right] ,
\end{aligned} \tag{E.24}$$

Appendix F

Appendix to Chapter 7

F.1 Excluded regions for quartic corrections

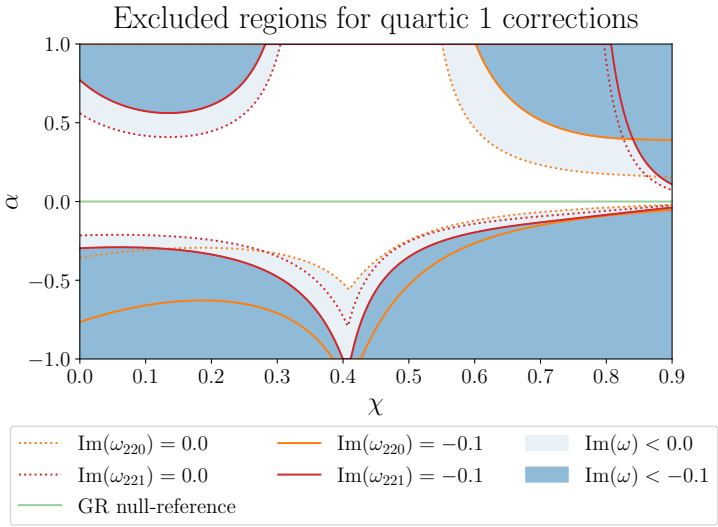


Figure F.1: Regions where $(2, 2, 0)$ and $(2, 2, 1)$ modes appear to grow exponentially $\mathrm{Im}[\omega] < 0$ (dotted lines) for quartic 1 corrections, and grow faster than $\mathrm{Im}[\omega] < -0.1$ (solid lines).

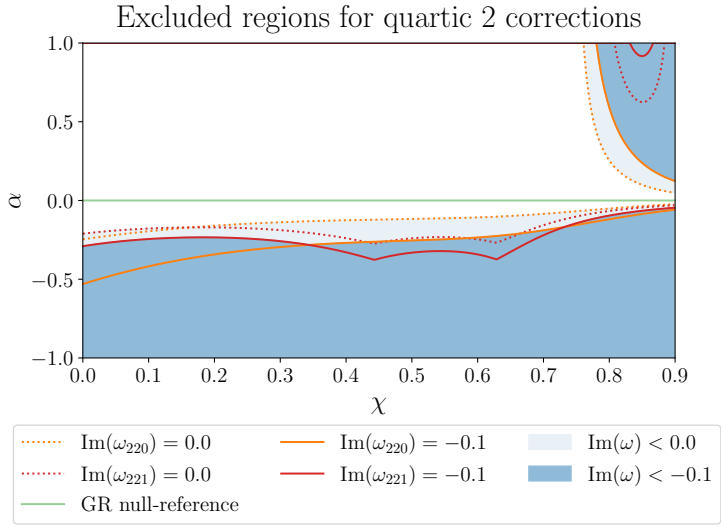


Figure F.2: Regions where $(2, 2, 0)$ and $(2, 2, 1)$ modes appear to grow exponentially $\mathrm{Im}[\omega] < 0$ (dotted lines) for quartic 2 corrections, and grow faster than $\mathrm{Im}[\omega] < -0.1$ (solid lines).

Bibliography

[1] A. Einstein, *The foundation of the general theory of relativity.* Annalen Phys. **49**, edited by J.-P. Hsu and D. Fine, 769–822 (1916).

[2] K. Schwarzschild, *On the gravitational field of a mass point according to Einstein's theory*, Sitzungsber. Preuss. Akad. Wiss. Berlin (Math. Phys.) **1916**, 189–196 (1916), arXiv:`physics/9905030`.

[3] A. S. Eddington, *A Comparison of Whitehead's and Einstein's Formulæ*, Nature **113**, 192–192 (1924).

[4] G. Lemaitre, *The expanding universe*, Gen. Rel. Grav. **29**, 641–680 (1997).

[5] D. Finkelstein, *Past-Future Asymmetry of the Gravitational Field of a Point Particle*, Phys. Rev. **110**, 965–967 (1958).

[6] H. Reissner, *Über die Eigengravitation des elektrischen Feldes nach der Einsteinschen Theorie*, Annalen Phys. **355**, 106–120 (1916).

[7] G. Nordström, *On the Energy of the Gravitation field in Einstein's Theory*, Koninklijke Nederlandse Akademie van Wetenschappen Proceedings Series B Physical Sciences **20**, 1238–1245 (1918).

[8] H. Weyl, *Zur Gravitationstheorie*, Annalen Phys. **359**, 117–145 (1917).

[9] G. B. Jeffery, *The Field of an Electron on Einstein's Theory of Gravitation*, Proceedings of the Royal Society of London Series A **99**, 123–134 (1921).

[10] R. P. Kerr, *Gravitational field of a spinning mass as an example of algebraically special metrics*, Phys. Rev. Lett. **11**, 237–238 (1963).

[11] E. T. Newman, R. Couch, K. Chinnapared, A. Exton, A. Prakash, and R. Torrence, *Metric of a Rotating, Charged Mass*, J. Math. Phys. **6**, 918–919 (1965).

[12] R. Penrose, *Gravitational Collapse and Space-Time Singularities*, Phys. Rev. Lett. **14**, 57–59 (1965).

[13] R. Penrose, *Gravitational collapse: The role of general relativity*, Riv. Nuovo Cim. **1**, 252–276 (1969).

[14] W. Israel, *Event Horizons in Static Vacuum Space-Times*, Phys. Rev. **164**, 1776–1779 (1967).

[15] B. Carter, *Axisymmetric Black Hole Has Only Two Degrees of Freedom*, Phys. Rev. Lett. **26**, 331–333 (1971).

[16] D. C. Robinson, *Uniqueness of the Kerr black hole*, Phys. Rev. Lett. **34**, 905–906 (1975).

[17] L. L. E. Braes and G. K. Miley, *Physical Sciences: Detection of Radio Emission from Cygnus X-1*, Nature **232**, 246–246 (1971).

[18] C. T. Bolton, *Identification of Cygnus X-1 with HDE 226868*, Nature **235**, 271–273 (1972).

[19] T. A. Matthews and A. R. Sandage, *Optical Identification of 3C 48, 3C 196, and 3C 286 with Stellar Objects.* The Astrophysical Journal **138**, 30 (1963).

[20] J. L. Greenstein and T. A. Matthews, *Red-Shift of the Unusual Radio Source: 3C 48*, Nature **197**, 1041–1042 (1963).

[21] K. Akiyama et al. (Event Horizon Telescope), *First M87 Event Horizon Telescope Results. I. The Shadow of the Supermassive Black Hole*, Astrophys. J. Lett. **875**, L1 (2019), arXiv:1906.11238 [astro-ph.GA].

[22] K. Akiyama et al. (Event Horizon Telescope), *First Sagittarius A* Event Horizon Telescope Results. I. The Shadow of the Supermassive Black Hole in the Center of the Milky Way*, Astrophys. J. Lett. **930**, L12 (2022), arXiv:2311.08680 [astro-ph.HE].

[23] H. Poincaré, *Sur la dynamique de l'électron*, Rendiconti del Circolo matematico di Palermo **21**, 129–176 (1906).

[24] A. Einstein, *Über Gravitationswellen*, Sitzungsber. Preuss. Akad. Wiss. Berlin (Math. Phys.) **1918**, 154–167 (1918).

[25] A. S. Eddington, *The propagation of gravitational waves*, Proc. Roy. Soc. Lond. A **102**, 268–282 (1922).

[26] A. Einstein and N. Rosen, *On Gravitational waves*, J. Franklin Inst. **223**, 43–54 (1937).

[27] F. A. E. Pirani, *Invariant Formulation of Gravitational Radiation Theory*, Phys. Rev. **105**, 1089–1099 (1957).

[28] R. A. Hulse and J. H. Taylor, *Discovery of a pulsar in a binary system*, Astrophys. J. Lett. **195**, L51–L53 (1975).

[29] J. H. Taylor, L. A. Fowler, and P. M. McCulloch, *Measurements of general relativistic effects in the binary pulsar PSR 1913+16*, Nature **277**, 437–440 (1979).

[30] B. P. Abbott et al. (LIGO Scientific, Virgo), *Observation of gravitational waves from a binary black hole merger*, Phys. Rev. Lett. **116**, 061102 (2016), arXiv:1602.03837 [gr-qc].

[31] T. D. Abbott et al. (LIGO Scientific, Virgo), *Improved analysis of GW150914 using a fully spin-precessing waveform Model*, Phys. Rev. X **6**, 041014 (2016), arXiv:1606.01210 [gr-qc].

[32] T. Regge and J. A. Wheeler, *Stability of a schwarzschild singularity*, Phys. Rev. **108**, 1063–1069 (1957).

[33] F. J. Zerilli, *Effective potential for even-parity Regge-Wheeler gravitational perturbation equations*, Phys. Rev. Lett. **24**, 737–738 (1970).

[34] C. Vishveshwara, *Stability of the schwarzschild metric*, Phys. Rev. D **1**, 2870–2879 (1970).

[35] S. Chandrasekhar, *On the equations governing the perturbations of the Schwarzschild black hole*, Proc. Roy. Soc. Lond. A **343**, 289–298 (1975).

[36] S. A. Teukolsky, *Rotating black holes - separable wave equations for gravitational and electromagnetic perturbations*, Phys. Rev. Lett. **29**, 1114–1118 (1972).

[37] F. Pretorius, *Evolution of binary black hole spacetimes*, Phys. Rev. Lett. **95**, 121101 (2005), arXiv:gr-qc/0507014.

[38] M. Campanelli, C. O. Lousto, P. Marronetti, and Y. Zlochower, *Accurate evolutions of orbiting black-hole binaries without excision*, Phys. Rev. Lett. **96**, 111101 (2006), arXiv:gr-qc/0511048.

[39] J. G. Baker, J. Centrella, D.-I. Choi, M. Koppitz, and J. van Meter, *Gravitational wave extraction from an inspiraling configuration of merging black holes*, Phys. Rev. Lett. **96**, 111102 (2006), arXiv:gr-qc/0511103.

[40] A. Buonanno, G. B. Cook, and F. Pretorius, *Inspiral, merger and ringdown of equal-mass black-hole binaries*, Phys. Rev. D **75**, 124018 (2007), arXiv:gr-qc/0610122.

[41] E. Berti, V. Cardoso, J. A. Gonzalez, U. Sperhake, M. Hannam, S. Husa, and B. Bruegmann, *Inspiral, merger and ringdown of unequal mass black hole binaries: A Multipolar analysis*, Phys. Rev. D **76**, 064034 (2007), arXiv:gr-qc/0703053.

[42] B. P. Abbott et al. (LIGO Scientific, Virgo), *Tests of general relativity with GW150914*, Phys. Rev. Lett. **116**, 221101 (2016), arXiv:1602.03841 [gr-qc].

[43] G. Carullo, *Black hole spectroscopy: status report*, Gen. Rel. Grav. **57**, 76 (2025).

[44] K. S. Stelle, *Classical gravity with higher derivatives*, Gen. Rel. Grav. **9**, 353–371 (1978).

[45] P. A. Cano and A. Ruipérez, *Leading higher-derivative corrections to Kerr geometry*, JHEP **05**, 189 (2019), arXiv:1901.01315 [gr-qc].

[46] J. L. Blázquez-Salcedo, C. F. B. Macedo, V. Cardoso, V. Ferrari, L. Gualtieri, F. S. Khoo, J. Kunz, and P. Pani, *Perturbed black holes in Einstein-dilaton-Gauss-Bonnet gravity: Stability, ringdown, and gravitational-wave emission*, Phys. Rev. D **94**, 104024 (2016), arXiv:1609.01286 [gr-qc].

[47] J. L. Blázquez-Salcedo, F. S. Khoo, and J. Kunz, *Quasinormal modes of Einstein-Gauss-Bonnet-dilaton black holes*, Phys. Rev. D **96**, 064008 (2017), arXiv:1706.03262 [gr-qc].

[48] V. Cardoso and L. Gualtieri, *Perturbations of Schwarzschild black holes in Dynamical Chern-Simons modified gravity*, Phys. Rev. D **80**, 064008 (2009), arXiv:0907.5008 [gr-qc].

[49] C. Molina, P. Pani, V. Cardoso, and L. Gualtieri, *Gravitational signature of Schwarzschild black holes in dynamical Chern-Simons gravity*, Phys. Rev. D **81**, 124021 (2010), arXiv:1004.4007 [gr-qc].

[50] V. Cardoso, M. Kimura, A. Maselli, and L. Senatore, *Black holes in an effective field theory extension of general relativity*, Phys. Rev. Lett. **121**, 251105 (2018), arXiv:1808.08962 [gr-qc].

[51] R. McManus, E. Berti, C. F. Macedo, M. Kimura, A. Maselli, and V. Cardoso, *Parametrized black hole quasinormal ringdown. II. Coupled equations and quadratic corrections for nonrotating black holes*, Phys. Rev. D **100**, 044061 (2019), arXiv:1906.05155 [gr-qc].

[52] C. de Rham, J. Francfort, and J. Zhang, *Black hole gravitational waves in the effective field theory of gravity*, Phys. Rev. D **102**, 024079 (2020), arXiv:2005.13923 [hep-th].

[53] O. J. Tattersall and P. G. Ferreira, *Quasinormal modes of black holes in Horndeski gravity*, Phys. Rev. D **97**, 104047 (2018), arXiv:1804.08950 [gr-qc].

[54] R. Konoplya and A. Zinhailo, *Quasinormal modes, stability and shadows of a black hole in the novel 4D Einstein-Gauss-Bonnet gravity*, Eur. Phys. J. C **80**, 1049 (2020), arXiv:2003.01188 [gr-qc].

[55] F. Moura and J. Rodrigues, *Asymptotic quasinormal modes of string-theoretical d-dimensional black holes*, JHEP **08**, 078 (2021), arXiv:2105.02616 [hep-th].

[56] O. J. Tattersall, P. G. Ferreira, and M. Lagos, *General theories of linear gravitational perturbations to a Schwarzschild Black Hole*, Phys. Rev. D **97**, 044021 (2018), arXiv:1711.01992 [gr-qc].

[57] V. Cardoso, M. Kimura, A. Maselli, E. Berti, C. F. Macedo, and R. McManus, *Parametrized black hole quasinormal ringdown: Decoupled equations for nonrotating black holes*, Phys. Rev. D **99**, 104077 (2019), arXiv:1901.01265 [gr-qc].

[58] R. Brito, A. Buonanno, and V. Raymond, *Black-hole spectroscopy by making full use of gravitational-wave modeling*, Phys. Rev. D **98**, 084038 (2018), arXiv:1805.00293 [gr-qc].

[59] G. Carullo et al., *Empirical tests of the black hole no-hair conjecture using gravitational-wave observations*, Phys. Rev. D **98**, 104020 (2018), arXiv:1805.04760 [gr-qc].

[60] A. Maselli, P. Pani, L. Gualtieri, and E. Berti, *Parametrized ringdown spin expansion coefficients: a data-analysis framework for black-hole spectroscopy with multiple events*, Phys. Rev. D **101**, 024043 (2020), arXiv:1910.12893 [gr-qc].

[61] S. H. Völkel, N. Franchini, and E. Barausse, *Theory-agnostic reconstruction of potential and couplings from quasinormal modes*, Phys. Rev. D **105**, 084046 (2022), arXiv:2202.08655 [gr-qc].

[62] K. Martel and E. Poisson, *Gravitational perturbations of the Schwarzschild spacetime: A Practical covariant and gauge-invariant formalism*, Phys. Rev. D **71**, 104003 (2005), arXiv:gr-qc/0502028.

[63] E. W. Leaver, *Spectral decomposition of the perturbation response of the Schwarzschild geometry*, Phys. Rev. D **34**, 384–408 (1986).

[64] A. Pound and B. Wardell, *Black hole perturbation theory and gravitational self-force*, arXiv:2101.04592 [gr-qc], 10.1007/978-981-15-4702-7_38-1 (2021), arXiv:2101.04592 [gr-qc].

[65] E. Newman and R. Penrose, *An Approach to gravitational radiation by a method of spin coefficients*, J. Math. Phys. **3**, 566–578 (1962).

[66] A. Z. Petrov, *The Classification of spaces defining gravitational fields*, Gen. Rel. Grav. **32**, 1661–1663 (2000).

[67] R. H. Boyer and R. W. Lindquist, *Maximal analytic extension of the Kerr metric*, J. Math. Phys. **8**, 265 (1967).

[68] R. Penrose and R. M. Floyd, *Extraction of Rotational Energy from a Black Hole*, Nature **229**, 177–179 (1971).

[69] J. D. Bekenstein, *Extraction of energy and charge from a black hole*, Phys. Rev. D **7**, 949–953 (1973).

[70] J. N. Goldberg and R. K. Sachs, *A theorem on Petrov types*, Acta Physica Polonica B, Proceedings Supplement **22**, 13 (1962).

[71] E. Leaver, *An Analytic representation for the quasi normal modes of Kerr black holes*, Proc. Roy. Soc. Lond. A **402**, 285–298 (1985).

[72] P. A. Cano, K. Fransen, T. Hertog, and S. Maenaut, *Gravitational ringing of rotating black holes in higher-derivative gravity*, Phys. Rev. D **105**, 024064 (2022), arXiv:2110.11378 [gr-qc].

[73] F. Moura and J. Rodrigues, *Eikonal quasinormal modes and shadow of string-corrected d-dimensional black holes*, Phys. Lett. B **819**, 136407 (2021), arXiv:2103.09302 [hep-th].

[74] K. Glampedakis and H. O. Silva, *Eikonal quasinormal modes of black holes beyond General Relativity*, Phys. Rev. D **100**, 044040 (2019), arXiv:1906.05455 [gr-qc].

[75] H. O. Silva and K. Glampedakis, *Eikonal quasinormal modes of black holes beyond general relativity. II. Generalized scalar-tensor perturbations*, Phys. Rev. D **101**, 044051 (2020), arXiv:1912.09286 [gr-qc].

[76] A. Bryant, H. O. Silva, K. Yagi, and K. Glampedakis, *Eikonal quasinormal modes of black holes beyond general relativity. III. Scalar Gauss-Bonnet gravity*, Phys. Rev. D **104**, 044051 (2021), arXiv:2106.09657 [gr-qc].

[77] P. A. Cano, K. Fransen, and T. Hertog, *Ringing of rotating black holes in higher-derivative gravity*, Phys. Rev. D **102**, 044047 (2020), arXiv:2005.03671 [gr-qc].

[78] P. Pani, V. Cardoso, L. Gualtieri, E. Berti, and A. Ishibashi, *Perturbations of slowly rotating black holes: massive vector fields in the Kerr metric*, Phys. Rev. D **86**, 104017 (2012), arXiv:1209.0773 [gr-qc].

[79] P. Pani, *Advanced methods in black-hole perturbation theory*, Int. J. Mod. Phys. A **28**, edited by V. Cardoso, L. Gualtieri, C. Herdeiro, and U. Sperhake, 1340018 (2013), arXiv:1305.6759 [gr-qc].

[80] L. Pierini and L. Gualtieri, *Quasi-normal modes of rotating black holes in Einstein-dilaton Gauss-Bonnet gravity: the first order in rotation*, Phys. Rev. D **103**, 124017 (2021), arXiv:2103.09870 [gr-qc].

[81] P. Wagle, N. Yunes, and H. O. Silva, *Quasinormal modes of slowly-rotating black holes in dynamical Chern-Simons gravity*, Phys. Rev. D **105**, 124003 (2022), arXiv:2103.09913 [gr-qc].

[82] M. Srivastava, Y. Chen, and S. Shankaranarayanan, *Analytical computation of quasinormal modes of slowly rotating black holes in dynamical Chern-Simons gravity*, Phys. Rev. D **104**, 064034 (2021), arXiv:2106.06209 [gr-qc].

[83] S. Endlich, V. Gorbenko, J. Huang, and L. Senatore, *An effective formalism for testing extensions to General Relativity with gravitational waves*, JHEP **09**, 122 (2017), arXiv:1704.01590 [gr-qc].

[84] F. J. Zerilli, *Gravitational field of a particle falling in a Schwarzschild geometry analyzed in tensor harmonics*, Phys. Rev. D **2**, 2141–2160 (1970).

[85] A. Zimmerman, H. Yang, Z. Mark, Y. Chen, and L. Lehner, *Quasinormal modes beyond kerr*, Astrophys. Space Sci. Proc. **40**, edited by C. F. Sopuerta, 217–223 (2015), arXiv:1406.4206 [gr-qc].

[86] Z. Mark, H. Yang, A. Zimmerman, and Y. Chen, *Quasinormal modes of weakly charged Kerr-Newman spacetimes*, Phys. Rev. D **91**, 044025 (2015), arXiv:1409.5800 [gr-qc].

[87] D. Li, P. Wagle, Y. Chen, and N. Yunes, *Perturbations of spinning black holes beyond General Relativity: Modified Teukolsky equation*, Phys. Rev. X **13**, 021029 (2023), arXiv:2206.10652 [gr-qc].

[88] A. Hussain and A. Zimmerman, *Approach to computing spectral shifts for black holes beyond Kerr*, Phys. Rev. D **106**, 104018 (2022), arXiv:2206.10653 [gr-qc].

[89] P. A. Cano, K. Fransen, T. Hertog, and S. Maenaut, *Universal Teukolsky equations and black hole perturbations in higher-derivative gravity*, Phys. Rev. D **108**, 024040 (2023), arXiv:2304.02663 [gr-qc].

[90] M. Campanelli and C. O. Lousto, *Second order gauge invariant gravitational perturbations of a Kerr black hole*, Phys. Rev. D **59**, 124022 (1999), arXiv:gr-qc/9811019.

[91] R. Penrose and W. Rindler, *Spinors and space-time: Volume 1, Two-spinor calculus and relativistic fields*, Vol. 1 (Cambridge Univ. Press, 1984).

[92] R. H. Price, *Nonspherical perturbations of relativistic gravitational collapse. II. Integer-spin, zero-rest-mass fields*, Phys. Rev. D **5**, 2439–2454 (1972).

[93] J. M. Bardeen and W. H. Press, *Radiation fields in the Schwarzschild background*, J. Math. Phys. **14**, 7–19 (1973).

[94] S. A. Teukolsky, *Perturbations of a rotating black hole. 1. Fundamental equations for gravitational electromagnetic and neutrino field perturbations*, Astrophys. J. **185**, 635–647 (1973).

[95] S. A. Teukolsky and W. Press, *Perturbations of a rotating black hole. III-Interaction of the hole with gravitational and electromagnetic radiation*, Astrophys. J. **193**, 443–461 (1974).

[96] R. Abbott et al. (LIGO Scientific, VIRGO, KAGRA), *Tests of general relativity with GWTC-3*, arXiv:2112.06861 [gr-qc] (2021), arXiv:2112.06861 [gr-qc].

[97] P. Bueno, P. A. Cano, F. Goelen, T. Hertog, and B. Vercnocke, *Echoes of kerr-like wormholes*, Phys. Rev. D **97**, 024040 (2018), arXiv:1711.00391 [gr-qc].

[98] N. Oshita and N. Afshordi, *Probing microstructure of black hole spacetimes with gravitational wave echoes*, Phys. Rev. D **99**, 044002 (2019), arXiv:1807.10287 [gr-qc].

[99] K. Fransen, G. Koekoek, R. Tielemans, and B. Vercnocke, *Modeling and detecting resonant tides of exotic compact objects*, Phys. Rev. D **104**, 044044 (2021), arXiv:2005.12286 [gr-qc].

[100] H.-P. Nollert, *About the significance of quasinormal modes of black holes*, Phys. Rev. D **53**, 4397–4402 (1996), arXiv:gr-qc/9602032.

[101] E. Gasperin and J. L. Jaramillo, *Energy scales and black hole pseudospectra: the structural role of the scalar product*, Class. Quant. Grav. **39**, 115010 (2022), arXiv:2107.12865 [gr-qc].

[102] J. L. Jaramillo, R. Panosso Macedo, and L. A. Sheikh, *Gravitational wave signatures of black hole quasinormal mode instability*, Phys. Rev. Lett. **128**, 211102 (2022), arXiv:2105.03451 [gr-qc].

[103] E. Berti, V. Cardoso, M. H.-Y. Cheung, F. Di Filippo, F. Duque, P. Martens, and S. Mukohyama, *Stability of the fundamental quasinormal mode in time-domain observations against small perturbations*, Phys. Rev. D **106**, 084011 (2022), arXiv:2205.08547 [gr-qc].

[104] H. S. Reall and J. E. Santos, *Higher derivative corrections to Kerr black hole thermodynamics*, JHEP **04**, 021 (2019), arXiv:1901.11535 [hep-th].

[105] P. A. Cano, B. Ganchev, D. R. Mayerson, and A. Ruipérez, *Black hole multipoles in higher-derivative gravity*, JHEP **12**, 120 (2022), arXiv:2208.01044 [gr-qc].

[106] S. R. Dolan, C. Kavanagh, and B. Wardell, *Gravitational perturbations of rotating black holes in lorenz gauge*, Phys. Rev. Lett. **128**, 151101 (2022), arXiv:2108.06344 [gr-qc].

[107] E. Berti, V. Cardoso, and M. Casals, *Eigenvalues and eigenfunctions of spin-weighted spheroidal harmonics in four and higher dimensions*, Phys. Rev. D **73**, 024013 (2006), arXiv:gr-qc/0511111.

[108] R. Ghosh, N. Franchini, S. H. Völkel, and E. Barausse, *Quasi-normal modes of non-separable perturbation equations: the scalar non-Kerr case*, Phys. Rev. D **108**, 024038 (2023), arXiv:2303.00088 [gr-qc].

[109] P. A. Cano, A. Deich, and N. Yunes, *Accuracy of the slow-rotation approximation for black holes in modified gravity in light of astrophysical observables*, Phys. Rev. D **109**, 024048 (2024), arXiv:2305.15341 [gr-qc].

[110] S. H. Völkel, N. Franchini, E. Barausse, and E. Berti, *Constraining modifications of black hole perturbation potentials near the light ring with quasinormal modes*, Phys. Rev. D **106**, 124036 (2022), arXiv:2209.10564 [gr-qc].

[111] N. Franchini and S. H. Völkel, *Parametrized quasinormal mode framework for non-Schwarzschild metrics*, Phys. Rev. D **107**, 124063 (2023), arXiv:2210.14020 [gr-qc].

[112] P. A. Cano, L. Capuano, N. Franchini, S. Maenaut, and S. H. Völkel, *Parametrized quasinormal mode framework for modified Teukolsky equations*, Phys. Rev. D **110**, 104007 (2024), arXiv:2407.15947 [gr-qc].

[113] P. A. Cano, L. Capuano, N. Franchini, S. Maenaut, and S. H. Völkel, *Higher-derivative corrections to the Kerr quasinormal mode spectrum*, Phys. Rev. D **110**, 124057 (2024), arXiv:2409.04517 [gr-qc].

[114] M. Kimura, *Note on the parametrized black hole quasinormal ringdown formalism*, Phys. Rev. D **101**, 064031 (2020), arXiv:2001.09613 [gr-qc].

[115] P. A. Cano, K. Fransen, T. Hertog, and S. Maenaut, *Quasinormal modes of rotating black holes in higher-derivative gravity*, Phys. Rev. D **108**, 124032 (2023), arXiv:2307.07431 [gr-qc].

[116] S. Völkel, *Sebastianvoelkel/parametrized_qnm_framework*, July 24, 2024.

[117] E. Berti, V. Cardoso, and A. O. Starinets, *Quasinormal modes of black holes and black branes*, Class. Quant. Grav. **26**, 163001 (2009), arXiv:0905.2975 [gr-qc].

[118] E. Berti, V. Cardoso, and C. M. Will, *On gravitational-wave spectroscopy of massive black holes with the space interferometer LISA*, Phys. Rev. D **73**, 064030 (2006), arXiv:gr-qc/0512160.

[119] A. A. Starobinsky, *Amplification of waves reflected from a rotating "black hole"*. Sov. Phys. JETP **37**, 28–32 (1973).

[120] S. Chandrasekhar, *The mathematical theory of black holes*, Fundam. Theor. Phys. **9**, edited by B. Bertotti, F. de Felice, and A. Pascolini, 5–26 (1984).

[121] P. P. Fiziev, *Teukolsky-starobinsky identities: a novel derivation and generalizations*, Phys. Rev. D **80**, 124001 (2009), arXiv:0906.5108 [gr-qc].

[122] R. M. Wald, *On perturbations of a Kerr black hole*, J. Math. Phys. **14**, 1453–1461 (1973).

[123] D. Li, A. Hussain, P. Wagle, Y. Chen, N. Yunes, and A. Zimmerman, *Isospectrality breaking in the Teukolsky formalism*, Phys. Rev. D **109**, 104026 (2024), arXiv:2310.06033 [gr-qc].

[124] P. Cano, *Pacmn91/BeyondKerrQNM*, Feb. 21, 2025.

[125] H.-P. Nollert and R. H. Price, *Quantifying excitations of quasinormal mode systems*, J. Math. Phys. **40**, 980–1010 (1999), arXiv:gr-qc/9810074.

[126] J. L. Jaramillo, R. Panosso Macedo, and L. Al Sheikh, *Pseudospectrum and Black Hole Quasinormal Mode Instability*, Phys. Rev. X **11**, 031003 (2021), arXiv:2004.06434 [gr-qc].

[127] M. H.-Y. Cheung, K. Destounis, R. P. Macedo, E. Berti, and V. Cardoso, *Destabilizing the fundamental mode of black holes: The elephant and the flea*, Phys. Rev. Lett. **128**, 111103 (2022), arXiv:2111.05415 [gr-qc].

[128] R. A. Konoplya, *Quasinormal modes in higher-derivative gravity: Testing the black hole parametrization and sensitivity of overtones*, Phys. Rev. D **107**, 064039 (2023), arXiv:2210.14506 [gr-qc].

[129] R. A. Konoplya and A. Zhidenko, *First few overtones probe the event horizon geometry*, JHEAp **44**, 291 (2024), arXiv:2209.00679 [gr-qc].

[130] H. O. Silva, G. Tambalo, K. Glampedakis, K. Yagi, and J. Steinhoff, *Quasinormal modes and their excitation beyond general relativity*, Phys. Rev. D **110**, 024042 (2024), arXiv:2404.11110 [gr-qc].

[131] P. Wagle, D. Li, Y. Chen, and N. Yunes, *Perturbations of spinning black holes in dynamical Chern-Simons gravity: Slow rotation equations*, Phys. Rev. D **109**, 104029 (2024), arXiv:2311.07706 [gr-qc].

[132] V. Cardoso, A. S. Miranda, E. Berti, H. Witek, and V. T. Zanchin, *Geodesic stability, Lyapunov exponents and quasinormal modes*, Phys. Rev. D **79**, 064016 (2009), arXiv:0812.1806 [hep-th].

[133] H. Yang, D. A. Nichols, F. Zhang, A. Zimmerman, Z. Zhang, and Y. Chen, *Quasinormal-mode spectrum of Kerr black holes and its geometric interpretation*, Phys. Rev. D **86**, 104006 (2012), arXiv:1207.4253 [gr-qc].

[134] P. A. Cano and M. David, *Isospectrality in Effective Field Theory Extensions of General Relativity*, arXiv:2407.12080 [hep-th] (2024), arXiv:2407.12080 [hep-th].

[135] H. Yang, F. Zhang, A. Zimmerman, D. A. Nichols, E. Berti, and Y. Chen, *Branching of quasinormal modes for nearly extremal Kerr black holes*, Phys. Rev. D **87**, 041502 (2013), arXiv:1212.3271 [gr-qc].

[136] G. T. Horowitz, M. Kolanowski, G. N. Remmen, and J. E. Santos, *Extremal Kerr black holes as amplifiers of new physics*, Phys. Rev. Lett. **131**, 091402 (2023), arXiv:2303.07358 [hep-th].

[137] G. T. Horowitz, M. Kolanowski, G. N. Remmen, and J. E. Santos, *Sudden breakdown of effective field theory near cool Kerr-Newman black holes*, JHEP **05**, 122 (2024), arXiv:2403.00051 [hep-th].

[138] C. Y. .-. Chen, C. de Rham, and A. J. Tolley, *Deformations of extremal black holes and the UV*, Phys. Rev. D **111**, 024056 (2025), arXiv:2408.05549 [hep-th].

[139] P. A. Cano and M. David, *Teukolsky equation for near-extremal black holes beyond general relativity: Near-horizon analysis*, Phys. Rev. D **110**, 064067 (2024), arXiv:2407.02017 [gr-qc].

[140] S. Maenaut, G. Carullo, P. A. Cano, A. Liu, V. Cardoso, T. Hertog, and T. G. F. Li, *Ringdown Analysis of Rotating Black Holes in Effective Field Theory Extensions of General Relativity*, (Nov. 2024) arXiv:2411.17893 [gr-qc].

[141] B. P. Abbott et al. (LIGO Scientific, Virgo), *A guide to LIGO–Virgo detector noise and extraction of transient gravitational-wave signals*, Class. Quant. Grav. **37**, 055002 (2020), arXiv:1908.11170 [gr-qc].

[142] B. Allen, J. D. E. Creighton, E. E. Flanagan, and J. D. Romano, *Robust statistics for deterministic and stochastic gravitational waves in nonGaussian noise. 1. Frequentist analyses*, Phys. Rev. D **65**, 122002 (2002), arXiv:gr-qc/0105100.

[143] M. Isi, M. Giesler, W. M. Farr, M. A. Scheel, and S. A. Teukolsky, *Testing the no-hair theorem with GW150914*, Phys. Rev. Lett. **123**, 111102 (2019), arXiv:1905.00869 [gr-qc].

[144] M. Isi and W. M. Farr, *Analyzing black-hole ringdowns*, arXiv:2107.05609 [gr-qc] (2021), arXiv:2107.05609 [gr-qc].

[145] H. Siegel, M. Isi, and W. M. Farr, *Analyzing black-hole ringdowns. II. Data conditioning*, Phys. Rev. D **111**, 044070 (2025), arXiv:2410.02704 [gr-qc].

[146] H. Lim, G. Khanna, A. Apte, and S. A. Hughes, *Exciting black hole modes via misaligned coalescences: II. The mode content of late-time coalescence waveforms*, Phys. Rev. D **100**, 084032 (2019), arXiv:1901.05902 [gr-qc].

[147] M. Casals, A. C. Ottewill, and N. Warburton, *High-order asymptotics for the Spin-Weighted Spheroidal Equation at large real frequency*, Proc. Roy. Soc. Lond. A **475**, 20180701 (2019), arXiv:1810.00432 [gr-qc].

[148] C. D. Capano, M. Cabero, J. Westerweck, J. Abedi, S. Kastha, A. H. Nitz, Y.-F. Wang, A. B. Nielsen, and B. Krishnan, *Multimode Quasinormal Spectrum from a Perturbed Black Hole*, Phys. Rev. Lett. **131**, 221402 (2023), arXiv:2105.05238 [gr-qc].

[149] G. Carullo, W. Del Pozzo, and J. Veitch, *Observational black hole spectroscopy: a time-domain multimode analysis of GW150914*, Phys. Rev. D **99**, 123029 (2019), arXiv:1902.07527 [gr-qc].

[150] B. Abbott et al. (LIGO Scientific, Virgo), *Tests of general relativity with the binary black hole signals from the LIGO-virgo catalog GWTC-1*, Phys. Rev. D **100**, 104036 (2019), arXiv:1903.04467 [gr-qc].

[151] B. J. Kelly and J. G. Baker, *Decoding mode mixing in black-hole merger ringdown*, Phys. Rev. D **87**, 084004 (2013), arXiv:1212.5553 [gr-qc].

[152] E. Berti and A. Klein, *Mixing of spherical and spheroidal modes in perturbed Kerr black holes*, Phys. Rev. D **90**, 064012 (2014), arXiv:1408.1860 [gr-qc].

[153] V. Gennari, G. Carullo, and W. Del Pozzo, *Searching for ringdown higher modes with a numerical relativity-informed post-merger model*, Eur. Phys. J. C **84**, 233 (2024), arXiv:2312.12515 [gr-qc].

[154] L. London, D. Shoemaker, and J. Healy, *Modeling ringdown: Beyond the fundamental quasinormal modes*, Phys. Rev. D **90**, 124032 (2014), arXiv:1404.3197 [gr-qc].

[155] M. Giesler, M. Isi, M. A. Scheel, and S. Teukolsky, *Black hole ringdown: The importance of overtones*, Phys. Rev. X **9**, 041060 (2019), arXiv:1903.08284 [gr-qc].

[156] I. Ota and C. Chirenti, *Overtones or higher harmonics? Prospects for testing the no-hair theorem with gravitational wave detections*, Phys. Rev. D **101**, 104005 (2020), arXiv:1911.00440 [gr-qc].

[157] X. Jiménez Forteza, S. Bhagwat, P. Pani, and V. Ferrari, *Spectroscopy of binary black hole ringdown using overtones and angular modes*, Phys. Rev. D **102**, 044053 (2020), arXiv:2005.03260 [gr-qc].

[158] G. Carullo, W. Del Pozzo, and J. Veitch, *<code>pyRing</code>: a time-domain ringdown analysis python package*, version 2.3.0, Zenodo, July 2023.

[159] X. Li, L. Sun, R. K. L. Lo, E. Payne, and Y. Chen, *Angular emission patterns of remnant black holes*, Phys. Rev. D **105**, 024016 (2022), arXiv:2110.03116 [gr-qc].

[160] V. Baibhav, M. H.-Y. Cheung, E. Berti, V. Cardoso, G. Carullo, R. Cotesta, W. Del Pozzo, and F. Duque, *Agnostic black hole spectroscopy: Quasinormal mode content of numerical relativity waveforms and limits of validity of linear perturbation theory*, Phys. Rev. D **108**, 104020 (2023), arXiv:2302.03050 [gr-qc].

[161] P. J. Nee, S. H. Völkel, and H. P. Pfeiffer, *Role of black hole quasinormal mode overtones for ringdown analysis*, Phys. Rev. D **108**, 044032 (2023), arXiv:2302.06634 [gr-qc].

[162] H. Zhu, J. L. Ripley, A. Cárdenas-Avendaño, and F. Pretorius, *Challenges in quasinormal mode extraction: Perspectives from numerical solutions to the Teukolsky equation*, Phys. Rev. D **109**, 044010 (2024), arXiv:2309.13204 [gr-qc].

[163] R. Cayuso, P. Figueras, T. França, and L. Lehner, *Modelling self-consistently beyond general relativity*, Phys. Rev. Lett. **131**, 111403 (2023), arXiv:2303.07246 [gr-qc].

[164] H. Siegel, M. Isi, and W. M. Farr, *Ringdown of GW190521: Hints of multiple quasinormal modes with a precessional interpretation*, Phys. Rev. D **108**, 064008 (2023), arXiv:2307.11975 [gr-qc].

[165] B. P. Abbott et al. (LIGO Scientific, Virgo), *GWTC-1: a gravitational-wave transient catalog of compact binary mergers observed by LIGO and virgo during the first and second observing runs*, Phys. Rev. X **9**, 031040 (2019), arXiv:1811.12907 [astro-ph.HE].

[166] R. Abbott et al. (LIGO Scientific, Virgo), *GWTC-2: Compact binary coalescences observed by LIGO and virgo during the first half of the third observing run*, Phys. Rev. X **11**, 021053 (2021), arXiv:2010.14527 [gr-qc].

[167] R. Abbott et al. (KAGRA, VIRGO, LIGO Scientific), *GWTC-3: Compact Binary Coalescences Observed by LIGO and Virgo during the Second Part of the Third Observing Run*, Phys. Rev. X **13**, 041039 (2023), arXiv:2111.03606 [gr-qc].

[168] R. Abbott et al. (LIGO Scientific, Virgo), *GW190521: a binary black hole merger with a total mass of* 150 $M_\odot$, Phys. Rev. Lett. **125**, 101102 (2020), arXiv:2009.01075 [gr-qc].

[169] R. Abbott et al. (LIGO Scientific, Virgo), *Properties and astrophysical implications of the* 150 $M_\odot$ *binary black hole merger GW190521*, Astrophys. J. Lett. **900**, L13 (2020), arXiv:2009.01190 [astro-ph.HE].

[170] R. Abbott et al. (LIGO Scientific, Virgo), *Tests of general relativity with binary black holes from the second LIGO-Virgo gravitational-wave transient catalog*, Phys. Rev. D **103**, 122002 (2021), arXiv:2010.14529 [gr-qc].

[171] R. Cotesta, G. Carullo, E. Berti, and V. Cardoso, *Analysis of ringdown overtones in GW150914*, Phys. Rev. Lett. **129**, 111102 (2022), arXiv:2201.00822 [gr-qc].

[172] M. Isi and W. M. Farr, *Comment on "analysis of ringdown overtones in GW150914"*, Phys. Rev. Lett. **131**, 169001 (2023), arXiv:2310.13869 [astro-ph.HE].

[173] G. Carullo, R. Cotesta, E. Berti, and V. Cardoso, *Reply to comment on "analysis of ringdown overtones in GW150914"*, Phys. Rev. Lett. **131**, 169002 (2023), arXiv:2310.20625 [gr-qc].

[174] H. O. Silva, A. Ghosh, and A. Buonanno, *Black-hole ringdown as a probe of higher-curvature gravity theories*, Phys. Rev. D **107**, 044030 (2023), arXiv:2205.05132 [gr-qc].

[175] A. Zimmerman, C.-J. Haster, and K. Chatziioannou, *On combining information from multiple gravitational wave sources*, Phys. Rev. D **99**, 124044 (2019), arXiv:1903.11008 [astro-ph.IM].

[176] A. K.-W. Chung and N. Yunes, *Probing quadratic gravity with black-hole ringdown gravitational waves measured by LIGO-Virgo-KAGRA detectors*, arXiv:2506.14695 [gr-qc] (2025), arXiv:2506.14695 [gr-qc].

[177] M. Punturo et al., *The third generation of gravitational wave observatories and their science reach*, Class. Quant. Grav. **27**, edited by Z. Marka and S. Marka, 084007 (2010).

[178] D. Reitze et al., *Cosmic explorer: The U.S. contribution to gravitational-wave astronomy beyond LIGO*, Bull. Am. Astron. Soc. **51**, 035 (2019), arXiv:1907.04833 [astro-ph.IM].

[179] A. Maselli, S. Yi, L. Pierini, V. Vellucci, L. Reali, L. Gualtieri, and E. Berti, *Black hole spectroscopy beyond Kerr: Agnostic and theory-based tests with next-generation interferometers*, Phys. Rev. D **109**, 064060 (2024), arXiv:2311.14803 [gr-qc].

[180] S. M. Carroll, *Spacetime and Geometry: An Introduction to General Relativity* (Cambridge University Press, July 31, 2019).

[181] J. B. Hartle, *Gravity* (Cambridge University Press, Sept. 3, 2021).

[182] S. M. Carroll, *Lecture notes on general relativity*, arXiv:gr-qc/9712019 (1997), arXiv:gr-qc/9712019.

[183] Y. BenTov and J. Swearngin, *Gravitational shockwaves on rotating black holes*, Gen. Rel. Grav. **51**, 25 (2019), arXiv:1706.03430 [gr-qc].

[184] S. Aksteiner, "Geometry and analysis on black hole spacetimes", PhD thesis (Leibniz U., Hannover, 2014).

[185] H. P. Nollert, *Quasinormal modes of Schwarzschild black holes: The determination of quasinormal frequencies with very large imaginary parts*, Phys. Rev. D **47**, 5253–5258 (1993).

[186] K. Glampedakis, A. D. Johnson, and D. Kennefick, *Darboux transformation in black hole perturbation theory*, Phys. Rev. D **96**, 024036 (2017), arXiv:1702.06459 [gr-qc].

List of publications

P. A. Cano, K. Fransen, T. Hertog, and S. Maenaut, *Gravitational ringing of rotating black holes in higher-derivative gravity*, Phys. Rev. D **105**, 024064 (2022), arXiv:2110.11378 [gr-qc].

P. A. Cano, K. Fransen, T. Hertog, and S. Maenaut, *Universal Teukolsky equations and black hole perturbations in higher-derivative gravity*, Phys. Rev. D **108**, 024040 (2023), arXiv:2304.02663 [gr-qc].

P. A. Cano, K. Fransen, T. Hertog, and S. Maenaut, *Quasinormal modes of rotating black holes in higher-derivative gravity*, Phys. Rev. D **108**, 124032 (2023), arXiv:2307.07431 [gr-qc].

T. Hertog, S. Maenaut, B. Missoni, R. Tielemans, and T. Van Riet, *Stability of axion-saxion wormholes*, JHEP **11**, 151 (2024), arXiv:2405.02072 [hep-th].

P. A. Cano, L. Capuano, N. Franchini, S. Maenaut, and S. H. Völkel, *Parametrized quasinormal mode framework for modified Teukolsky equations*, Phys. Rev. D **110**, 104007 (2024), arXiv:2407.15947 [gr-qc].

P. A. Cano, L. Capuano, N. Franchini, S. Maenaut, and S. H. Völkel, *Higher-derivative corrections to the Kerr quasinormal mode spectrum*, Phys. Rev. D **110**, 124057 (2024), arXiv:2409.04517 [gr-qc].

Submitted for publication

S. Maenaut, G. Carullo, P. A. Cano, A. Liu, V. Cardoso, T. Hertog, and T. G. F. Li, *Ringdown Analysis of Rotating Black Holes in Effective Field Theory Extensions of General Relativity*, (Nov. 2024) arXiv:2411.17893 [gr-qc].

FACULTY OF SCIENCE
DEPARTMENT OF PHYSICS AND ASTRONOMY
INSTITUTE FOR THEORETICAL PHYSICS
Celestijnenlaan 200D box 2415
B-3001 Leuven

